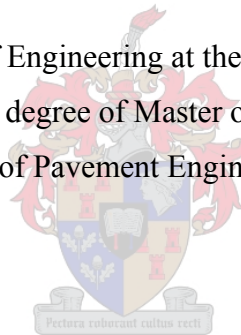


# **FACTORS INFLUENCING ASPHALT COMPACTIBILITY AND ITS RELATION TO ASPHALT RUTTING PERFORMANCE**

by

W. J. Douries B.Eng (Stell.)

A thesis submitted to the Faculty of Engineering at the University of Stellenbosch in partial fulfilment of the requirements for the degree of Master of Science in Engineering (Civil) in the field of Pavement Engineering



Prof. K.J. Jenkins

Study Leader

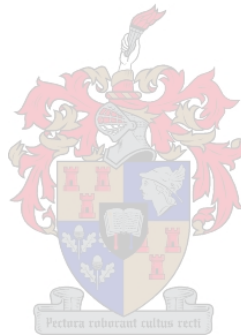
# DECLARATION

*“Declaration*

I, the undersigned, hereby declare that the work contained in this thesis is my own original work, except where specifically acknowledged in the text, and that I have not previously in its entirety or in part submitted it at any university for a degree.

Signed: .....  
William John Douries

Date: ..... ”



# SYNOPSIS

This thesis covers the factors affecting compactibility of hot mix asphalt including gradation, filler/binder ratios, binder types, binder content, polymer modification, temperature, volumetric properties etc. The study is not limited to compactibility as the property measured, but also on the influence of these factors on the mix's capacity to resist permanent deformation or rutting.

An experimental design was used with a variety of the above factors being included. Laboratory analysis of the mixes as well as accelerated pavement testing of different mix types using the one-third scale Model Mobile Load Simulator (MMLS3) was carried out. The analysis assists in identification of the factors that influence both compactibility and rut resistance, those influencing the one but not the other, and those factors having no significant influence. The compactibility of the mixes has been analysed in terms of voids in the mix at a specific binder content and compaction level. Special consideration was given to the characterisation of the filler and filler/binder system of some mixes.

It was found that gradation of a mix has a significant influence on compaction and the rutting performance. High filler/binder ratios were found to be the critical factors influencing the compactibility of the wearing course mixes investigated, but based on the limited tests performed, the reduction of the filler/binder ratios for improved compactibility did not significantly increase rutting under accelerated pavement testing.

As expected, the binder type has a significant influence on the rutting resistance as well as compactibility. In addition, an increase in binder content facilitated compaction, but decreased rutting resistance.

Polymer modification considerably improved the rutting resistance of a standard mix under the same loading conditions. Although some modifiers may improve rutting resistance, it requires higher compaction temperatures.

The addition of the antistripping agent Gripper L decreased the rutting, aggregate stripping and also the rate of rutting of the Quartzite LAMBS mix that result from the stripping failure

mechanism. Low densities can lead to considerable rutting and moisture damage, especially when a moisture susceptible aggregate is used.

In terms of compactibility as evaluated with the Superpave Gyrotory Compactor, it appears that there exists a temperature window in which compaction can be achieved, but in terms of rutting; even a small deviation in temperature can influence rutting results significantly. The control of the temperature during testing is critical if meaningful comparisons between different mixes with regard to rutting performance are to be made.

Linear elastic and finite element analysis has been performed to ascertain whether different specimen geometries would influence the stress distribution within the specimen, and subsequently the rutting results. It was found that the geometry of test specimens has an influence on the stress distribution within the specimens, which can influence the permanent deformation results. The briquette specimens tested in the laboratory also yielded higher rutting results for the same mix tested in the field. It is therefore important to use specimens that are most representative of field conditions.



# SAMEVATTING

Hierdie tesis ondersoek die faktore wat 'n invloed het op die kompakteerbaarheid van warm asfalt. Faktore sluit in onder andere gradering, vulstof/bindstof verhouding, tipe bindstof, bindstof inhoud, polimeer modifisering, temperatuur, volumetriese eienskappe, ens. Hierdie studie is nie net beperk tot kompakteerbaarheid as 'n gemete eienskap nie, maar ook die invloed van hierdie faktore op die mengsel se vermoë om weerstand te bied teen permanente deformatsie of spoorvorming.

'n Eksperimentele ontwerp wat 'n verskeidenheid van bogenoemde faktore insluit is gebruik. Laboratorium analise van die mengsels asook versnelde plaveisel toetse van die verskillende tipe mengsels is gedoen met die een-derde skaal Mobile Lammuleerder (MMLS3). Die analise help met die identifikasie van die faktore wat beide kompakteerbaarheid en spoorvorming beïnvloed, asook dié wat slegs die een maar nie die ander beïnvloed, en ook die faktore wat geen beduidende invloed het nie. Die kompakteerbaarheid is geëvalueer in terme van die hol ruimtes in die mengsel by 'n bepaalde bindstof inhoud en verdigtingsgraad. Spesiale aandag is geskenk aan die eienskappe van die vulstof en vulstof/bindstof wisselwerking van die mengsels.



Die gradering van 'n mengsel het 'n beduidende invloed op kompakteerbaarheid sowel as spoorvorming. Hoë vulstof/bindstof verhoudings is een van die kritiese faktore wat die kompakteerbaarheid van die betrokke mengsels beïnvloed, maar laer vulstof/bindstof verhoudings vir beter kompaksie het nie 'n beduidende toename in wielsporing teweeg gebring nie.

Soos verwag het die tipe bindstof 'n beduidende invloed op kompakteerbaarheid sowel as spoorvorming. 'n Toename in bindstof bevorder verdigting, maar lei tot groter wielsporing.

Polimeer modifisering verminder die wielsporing van 'n standard mengsel onder dieselfde beladingstoestand. Alhoewel modifisering wielsporing verminder, vereis dit hoër kompaksie temperature.

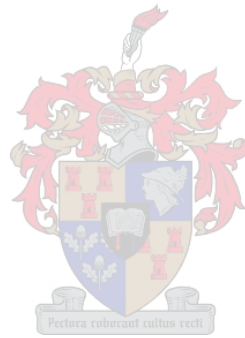
Die toevoeging van die teenstropingsmiddel GripperL verminder spoorvorming, aggremaat stroping asook die tempo van spoorvorming van die Kwartsiet LAMBS mengsel as gevolg van die stropingsmeganisme. Lae digthede kan lei tot aansienlike vogskade en spoorvorming; veral as die aggremaat vatbaar is vir die invloed van vog.

Daar blyk 'n temperatuur interval te wees waarin verdigting met die *Superpave Gyrotory Compactor* bereik kan word; maar selfs 'n klein temperatuurafwyking kan beduidende invloed op die resultate van spoorvorming hê. Temperatuurbeheer is baie belangrik indien sinvolle vergelykings tussen die sporinggedrag van verskillende mengsels gemaak moet word.

Lineêr elasties en eindige element analise is uitgevoer om te bepaal of verskillende toetskonfigurasies die spanningsverdeling binne die toetsmonsters en die spoorvorming affekteer. Dit is bevind dat die geometrie van toetsmonsters het 'n invloed op die spanningsverdeling in die monsters wat die sporingresultate kan beïnvloed. Die briketmonsters in die laboratorium gee ook groter spoordiepte teenoor dieselfde mengsel wat in die veld getoets is. Daarom is dit belangrik om verteenwoordigende monsters te gebruik.



*In Loving Memory of my Mother*



# ACKNOWLEDGEMENTS

I would like to thank the following people:

My Heavenly Father for His grace in giving me the strength and ability to complete my studies

My family and friends and those near and dear to me for their love, encouragement and support

Prof. K. Jenkins for his guidance, advice and suggestions

Prof. F. Hugo for his mentorship and the opportunity to study via the ITT internship

All my colleagues and peers at the ITT and Department of Civil Engineering for their interest and support

Everyone else who showed interest and concern throughout my studies



# CONTENTS

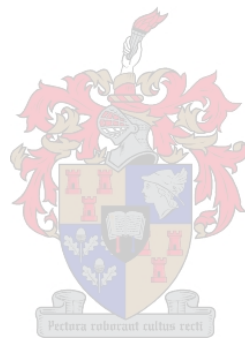
<b>Declaration.....</b>	<b>ii</b>
<b>Synopsis.....</b>	<b>iii</b>
<b>Samevatting .....</b>	<b>v</b>
<b>Acknowledgements.....</b>	<b>viii</b>
<b>Contents .....</b>	<b>ix</b>
<b>List of Figures.....</b>	<b>xv</b>
<b>List of Tables .....</b>	<b>xxii</b>
<b>List of symbols and Abbreviations .....</b>	<b>xxiv</b>
<b>1 INTRODUCTION.....</b>	<b>1</b>
<b>1.1 Background.....</b>	<b>1</b>
<b>1.2 Objectives of the Study .....</b>	<b>3</b>
<b>1.3 Scope of the study .....</b>	<b>4</b>
<b>1.4 Outline.....</b>	<b>5</b>
<b>1.5 Methodology .....</b>	<b>5</b>
<b>2 LITERATURE REVIEW .....</b>	<b>9</b>
<b>2.1 Scope of this chapter .....</b>	<b>9</b>
<b>2.2 Compaction and compactibility .....</b>	<b>9</b>
2.2.1 Mechanics of compaction.....	10
2.2.2 Factors influencing compaction and compactibility of HMA.....	11
2.2.3 Aggregate properties .....	12

2.2.4	Binders .....	13
2.2.5	Fillers.....	14
2.2.6	Temperature .....	18
2.2.7	Compaction methods.....	20
2.2.7.1	Laboratory compaction methods.....	20
2.2.7.2	Field compaction methods .....	21
2.2.7.2.1	Steel wheel rollers .....	21
2.2.7.2.2	Pneumatic Rollers .....	22
2.2.7.2.3	Vibratory Rollers.....	22
2.2.7.2.4	Laboratory and field compaction conditions.....	23
2.2.8	Other factors influencing compaction.....	24
2.2.9	Factors affecting HMA volumetrics.....	25
<b>2.3</b>	<b>Polymer modification.....</b>	<b>31</b>
2.3.1	Plastomer modifiers.....	32
2.3.2	Elastomer modifiers .....	33
<b>2.4</b>	<b>Permanent Deformation (Rutting) of HMA pavements .....</b>	<b>34</b>
2.4.1	Factors influencing permanent deformation .....	37
<b>2.5</b>	<b>Moisture Susceptibility .....</b>	<b>42</b>
2.5.1	Factors influencing moisture susceptibility.....	42
<b>2.6</b>	<b>Summary .....</b>	<b>46</b>
<b>3</b>	<b>INVESTIGATION OF FACTORS INFLUENCING COMPACTIBILITY .....</b>	<b>48</b>
<b>3.1</b>	<b>Introduction .....</b>	<b>48</b>
<b>3.2</b>	<b>Volumetrics .....</b>	<b>49</b>
<b>3.3</b>	<b>Test programme and methodology .....</b>	<b>52</b>
3.3.1	Materials.....	52
3.3.2	Test methods .....	58
3.3.2.1	Hydrometer tests .....	58
3.3.2.2	Softening point (Ring & Ball) tests.....	58
3.3.2.3	Gyratory compaction.....	60

3.3.2.4	Dynamic creep.....	62
3.3.2.5	Indirect tensile strength (ITS) .....	62
3.3.2.6	Stiffness (Dynamic Modulus) in Indirect Tensile mode .....	63
<b>3.4</b>	<b>Compactibility results .....</b>	<b>64</b>
3.4.1	Gyratory compaction vs. Marshall compaction .....	64
3.4.2	Gradation.....	68
3.4.3	Nature of the filler .....	71
3.4.4	Binder content .....	71
3.4.5	Filler content .....	72
3.4.6	Filler/binder ratio.....	73
3.4.7	Compaction temperature .....	79
3.4.8	Mechanical testing.....	80
<b>3.5</b>	<b>Conclusions .....</b>	<b>82</b>
<b>4</b>	<b>INFLUENCE OF COMPACTABILITY ON PAVEMENT RUTTING PERFORMANCE: CASE STUDIES.....</b>	<b>84</b>
<b>4.1</b>	<b>Introduction .....</b>	<b>84</b>
4.1.1	Background .....	84
4.1.2	Influence of compaction on asphalt properties and influence on rutting performance.....	84
4.1.3	Accelerated pavement testing (APT) .....	89
<b>4.2</b>	<b>CASE STUDY 1: Influence of filler/binder ratios on rut resistance .....</b>	<b>91</b>
4.2.1	Materials.....	91
4.2.2	Specimen preparation.....	93
4.2.3	Set up.....	93
4.2.4	Temperature control and measurements .....	94
4.2.5	Rut profile measurements.....	94
4.2.6	MMLS3 Rutting results.....	95
4.2.7	Conclusions of CASE STUDY 1 .....	97
<b>4.3</b>	<b>CASE STUDY 2: Influence of Polymer Modified Binders (PMBs) on rut resistance of intersections .....</b>	<b>98</b>

4.3.1	Materials and testing .....	100
4.3.2	Test results.....	100
4.3.3	Conclusions of CASE STUDY 2 .....	103
<b>4.4</b>	<b>CASE STUDY 3: Influence of antistripping agent on rutting and stripping .....</b>	<b>104</b>
4.4.1	Materials.....	105
4.4.2	Test setup.....	107
4.4.2.1	Temperature control and measurements .....	108
4.4.2.2	Rut profile measurements.....	109
4.4.3	MMLS3 Rutting results.....	110
4.4.4	Conclusions of CASE STUDY 3 .....	113
<b>4.5</b>	<b>CASE STUDY 4: Influence of binder type and gradation on rut resistance.....</b>	<b>114</b>
4.5.1	Indirect tensile fatigue testing .....	115
4.5.2	MMLS3 Results .....	116
4.5.3	Indirect tensile strength and fatigue results.....	120
4.5.4	Conclusions of CASE STUDY 4.....	121
<b>4.6</b>	<b>CASE STUDY 5: Influence of wet trafficking on rutting and fatigue life.....</b>	<b>122</b>
4.6.1	Stiffness testing (SASW) .....	124
4.6.2	Materials.....	125
4.6.3	Mix designs .....	127
4.6.4	Test results.....	129
4.6.4.1	Indirect Tensile Strength .....	129
4.6.4.2	MMLS3 Results .....	130
4.6.4.3	Indirect tensile fatigue tests.....	131
4.6.4.4	Discussion .....	133
4.6.5	Conclusions of CASE STUDY 5 .....	135
<b>4.7</b>	<b>Overall Conclusions .....</b>	<b>137</b>
<b>5</b>	<b>RELATING LABORATORY TO FIELD PERFORMANCE .....</b>	<b>139</b>
<b>5.1</b>	<b>Introduction .....</b>	<b>139</b>
<b>5.2</b>	<b>Mechanisms of permanent deformation .....</b>	<b>142</b>

<b>5.3</b>	<b>Effect of specimen geometry on stress distribution.....</b>	<b>150</b>
5.3.1	Linear Elastic Analysis with ELSYM5.....	151
5.3.2	Finite Element Analysis with ABAQUS.....	153
5.3.3	Summary of stress distribution analysis.....	155
<b>5.4</b>	<b>Rut prediction models.....</b>	<b>162</b>
<b>5.5</b>	<b>Rut prediction results.....</b>	<b>167</b>
<b>5.6</b>	<b>Validation of Prediction Models with MMLS3 Tests .....</b>	<b>172</b>
5.6.1	Materials.....	173
5.6.1.1	SABS BTB .....	173
5.6.1.2	COLTO Medium .....	173
5.6.2	MMLS3 Testing.....	174
5.6.2.1	Laboratory testing .....	174
5.6.2.2	Field testing.....	175
5.6.3	MMLS3 Test results.....	177
5.6.3.1	COLTO Medium 40/50.....	177
5.6.3.2	SABS BTB .....	178
5.6.4	Model vs. MMLS3 rutting.....	180
<b>5.7</b>	<b>Conclusions .....</b>	<b>181</b>
<b>6</b>	<b>CONCLUSIONS AND RECOMMENDATIONS.....</b>	<b>183</b>
<b>6.1</b>	<b>Conclusions .....</b>	<b>183</b>
<b>6.2</b>	<b>Recommendations .....</b>	<b>185</b>
	<b>References .....</b>	<b>186</b>
	<b>APPENDIX .....</b>	<b>200</b>
	<b>Appendix A .....</b>	<b>201</b>
	<b>Sensitivity Analysis of Stress Distribution between Different Specimen Geometries.....</b>	<b>201</b>
	<b>Appendix B .....</b>	<b>228</b>



# LIST OF FIGURES

Figure 1-1: Scope of the study .....	4
Figure 1-2: Methodology of the study.....	8
Figure 2-1: Variation in the compactibility of bituminous mixtures due to changes in composition (Hunter <i>et al</i> , 2000) .....	12
Figure 2-2: Schematic Illustrating Fixed and Free Binder (Anderson, 1987).....	15
Figure 2-3: Parameters to describe voids in filler/binder mortar (Cooley <i>et al</i> , 1998).....	16
Figure 2-4: Relationship indicating stiffening of filler/binder mastic (Cooley <i>et al</i> , 1998) .....	17
Figure 2-5: Effect of temperature on the compactibility of bituminous mixtures (Hunter <i>et al</i> , 2000) .....	19
Figure 2-6: Bitumen test data chart showing ‘ideal’ viscosities for optimal mixing and compaction (after Shell, 1991).....	19
Figure 2-7: Some factors affecting HMA compaction in the field (Sabita, 2000).....	25
Figure 2-8: Components of a compacted HMA specimen (Huner and Brown, 2001).....	26
Figure 2-9: The effect of binder content on VMA, voids and volume of binder (Verhaeghe <i>et al</i> , 1995) .....	27
Figure 2-10: The effect of compaction energy on optimum binder content (Verhaeghe <i>et al</i> , 1995) .....	28
Figure 2-11: Maximum Density Line Related to VMA (Chadbourn <i>et al</i> , 2000) .....	29
Figure 2-12: The effect of polymer modification on rheology (Hunter <i>et al</i> , 2000).....	32
Figure 2-13: Asphalt response to repeated loading.....	34
Figure 2-14: Consolidation in asphalt layer (FPCWV, 2000).....	34
Figure 2-15: Plastic flow in asphalt layer (Santucci, 2001) .....	35
Figure 2-16: Schematic Rut Curve (Bouldin <i>et al</i> , 1994) .....	37
Figure 2-17: Relative rutting rate vs. air voids (AAPA, 1999).....	39
Figure 2-18: Relations between ESALs to 10 mm Rut Depth, Binder Content, and Air Void Content, Fine Gradation (after J. Epps <i>et al</i> , 1999).....	40
Figure 2-19: Air void content versus retained mix strength-region of pessimum voids (Terrel and Al-Swailmi, 1993) .....	45
Figure 3-1: Volumetric Properties of Mixtures Re-Compacted with the SGC at Decreasing Temperatures @Ndesign (Bahia and Hanson, 2000).....	50

Figure 3-2: Effect of Temperature on Air Voids measured after Compaction Using Different Compaction Methods for HMA containing a Fine Crushed Gravel Mixture (Parker and Hossain, 1999).....	51
Figure 3-3: Average Percent Air Voids vs. Compaction Temperature (Huner and Brown, 2001) .....	51
Figure 3-4: Gradation of the experimental mix in relation to the 19mm COLTO Coarse.....	53
Figure 3-5: Gradation curves at various <i>n</i> -values .....	54
Figure 3-6: Particle size distribution of fillers .....	55
Figure 3-7: The Ring-and-Ball Softening Point Test.....	59
Figure 3-8: SGC Mould Configuration and Compaction Parameters.....	61
Figure 3-9: Marshall volumetric properties of 19mm COLTO Coarse mix as reported by supplier.....	65
Figure 3-10: Marshall volumetric properties of 19mm COLTO Coarse mix (University of Stellenbosch).....	66
Figure 3-11: The influence of the gradation exponent <i>n</i> on compactibility of 19mm COLTO Coarse mix.....	68
Figure 3-12: The influence of binder content on compactibility of 19mm COLTO Coarse Mix ( <i>n</i> = 0.3 and filler content = 6.5%).....	71
Figure 3-13: Mix design chart for $N_{des}$ VIM for 19mm COLTO Coarse mixes having an <i>n</i> -value of 0.3.....	72
Figure 3-14: The influence of filler content on compactibility of 19mm COLTO Coarse mix ( <i>P<sub>b</sub></i> = 4.5%; <i>n</i> -value = 0.3).....	73
Figure 3-15: Softening point test results on different fillers.....	74
Figure 3-16: Increase in softening point of mastic (in terms of filler/binder ratio) .....	75
Figure 3-17: Increase in softening point of mastic (in terms of % bulk volume of filler).....	75
Figure 3-18: Stiffening of study filler/binder mortars.....	76
Figure 3-19: Gyrotory compaction summary for experimental mix with Filler @ 5.5 % .....	78
Figure 3-20: Gyrotory compaction summary for experimental mix with Filler @ 6.5 % .....	79
Figure 3-21: The influence of temperature on the compactibility of the 19mm COLTO Coarse mix.....	79
Figure 4-1: Impact of Compaction on the Orientation and Interlock of Aggregate Particles in an Asphalt Mix (Santucci, 2001) .....	85
Figure 4-2: Relative fatigue life vs. air voids (AAPA, 1999) .....	87
Figure 4-3: Relative stiffness modulus vs. air voids (AAPA, 1999).....	87

Figure 4-4: Chart showing the relationship between density (expressed in terms of air voids remaining) and performance (NETTCP, 2002).....	88
Figure 4-5: Wheel Configuration of the MMLS Mk.3.....	90
Figure 4-6: Gradations of mixes with adjusted filler/binder ratios.....	92
Figure 4-7:MMLS3 Wooden mould and slab configuration.....	93
Figure 4-8: Slab configuration with transverse profile positions.....	94
Figure 4-9: Cumulative rutting curves for Test 1.....	95
Figure 4-10: Cumulative rutting curves for Test 2.....	96
Figure 4-11: Cumulative rutting curves – STD mix.....	101
Figure 4-12: Cumulative rutting curves – EVA mix.....	102
Figure 4-13: Cumulative rutting curves – LD mix.....	102
Figure 4-14: Gradation of Quartzite LAMBS mix.....	105
Figure 4-15: Gyratory compaction of Quartzite LAMBS mixes.....	106
Figure 4-16: Specimens cut to fit in water bath: Plan view.....	107
Figure 4-17: Plan view of MMLS3 testing under water: Diagrammatical.....	108
Figure 4-18: Rut profile measurements.....	109
Figure 4-19: Cumulative rutting for Quartzite LAMBS.....	110
Figure 4-20: Linear relation of log plot – Quartzite LAMBS.....	111
Figure 4-21: Quartzite LAMBS specimens after MMLS3 trafficking.....	112
Figure 4-22: Quartzite LAMBS specimens (with Gripper L) after MMLS3 trafficking.....	112
Figure 4-23: Cumulative rutting for COLTO Medium mixes.....	116
Figure 4-24: Cumulative rutting for BTB mixes.....	117
Figure 4-25: Cumulative rutting for LAMBS mixes.....	117
Figure 4-26: Cumulative rutting at different temperatures for BTB 40/50.....	118
Figure 4-27: Cumulative rutting for COLTO Medium 40/50 at different temperatures.....	119
Figure 4-28: Slope of rutting curve BTB 40/50.....	120
Figure 4-29: Gradations of Texas study mixtures.....	128
Figure 5-1: Outline for Chapter 5.....	141
Figure 5-2: Burgers’ model.....	143
Figure 5-3: Deformation response of a viscoelastic material under constant load.....	143
Figure 5-4: Viscoelastic behaviour.....	144
Figure 5-5: Elastic and Viscous behaviour.....	145
Figure 5-6: Variation of Permanent Shear Strain in RSST-CH on Specimens of the Same Mix Subjected to Short-Term and Long-Term Ageing (Sousa, 1994).....	149

Figure 5-7: Diagram illustrating the stress analysis for different specimen geometries.....	152
Figure 5-8: Illustration of briquette deformation (not to scale) .....	154
Figure 5-9: Illustration of slab deformation (not to scale) .....	154
Figure 5-10: The coordinate system for the stress distribution analysis.....	155
Figure 5-11: Deviator stress ( $\sigma_1 - \sigma_3$ ) contours (kPa) for Briquette width 150 mm .....	161
Figure 5-12: Deviator stress ( $\sigma_1 - \sigma_3$ ) contours (kPa) for slab .....	162
Figure 5-13: Composition and characteristics of Francken mixes (Francken, 1977) .....	166
Figure 5-14: Rut prediction profiles for 150mm briquette – ELSYM5 .....	168
Figure 5-15: Rut prediction profiles for 150mm briquette – ELSYM5 .....	169
Figure 5-16: Briquette full friction rut prediction profiles for Monismith-model .....	170
Figure 5-17: Rut prediction with time for briquette specimens .....	171
Figure 5-18: Validation of rutting models.....	172
Figure 5-19: Gradation for SABS BTB.....	173
Figure 5-20: Gradations for COLTO Medium 40/50.....	174
Figure 5-21: Pictorial View of Setup for Typical Wet Trafficking Test.....	176
Figure 5-22: Typical Wet Trafficking Test in Progress.....	176
Figure 5-23: Cumulative Rutting Curves –COLTO Medium 40/50.....	177
Figure 5-24: Cumulative Rutting Curves –SABS BTB.....	178
Figure 5-25: Results of actual and predicted rutting.....	180
	
Figure A - 1: ELSYM 5 Vertical Stress Contours (in kPa) for Asphalt thickness 1m; Stiffness 1000 MPa, $\nu = 0.45$ .....	202
Figure A - 2: ELSYM 5 Vertical Stress Contours (in kPa) for Asphalt thickness 1m; Stiffness 1500 MPa; $\nu = 0.45$ .....	203
Figure A - 3: ELSYM 5 Vertical Stress Contours (in kPa) for Asphalt thickness 40 mm; Stiffness 1500 MPa; $\nu = 0.45$ .....	203
Figure A - 4: ELSYM 5 Vertical Stress Contours (in kPa) for Asphalt thickness 40 mm; Stiffness 1000 MPa; $\nu = 0.45$ .....	204
Figure A - 5: ELSYM 5 Shear Stress Contours (in kPa) for Asphalt thickness 1m; Stiffness 1000 MPa; $\nu = 0.45$ .....	205
Figure A - 6: ELSYM 5 Shear Stress Contours (in kPa) for Asphalt thickness 1m; Stiffness 1500 MPa; $\nu = 0.45$ .....	205

Figure A - 7: ELSYM 5 Shear Stress Contours (in kPa) for Asphalt thickness 60 mm; Stiffness 1500 MPa; $\nu = 0.45$ .....	206
Figure A - 8: ELSYM 5 Shear Stress Contours (in kPa) for Asphalt thickness 60 mm; Stiffness 1000 MPa; $\nu = 0.45$ .....	206
Figure A - 9: ELSYM 5 Shear Stress Contours (in kPa) for Asphalt thickness 40 mm; Stiffness 1500 MPa; $\nu = 0.45$ .....	207
Figure A - 10: ELSYM 5 Shear Stress Contours (in kPa) for Asphalt thickness 40 mm; Stiffness 1000 MPa; $\nu = 0.45$ .....	207
Figure A - 11: ELSYM 5 Horizontal Stress Contours (in kPa) for Asphalt thickness 1m; Stiffness 1500 MPa; $\nu = 0.45$ .....	208
Figure A - 12: ELSYM 5 Horizontal Stress Contours (in kPa) for Asphalt thickness 1m; Stiffness 1000 MPa; $\nu = 0.45$ .....	209
Figure A - 13: ELSYM 5 Horizontal Stress Contours (in kPa) for Asphalt thickness 40 mm; Stiffness 1000 MPa; $\nu = 0.45$ .....	209
Figure A - 14: ELSYM 5 Horizontal Stress Contours (in kPa) for Asphalt thickness 60 mm; Stiffness 1500 MPa; $\nu = 0.45$ .....	210
Figure A - 15: ELSYM 5 Horizontal Stress Contours (in kPa) for Asphalt thickness 60 mm; Stiffness 1500 MPa; $\nu = 0.45$ .....	210
Figure A - 16: ELSYM 5 Horizontal Stress Contours (in kPa) for Asphalt thickness 60 mm; Stiffness 1000 MPa; $\nu = 0.45$ .....	211
Figure A - 17: ELSYM 5 Horizontal Stress Contours (in kPa) for Asphalt thickness 40 mm; Stiffness 1500 MPa; $\nu = 0.45$ .....	211
Figure A - 18: ELSYM 5 Deviator Stress ( $\sigma_1 - \sigma_3$ ) Contours (in kPa) for Asphalt thickness 1m; Stiffness 1000 MPa; $\nu = 0.45$ .....	212
Figure A - 19: ELSYM 5 Deviator Stress ( $\sigma_1 - \sigma_3$ ) Contours (in kPa) for Asphalt thickness 1m; Stiffness 1500 MPa; $\nu = 0.45$ .....	212
Figure A - 20: ELSYM 5 Deviator Stress ( $\sigma_1 - \sigma_3$ ) Contours (in kPa) for Asphalt thickness 1m; Stiffness 500 MPa; $\nu = 0.45$ .....	213
Figure A - 21: ELSYM 5 Deviator Stress ( $\sigma_1 - \sigma_3$ ) Contours (in kPa) for Asphalt thickness 60 mm; Stiffness 1500 MPa; $\nu = 0.45$ .....	213
Figure A - 22: ELSYM 5 Deviator Stress ( $\sigma_1 - \sigma_3$ ) Contours (in kPa) for Asphalt thickness 60 mm; Stiffness 1000 MPa; $\nu = 0.45$ .....	214

Figure A - 23: ELSYM 5 Deviator Stress ( $\sigma_1 - \sigma_3$ ) Contours (in kPa) for Asphalt thickness 40 mm; Stiffness 1500 MPa;  $\nu = 0.45$  ..... 214

Figure A - 24: ELSYM 5 Deviator Stress ( $\sigma_1 - \sigma_3$ ) Contours (in kPa) for Asphalt thickness 40 mm; Stiffness 1000 MPa;  $\nu = 0.45$  ..... 215

Figure A - 25: ABAQUS Vertical Stress Contours (in kPa) for Briquette 150mm width; Thickness 60 mm; Stiffness 1500 MPa;  $\nu = 0.45$  ..... 217

Figure A - 26: ABAQUS Vertical Stress Contours (in kPa) for Briquette 120mm width; Thickness 60 mm; Stiffness 1500 MPa;  $\nu = 0.45$  ..... 218

Figure A - 27: ABAQUS Vertical Stress Contours (in kPa) for Briquette 100mm width; Thickness 60 mm; Stiffness 1500 MPa;  $\nu = 0.45$  ..... 218

Figure A - 28: ABAQUS Vertical Stress Contours (in kPa) for Slab 600 mm width; Thickness 40 mm; Stiffness 1500 MPa;  $\nu = 0.45$  ..... 219

Figure A - 29: ABAQUS Shear Stress Contours (in kPa) for Briquette 150mm width; Thickness 60 mm; Stiffness 1500 MPa;  $\nu = 0.45$  ..... 220

Figure A - 30: ABAQUS Shear Stress Contours (in kPa) for Briquette 120mm width; Thickness 60 mm; Stiffness 1500 MPa;  $\nu = 0.45$  ..... 220

Figure A - 31: ABAQUS Shear Stress Contours (in kPa) for Briquette 100mm width; Thickness 60 mm; Stiffness 1500 MPa;  $\nu = 0.45$  ..... 221

Figure A - 32: ABAQUS Shear Stress Contours (in kPa) for Slab 600 mm width; Thickness 40 mm; Stiffness 1500 MPa;  $\nu = 0.45$  ..... 221

Figure A - 33: ABAQUS Horizontal Stress Contours (in kPa) for Briquette 150mm width; Thickness 60 mm; Stiffness 1500 MPa;  $\nu = 0.45$  ..... 222

Figure A - 34: ABAQUS Horizontal Stress Contours (in kPa) for Briquette 120mm width; Thickness 60 mm; Stiffness 1500 MPa;  $\nu = 0.45$  ..... 223

Figure A - 35: ABAQUS Horizontal Stress Contours (in kPa) for Briquette 100mm width; Thickness 60 mm; Stiffness 1500 MPa;  $\nu = 0.45$  ..... 223

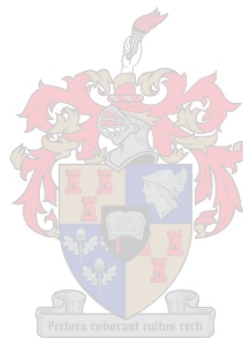
Figure A - 36: ABAQUS Horizontal Stress Contours (in kPa) for Slab 600 mm width; Thickness 40 mm; Stiffness 1500 MPa;  $\nu = 0.45$  ..... 224

Figure A - 37: ABAQUS Deviator Stress ( $\sigma_1 - \sigma_3$ ) Contours (in kPa) for Briquette 150mm width; Thickness 60 mm; Stiffness 1500 MPa;  $\nu = 0.45$  ..... 225

Figure A - 38: ABAQUS Deviator Stress ( $\sigma_1 - \sigma_3$ ) Contours (in kPa) for Briquette 120mm width; Thickness 60 mm; Stiffness 1500 MPa;  $\nu = 0.45$  ..... 226

Figure A - 39: ABAQUS Deviator Stress ( $\sigma_1 - \sigma_3$ ) Contours (in kPa) for Briquette 100mm width; Thickness 60 mm; Stiffness 1500 MPa;  $\nu = 0.45$  ..... 226

Figure A - 40: ABAQUS Deviator Stress ( $\sigma_1 - \sigma_3$ ) Contours (in kPa) for Slab 600 mm width; Thickness 40 mm; Stiffness 1500 MPa;  $\nu = 0.45$  ..... 227



## LIST OF TABLES

Table 1-1: Factors evaluated in Compaction and Rutting studies.....	6
Table 2-1: Guidelines for selecting the amplitude of vibration (after Kennedy <i>et al</i> , 1984).....	23
Table 2-2: Influences on Compaction (after Asphalt Institute, 1980).....	46
Table 2-3: Influences on Rut resistance (Collop, 2002).....	47
Table 3-1: Test matrix for compactibility variables.....	52
Table 3-2: Binders for compactibility mixes.....	56
Table 3-3: Gradation of COLTO Medium wearing course mixes .....	56
Table 3-4: Gradation of LAMBS mixes.....	57
Table 3-5: Gradation of BTB mixes.....	57
Table 3-6: Superpave compaction criteria (Blankenship <i>et al</i> , 1994).....	60
Table 3-7: Recommended Superpave compaction matrix (Blankenship <i>et al</i> , 1994).....	61
Table 3-8: Gyratory VIM @ $N_{des}$ for different binder contents and traffic levels .....	65
Table 3-9: Gyratory compaction results - COLTO Medium.....	69
Table 3-10: Gyratory compaction results - BTB.....	70
Table 3-11: Gyratory compaction results - LAMBS.....	70
Table 3-12: Rigden voids of fillers .....	73
Table 3-13: Gyratory VIM @ $N_{des}$ for different binder contents and traffic levels (Experimental mix with filler content of 5.5 %).....	77
Table 3-14: Gyratory VIM @ $N_{des}$ for different binder contents and traffic levels (Experimental mix with filler content of 6.5 %).....	77
Table 3-15: Mechanical test results on 19mm COLTO Coarse mix.....	80
Table 3-16: Dynamic creep test results on experimental mixes.....	81
Table 4-1: Properties of mixes with adjusted filler/binder ratios.....	92
Table 4-2: MMLS3 Test sequence for mixes with adjusted filler/binder ratios .....	92
Table 4-3: Summary of results.....	97
Table 4-4: Ranking of mixes.....	97
Table 4-5: Binder and filler contents of PMB mixes .....	99
Table 4-6: Test sequence for PMB mixes .....	99
Table 4-7: Mixing and Compaction temperatures for different modifiers (Distin, 2002) .....	100
Table 4-8: Compaction and Rutting results for PMB mixes.....	103

Table 4-9: Characteristics of GripperL (Kao Corporation S.A., 2001).....	107
Table 4-10: Test matrix for the effect of binder type and gradation on rut resistance.....	114
Table 4-11: Indirect tensile strength test results (in kPa).....	120
Table 4-12: Indirect tensile fatigue test results (in cycles to failure).....	120
Table 4-13: MMLS3 specimen sequence.....	123
Table 4-14: Mix types tested with the MMLS3 .....	125
Table 4-15: FAA and CAA of aggregate .....	127
Table 4-16: Mix design information .....	127
Table 4-17: Mixing and compaction temperatures of Texas study binders .....	128
Table 4-18: ITS results.....	129
Table 4-19: MMLS3 test summary .....	130
Table 4-20: Indirect tensile fatigue results – Untrafficked .....	132
Table 4-21: Indirect tensile fatigue results - Trafficked.....	132
Table 4-22: Average indirect tensile fatigue values.....	133
Table 4-23: Summary of test results .....	135
Table 5-1: Influence of asphalt modulus on stress distribution (asphalt thickness 40mm) .....	156
Table 5-2: Influence of asphalt modulus on stress distribution (asphalt thickness 60mm) .....	157
Table 5-3: Influence of asphalt thickness on stress distribution .....	158
Table 5-4: Influence of friction on the 150mm briquette specimen (ABAQUS).....	159
Table 5-5: Influence of specimen width on stress distribution .....	160
Table 5-6: Rut prediction after 150 000 axles.....	171
Table 5-7: Average temperatures for SABS BTB Field tests (60mm from centerline).....	178

# LIST OF SYMBOLS AND ABBREVIATIONS

AAPA	:	Australian Asphalt Pavement Association
APT	:	Accelerated Pavement Testing
ASTM	:	American Society for Testing and Materials
BRD	:	Bulk Relative Density
BTB	:	Bitumen Treated Base
CAA	:	Coarse Aggregate Angularity
CBD	:	Central Business District
COLTO	:	Committee for Land Transport Officials
CSIR	:	Council for Scientific and Industrial Research
CTCC	:	Cape Town City Council
CTIA	:	Cape Town International Airport
DOT	:	Department of Transportation
ESAL	:	Equivalent Single Axle Load
EVA	:	Ethylene vinyl acetate
FAA	:	Fine Aggregate Angularity
FEA	:	Finite Element Analysis
FEM	:	Finite Element Method
FHWA	:	Federal Highway Administration
FPCWV	:	Flexible Pavements Council of West Virginia
G*	:	Complex Shear Modulus
G <sub>mm</sub>	:	Maximum Theoretical Relative Density
HMA	:	Hot Mix Asphalt
HWTD	:	Hamburg Wheel-Tracking Device
ITS	:	Indirect Tensile Strength
LAMBS	:	Large Aggregate Mix for Bases
MMLS3	:	Model Mobile Load Simulator Mk3
MTRD	:	Maximum Theoretical Relative Density
MTS	:	Materials Testing System
NAPA	:	National Asphalt Pavement Association
N <sub>f</sub>	:	Indirect tensile fatigue life
OCW	:	Opzoekingscentrum voor de Wegenbouw

Pb	:	Percentage bitumen by mass
PMB	:	Polymer Modified Binder
RSST-CH	:	Repetitive Simple Shear Test at Constant Height
SABITA	:	Southern African Bitumen and Tar Association
SABS	:	South African Bureau for Standards
SASW	:	Spectral Analysis of Surface Waves
SBR	:	Styrene-butadiene-rubber
SBS	:	Styrene-butadiene-styrene
SGC	:	Superpave Gyrotory Compactor
SHRP	:	Strategic Highway Research Program
SMA	:	Stone Mastic Asphalt
TxDOT	:	Texas Department of Transportation
TxMLS	:	Texas Mobile Load Simulator
USACE	:	United States Army Corps of Engineers
V <sub>be</sub>	:	Volume of effective binder
VFB	:	Voids filled with binder
VIM	:	Voids in the mix
VMA	:	Voids in the Mineral Aggregate
$\delta$	:	phase angle



# 1 INTRODUCTION

## 1.1 Background

Compaction is recognised as probably the most important factor affecting the performance of hot mix asphalt (HMA) pavements. It is therefore vital that the density of the asphalt be controlled to ensure adequate performance. A mix may be well designed with all the desired properties, but if it is not compacted to a satisfactory density level, it will not perform properly in the field. Low densities may result in (AAPA, 1998(b)):

- Reduced resistance to rutting
- Reduced fatigue life
- Reduced pavement stiffness
- Increased permeability and hence increase in age hardening effects, earlier onset of ravelling, and risk of moisture damage to asphalt and underlying layers

On the other hand, Hunter *et al* (2000) warned that although worthwhile extensions in the pavement life could be achieved with increased compaction, over-compaction might result in excessive rutting, shoving or bleeding. Permanent deformation, being one of the major pavement distress modes, may lead to safety problems during wet weather, such as impaired vehicle steering and hydroplaning and slippery surfaces.

Compactibility can be defined as “*a concept related to the ease with which a material can be compacted*” (Hunter *et al*, 2000). There are many factors that influence the compactibility of asphalt, including the material properties and environmental conditions. Amongst the material properties are aggregate gradation and properties, binder content and binder properties, filler content and properties. Most of the material properties affecting compactibility also influence permanent deformation. All of the aggregate properties that are beneficial in terms of improving the mix’s resistance to permanent deformation typically decrease the compactibility of such a mix (Chadborn *et al*, 2000). Thus, increased compactive effort is required to achieve the desired density level needed in the mix. Increase in binder content may increase the compactibility of a particular mix to an extent, but may decrease the resistance to permanent deformation.

It can thus be seen that some of the factors favourable for compactibility may not be favourable for resistance to permanent deformation. This illustrates the complexity of asphalt behaviour and asphalt mix design.

The occurrence of permanent deformation on our roads has increased over the past few years due to increases in heavy vehicle volumes, axle loading and tyre pressures. This increased the demands placed on the binders used in pavement construction and this necessitated the development of binders with a higher level of performance. This led to the introduction of polymer modified binders (PMBs) in an effort to reduce early pavement distress and to extend the service life of the pavement (King *et al*, 1986). This is achieved through increased asphalt stiffness, improved elasticity and strengthening the binder-aggregate bond at high temperatures while increasing strain tolerance and improving fatigue resistance at low temperatures.

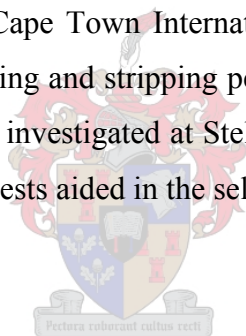
There is a strong tendency towards performance related specifications for asphalt construction, and hence the need for performance related test methods. Controlling volumetric properties alone is not sufficient to ensure good performance. Empirical tests are frequently used to estimate the lifetime of an asphalt pavement. However, these tests determine only certain properties of the asphalt and cannot always relate to the actual asphalt field performance. Accelerated pavement testing (APT) is a tool that can be used for the performance evaluation of new pavement materials (e.g. reinforced asphalt, cement treated bases, etc.), distress mechanisms such as impact of water, pavement distress and selection of rehabilitation strategies (Hugo, 2000). All of these distresses can result in loss of performance but rutting is the one distress that is most likely to be a sudden failure as a result of unsatisfactory HMA (Brown *et al*, 2001).

The one-third scale Model Mobile Load Simulator (MMLS3) is a small-scale APT device that has been shown to be a very cost-effective tool for evaluating performance. It can do so by evaluating the response and performance of dry, heated, and wet (surface) layers of full-scale in service pavements (Smit *et al*, 1999; Walubita *et al*, 2000). It can also be used to evaluate the performance of different materials. Rut depth criteria for acceptable performance were initially proposed by A. Epps *et al* (2001). These have been further developed in other studies in the USA and SA (Smit *et al*, 2003; Hugo *et al*, 2004)

In Stellenbosch, an apparatus has been constructed to evaluate the moisture susceptibility of laboratory compacted asphalt briquette specimens under water using the MMLS3 (Du Preez, 2001). The performance of different materials can be compared and ranked in terms of stripping and rutting performance.

Recently, concern has been raised over the compactibility of typical asphalt wearing course mixes used in the Western Cape, South Africa. The harshness of these particular mixes has several disadvantages with regard to production costs and quality of the end product. An investigation was carried out to identify the reason for the harshness of these mixes and to recommend strategies to improve the compactibility of these mixes. Measures and recommendations towards improved compactibility and the resulting effect on the rutting resistance will be presented in this thesis.

Compactibility and resistance to permanent deformation were also important considerations in the mix design validation phase of Cape Town International Airport Taxiway Rehabilitation project in 2001. The compaction, rutting and stripping performance of candidate mixes for use in the rehabilitation construction was investigated at Stellenbosch University. It will be shown in this thesis how these performance tests aided in the selection of the appropriate mixes for the different layers in the rehabilitation.



## **1.2 Objectives of the Study**

The objective of this study was to investigate the influence of compactibility and resistance to permanent deformation on pavement performance in terms of rutting and resistance to moisture damage.

From an analysis of the findings the factors that influence both compactibility and rut resistance were identified. In the same vein, those influencing the one but not the other, and those factors having no significant influence were identified.

### 1.3 Scope of the study

This study focused on factors affecting the compactibility of asphalt including gradation, filler/binder ratios, binder types, binder content, temperature, volumetric properties etc. The influence of these factors on the mix’s capacity to resist permanent deformation or rutting was also investigated. The influence of compaction on the moisture susceptibility of some of the mixes was also included in the study. The various components of the study are summarised in Figure 1-1.

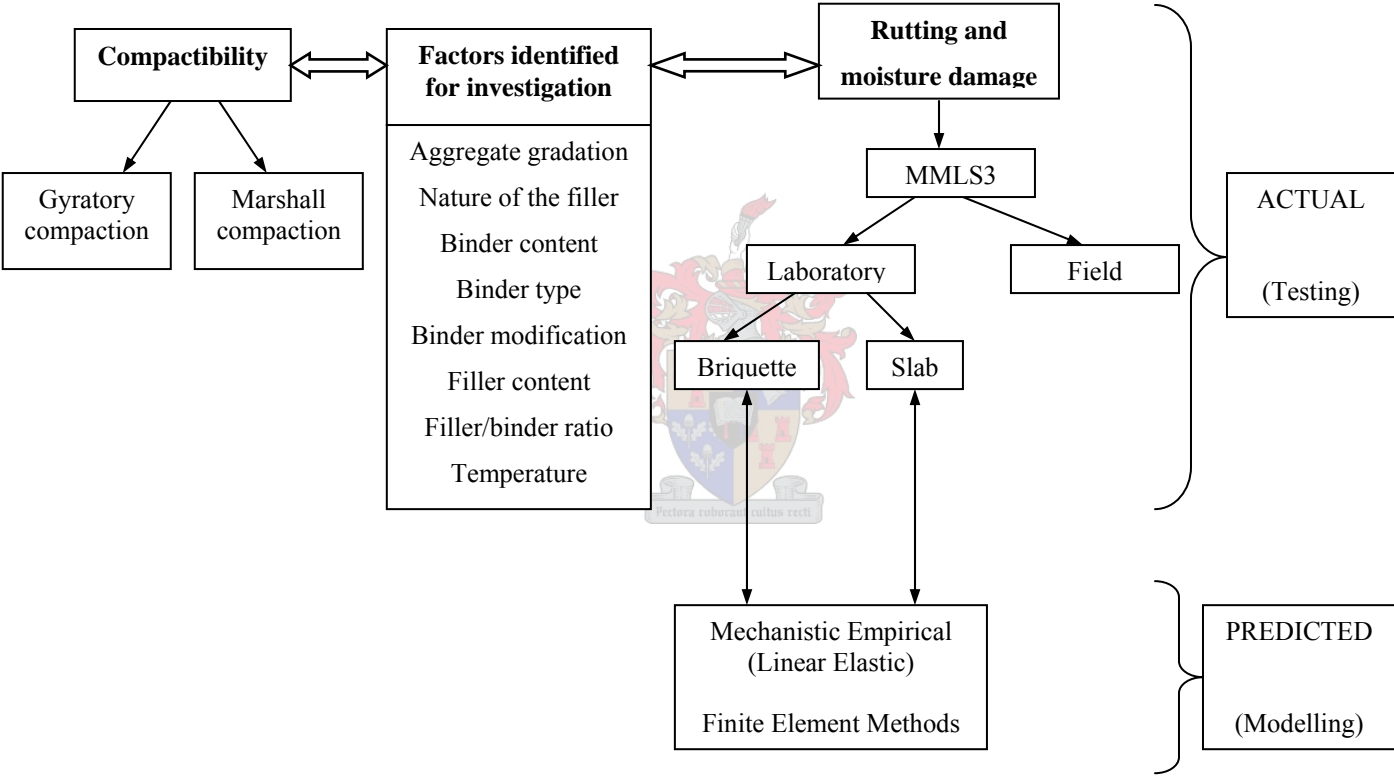


Figure 1-1: Scope of the study

## 1.4 Outline

Chapter 1 gives the background to the study. The objectives, scope and experimental methodology are outlined.

Chapter 2 reports the findings of a literature study into HMA compaction and compactibility, permanent deformation and moisture susceptibility.

Chapter 3 reports the test results of the various factors affecting the compactibility of HMA.

Chapter 4 describes the influence of compactibility on pavement performance, in terms of pavement rutting and moisture damage using the MMLS3 as APT tool.

Chapter 5 reports findings on relating laboratory rutting performance to field performance.

Chapter 6 comprises the conclusions and recommendations of the study.



## 1.5 Methodology

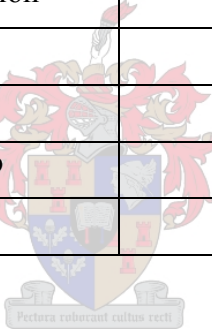
A summary of the factors influencing compactibility and rutting and the related number of variables that were investigated is presented in Table 1-1.

The methodology consisting of sample preparation, test set up, data collection and measurement, APT in the laboratory and field, mechanical testing, volumetric evaluation and comparative analyses is illustrated in Figure 1-2.

All the specimens for the compactibility studies were primarily compacted using the SGC with some correlation with Marshall compaction. The compaction temperature varied between 135 °C and 150 °C, depending on the type of binder used.

**Table 1-1: Factors evaluated in Compaction and Rutting studies**

<b>COMPACTION</b>	
<b>Factor</b>	<b>Number of variables</b>
Aggregate gradation	6
Filler type	4
Filler content	2
Binder type	3
Binder content	3
Filler/binder ratio	4
Compaction temperature	2
<b>RUTTING</b>	
<b>Factor</b>	<b>Number of variables</b>
Aggregate type	3
Aggregate gradation	4
Binder type	3
Binder content	4
Filler/binder ratio	5
Air voids	2



Filler/binder mastics were made at different percentages of percent bulk volume of filler. The mixing of the filler and binder consisted of preheating fillers in an oven at 140 – 150 °C and adding them gradually to fluid bitumen in the same temperatures range. Softening point tests were done to in order to characterise the stiffening effect of the filler on the binder.

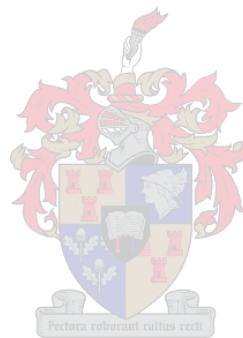
MMLS3 test specimens were generally compacted to approximately 7 percent VIM. All the MMLS3 tests were run up to a maximum number of MMLS3 axles of between 100 000 and 250 000 axles. Temperature measurements were recorded during MMLS3 trafficking and rutting profiles were measured after specific intervals.

Mechanical testing included dynamic creep, indirect tensile strength and stiffness tests in the indirect tensile mode to evaluate the performance properties of some of the mixes. This was done to establish whether the mixes satisfy the respective criteria typically established for

wearing course mixes. Indirect tensile fatigue and SASW testing were also performed on wet trafficked specimens to gauge the relative damage caused by wet trafficking.

The influence of test mode was evaluated. This was done by analysing the difference in stress distribution between slabs and briquettes. ABAQUS and ELSYM5 were utilised to estimate the stress distribution. Rutting models were used to predict the expected difference in rutting between the slab and briquette specimens. Comparisons were also made between laboratory and field rutting results.

The author was primarily involved in all of the research reported in this study and where it is not the case, it will be referenced accordingly.



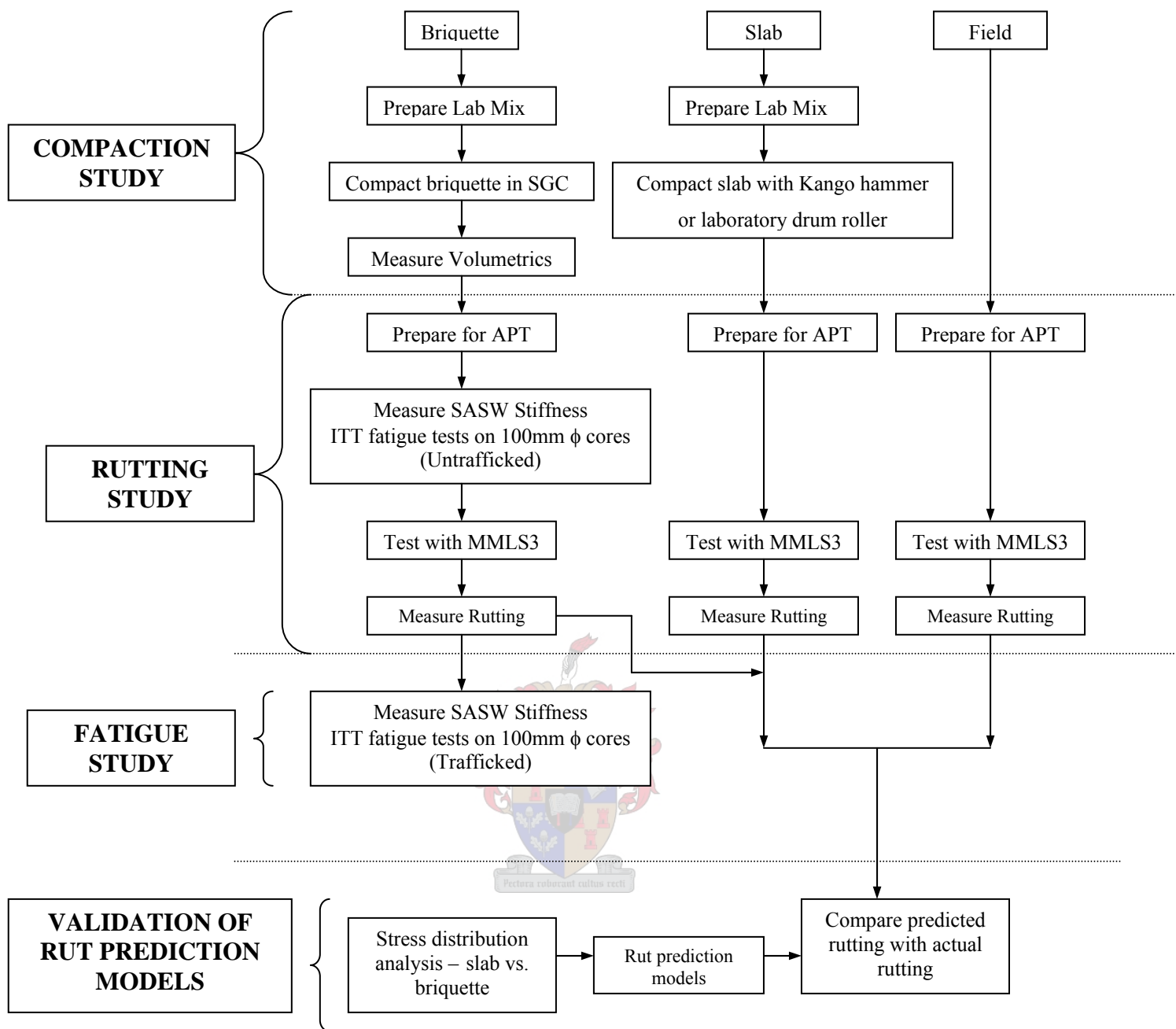


**Figure 1-2: Methodology of the study**

## 2 LITERATURE REVIEW

### 2.1 Scope of this chapter

This chapter presents a literature review pertaining to:

- Compaction and compactibility
- Permanent deformation
- Moisture susceptibility, and
- Polymer modification

### 2.2 Compaction and compactibility

The quality of HMA pavement layers depends on a number of factors including mix designs, nature and condition of the underlying layers, production and construction. If all these factors are satisfactorily dealt with, the pavement should perform well and ensure adequate comfort to the road users

An asphalt mix may be well designed and well produced, but when that mix is not properly compacted in the field, the pavement performance will be poor. This could also mean that a poorly designed mix that is properly compacted may perform better than a well-designed mix, which is not properly compacted to the desired density. Failure to achieve the desired compaction will result in, amongst others reduced pavement stiffness, reduced fatigue life, reduced resistance to rutting and increased permeability and subsequent risk of moisture damage. For the abovementioned reasons, various researchers regard the degree of HMA compaction as the single most important factor that affects the ultimate performance of that pavement under traffic loading.

Roberts *et al* (1991) define **compaction** as “*the process by which the volume of air in an asphalt mixture is reduced by the application of external forces*”. These external forces are in the form of pressure, initially from the screed of the paver and subsequently from the rollers (Hunter *et al*, 2000). The expulsion of air enables the mix to occupy a smaller space thereby increasing the density. The compacted mixture should have sufficient voids to allow the binder to expand and contract as temperature changes without filling the voids resulting in flushing.

Hunter *et al* (2000) define **compactibility** as “a concept related to the ease with which a material can be compacted”. It is normally expressed in relative terms. All materials have an optimum void content. A material with a high compactibility requires less compaction to achieve those desired voids content. In this thesis this material will be HMA.

### 2.2.1 Mechanics of compaction

To achieve effective compaction, the compactive forces exerted by the roller must exceed the forces resisting compaction within the asphalt mixture (Roberts *et al*, 1991). The mixture’s resistance is a result of the combined effect of the aggregate and the bituminous binder, which fills the voids between the aggregates. Asphalt compaction can be related to the mechanics of soil compaction (Robert *et al*, 1991; De Sombre *et al*, 1998). Densification of a soil or a particle medium can occur in three different ways:

- Reorientation of particles
- Fracture of the grains or bonds between them
- Bending or distortion of particles and their absorbed layers

The shear strength of the material must be overcome in order to compact the material. Coulomb’s equation can be used to define the shear strength:

$$\tau = c + \sigma \tan \phi$$

**Equation 2-1**

where

$\tau$	= shear stress
$c$	= cohesion
$\sigma$	= confining pressure
$\phi$	= angle of internal friction

During compaction, an asphalt mixture may be considered as behaving somewhere between a cohesive and non-cohesive soil. Compaction is accomplished by distortion and reorientation of particles much like a cohesive soil. As the binder content increases, the cohesion decreases, making the mixture easier to compact. An asphalt mixture also behaves similarly to a non-cohesive soil in that the friction between the aggregate particles resists the reorientation of the particles. The less angular the aggregate, the easier the mixture is to compact. Since asphalt mixtures behave much like soils, Coulomb’s equation can also be used to quantify the amount of shear stress in an asphalt mixture (De Sombre *et al*, 1998).

With asphalt, the amount and nature of the binder and filler used, and the temperature of the mix influence the cohesion of the mix. Compaction temperatures are high, thus giving low cohesion. As temperature decreases, so cohesion increases. The angle of internal friction is influenced by the binder content, temperature and the aggregate properties. Optimum compaction with the minimum effort can be achieved by minimising the cohesion and angle of internal friction; thus minimising the shear strength. This can be achieved by increasing the binder content in the mix to decrease the cohesion. More rounded particles and fewer angular particles, or an increased binder content can reduce the angle of internal friction. Changing these parameters may however change the mix properties, which may result in undesirable effects such as a loss of stability (De Sombre *et al*, 1998). Working in the proper temperature range will also reduce cohesion in the binder and interparticle friction by making the binder fluid enough to act as a lubricator while being stiff enough to resist shoving out from under the rollers.

### **2.2.2 Factors influencing compaction and compactibility of HMA**

Many factors influence the compaction and hence the compactibility of HMA. The Asphalt Institute (1980) categorised these factors into five classes, namely:

- 1) Material properties
  - a) Aggregate properties
  - b) Binder properties
- 2) Layer thickness
- 3) Mix temperature
- 4) Weather conditions, and
- 5) Compaction forces

Figure 2-1 illustrates the effects that some of these factors have on the compactibility of asphalt mixes.

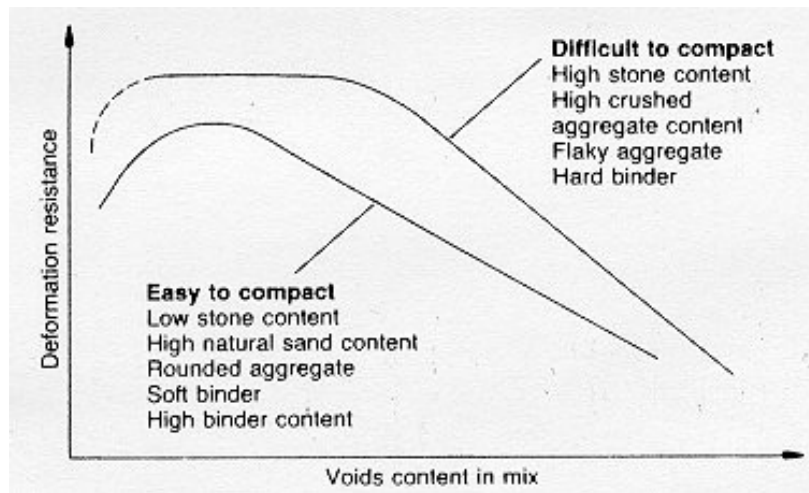


**Figure 2-1: Variation in the compactibility of bituminous mixtures due to changes in composition (Hunter *et al*, 2000)**

### 2.2.3 Aggregate properties

Aggregate gradation is the distribution of particle sizes expressed as a percentage of the total mass. Gradation is determined by sieve analysis. Roberts *et al* (1991) and Bahia *et al* (1998) pointed out that the aggregate gradation plays a significant role in the densification and performance of asphalt mixtures by affecting almost all the most important properties of HMA, including:

- 1) Stiffness
- 2) Stability
- 3) Durability
- 4) Permeability
- 5) Workability
- 6) Fatigue resistance
- 7) Skid resistance, and
- 8) Resistance to moisture damage

A continuously graded aggregate, from coarse to fine, may be easier to compact than a mixture with any other aggregate gradation. A harsh mix typically requires a significant increase in compactive effort to obtain the desired level of density. An over-sanded or finely graded mix, on the other hand, tends to be extremely workable. Because of the inherent tender nature of such an over-sanded mix, it might still be difficult to achieve proper compaction on such a mix.

Three properties of the coarse aggregate particles used in an asphalt mixture that can affect the ability to obtain the proper level of density include (USACE, 1991):

- 1) The particle shape of the aggregate
- 2) The number of fractured faces (angularity), and
- 3) The surface texture

A cubical or block-shaped aggregate needs a greater compactive effort than a rounded particle shape to achieve a certain degree of compaction. Aggregates with a rough surface texture are harder to compact than aggregates with a smooth surface texture. As the nominal maximum size of the aggregate increases, and as the hardness of the aggregate increases, the compactive effort needed to obtain a specific level of density also increases. Mixes that contains an excess of midsize fine aggregate (between 0.6 and 0.3 mm sieves) also are difficult to compact because of their lack of internal cohesion, they tend to displace laterally rather than compress vertically. Tayebali *et al* (1996) concluded that mixtures containing 100 percent crushed fine aggregate are more difficult to place and compact than mixtures containing at least some percentage of natural fine aggregate.



#### **2.2.4 Binders**

Binder viscosity affects compaction greatly (Asphalt Institute, 1980). Viscosity depends on:

- Binder type
- Temperature
- Loading time i.e. speed and frequency of loading

High viscosity tends to hold back movement of aggregate particles when the mix is rolled. If the viscosity is too low, the particles move easily during compaction, but not enough cohesion develops to hold the particles in position once compaction is completed. While hot, the bitumen acts as a lubricant, overcoming the interparticle friction of the aggregate. Once the mix has cooled, the bitumen acts as a binder holding the aggregate particles together.

The grade and amount of binder used in the mix affects the ability to compact the mix (USACE, 1991). A higher viscosity or lower penetration binder will generally result in a stiffer mix at a given mix temperature and therefore require a greater compactive effort. This stiffness tendency, however, is affected by the temperature-viscosity relationship for each particular binder.

The degree of binder hardening that occurs during the manufacture of the mix also affects the compactibility (USACE, 1991). Different binders harden differently during the mixing process, and that hardening is related, in part, to the chemical properties of each binder and its temperature susceptibility. Higher manufacturing temperatures typically produce stiffer mixes.

The binder content of the mix also influences its compactibility (USACE, 1991). In general, a mix with too little binder may be stiff and require an increase in compactive effort, whereas a mix with too much binder may shove under roller compaction.

### 2.2.5 Fillers

Various researchers have reported on the stiffening effect of filler addition to bitumen. Kandhal (1981) refers to the dual role that mineral fillers play in asphalt mixtures.

- First, they are a part of the mineral aggregate – they fill the interstices and provide contact points between larger aggregate particles and, thereby strengthen the mixtures.
- Second, when mixed with bitumen, mineral fillers form a high-consistency binder or matrix, which cements larger aggregate particles together.

Craus *et al* (1978), Huscheck and Angst (1980), Anderson (1987), and Kavussi and Hicks (1997) emphasized the role that the filler plays in determining the properties and the behaviour of asphalt mixes. The filler contributes to different aspects of the mechanical properties of a mix, such as:

- Workability,
- Compaction characteristics,
- Stiffening and extending the binder, thus affecting mix stiffness,
- Moisture resistance,
- Ageing characteristics,
- Voids in the mix

This influence is more dependent upon the properties of the filler-binder mastic.

According to Anderson (1987), the voids in compacted filler will take on some minimum configuration. When binder is added to the filler, the binder must first fill the voids. Any binder within these voids is called *fixed binder* because it is fixed within the minimum void structure.

Binder in excess of the *fixed binder* is called *free binder* because it is free of the voids and is free to lubricate the filler particles. This *free binder* pushes the particles apart, lubricating the filler/binder mixture and thereby enhancing its fluidity. This is illustrated in Figure 2-2 where the free and fixed binder is defined. In the illustration, the term *asphalt* refers to *bitumen* or *binder* in the South African context.

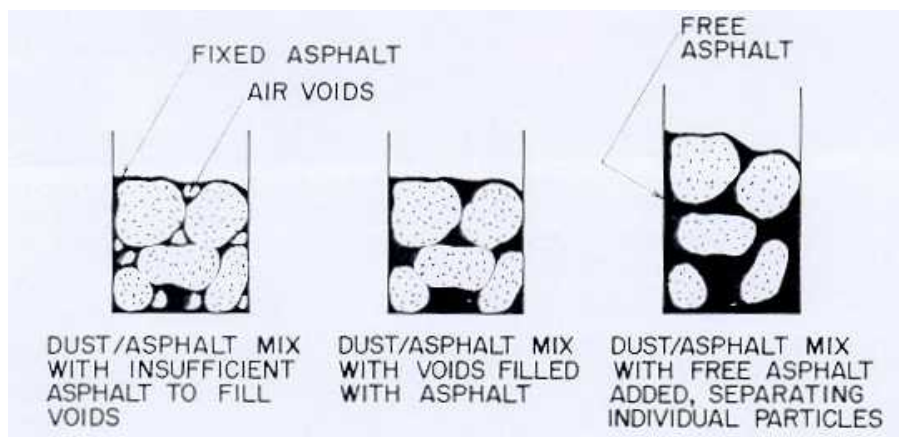


**Figure 2-2: Schematic Illustrating Fixed and Free Binder (Anderson, 1987)**

Tunncliffe (1967) concluded that the properties of the filler/binder mastic are controlled by the concentration of filler, or filler/binder ratio. He found that there is a definite increase in binder viscosity as the filler concentration increases and concluded that the shear resistance of such a mix will also increase. Kari (1967) found that there exists an optimum cohesion (as expressed by filler/binder ratio (by volume)) for maximum compaction under a roller. There is also a maximum filler/binder ratio at which maximum density is achieved.

Dukatz and Anderson (1980) stated that compaction and field performance of paving mixtures could be influenced by the type and concentration of filler. Kandhal (1981) and Cooley *et al* (1998) concluded that some fillers could have a considerable stiffening effect on the binder, while other fillers may not. This can make the mixture brittle and/or difficult to compact in the field (Kandhal, 1981). Thus, different fillers will stiffen a binder differently.

Many researchers used the void content in fines (generally called *Rigden voids*) compacted to maximum density to characterise the fines. The most common methods used to express the stiffening potential of a filler includes (Anderson *et al*, 1982; Cooley *et al*, 1998):

- 1) A stiffening ratio using kinematic viscosities of a filler/binder mastic and a neat binder,

- 2) Penetration values (25 °C) of a filler/binder mastic and a neat binder
- 3) The increase in the ring and ball softening point temperature due to the addition of fillers

The amount of filler in mastic can be defined in terms of percentage bulk volume of filler (Cooley *et al*, 1998):

$$\%V_{db} = \frac{V_{db}}{V_a + V_{ds}} \cdot 100$$

**Equation 2-2**

where:

- $\%V_{db}$  = Percent bulk volume of filler
- $V_{db}$  = Bulk volume of compacted filler
- $V_a$  = Volume of binder
- $V_{ds}$  = Volume of dust particles

These parameters used to describe filler/bitumen systems are shown in Figure 2-3.

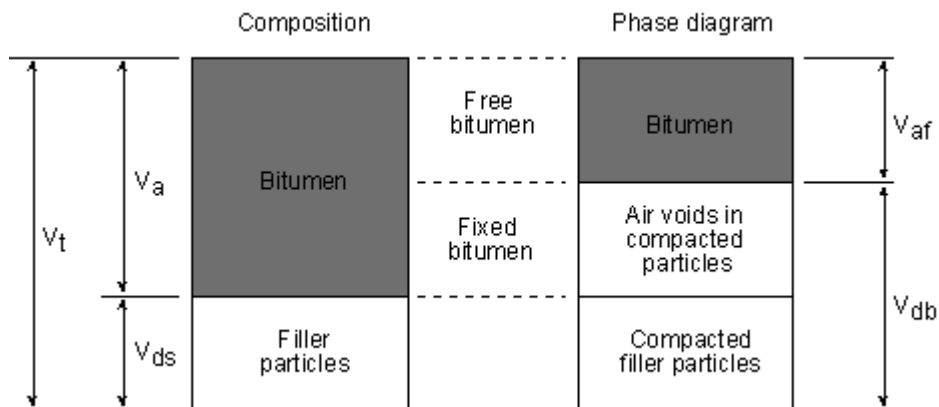


**Figure 2-3: Parameters to describe voids in filler/binder mortar (Cooley *et al*, 1998)**

Cooley *et al* (1998) tested a variety of filler/binder systems and found the relationship shown in Figure 2-4. They selected a limiting value of bulk volume of filler of 55 percent based on tests

at both high service temperatures (softening point) and mixing, transport and compaction temperatures.

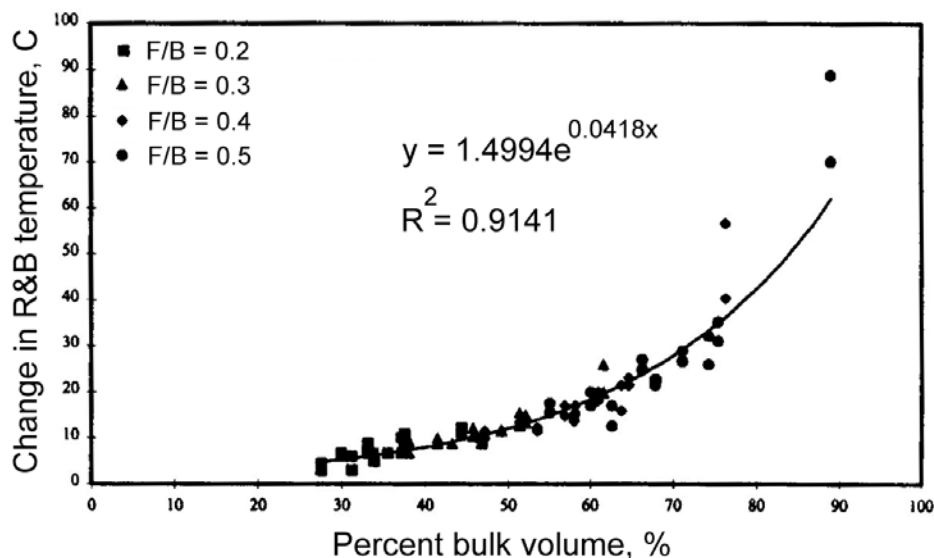


**Figure 2-4: Relationship indicating stiffening of filler/binder mastic (Cooley *et al*, 1998)**

Anderson *et al* (1982) concluded that the stiffening that occurs in filler/binder mastics is more apparent in the softening point test results than in viscosity or penetration results. Huschek and Angst (1980), Kandhal (1981) and Cooley *et al* (1998) related the stiffening potential of filler in a filler-binder system (mastic) to the volumetric properties of dry-compacted fillers. They also used the Rigden’s voids test to establish limiting criteria for a filler-binder mastic. The property used for the criteria was the percent bulk volume of filler. Kandhal (1981) found that considerable stiffening occurs at a 60 percent bulk volume and suggested a limiting value of 50 percent bulk volume. He also suggested a limit on changes in softening point temperature of 11.5 °C. Values above this may result in mastics that are too stiff. These stiff mastics in HMA may require “higher mixing and compaction temperatures, prompt rolling, etc.” The concept of using bulk volume concentration of fines appears good because it is regulated by four basic properties of fines (Kandhal, 1981):

- Particle shape,
- Particle size,
- Particle size distribution, and
- Particle surface texture

Huschek and Angst (1980) used the tensile strength and elongation at rupture of filler-binder mastics at a temperature of  $-15\text{ }^{\circ}\text{C}$  to conclude that the tensile strength of HMA reaches a maximum at a percent bulk volume of 60. This value agreed with the 60 percent value obtained by Kandhal (1981). Roberts *et al* (1991) stated that the filler-bitumen factor is quite important for compaction, as it affects the mass viscosity of the matrix that surrounds the coarse aggregate particles. Using the change in height during laboratory compaction (kneading compaction) as a measure of compactibility, Dukatz and Anderson (1980) found that the amount and type of mineral filler might, in some instances, cause compaction problems by stiffening mixtures.

Results from these studies illustrate that the volumetric properties of dry compacted fillers can be used to determine the stiffening potential of a specific filler to a binder. It is also apparent that too high a filler content may stiffen the mix, which may compromise the workability and compactibility. Also, there is an optimum filler-binder ratio for optimum cohesion and maximum density.

### **2.2.6 Temperature**

Mix temperature is a principal factor affecting compaction (Asphalt Institute, 1980). The critical mix temperature is the temperature at the time of compaction. This should determine the temperature at which the plant is producing the mixture. The mixing temperature is as important as the compaction temperature to ensure proper coating of the aggregate. Compaction can only occur while the binder is fluid enough to act as a lubricant. The workability of an asphalt mix is also affected by the temperature susceptibility of the binder (USACE, 1991). For a highly temperature-susceptible binder, less time will be available for compaction because the mix will change stiffness more quickly with a change in temperature than will a mix containing a less temperature-susceptible binder.

De Sombre *et al* (1998) stated that problems with field compaction of pavements might occur because of a lack of control over the beginning and ending compaction temperatures. Hunter *et al* (2000) also reported that an increase in temperature increases the compactibility of an asphalt mix. At relatively high temperature, the binder is sufficiently fluid to act as a lubricant between aggregate particles, reducing the internal friction of the mixture and assisting in achieving good aggregate interlock. Hunter *et al* (2000) therefore suggest raising the specified delivery temperature of the mix to solve compaction difficulties. However, the temperature at

any stage should not be higher than those specified for a particular binder, because it may lead to ageing which will result in a stiffer mix than expected. Figure 2-5 illustrates the effect of temperature on compactibility of a particular mix. Observing Figure 2-6, it can be seen that optimum temperature and viscosity ranges exist for optimum compaction. Too high temperatures will result in mixes that are too workable and when the temperatures are too low, than the mix will be too stiff to compact. It is therefore important to remain in this optimum temperature range to achieve proper compaction.

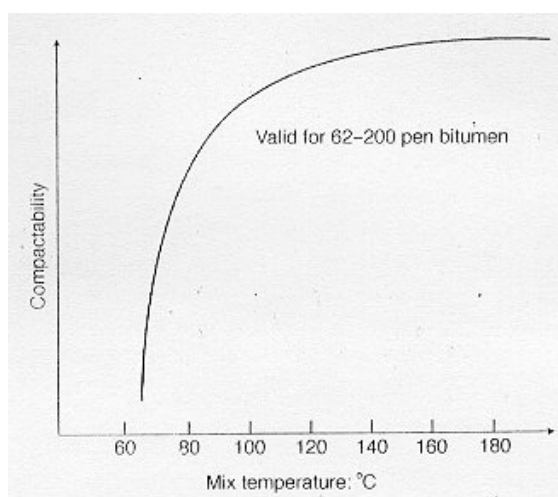


**Figure 2-5: Effect of temperature on the compactibility of bituminous mixtures (Hunter *et al*, 2000)**

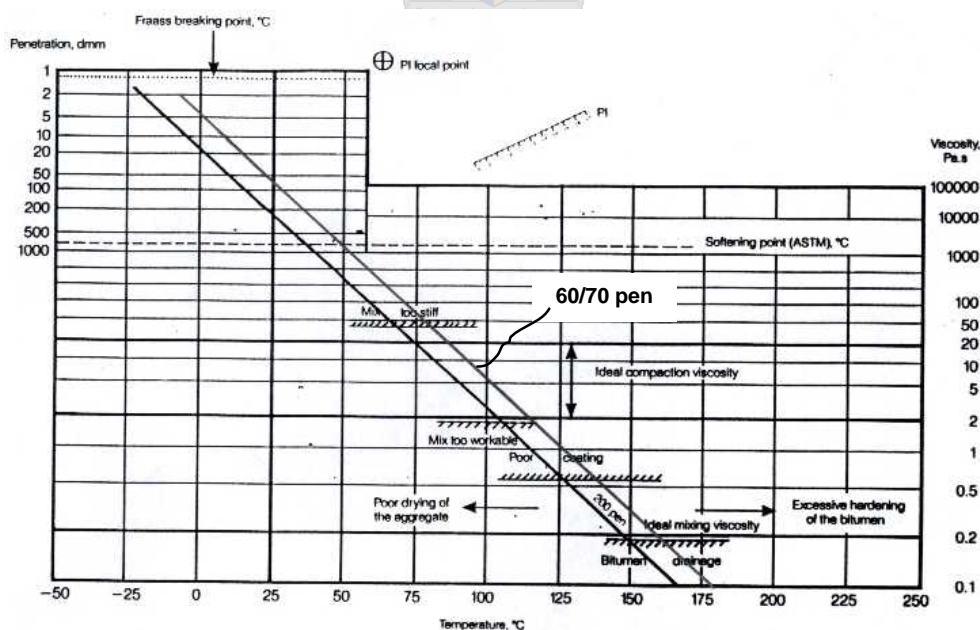


**Figure 2-6: Bitumen test data chart showing ‘ideal’ viscosities for optimal mixing and compaction (after Shell, 1991)**

## **2.2.7 Compaction methods**

The purpose of laboratory compaction is to simulate, as closely as possible, the degree of density produced in the field by the rollers and the density of the mix after some time under traffic. Laboratory compaction methods differ from field compaction methods and this results in differences in compaction.

### **2.2.7.1 Laboratory compaction methods**

Different laboratory compaction methods are being used. This includes the Marshall hammer, Gyratory Compactor, kneading compactor and rolling wheel compactor (NAPA, 1997). Most frequently used in South Africa is the Marshall hammer. The Superpave Gyratory Compactor is also used, but to a lesser extent.

For the Marshall hammer, the optimum binder content is a function of the amount of compactive effort used to densify the mix. Typically, two different compactive efforts (50 blows per side and 75 blows per side) are used in the laboratory to simulate the amount of compaction that will take place under both the rollers at the time of construction and under traffic with time. Because the Marshall hammer compacts by impact, it is believed that it does not simulate field compaction (Hughes *et al*, 1989). Its advantages are practical features such as convenience, portability, etc. Even though the Marshall hammer is the most often used, it has been found to have the least correlation with field roller compaction (NAPA, 1997).

The gyratory compactor simulates the kneading action of rollers used to compact asphalt pavements by applying a vertical load to an asphalt mixture while gyrating a mould tilted at a specified angle (refer Section 3.3.2.3). According Button *et al* (1994), gyratory compaction most often reproduce specimens similar to pavement cores. Button *et al* (1994) studied the correlation of laboratory compaction to field compaction and found that although the air void distribution of gyratory compacted specimens may be less similar to pavement cores than rolling wheel compacted specimens; this difference did not adversely affect the mix properties measured for their study.

### **2.2.7.2 Field compaction methods**

There are three basic types of rollers used for field compaction: the static steel wheel roller, the rubber tyre or pneumatic roller, and the vibratory roller. Only the most important features of rollers related to field compaction will be discussed here. For more detail, the reader is referred publications of the Asphalt Institute (1978, 1980), Kennedy *et al* (1984), Hughes *et al* (1989) Sabita (1992) and Hunter *et al* (1995).

#### **2.2.7.2.1 Steel wheel rollers**

Steel wheel rollers compact the asphalt with a compressive force. The total force that the roller applies is a function of the total load applied over the contact area, known as the contact pressure. The total load applied is a function of the weight of the roller and the rotational force provided by the wheels.

As the roller compacts the asphalt, the contact pressure increases and the contact area decreases. The contact pressure is dependent on the depth of penetration of the roller into the asphalt. The greater the depth of penetration, the greater the contact area and thus the lower the contact pressure. This means that on the first pass, the roller “sinks” into the asphalt, and the area of contact between the steel drum and the asphalt is large. As the roller makes additional passes, the asphalt becomes more resistant to the compressive force and begins to support the roller. The depth of penetration decreases, the total area of contact between the roller and the asphalt decreases, and the contact pressure increases. Thus, the compactive effort obtained by the roller is decreased.

Steel wheel rollers with larger diameter drums penetrate into the asphalt to a lesser degree than rollers with smaller diameter drums since the contact area is much larger. In other words, larger diameter drums are supported to a greater degree than smaller diameter drums since the force imparted by the drum is spread out over greater contact arc. A reduction in the total depth of penetration of the roller into the asphalt reduces the horizontal resistance to which the roller is subject on the first few passes. Reducing the horizontal resistance maximizes the downward force while minimizing the horizontal force. The horizontal force, when excessive, can result in the appearance of waves in front of the roller drum.

### **2.2.7.2.2 Pneumatic Rollers**

Pneumatic rollers use inflated rubber tyres instead of steel wheels to apply a compressive force to the asphalt. The total compactive force provided by a pneumatic roller is function of wheel load, depth of penetration, and the characteristics of the rubber tyres, including tyre pressure, tyre diameter, and the ply rating.

All of the tyres should be the same size, ply and tyre pressure. The area of each tyre footprint and the wheel load of the roller are the primary factors in judging the effectiveness of a pneumatic roller. The greater the contact pressure between the tyre and the asphalt, the greater the compactive effort applied by the roller. Low pressure results in bulging of the tyres with little effect on the asphalt; whilst high pressure results in excessive mix displacement. The action of multiple tires also promotes a “kneading” effect in the asphalt.

### **2.2.7.2.3 Vibratory Rollers**

Vibratory rollers use a combination of static force (similar to steel wheel rollers) and dynamic force to compact the asphalt. The static force is determined by the weight of the rolls and frame and the dynamic force is determined by the frequency and amplitude of vibrations. Conditions in the field as well as properties of the mixture will influence the decision to use higher or lower amplitudes. Table 2-1 describes some of the circumstances that would affect the decision to use high or low amplitude settings.

Frequency is the rate at which the drum impacts the pavement in a downward motion. Higher amplitude settings produce higher energy impacts, while low amplitude settings produce lower energy impacts. High frequency settings increase the number of impacts within a given time. An increase in the applied amplitude of vibration increases the compactive effort applied to the pavement.

The impact spacing is a function of the frequency of vibration and the travel speed of the roller. A decrease in frequency and an increase in roller speed both serve to increase the distance between impacts. Conversely, an increase in frequency and a decrease in roller speed both cause an increase in the impact spacing, thereby increasing the compactive effort applied by the roller.

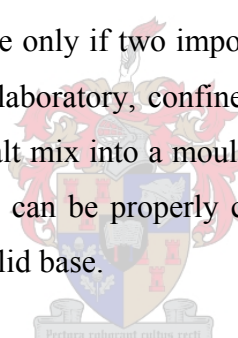
**Table 2-1: Guidelines for selecting the amplitude of vibration (after Kennedy *et al*, 1984)**

Lower Amplitudes	Parameter Level	PARAMETER	Parameter Level	Higher Amplitudes
	Thin* < 50mm	Mat Thickness	Thick > 50mm	
	Rigid	Base Support	Flexible	
	Low	Binder Viscosity	High	
	Rounded	Aggregate	Angular	
	Smooth	Aggregate Surface Texture	Rough	
	Poorly graded	Aggregate Gradation	Dense	
	High	Temperature (Mix, Base or Air)	Low	

\* For very thin layers, especially on rigid base supports, vibration is not recommended, to avoid fracturing aggregate

#### **2.2.7.2.4 Laboratory and field compaction conditions**

Compaction of a pavement is possible only if two important conditions exist, i.e. confinement and correct mix temperature. In the laboratory, confinement occurs in the laboratory when a ram or hammer compresses the asphalt mix into a mould. The mould and ram confine the mix from every direction so that the mix can be properly compacted. Also, in the laboratory the asphalt mix is compacted against a solid base.



When compacting in the field, confinement from the bottom comes from the base, which means that the base must be stable. A wide variety of base types and stiffnesses are encountered in the field. The ability to obtain a particular density level depends in part on the rigidity of the base and on the type of rollers used. The rollers provide confinement from the top and confinement from the sides comes internally from the surrounding mix being compacted. This surrounding mix must resist flow and shoving. The mix's ability to resist flow is important for confinement and is affected by aggregate friction and binder temperature. The differences between some pavement base conditions and laboratory base conditions can be significant (USACE, 1991).

Laboratory compaction does not take very long, usually within 2 or 3 minutes. This is in direct contrast to actual roller operations in the field, which use an infinite variety of roller combinations, roller passes, and roller patterns and in which final density levels might not be obtained until 30 minutes or longer after the mix is placed by the paver. Also, during the

laboratory compaction process, the mix temperature is relatively constant. On the pavement, the temperature of the mix is continually decreasing with time. In the laboratory, the compaction is usually applied before the mix temperature drops to 115 or 105 °C. in the field, the mix may cool down to 80 °C or less before the compaction process is completed.

### ***2.2.8 Other factors influencing compaction***

Other factors related to compaction in the field include:

- The air and base temperature
- Wind speed, and
- Solar radiation
- The surface texture of the underlying layer
- Whether a tack coat has been applied

All other factors being equal, the lower the ambient air temperature, the faster the hot mix cools off (Asphalt Institute, 1980; USACE, 1991). Consequently, less time are available for proper compaction. Base temperature is actually more important than air temperature in determining the time available for compaction. It is often assumed that air and base temperature are the same. This is not necessarily true, particularly in cool weather. A moist base layer significantly increases the cooling rate of the hot mix (USACE, 1991). The wind is also a major factor affecting compaction. The stronger the wind, the faster the mix cools, especially in cold weather.

As the temperature of the ambient air and existing pavement surface increases, the time for the mix to cool down also increases. The temperature of the ambient air and base surface are important, but not nearly as crucial as the layer thickness in determining the time available for compaction. Thicker layers of HMA allow more time to achieve proper densities than thinner layers. The effect of the mix temperature is more significant at thinner layers and lower base temperatures. The amount of solar flux is more important in its effect on base temperature than its effect on mix temperature. The base temperature will be higher on a sunny day, for a particular ambient air temperature, than it will be on a day with heavy cloud cover. This higher base temperature will reduce the rate of cooling of the mix and increase the time available for compaction.

SABITA Manual 22 (Sabita, 2000) has more information on how to deal with paving and compaction in adverse weather conditions. Figure 2-7 is just one of the useful guidelines contained in this manual.

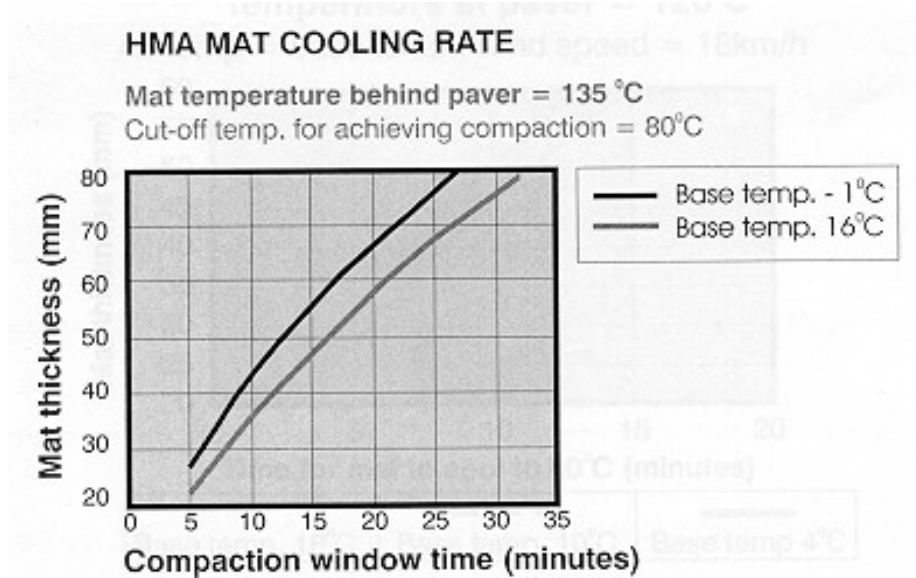


Figure 2-7: Some factors affecting HMA compaction in the field (Sabita, 2000)

### 2.2.9 Factors affecting HMA volumetrics

A basic understanding of mass-volume relationships of compacted asphalt is important from both a mix design and a construction viewpoint. Mix design is a volumetric process with the purpose of determining the volume of bitumen and aggregates required to produce a mix with the desired properties. However, measurements in the laboratory or field of the volume of aggregates and bitumen are very difficult and impractical. Therefore, to simplify the measurement problem, masses are used instead of volume, and the relative density is used to convert from mass to volume. The component diagram in Figure 2-8 is an example of a spatial model. (In this diagram, the term “asphalt” refers to “bitumen”). From this component diagram it is clear that when converting the total mass of aggregate to volume, the differences in densities of the coarse aggregate, fine aggregate and filler have to be taken into account. The reader is also referred to Van de Ven *et al* (1999) for a comprehensive discussion on spatial composition.



Figure 2-9 demonstrates how these parameters interact with variation in binder content for a certain compaction level. From this figure it is evident that an increase in binder leads to a decrease in VMA. Also, the VMA decrease with an increase in binder content, up to a point. When the minimum VMA is reached, the VIM becomes overfilled with binder and the aggregates are forced apart. The binder acts as a lubricant between the aggregates and reduces point-to-point contact pressures. When the asphalt mix is further compacted by traffic, the loads are carried by the binder rather than the aggregate structure. This result in fewer voids and without the aggregate skeleton resisting the applied shear stresses, the mix develops large permanent shear strains, which leads to rutting and bleeding. When the air void level is low enough for the binder to prevent point-to-point contact in the aggregate structure, the mix loses its stability.

Since VMA includes air voids and the effective binder content, increasing the air voids in the compacted mixture will increase the VMA and allow more binder into the mix.

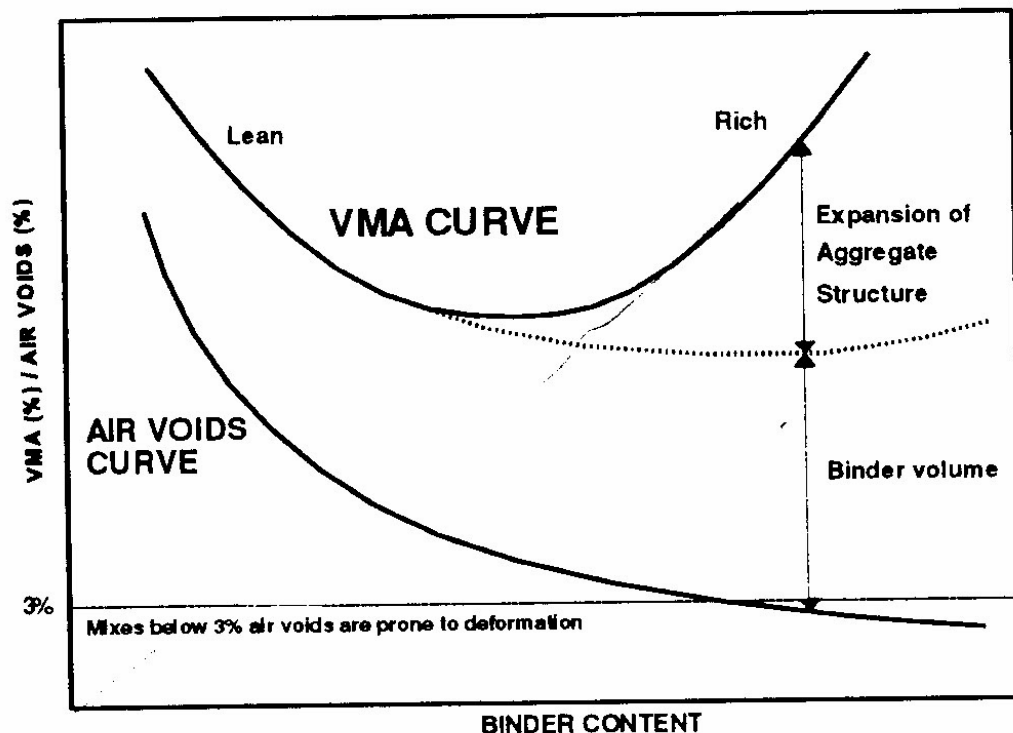


Figure 2-9: The effect of binder content on VMA, voids and volume of binder (Verhaeghe *et al*, 1995)

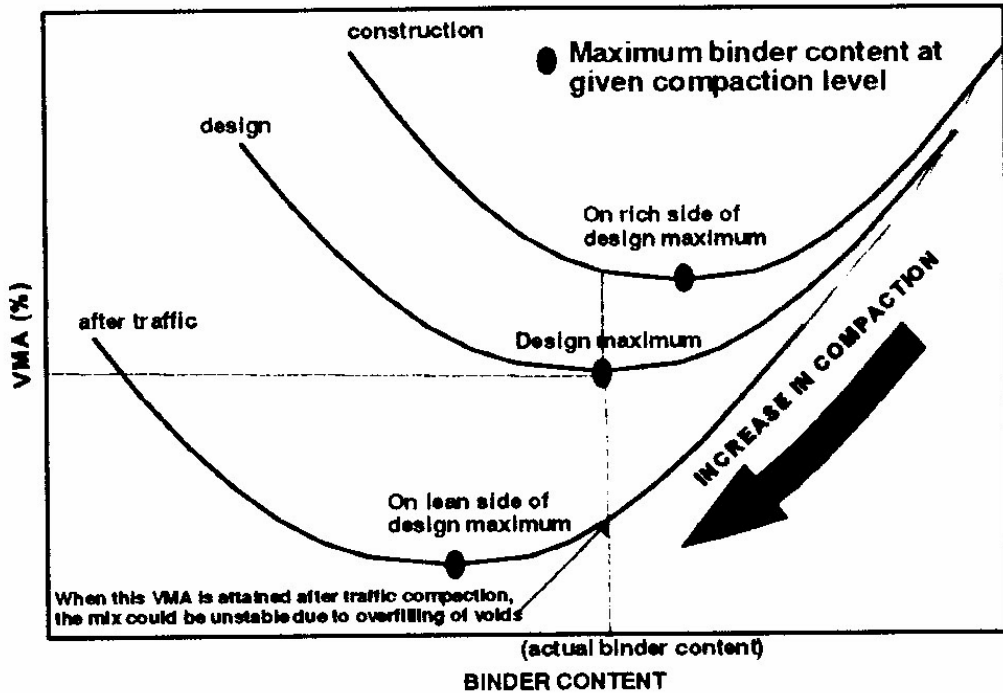


Figure 2-10: The effect of compaction energy on optimum binder content (Verhaeghe *et al*, 1995)

The extent to which an asphalt mixture can be compacted is related to aggregate gradation, aggregate surface characteristics, amount and type of binder, and binder absorption by the aggregate (Chadbourn *et al*, 2000). It can thus be seen that these properties will have an important influence on volumetric properties.

Aggregate gradation has a dominant effect on the volumetric properties of an HMA mix (NAPA, 1997). In particular, changes in the aggregate characteristics directly affect the VMA in the mix as well as the air void content. Chadbourn *et al* (2000) pointed out that the two factors relating to aggregate gradation having the most influence on VMA are density, or the ability of the aggregate particles to pack together, and the aggregate surface area.

Nijboer (1943) has indicated that maximum density mixes are obtained from gradations having a gradation exponent,  $n$ , of 0.45. It means that, in terms of volumetrics, these mixes will have the lowest air void content and the lowest VMA. Cooper *et al* (1985) found that a low VMA is a requirement for good resistance to permanent deformation. However, it is undesirable to design mixes which fall on the maximum density line in case these mixes have low VMA or

not enough space to allow sufficient bitumen for compaction and durability and may be prone to overfilling with trafficking. Deviating from the maximum density line in either the fine or the coarse direction (see Figure 2-11) will tend to increase the VMA of the compacted mix (Chadbourn *et al*, 2000).

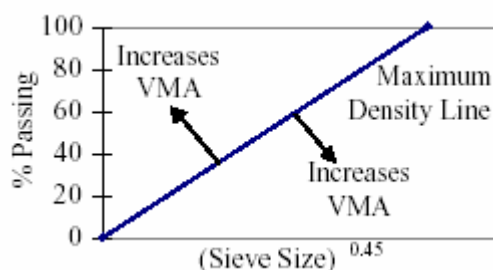
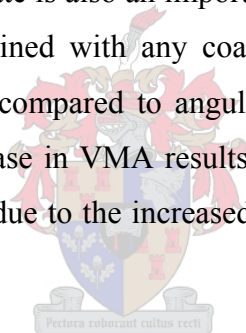


**Figure 2-11: Maximum Density Line Related to VMA (Chadbourn *et al*, 2000)**

The particle shape of the fine aggregate is also an important factor affecting the VMA (NAPA, 1997). Rounded, natural sand combined with any coarse aggregate material will generally result in a mix with a lower VMA compared to angular, manufactured sand with the same coarse aggregate material. The increase in VMA results from the angular aggregates creating more void space during compaction due to the increased number of sharp edges and fractured faces.



Rounded aggregate particles reduce the internal friction and result in a dense arrangement, consequently lowering the air void content and VMA. Aggregates with rough surface textures have a high level of internal friction, higher air void contents, and higher VMA (Chadbourn *et al*, 2000). Kandhal and Maqbool (1991) stated that although some absorption may lead to improved strength in a compacted mixture through particle adhesion, the portion of the binder that is absorbed is no longer available as binder. Therefore, aggregates with a large void volume and/or pore size will have a reduced effective binder content. This will lead to a decrease in VMA provided the air voids remain constant.

Changes in the VMA value in a HMA mix are typically not significantly affected by any properties of the binder (NAPA, 1997). Roberts *et al* (1991) reported that too much binder in the mix causes the loss of internal friction between aggregate particles and results in the loads being carried by the binder rather than the aggregate structure. The VFB are inversely related

to the air voids. As the percentage of air voids approaches zero, the percentage of VFB approaches 100. The asphalt mix is initially constructed to some percentage of VFB (usually 50 – 70 percent). This percentage of VFB increases as the asphalt mix continues to densify under traffic. When the VFB exceeds approximately 80 – 85 percent, the asphalt mix typically becomes unstable and rutting is likely to occur. Coree and Hislop (2000) found that two factors clearly stand out that differentiate sound from unsound mixtures are: a sufficient coating of binder ( $V_{bc}$ ) and not overly saturating the VMA with binder (VFB).

For a given binder content, a mix with low VMA may have a low air void content and have the potential to flush, bleed and/or rut under traffic. For mixes with the same binder content, the mix with a higher VMA may have a much higher air void content. If the air void contents are excessively high, the mix might have the tendency to ravel or disintegrate under service (NAPA, 1997). It is possible that the VMA, as well as VIM of a particular mix may increase by some degree if the aggregate is very absorptive and if the mix is kept in the surge or storage silo for a period of time at a high temperature (NAPA, 1997). However, for most aggregates used in HMA, this change in VMA is very small.

Chadbourn *et al* (2000) refer to a phenomenon called “*VMA collapse*”, which develops when the VMA after construction is significantly lower than the design VMA. This “*VMA collapse*” can be related to some durability related failures. Potential causes include:

- The generation of fines: – may be due to construction-related aggregate degradation, and can decrease VMA by increasing the surface area of the aggregate blend.
- High production temperatures and long storage or cure times: – can result in increased binder absorption into the aggregate relative to the mix design, making less binder available to coat the particles.

Establishing an adequate VMA during mix design and in the field will help establish adequate binder film thickness without excessive bleeding or flushing. In general, if an HMA has about the same binder film thickness from mix design to production, there will be little or no change in VMA (Chadbourn *et al*, 2000).

Minimum percentage contents of VMA are recommended by the Asphalt Institute to ensure that the mixture is neither deficient in binder nor air voids. There should be enough room in the aggregate structure to take sufficient binder for durability of the mixture while still leaving a sufficient volume of air voids to avoid problems with plastic deformation (rutting). Limits

placed on VFB, control the balance between the effective binder content, i.e. excluding binder absorbed into the pores of the aggregate, and air voids content.

## 2.3 Polymer modification

Increased truck volumes, increased truck loading and increased tyre pressures are the main reasons for the increase in rutting on HMA pavements (Kandhal *et al*, 1990). These increases over the years have increased the demands placed on the binders used in road construction. It has been found that unmodified binders have been less capable of satisfying all of the following requirements with regard to bituminous binders (Hunter *et al*, 2000):

- Sufficient flexibility to absorb traffic stresses and prevent fatigue cracking
- Sufficient cohesion to bind the materials together
- Sufficient adhesion to prevent mineral erosion
- A broad in-service temperature range

This identified the need to develop binders with a higher level of performance. Bitumen is a thermoplastic, viscoelastic material and therefore susceptible to the effects of temperature, loading stress and frequency. The most common method of reducing the temperature susceptibility of bitumen is by the addition of polymers. King *et al* (1986), Maccarrone *et al* (1995), Hunter *et al* (2000) and other researchers have reported on the following beneficial effects of polymer modification:

- Increase in softening point
- Decrease in penetration
- Suppression of the Fraass breaking point
- Increase in viscosity
- Improved deformation resistance
- Improved fatigue resistance
- Increased durability
- Increased binder adhesion, cohesion and elasticity.
- Improved flexibility, workability, ductility and toughness
- Reduces thermal cracking, fatigue damage and temperature susceptibility.

One can summarise that PMBs are used in an effort to reduce early pavement distress and to extend the service life of the pavement (King *et al*, 1986).

The increase in softening point means a greater rate of increase in stiffness on cooling with a consequent effect on ability to achieve effective compaction (AAPA, 1998). In practice, PMBs are often handled at marginally higher temperatures and viscosities than unmodified bitumen. However, Khatri *et al* (2001) warns against excessive heating, because it can cause damage to binders, particularly those containing additives. Many of the modified binders show significant shear dependency, which plays a major role in compaction.

The most common polymer modifiers can be classified into:

- Thermoplastic (Plastomer) modifiers
- Elastomer modifiers

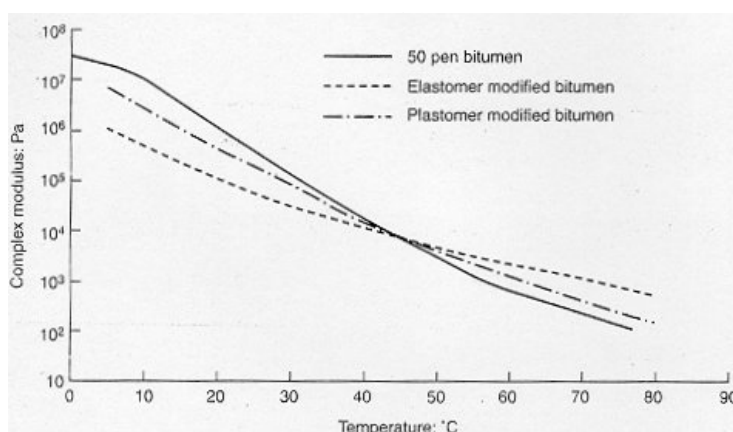


**Figure 2-12: The effect of polymer modification on rheology (Hunter *et al*, 2000)**

### 2.3.1 Plastomer modifiers

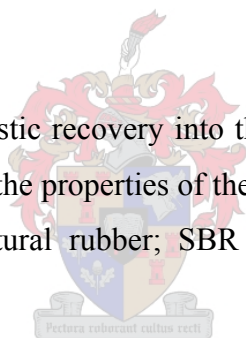
Thermoplastic polymers often referred to as plastomers, have a similar although less dramatic temperature susceptibility to bitumen in that they are hard at low temperature and fluid at high temperature. Plastomers tend to influence the penetration of the bitumen more than the softening point. The softening point increases as the concentration of the polymer in the bitumen rises until a maximum softening point is reached. Beyond this concentration there is no increase in the softening point even at significantly higher polymer contents.

King *et al* (1992) reported that binder related pavement failures are usually caused by one of the following problems: the binder is too low in stiffness at high temperatures to resist permanent deformation; the mixture is unable to withstand moisture related debonding of binder and aggregate; or the binder becomes too brittle at low temperatures to resist cracking caused by some combination of thermal stresses, repeated loading, low temperature physical hardening or oxidative ageing.

Among the plastomers most commonly used are ethylene vinyl acetate (EVA) .EVA was originally used to increase stiffness of HMA and hence improve its performance. However, an unexpected additional benefit of the modification was improved workability at low temperatures (Hunter *et al*, 2000). Plastomers also form a tougher; more rigid binder compared to elastomeric types, and are particularly used in asphalt to improve deformation resistance as well as for increased durability (AAPA, 1998).

### ***2.3.2 Elastomer modifiers***

Elastomeric modifiers introduced elastic recovery into the modified binder. It has been found to make significant improvements to the properties of the bitumen (Hunter *et al*, 2000). Among those most commonly used are natural rubber; SBR (Styrene-butadiene-rubber) and SBS (Styrene-butadiene-styrene).



A typical example of the use of a random elastomeric polymer is the inclusion of natural rubber latex in porous asphalt wearing course. The effect of the modification is primarily to increase the viscosity, minimise binder drainage and increase the bitumen film thickness on the aggregate. Increased durability is also noted.

With increased polymer concentration, the complex modulus ( $G^*$ ) increases while  $\tan \delta$  decreases. Therefore, with increasing polymer content, the binder and the mix will be more resistant to permanent deformation.

## 2.4 Permanent Deformation (Rutting) of HMA pavements

Permanent deformation is caused by the progressive movement of materials under repeated loads either in the asphalt pavement or the underlying base. This can occur either through consolidation or through plastic flow (Roberts *et al*, 1991). This deformation can be illustrated like in Figure 2-13.

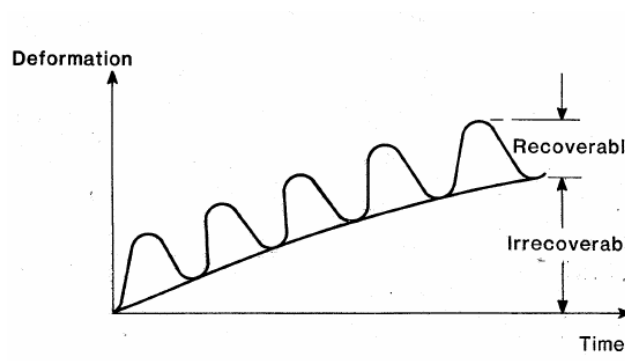


Figure 2-13: Asphalt response to repeated loading

Consolidation (Figure 2-14) is the further compaction of HMA pavement by traffic after construction. When compaction is poor, the channelised traffic provides a repeated kneading action in the wheel track areas and completes the consolidation to the design air voids. A substantial amount of rutting can occur if very thick asphalt layers are consolidated by the traffic.

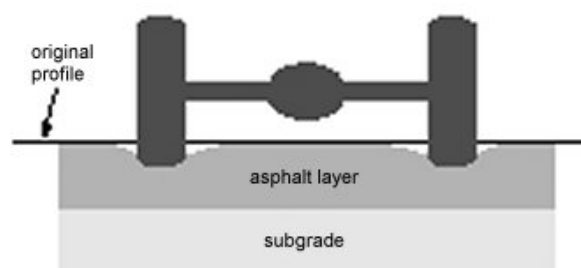
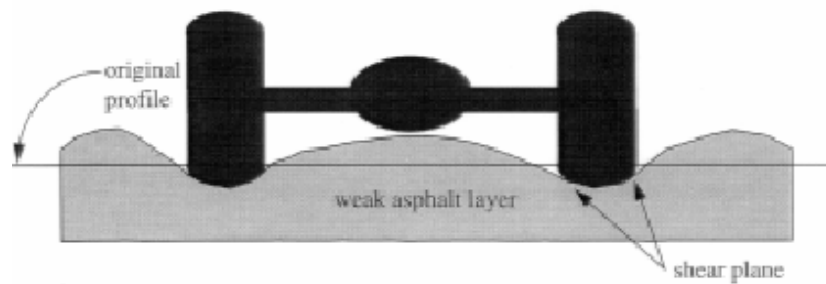


Figure 2-14: Consolidation in asphalt layer (FPCWV, 2000)

Rutting also results from lateral plastic flow (Figure 2-15) of the HMA from the wheel tracks. Use of excessive binder in the mix is the most common cause for this phenomenon (Santucci, 2001).



**Figure 2-15: Plastic flow in asphalt layer (Santucci, 2001)**

Rutting typically occurs during the summer months when pavement temperatures are high. Higher traffic volumes and higher tyre pressures have increased the potential for rutting in recent years (Cooley *et al*, 2000). Bissada (1983) found that in the case of heavy traffic conditions and high in-service pavement temperatures, a change of about 0.5 percent in the binder content will result in a drastic change in permanent deformation.

Sousa and Weissman (1994) concluded the following with regard to the effect of the number of wheel passes on a transverse surface profile:

- 1) In the initial stage of trafficking, the increase of irreversible deformation below the tyres is distinctly greater than the increase in the upheaval zones. In this initial phase, traffic compaction has an important influence on rutting.
- 2) After the initial stage, the volume decrement beneath the tyres is approximately equal to the volume increment in the adjacent upheaval zones. This is an indication that compaction under traffic is completed for the most part and that further rutting is caused essentially by displacement with constancy of volume. This phase is considered to be representative of the deformation behaviour for the greater part of the life of a pavement.

For properly compacted pavements, shear deformations, caused primarily by large shear stresses in the upper portions of the asphalt layer(s), are dominant (Sousa *et al*, 1991). Repetitive loading in shear is required in order to accurately measure, in the laboratory, the influence of mixture composition on resistance to permanent deformation. Because the rate at which permanent deformation accumulates increases rapidly with higher temperatures, laboratory testing must be conducted at temperatures simulating the highest levels expected in

the paving mixture in service. Bouldin *et al* (1994) pointed out that it is not only important to do rutting tests at realistic loading times but also to carry out the test at the highest expected pavement temperature to prevent premature rutting of the mix.

In the development of the rut depth it is also necessary to recognise the evolution of the void content in a pavement section (Sousa, 1994). When the air voids drop below two to three percent, the binder acts as a lubricant between the aggregates and reduces point-to-point contact pressures. Without the aggregate skeleton resisting the shear stresses that appear near the edge of the tyres, the mix rapidly develops large permanent shear strains, which, in turn, cause the development of the rut. As the mixture densifies, it steadily develops better aggregate interlock and resistance to shear stresses. The mix loses stability only when the reduction of the air void content causes the binder to prevent point-to-point contact in the aggregate. Sousa and Weissman (1994) also point out that as an asphalt mix ages, the binder stiffens and the elastic strains decrease and the permanent deformation accumulated at each load application decreases.

Bouldin *et al* (1994) explains the development of permanent deformation by means of a rut curve (Figure 2-16). In the initial range the material is considered to experience additional compaction and/or rearrangement of the aggregate skeleton. The relatively high local pressures results in the reorientation, which ultimately leads to an improved aggregate interlock. Consequently, the slope (or rut rate) reduces as the modulus of the mixture increases. In the second range, the linear range, the rate of deformation is slower. In some cases no significant linear range occurs because the material is very unstable or the loading conditions are so severe that it reaches the tertiary range before reaching a constant slope. The tertiary range (also sometimes referred to as the tertiary flow phase) is reached when the rut rate begins to increase again. In this range we observe large scale aggregate movements, which are accompanied by significant volumetric effects, i.e., the material exhibits dilatancy.

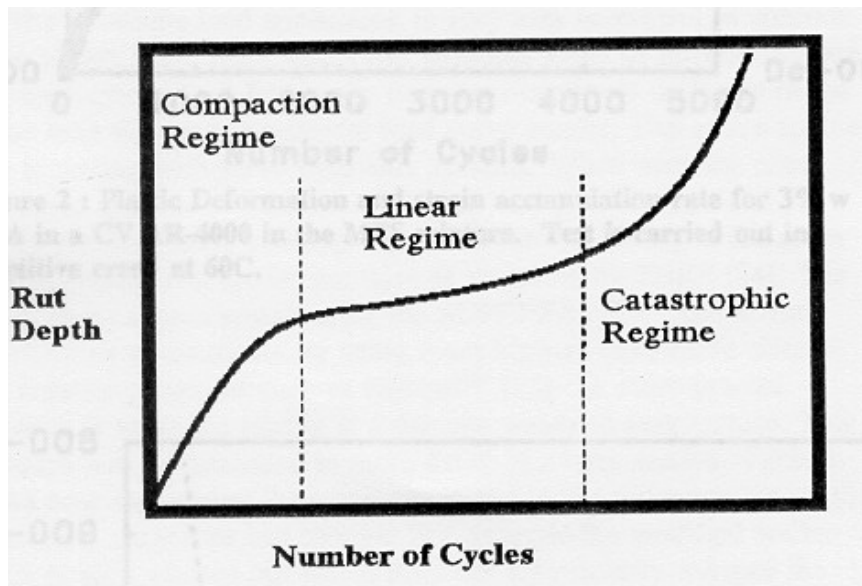


**Figure 2-16: Schematic Rut Curve (Bouldin *et al*, 1994)**

### **2.4.1 Factors influencing permanent deformation**

There are many factors influencing the permanent deformation of HMA pavements, however, Molenaar (2001) pointed out that the four most important factors are:

- The grading curve
- The binder content
- The degree of compaction, and
- The softening point of the binder



The gradation of aggregates is a very important property that determines the stability of a mix (Kandhal and Mallick, 1999). Mixes containing different aggregate gradations are likely to have different stability and different rutting potential. Mixes containing different aggregates, but with same gradation can show significantly different rutting potential. Apart from gradation and type of aggregate, the maximum size of aggregate is also believed to have significant effect on rutting potential. Cooper *et al* (1985) found that good resistance to permanent deformation requires a low VMA.

The rutting resistance of an asphalt mix depends on the shear resistance of that mix (Santucci, 2001). If the shear stress created by repeated wheel load applications exceeds the shear strength of the mix, then rutting will occur. Cubical, rough-textured aggregates are more resistant to the

shearing action of traffic than rounded, smooth-textured aggregates. Mixes containing natural aggregates (especially the natural river sands) are generally more susceptible to rutting, shoving and bleeding than mixtures containing 100 percent crushed fine aggregate (Tayebali *et al*, 1996).

Hesp *et al* (2001) reported the significant effect of filler particle size and gradation, fine aggregate angularity and aggregate gradation on the high temperature permanent deformation characteristics of an asphalt mixture. Tayebali *et al* (1996) reported that increasing the amount of mineral filler has beneficial effect on the rutting performance. However, although the rutting performance is enhanced, it should be noted that at higher mineral filler content, the binder content is reduced which may have a detrimental effect on other mixture properties such as fatigue, thermal cracking, and raveling. Roberts *et al* (1991) also warned against the use of excessive fines.

Santucci (2001) stated that the binder in the mix also affects the rut resistance but to a lesser degree than the aggregate characteristics. A mix made with a softer binder will be less resistant to rutting at high temperature than a comparable mix with a harder binder. On the WesTrack test track, the greatest amount of rutting has been associated with the high binder content mixtures (J. Epps *et al*, 1998).



Roberts *et al* (1991) stated that the consistency (penetration or viscosity) of the binder plays a relatively small role in the rut resistance of HMA if well graded, angular and rough textured aggregates are used. Huber and Heiman (1987) also reported that the penetration and viscosity of the binder do not demonstrate a significant effect on rutting rate. Bolk *et al* (1982) reported that, in general, the binder content is found to have a substantially greater effect than the filler content on the deformation resistance. The extent of the effect is, however, dependent on the type and nature of the filler. Smit (1995) found that the rutting performance of a pavement was apparently better at a lower than optimum binder content and increased with ageing of the asphalt.

Roberts *et al* (1991) reported that too much binder in the mix causes the loss of internal friction between aggregate particles and results in the loads being carried by the binder rather than the aggregate structure. When the VFB exceed approximately 80 – 85 percent, the asphalt mix typically becomes unstable and rutting is likely to occur. Goodrich (1991) argued that there

was little effect of the binder on the high temperature properties while Valkering *et al* (1990) and Bouldin and Collins (1992) had seen significant improvements in the rut resistance when using stiff or highly elastic binders when tested using wheel tracking devices.

Brown and Cross (1989) pointed low air voids in the laboratory compacted asphalt mixture as one of the best indicators of rutting. Bouldin *et al* (1994) also highlighted the pronounced effect of air voids on the rut resistance of an asphalt material. Various researchers stressed the importance of proper compaction to decrease the potential for rutting. Cross and Brown (1991) stated that in-place air voids above approximately three percent are needed to decrease the probability of premature rutting throughout the life of the pavement. Below this level, rutting is likely to occur due to plastic flow (Roberts *et al*, 1991). The air voids will also affect the rate of rutting (AAPA, 1999). Figure 2-17 gives an indication of relative rutting rate of a mix designed for five percent voids and compacted to different voids levels.

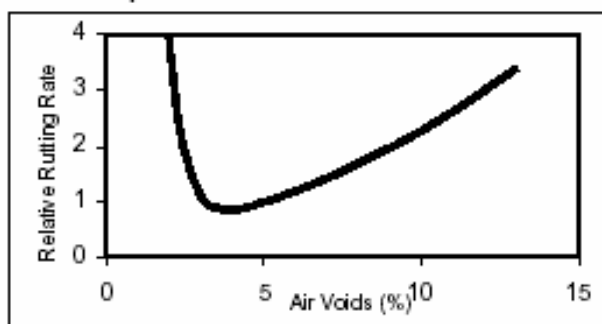


**Figure 2-17: Relative rutting rate vs. air voids (AAPA, 1999)**

An analysis of results from a full-scale pavement test track in Nevada (WesTrack) showed that a reduction in air void content improved the rut resistance of most asphalt pavement sections (J. Epps *et al*, 1999). Figure 2-18 illustrates the influence of air void content on the predicted number of equivalent single axle loads (ESALs) to a 10 mm rut depth.

Bitumen shows a lower modulus when measured at low frequency than it does at high frequency. This explains why asphalt pavements can be susceptible to permanent deformation when subjected to slow moving (i.e. low frequency) traffic (Hunter *et al* 2000) Although temperature has the greatest effect on the properties of the bitumen, it is also important to consider the effects of time.

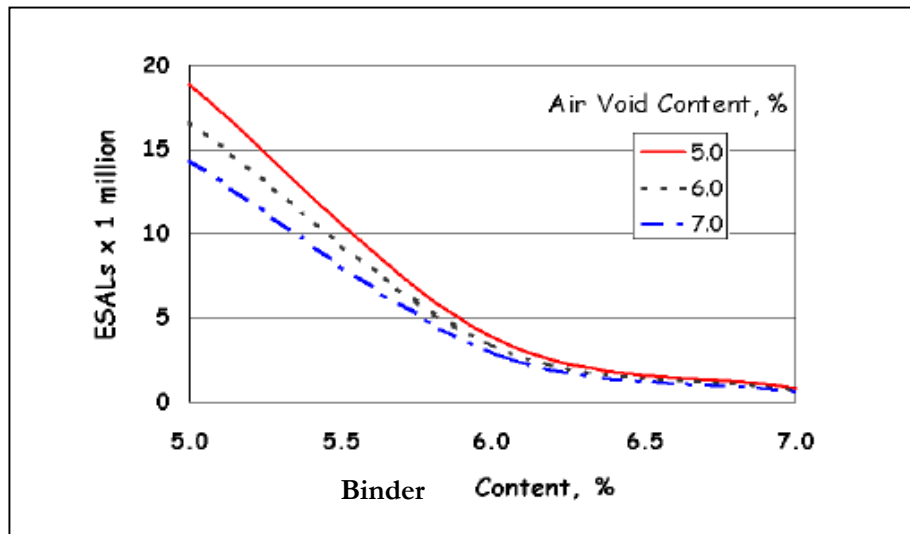


**Figure 2-18: Relations between ESALs to 10 mm Rut Depth, Binder Content, and Air Void Content, Fine Gradation (after J. Epps *et al*, 1999)**

Cross and Brown (1991), Kandhal *et al* (1998 (b)), Hunter *et al* (2000) and Brown *et al* (2001) reported that rutting due to shear failure generally occurs in the top 100 – 150 mm of the pavement. However, it can occur deeper if satisfactory materials are not used.

Rutting in an asphalt mix normally occurs in the early years of a pavement's life when the binder is relatively low in viscosity. Rutting is less likely to occur in a pavement after the asphalt binder has aged with exposure to the elements to a higher viscosity.

Bouldin *et al* (1994) stated that the reason why the static creep test fails in ranking mixtures with respect to permanent deformation is that this test does not capture elastic recoil and the time dependency of the material properties. Valkering *et al* (1990) also found that, with regard to permanent deformation, the static creep test did not correlate well with wheel tracking results. Dynamic creep tests, however, correlated well with the wheel tracking results.

For rutting resistance, a high complex shear modulus,  $G^*$  and a low phase angle  $\delta$  are desirable (Bahia and Anderson, 1995). The higher the  $G^*$  value, the stiffer and thus the more resistant to rutting the binder will be. The lower the  $\delta$  value, the more elastic the binder. Based on the dissipated energy concept, these two values were combined to develop the rutting parameter of  $G^*/\sin \delta$  (Bahia and Anderson, 1995).

A number of projects have been conducted to address the reliability of  $G^*/\sin\delta$  in predicting rutting. Leahy *et al* (1994), according to the results from wheel-tracking tests and repeated shear tests, found that the correlation between  $G^*/\sin\delta$  and the measure of permanent deformation response were generally poor. They concluded that the weak correlations are partly the result of the dominant effect of aggregate characteristics on permanent deformation response. On the other hand, a study conducted by Bouldin *et al* (1994), based on the results from wheel tracking tests, concluded that there is a good correlation between  $G^*/\sin\delta$  and the permanent deformation.

Izzo *et al* (1995) found that the Georgia Loaded –Wheel Tester provided a very good relationship between  $G^*/\sin\delta$  and rutting susceptibility. They also found that the French Pavement Rutting Tester and Hamburg Wheel-Tracking Device provide reasonably good relationships; and the Gyrotory Testing Machine data did not differentiate the mixtures according to rutting susceptibility.

General observations from these studies suggest that the relation between  $G^*/\sin\delta$  and mixture performance (rutting) depends on testing methods and conditions (Zhang and Huber, 1996). The  $G^*/\sin\delta$  may be used to identify those binders that will not perform well regardless of the mixture in which they are used. In other words, this is very useful parameter for quality control or screening for binder producers. Without consideration of the interactions of constituents in a mixture it is impossible to directly relate this parameter to actual pavement performance.

Recent research (Bahia, 2001) indicated that the Superpave rutting parameter  $G^*/\sin\delta$  showed poor correlation with laboratory measured rutting. This parameter was not found to be useful in describing the accumulation of permanent flow, which is important in rutting evaluation. They are now researching other possibilities for a rheological parameter that could be used as a more effective indicator or the role of binder in mixture behaviour than  $G^*/\sin\delta$ .

Various researchers reported on the improvement in rut resistance through polymer modification. Valkering *et al* (1990) reported on the improved rutting resistance by polymer modification as evaluated by wheel tracking tests.

## 2.5 Moisture Susceptibility

Stripping is a failure mechanism on asphalt road pavements that may lead to premature failure, and consequently have an adverse effect on that pavement life and performance. Extreme cases such as disintegration of the asphalt layer and formation of potholes are evident on some of our roads in South Africa.

Many definitions for stripping exist in the literature, but Kiggundu and Roberts (1988) provided a more complete definition. They defined stripping as “*the progressive functional deterioration of a pavement mixture by loss of the adhesive bond between the binder and the aggregate surface and/or loss of the cohesive resistance within the binder principally from the action of water*”.

Despite the variations in definitions, they all acknowledge the presence of water as a major factor in the stripping mechanism of an asphalt pavement. Other factors influencing stripping include (Robert *et al*, 1991):

- 1) The type and use of the mix
- 2) Binder characteristics
- 3) Aggregate characteristics
- 4) Environment
- 5) Traffic
- 6) Construction practice, and
- 7) The use of anti-stripping additives



### 2.5.1 Factors influencing moisture susceptibility

Stripping has been related to a very large number of factors and combinations of factors (Kiggundu and Roberts, 1988; Kandhal, 1992; Kandhal and Rickards, 2001).

This includes:

- 1) Inadequate pavement drainage
- 2) Inadequate compaction of HMA pavement
- 3) Excessive dust coating on aggregate
- 4) Inadequate drying of aggregates
- 5) Decreased binder contents in HMA mixtures (reducing binder film thickness) to obtain increased rut resistance

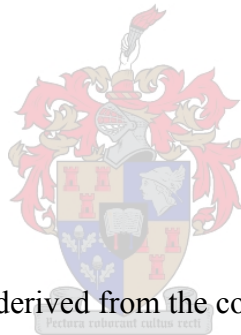
- 6) The use of siliceous aggregates which are relatively more prone to stripping, to obtain increased skid resistance in HMA pavements
- 7) Substantial increase in truck traffic and tyre pressures

Stripping leads to loss in quality of mixture and ultimately failure of the pavement as a result of raveling, rutting or cracking (Brown *et al*, 2001). There are three mechanisms by which moisture can degrade the integrity of a HMA matrix: (Brown *et al*, 2001).

- Loss of cohesion (strength) of the binder film that may be due to several mechanisms
- Failure of the adhesion (bond) between the aggregate and binder (stripping), and
- Degradation or fracture of individual aggregate particles

There may be as many as five different mechanisms by which stripping of binder from an aggregate surface may occur (Roberts *et al*, 1991). These five mechanisms include:

- 1) Detachment,
- 2) Displacement,
- 3) Spontaneous emulsification,
- 4) Pore pressure, and
- 5) Hydraulic scouring



The strength of an asphalt mixture is derived from the cohesive resistance of binder and grain interlock and frictional resistance of aggregates (Roberts *et al*, 1991). The cohesive resistance is only fully available if a good bond exists between the binder and the aggregate. If the bond is poor, failure occurs at the binder-aggregate interface and may result in premature failure of the mix and the HMA pavement. The most frequently referenced relationship between the binder characteristics and moisture susceptibility relates stripping to the viscosity of the binder in service (Roberts *et al*, 1991). High viscosity binders have generally been observed to resist displacement by water better than those of low viscosity. Low viscosity however, is desirable during mixing operations because of its better aggregate coating. However, Cheng *et al* (2002) mentioned that aged pavements are more vulnerable to stripping because ageing reduces both binder cohesion and adhesion with aggregates.

It is possible for a properly designed mix to strip if field compaction produces void contents high enough to permit water to enter the HMA pavement layer. High air void content, the

presence of water, high stress and high temperature are essential ingredients to promote stripping (Kandhal and Rickards, 2001)

The presence of dust and clay coatings on the coarse and/or fine aggregate can inhibit coating between the binder and aggregate and provide channels for penetrating water (Kandhal *et al*, 1998(a)). The binder coats the dust coating and is not in contact with the aggregate surface, resulting in stripping. The potential for premature stripping is enhanced further if the mix consists of an aggregate that is prone to stripping (Kandhal and Rickards, 2001).

Kandhal *et al* (1989) did several case studies and found that in many cases the stripping of asphalt pavements may not be a general phenomenon but rather a localised in areas that are over saturated with water and/or water vapour due to inadequate subsurface drainage conditions. Excessive pore pressure build-up has also been reported as the cause of stripping in some mixtures. The pressure build-up is caused by traffic and results in the water being in frequent motion. This happens when the air voids in the asphalt may become saturated with water even from vapour condensation due to water in the subgrade or subbase. A temperature rise after this saturation can cause expansion of the water trapped in the mixture voids resulting in significant void pressure when the voids are saturated.

Terrel and Al-Swailmi (1993) reported that asphalt with voids either higher or lower than the pessimum range resists water damage more than those within the “pessimum” range. The “pessimum” range is defined as the void range between 7 and 13 percent (the middle region in Figure 2-19) where the asphalt mix is at risk of becoming saturated with water. It is called the “pessimum” range because it represents the opposite of optimum. Figure 2-19 shows the general relationship between air voids and relative strength of HMA mixtures following water conditioning. The amount of strength loss depends upon the amount and nature of the voids. As shown in Figure 2-19, at less than four percent voids, the mixture is virtually impermeable to water, so it is essentially unaffected. Unfortunately, the pessimum range is where many pavements get constructed. Heavy traffic, which causes pore pressure within the saturated mix, can then lead to separation or stripping of the binder from the aggregate surface. As the voids increase to 15 percent and beyond, the mix strength becomes less affected by water because the mixture is now free draining. The objective is to stay out of the “pessimum” void range to minimise stripping problem. This can be done through proper mix design and compaction control procedures.

High air voids content is shown to contribute to rapid hardening and poor retained mix strength (stripping resistance) (Santucci *et al*, 1985). Damage to the mix can come from internal moisture trapped in the aggregate or from external moisture. The combination of moisture and traffic action can result in rapid pavement deterioration in the form of ravelling, stripping, or reduced mix strength. Poor compaction (and hence air void contents) contributes to the detrimental effects of water on the strength of the mix.

Walubita (2000) found that under wet trafficking with water on the pavement surface, moisture leads to a reduction in asphalt stiffness, stripping, cracking, degradation and loss in fatigue life. It is apparent that the fatigue life expectancy of asphalt materials susceptible to moisture damage is significantly reduced by wet trafficking, so that even light axle loads with high tyre pressures (690 kPa) cause substantial damage.

Brown *et al* (2001) stated that environmental factors such as temperature and moisture could have a profound effect on the durability of HMA pavements. When critical environmental conditions are coupled with poor materials and traffic, premature failure may result as a result of stripping of the binder from the aggregate particles.

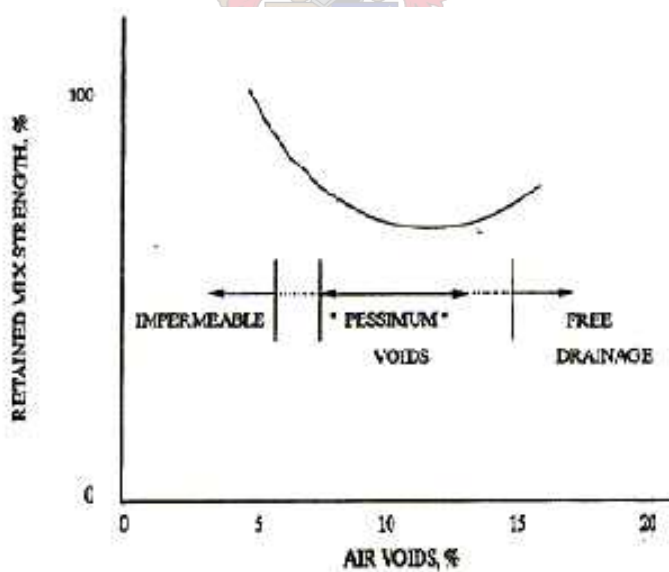


**Figure 2-19: Air void content versus retained mix strength-region of pessimum voids (Terrel and Al-Swailmi, 1993)**

## 2.6 Summary

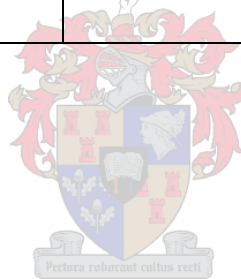
The most important factors influencing the compactibility and rut resistance of HMA pavements can be summarised as in Table 2-2 and Table 2-3.

**Table 2-2: Influences on Compaction (after Asphalt Institute, 1980)**

ITEMS	EFFECTS
<b>Aggregate</b>	
Smooth surfaced	Low interparticle friction
Rough surfaced	High interparticle friction
Unsound	Breaks under steel-wheeled rollers
Absorptive	Dries mix – difficult to compact
<b>Binder</b>	
Viscosity	
High	Particle movement restricted
Low	Particles move easily during compaction
Quantity	
High	Unstable and plastic under roller
Low	Reduced lubrication -difficult compaction
<b>Mix</b>	
Excess coarse aggregate	Harsh mix -difficult to compact
Over sanded	Too workable -difficult to compact
Too much filler	Stiffens mix – difficult to compact
Too little filler	Low cohesion – mix may come apart
<b>Mix temperature</b>	
High	Difficult to compact – mix lacks cohesion
Low	Difficult to compact – mix too stiff
<b>Mat thickness</b>	
Thick	Hold heat – more time to compact
Thin	Lose heat – less time to compact
<b>Weather conditions</b>	
Low air temperature	Cools mix rapidly
Low surface temperature	Cools mix rapidly
Wind	Cools mix – crusts surface

**Table 2-3: Influences on Rut resistance (Collop, 2002)**

	<b>Factor</b>	<b>Change in factor</b>	<b>Effect on Rut resistance</b>
<b>Aggregate</b>	Surface texture	Smooth to rough	Increase
	Gradation	Gap to continuous	Increase
	Shape	Rounded to angular	Increase
	Size	Increase in maximum size	Increase
<b>Binder</b>	Stiffness	Increase	Increase
<b>Mix</b>	Binder content	Increase	Decrease
	Air void content (>3percent)	Increase	Decrease
	VMA	Increase	Decrease
<b>Test/field conditions</b>	Temperature	Increase	Decrease
	State of stress/strain	Increase in tyre contact pressure	Decrease
	Load repetitions	Increase	Decrease
	Water	Dry to wet	Decrease if mix is water sensitive



# 3 INVESTIGATION OF FACTORS INFLUENCING COMPACTIBILITY

In this chapter, some of the factors influencing compactibility are evaluated by means of laboratory testing and presented. Compactibility has been analysed as a volumetric property of an asphalt mixture directly related to the VIM. Therefore, the compactibility of a mix was judged in terms of VIM at a specific compaction level. The test specimens were primarily compacted using the SGC, with some correlation with Marshall compaction.

## 3.1 Introduction

When an asphalt mixture is designed in the laboratory, it should be compacted to a density representative of field density after traffic compaction. It is desirable that the design mix has similar uniform properties and characteristics as the plant-produced mix. It is often assumed that the plant will be able to duplicate the mix produced in the laboratory, which is not necessarily true (NAPA, 1997). There are often slight differences between the aggregate and binder used in the laboratory and those used in the plant. The differences between laboratory and plant produced mixes are more often than not noticeable because of differences between aggregate properties. This may result in differences between the volumetric properties of the laboratory mix and the plant mix.

Sousa *et al* (1991) studied the effect of compaction methods on the permanent deformation characteristics of laboratory specimens. They found that different compactors tend to produce specimens that, although of the same composition, have quite different engineering properties. The compactors used were the Texas gyratory, kneading, and rolling wheel apparatus. Rolling wheel compaction was recommended to simulate field compaction most closely, however, gyratory compaction may be considered more convenient for the preparation of small specimens. It is thus important to select the appropriate compaction method that will closely simulate field compaction. The selection of the appropriate laboratory compaction level is also critical to design a mix that will perform adequately in the field.

## 3.2 Volumetrics

The relationship between the air void content and compaction level (density) of an asphalt mix is widely documented. Air void content and other volumetric properties of asphalt are very important factors in determining the long-term strength and durability of the mixture (NAPA, 1997). It is therefore understandable that there are certain limiting criteria for these volumetric properties to ensure adequate performance.

In Chapter 2, the factors affecting asphalt volumetrics were highlighted. Summarising these:

- Dense gradations, more rounded aggregates and smooth or polished aggregates decreases VMA
- Increased binder absorption results in lower effective binder content and lower VMA (for the same level of compaction)
- Higher filler contents increase surface area, decrease film thickness, and tend to lower VMA
- Higher temperatures decrease binder viscosity, which results in more binder absorption, lower effective binder and lower VMA

Re-heating of asphalt samples occurs after transporting the sample to the laboratory for testing, or when verification samples must be tested. Bahia and Hanson (2000) studied the effect of compaction temperature on the volumetrics of asphalt specimens as compacted with the SGC. Samples were compacted with the SGC at temperatures from 80 °C to 155 °C and volumetrics measured to determine VIM, VMA, and VFB. They found that the binder viscosity changed by 3-orders of magnitude between 80 °C and 155 °C, but compaction temperature had little to no effect on volumetric properties of the compacted samples (Figure 3-1). There was however some concern with the methods which were used in this study.

Coarse Gradation, Limestone			
Temperature, °C	Air Voids, %	VMA, %	VFA, %
155	4.3	14.5	70.3
145	5.1	15.2	66.3
130	4.5	14.6	69.5
115	4.7	14.8	68.5
80	4.8	14.9	67.7
Fine Gradation, Crushed Gravel			
155	4.2	14.9	72.1
145	3.7	14.5	74.6
130	4.0	14.7	73.1
115	3.6	14.4	74.9
100	3.7	14.5	74.6
80	4.2	14.9	71.9

**Figure 3-1: Volumetric Properties of Mixtures Re-Compacted with the SGC at Decreasing Temperatures @N<sub>design</sub> (Bahia and Hanson, 2000)**

In another study by Parker and Hossain (1999), other modes of laboratory compaction were evaluated along with the SGC. In this study, similar mixture samples were compacted on four different compactors utilising three different compaction temperatures. These test temperatures were 160 °C, 115 °C, and 80 °C. The results of this work showed that all four compactors differed in terms of sensitivity to temperature, with the SGC being the least sensitive (Figure 3-2). From these results it can be observed that except for the SGC, the density of the samples significantly increased with increasing temperature. This is what one would expect.

Huner and Brown (2001) also studied the effect of variability in compaction temperature on the volumetrics of a HMA mixture. Samples of each of the eight mixture types were compacted with the same number of gyrations on the SGC but at three different temperatures. The three compaction temperatures evaluated were; the standard target compaction temperature for the specific binder used, target temperature -14 °C and target temperature +14 °C. The results have shown there is no significant difference seen between volumetric properties of these mixes (Figure 3-3). Huner and Brown reported that only two binder types were evaluated and the behaviour of other types could not be commented on. They concluded that the reason why modifying the compaction temperature had no significant effect was due to the fact that the SGC is really a constant strain compactor. The gyration angle is set at 1.25 ° and this is basically applied regardless of mix stiffness. So as the mix gets stiffer the load required to

achieve the 1.25 ° angle is simply increased. In effect, mixes at lower temperatures are compacted with higher compaction effort since the strain is the same and the load is higher.

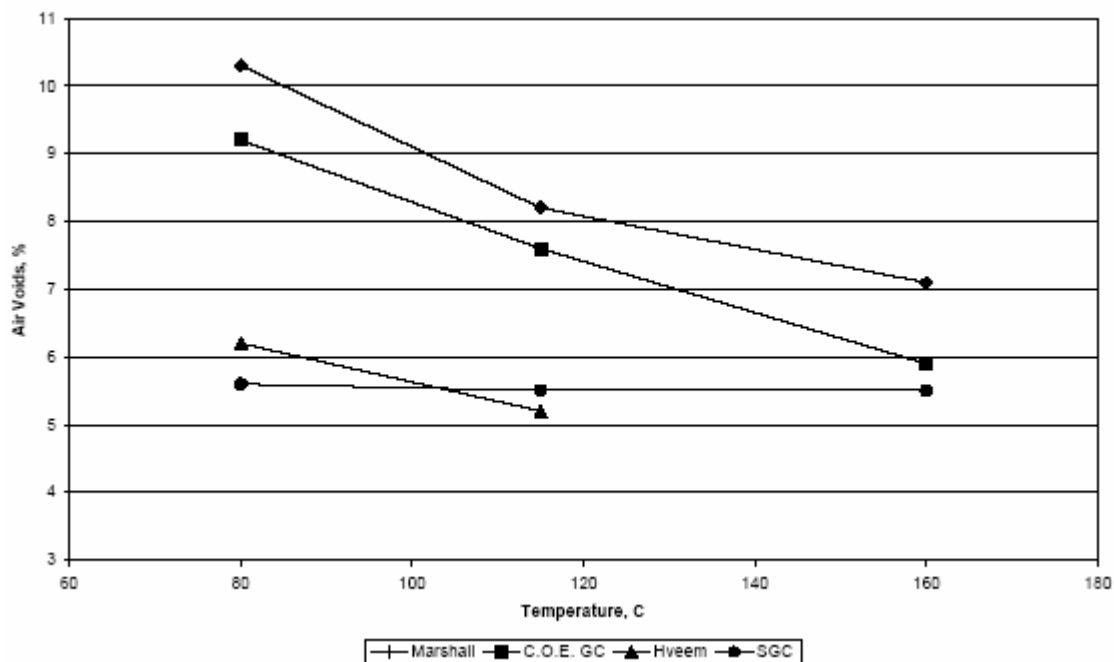
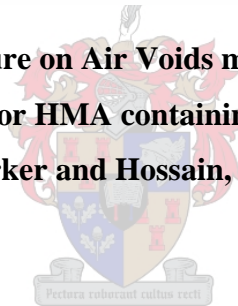


**Figure 3-2: Effect of Temperature on Air Voids measured after Compaction Using Different Compaction Methods for HMA containing a Fine Crushed Gravel Mixture (Parker and Hossain, 1999)**



Mixture Type	Asphalt Content, %	Target Temp. -14° C (VTM)	Target Temp. (VTM)	Target Temp. +14° C (VTM)
LOW-64-F	4.5	4.1	4.2	4.0
LOW-64-C	5.1	3.3	3.2	3.1
LOW-76-F	4.5	3.4	3.5	3.2
LOW-76-C	4.9	4.1	4.1	3.9
HIGH-64-F	5.6	4.4	4.3	4.2
HIGH-64-C	5.3	5.0	4.5	4.4
HIGH-76-F	5.5	4.0	4.0	4.1
HIGH-76-C	5.2	4.0	3.8	3.9

**Figure 3-3: Average Percent Air Voids vs. Compaction Temperature (Huner and Brown, 2001)**

### 3.3 Test programme and methodology

To evaluate the influence of various factors on compactibility, studies were conducted at the University of Stellenbosch (Smit *et al*, 2000; Jenkins and Douries, 2001(a)). These studies included variation of various factors to assess whether they have a significant influence on compactibility. Those factors are summarized in Table 3-1. The author's involvement in the study by Smit *et al* (2000) was confined to the work reported in section 3.4.6.

**Table 3-1: Test matrix for compactibility variables**

<b>FACTOR</b>	<b>VARIABLES</b>	<b>TEST</b>
<b>Gradation</b>	Gradation exponent (n) = 0.2, 0.3, 0.4, 0.5, 0.6, 0.7	Gyratory compacted Temperature 135 °C
<b>Nature of the filler</b>	M1 --Contermanskloof M2 -- Port Elizabeth M3 -- Eerste River M4 -- Eikenhof	Hydrometer tests (ASTM D422-63) Rigden voids
<b>Binder content</b>	4.5, 5.0, 5.5 and 6.0 %	Gyratory compaction Temperature 135°C
<b>Filler content</b>	4.0 and 6.5 %	Gyratory compaction Temperature 135°C
<b>Filler/binder ratio</b>	Percentage bulk volume of filler -- 30, 50, 60 and 70 %	Softening point test (ASTM D36-95)
<b>Compaction temperature</b>	100 and 160 °C	Gyratory compacted

#### 3.3.1 Materials

The first investigation was limited to the compactibility of a typical 19 mm wearing course mix used in the Western Cape. This particular mix has a gradation that falls within the COLTO gradation specification (COLTO, 1998) and has a design binder content of 4.7 percent and a filler content of 7.7 percent (Figure 3-4). The aggregate was Hornfels from the Peninsula quarry and 60/70-pen grade bitumen from the CALREF refinery. The penetration of the bitumen was measured as 63 and the softening point as 48 °C. No natural sand or active fillers

(such as lime or cement) were used in the mixes. Unless otherwise stated, all mixes were compacted using the SGC after being aged in a draft oven at 150 °C for one hour. The mixing temperatures of the mixes were between 150 °C and 160 °C and the compaction temperature of 135 °C.

To evaluate the influence of filler content on the compactibility of the 19mm COLTO Coarse mix, two different filler contents (4.0 and 6.5%) were considered (Table 3-1). In the latter stage of the study, experimental mixes were made by slightly coarsening the gradation of the original 19mm COLTO Coarse mix and varying the filler content (5.5 and 6.5 percent). It should be noted that these filler contents differ. Figure 3-4 shows the gradation of the experimental mix (5.5 percent filler) compared to the original 19mm COLTO Coarse mix. The COLTO gradation specification limits have also been plotted (as dotted lines).

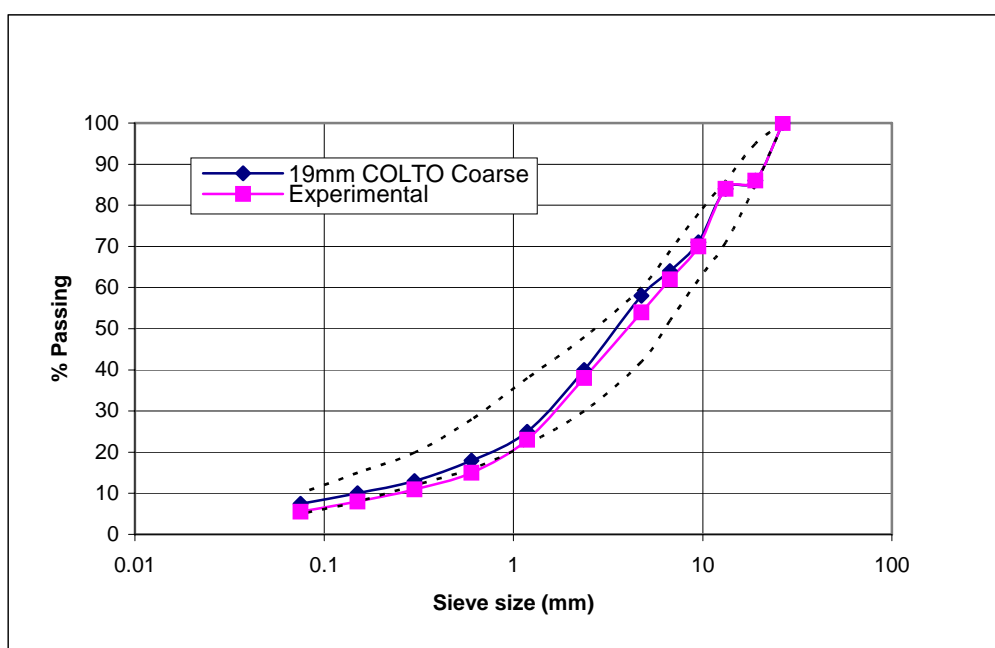


**Figure 3-4: Gradation of the experimental mix in relation to the 19mm COLTO Coarse**

Further testing included alternative wearing course mixes established using the gradation equation developed by Cooper *et al* (1985), shown below:

$$P = \frac{(100 - F)(d^n - 0.075^n)}{(D^n - 0.075^n)} + F$$

**Equation 3-1**

where:

- $P$  = Percentage passing a sieve size of  $d$  mm
- $D$  = Maximum aggregate size, mm
- $F$  = Filler content ( $< 0.075$  mm material)
- $n$  = a gradation exponent between 0 and 1

The gradation exponent,  $n$ , was varied to examine the influence of gradation on compactibility. Values of 0.2, 0.3, 0.4, 0.5, 0.6 and 0.7 were used. Figure 3-5 shows some of the mix gradations for different  $n$ -values having a maximum aggregate size of 19 mm and a filler content of 6.5 percent. The COLTO gradation specification limits have been plotted as dotted lines.

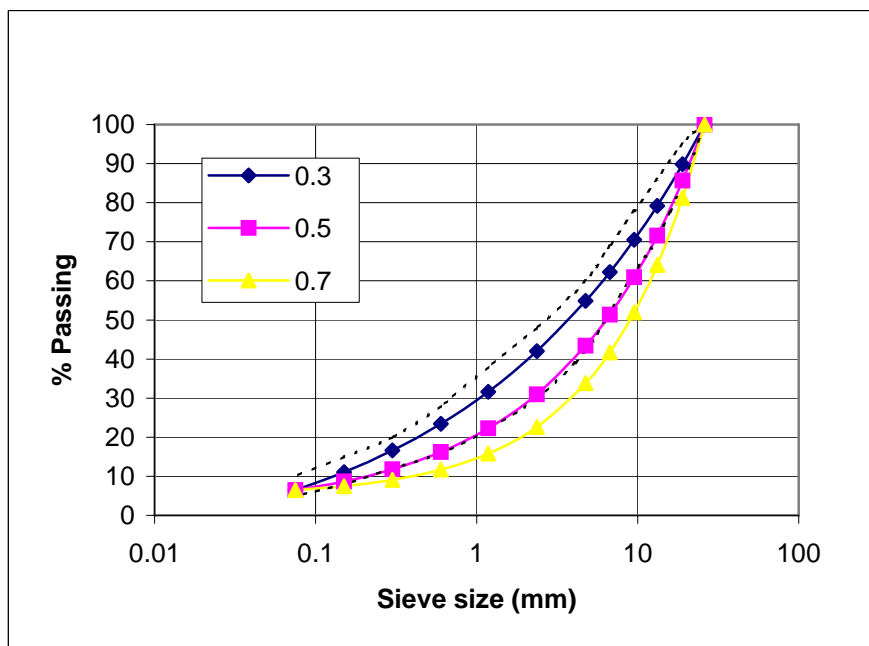


**Figure 3-5: Gradation curves at various  $n$ -values**

To evaluate the impact of the filler on compactibility, four fillers from different sources were investigated. These were designated M1, M2, M3 and M4 (refer Table 3-1). Hydrometer tests (ASTM method D422-63) were done on the four fillers to obtain the particle size distributions (Figure 3-6).

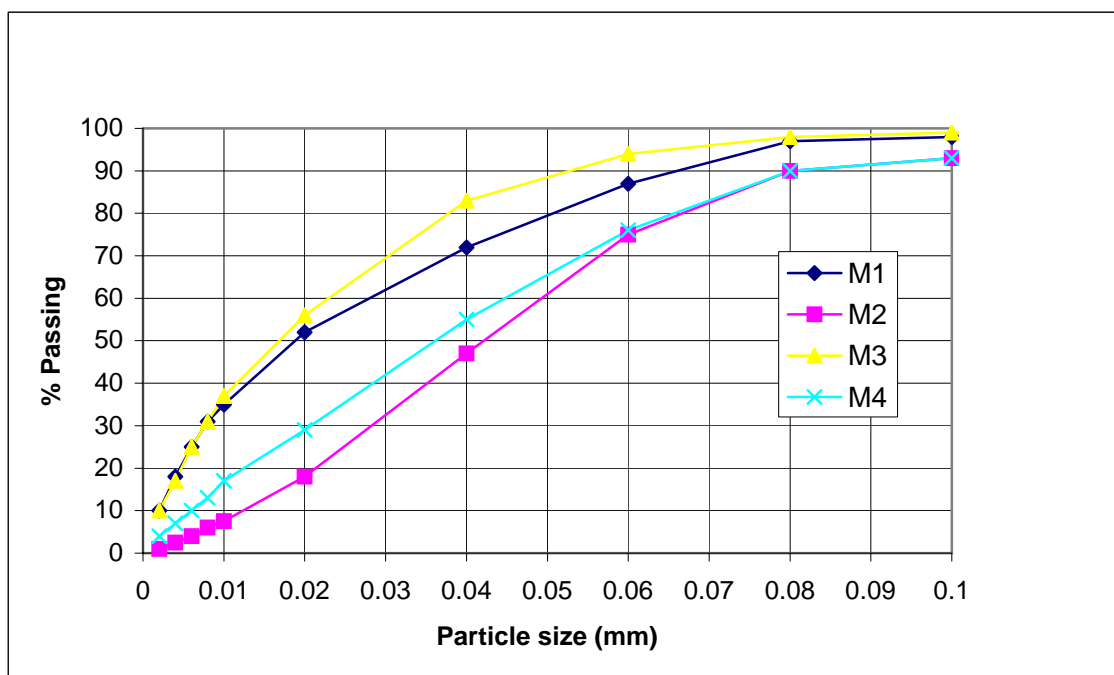


**Figure 3-6: Particle size distribution of fillers**

Filler/binder mastics were made from the four fillers at different percentages of percent bulk volume of filler: 30, 50, 60 and 70 percent. The mixing of the filler and binder consisted of preheating fillers in an oven at 140 – 150 °C and adding them gradually to fluid bitumen in the same temperature range. This mixing was performed over a hot plate using a constant stirring for 2 to 3 minutes until the hot mass was smooth and uniform. Afterwards the softening point was determined.

In another investigation (Jenkins and Douries, 2001(a)), nine different asphalt mixes were tested. The mixes were:

1. Three COLTO Medium mixes having a maximum aggregate size of 13 mm,
2. Three LAMBS (Large Aggregate Mix for Bases) mixes having a maximum aggregate size of 26 mm,
3. Three BTB (Bitumen Treated Base) mixes, having a maximum aggregate size of 19 mm

The binders for these mixes were as in Table 3-2.

**Table 3-2: Binders for compactibility mixes**

Mix	1	2	3
COLTO Medium	60/70	60/70 + Gilsonite	40/50
LAMBS	60/70	40/50	40/50 (no sand)
BTB	60/70 + Gilsonite	40/50	40/50 + Gilsonite

**Table 3-3: Gradation of COLTO Medium wearing course mixes**

Sieve size (mm)	Target	60/70	60/70 + 40/50	Gilsonite
	% passing	% passing	% passing	% passing
19.0	100	100	100	100
13.2	99	100	100	99
9.5	88	90	90	86
6.7	77	76	76	74
4.75	68	69	68	69
2.36	45	46	44	46
1.18	28	28	27	29
0.6	18	19	18	19
0.3	12	13	13	13
0.15	9	10	10	9
0.075	7.2	8.1	8.3	7.5
Pb	5.4 %	5.5 %	5.4 %	5.5 %
MTRD		2.508	2.516	2.521

**Table 3-4: Gradation of LAMBS mixes**

Sieve Size (mm)	Target	60/70	40/50
	% passing	% passing	% passing
37.5	100	100	100
26.5	88	87	89
19.0	71	73	69
13.2	68	68	64
9.5	59	62	57
6.7	50	51	49
4.75	46	46	45
2.36	32	34	34
1.18	22	25	25
0.6	17	17	17
0.3	11	11	11
0.15	7	7	7
0.075	5.5	5.4	5.9
Pb	4.0%	3.9%	3.8%
MTRD		2.568	2.563

**Table 3-5: Gradation of BTB mixes**

Sieve Size (mm)	Target	40/50	40/50 + Gilsonite	60/70 + Gilsonite
	% passing	% passing	% passing	% passing
26.5	100	100	100	100
19.0	91	91	90	87
13.2	85	86	84	84
9.5	74	73	72	71
6.7	63	63	63	62
4.75	58	57	58	58
2.36	41	38	39	38
1.18	24	22	24	23
0.6	16	14	16	15
0.3	11	10	12	11
0.15	9	8	9	9
0.075	7.2	6.8	7.4	7.3
Pb	4.5%	4.5%	4.5%	4.5%
MTRD		2.548	2.547	2.561

The aggregate was Hornfels from the Eerste River quarry, the 60/70-pen grade binder from the CALREF refinery and the 40/50-pen grade binder from the SAPREF refinery. All the mixes were received in paper bags ( $\pm 4.5$  kg) and reheated in a draft oven to approximately 150 °C. The mixes were compacted with the SGC at temperatures of approximately 140 °C (60/70-pen grade) and 145 °C (40/50-pen grade).

### **3.3.2 Test methods**

Various tests methods were used in this study. This included:

- Hydrometer tests
- Softening point (Ring & Ball) tests
- Gyrotory compaction
- Dynamic creep
- Indirect tensile strength (ITS)
- Stiffness (Dynamic Modulus) in Indirect Tensile mode

#### **3.3.2.1 Hydrometer tests**

Hydrometer tests were performed on the different fillers to determine the particle size distribution. These tests were done according ASTM Test method D422-63. This test method covers the quantitative determination of the distribution of particle sizes in soils. The distribution of particle sizes larger than 0.075 mm is determined by sieving, while a sedimentation process using a hydrometer determines the distribution of particle sizes smaller than 0.075 mm. It is based on Stoke's Law – larger particles travel faster through water and settle first. The hydrometer is used to monitor the density of soil suspension at any given time. A plot of suspension density vs. elapsed time gives the particle size distribution.

#### **3.3.2.2 Softening point (Ring & Ball) tests**

The softening point test is a valuable consistency test for penetration grade bitumens. It is also an indirect measure of viscosity or, rather, the temperature at which a given viscosity is evident. For bitumen of a given penetration (determined at 25 °C), the higher the softening point the lower the temperature sensitivity. This test is carried out by the Ring and Ball method, which consists of suspending a brass ring containing the test sample of bitumen in

water at a given temperature. A steel ball is placed upon the bituminous material; the water is then heated at the rate of 5 °C increase per minute. The temperature at which the softened bituminous material first touches a metal plate at a specified distance below the ring is recorded as the softening point of the sample. This test method is described in detail in ASTM Test method D36-95.

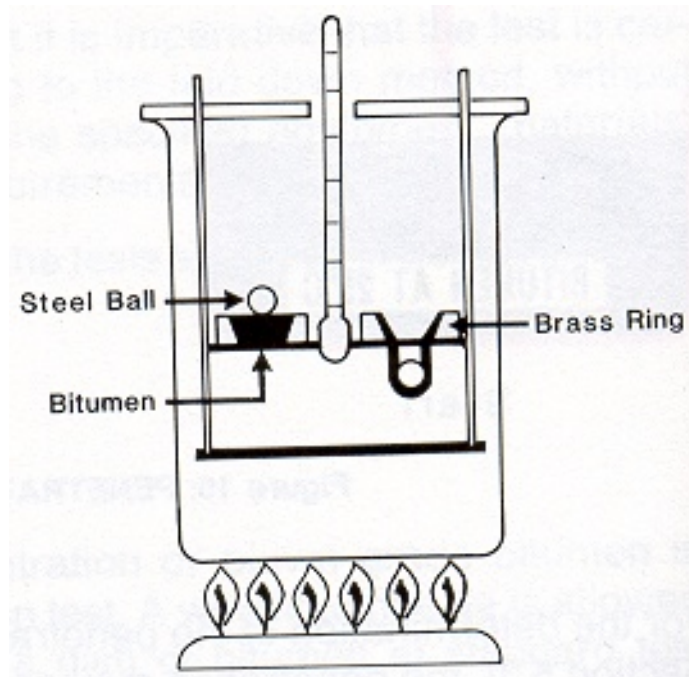


**Figure 3-7: The Ring-and-Ball Softening Point Test**

The Belgium (OCW, 1997) mix design method uses the resulting increase in the softening point of a filler/binder mixture with the addition of the filler to determine the optimum mastic composition. This increase in softening point depends on the filler/binder ratio and the volume of voids in the filler (Rigden's voids). Based on the Belgium experience, a mastic composition that ensures an increase in softening point temperature of between 12 °C and 16 °C is required to balance the mix requirements in terms of durability (flexible mastic) and stability (stiff mastic).

For this thesis, softening point test were done on pure bitumen as well as different filler/binder mastics at different percentages of bulk volume of filler.

### 3.3.2.3 Gyrotory compaction

The gyrotory compaction tests were done according to an American mix design procedure (Superpave) that relates number of gyrations (compactive effort) to four traffic levels as shown in Table 3-7 (Blankenship *et al*, 1994). These have been designated A to D with increasing traffic. Superpave has three compaction parameters, which have the following relevance:

- $N_{des}$  corresponds to the expected amount of traffic at the end of a 20-year design life.
- $N_{ini}$  is a small number of gyrations that simulates mixture behaviour during breakdown rolling.
- $N_{max}$  is a large number of gyrations that simulates mixture behaviour in an extreme stress situation.

Design parameters are established on the basis of air void content at  $N_{ini}$ ,  $N_{des}$  and  $N_{max}$ . Table 3-6 indicates the Superpave criteria at these levels in terms of percentage Rice density (%Gmm).

**Table 3-6: Superpave compaction criteria (Blankenship *et al*, 1994)**

Gyration Level	Criterion for %Gmm
$N_{ini}$	< 89
$N_{des}$	= 96
$N_{max}$	< 98

The gyrotory compactor simulates the kneading action of rollers used to compact asphalt pavements by applying a vertical load to an asphalt mixture while gyrating a mould tilted at a specified angle (see Figure 3-8). The compactor places 600 kPa of pressure on the specimen and operates at 30 rpm. The SGC also provides a measure of compactibility by recording the height of the specimen during compaction. Using the measured bulk relative density of the final specimen and the recorded change in height during compaction, the change in density (%Gmm) with number of gyrations can be calculated. This gives an indication of the densification during compaction. It is typically plotted on a semi-log scale. A smooth sided cylinder is assumed initially and then later corrected based on the measured value for bulk relative density.

**Table 3-7: Recommended Superpave compaction matrix (Blankenship *et al*, 1994)**

Design Traffic Level (million ESALs)	Compaction parameters			Typical roadway application
	Nini	Ndes	Nmax	
<b>A (&lt; 1)</b>	6	50	74	Local roads, country roads and city streets where truck traffic is at a very minimal level.
<b>B (0.1 – 1)</b>	7	70	107	Collector roads or access streets. Medium trafficked city streets and the majority of country roads would be applicable to this level.
<b>C (1 – 30)</b>	8	100	158	Two-lane, multilane and partially divided or completely controlled access roadways. Medium to highly trafficked city streets.
<b>D (&gt; 30)</b>	9	130	212	National routes, both rural and urban in nature. Truck climbing lanes on two lane roadways.

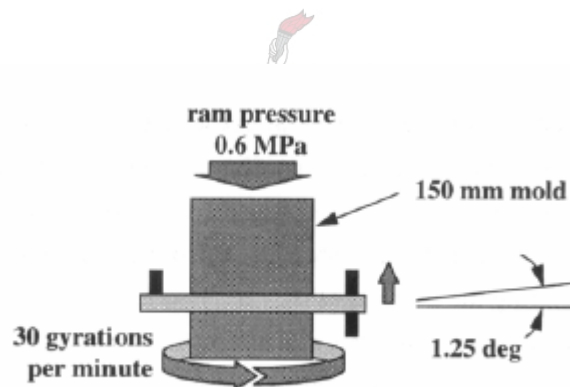


**Figure 3-8: SGC Mould Configuration and Compaction Parameters**

### 3.3.2.4 Dynamic creep

The dynamic creep test is used in South Africa to evaluate the resistance to permanent deformation of asphalt mixes. It is calculated as follows:

$$E_{DC} = \frac{\sigma}{\left(\frac{\Delta V}{t}\right)}$$

**Equation 3-2**

where:

- $E_{DC}$  = Dynamic creep modulus, MPa
- $\sigma$  = Applied stress = 0.1 MPa
- $\Delta V$  = Permanent vertical deformation, mm
- $t$  = Thickness of sample, mm

The conditions for this test are:

- Load type – 0.5 Hz haversquare wave
- Load magnitude – 100 kPa
- Test temperature – 40 °C
- Test duration – 3600 cycles (2 hours)
- Conditioning cycles before testing – 30 cycles

### 3.3.2.5 Indirect tensile strength (ITS)

The indirect tensile splitting test is used in South Africa to evaluate the tensile strength of an asphalt material. A minimum tensile strength of 800 kPa determined using the diametral test is often specified.

The test was done at a temperature of  $20 \pm 0.5$  °C and a displacement rate of 50 mm/min. Specimens were conditioned at  $20 \pm 0.5$  °C in the MTS (Materials Testing System) test chamber for at least 2 hours.

The indirect tensile strength is calculated as follows:

$$ITS = \frac{2P}{\pi D}$$

**Equation 3-3**

where:

*ITS* = Indirect Tensile Strength, MPa

*P* = Applied load, N

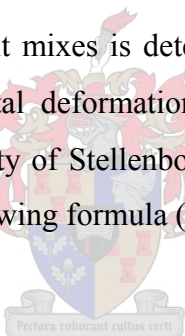
*t* = Thickness of sample, mm

*D* = Sample diameter, mm

### 3.3.2.6 Stiffness (Dynamic Modulus) in Indirect Tensile mode

In South Africa, the stiffness of asphalt mixes is determined in the diametral indirect tensile mode at  $20 \pm 0.5$  °C, using horizontal deformations and assuming a Poisson's ratio. An approach often adopted at the University of Stellenbosch is to calculate the dynamic stiffness from vertical deflections using the following formula (ASTM D4123-82)::

$$E = \frac{3.59 \cdot P}{t \cdot \Delta V}$$



**Equation 3-4**

where:

*E* = Dynamic modulus, MPa

*P* = Dynamic load, N

*t* = Thickness of sample, mm

$\Delta V$  = Amplitude of the vertical deflection, mm

This approach has the advantage in that

- 1) The vertical deflections are an order of magnitude larger than the horizontal deflections and therefore measured more accurately, and
- 2) Poisson's ratio does not have to be assumed.

## 3.4 Compactibility results

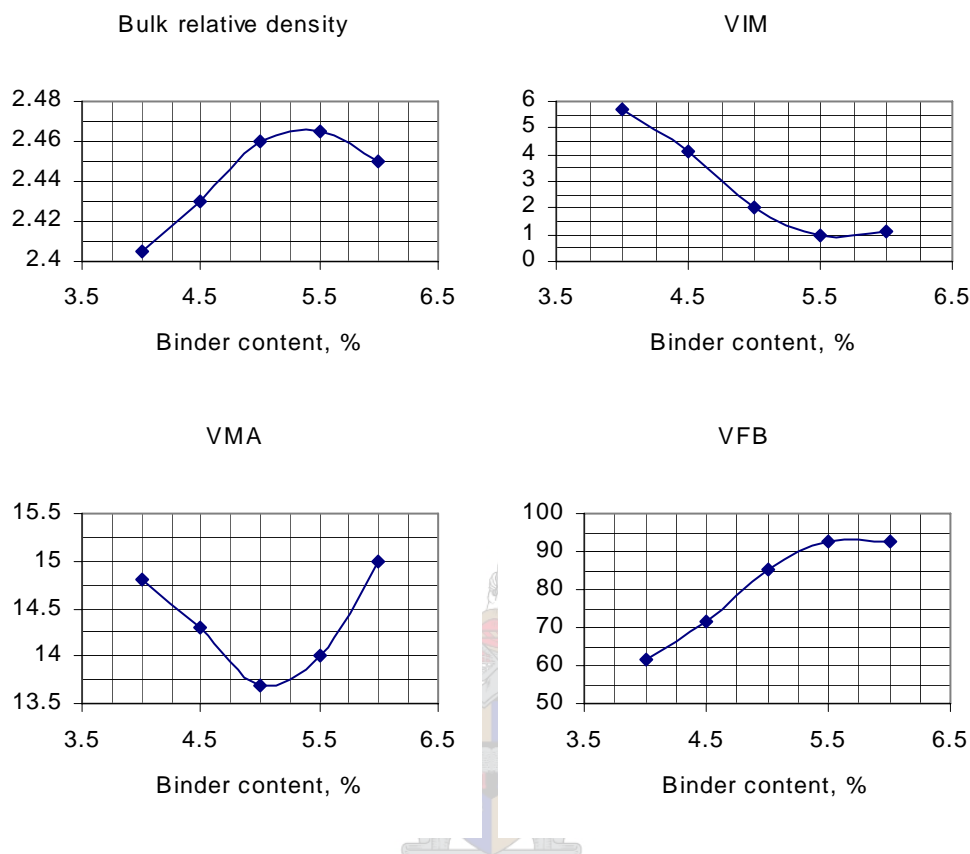
### 3.4.1 Gyratory compaction vs. Marshall compaction

Figure 3-9 shows the volumetric properties of the 19mm COLTO Coarse mix as reported by the asphalt supplier in February 2000 (Smit *et al*, 2000). These properties were determined from 100 mm diameter Marshall specimens. It should be noted that this mix as reported was manufactured in the plant and not made up in the laboratory. Small variations in gradation and binder content consistent with plant mixes can therefore be expected. The asphalt supplier made the point that this approach allows a better understanding of the mix volumetric properties anticipated in the field. Under Marshall compaction and a design binder content of 4.7 percent, the VIM in the mix is at 2.5 percent, indicating that the mix compacts quite readily. The minimum VMA occurs at a binder content of 5.0 percent. At a binder content of 5.5 percent the VIM are at the one percent level. At this point the mix has become overfilled with bitumen. Figure 3-9 summarises the volumetric properties of the 19mm COLTO Medium mix at different binder contents (as reported by the asphalt supplier).

A Marshall mix design was done at the University of Stellenbosch by Smit *et al* (2000) to confirm the volumetric properties of the 19mm COLTO Coarse mix as reported by the asphalt supplier. Mixes were compacted at a temperature of 135 °C directly after mixing at a temperature of 160 °C (without ageing). These mixes were made up in the laboratory using sieved aggregate gradings. The results of this Marshall mix design are shown in Figure 3-10. The volumetric properties shown on this figure differ significantly from those in Figure 3-9. At the design binder content of 4.7 percent, the VIM after Marshall compaction are in excess of 5 percent indicating that the mix is relatively harsh and difficult to compact. The minimum VMA occurs at a binder content of 5.5 percent and there is a definite increase in the VFB with the addition of binder beyond 5.5 percent. The reason for the discrepancy between the results is unknown. One possible reason could be differences between the laboratory and plant mixes.

Gyratory compaction tests were done to investigate the compactibility of the 19mm COLTO Coarse mix in more detail. These were done on the laboratory mix at various binder contents (4.5, 5.0, 5.5 and 6.0 percent). Two specimens were compacted at each of the four binder contents at a compaction temperature of 135 °C. A maximum of 288 gyrations were applied to the compacted specimens. This is a large number of gyrations and the density of the mix after this many gyrations therefore represents the refusal density of the mix. At refusal density, a

mix will not densify significantly further. It is critical that a mix, at refusal density, has sufficient voids (at least 1 to 2 percent) to prevent the mix becoming unstable if the aggregate skeleton becomes overfilled with bitumen. Table 3-8 indicates the gyratory volumetric properties at  $N_{des}$  for the different binder contents and traffic levels.



**Figure 3-9: Marshall volumetric properties of 19mm COLTO Coarse mix as reported by supplier**

**Table 3-8: Gyratory VIM @  $N_{des}$  for different binder contents and traffic levels**

Traffic class	Binder content			
	4.5%	5.0%	5.5%	6.0%
<b>A</b>	8.3%	6.4%	5.0%	4.9%
<b>B</b>	7.3%	5.2%	3.9%	3.6%
<b>C</b>	6.1%	4.1%	2.8%	2.5%
<b>D</b>	5.4%	3.3%	2.0%	1.7%
<b>Marshall</b>	7.1%	5.0%	2.7%	1.8%

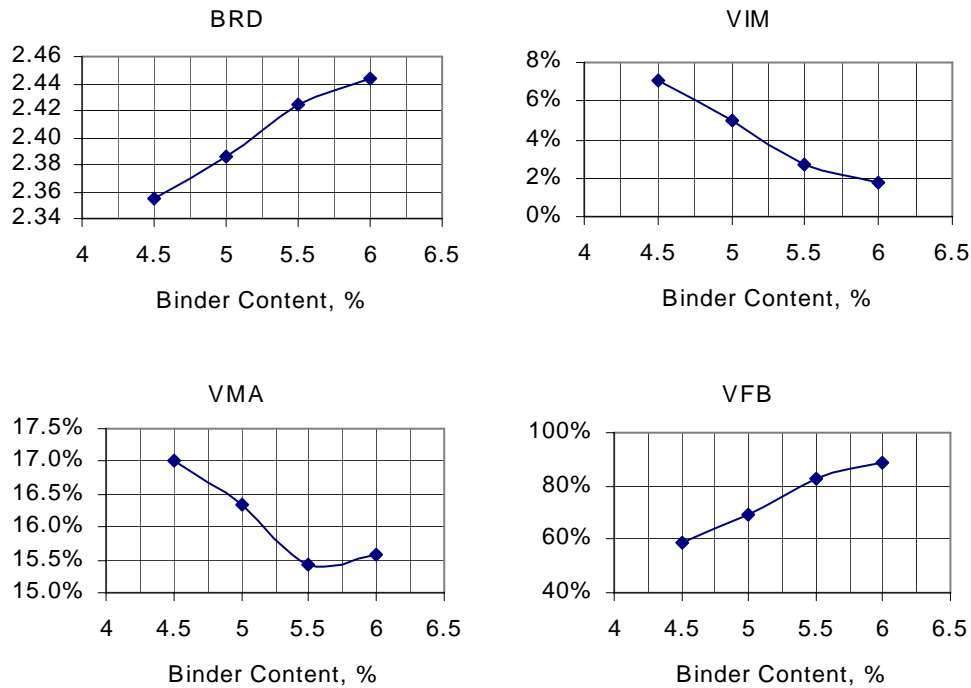


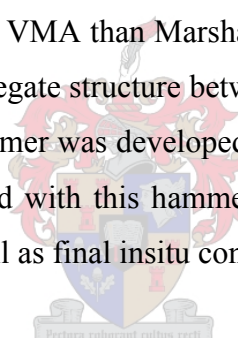
**Figure 3-10: Marshall volumetric properties of 19mm COLTO Coarse mix (University of Stellenbosch)**

A comparison of VIM from Table 3-8 indicates that Marshall compaction does not necessarily correspond with a fixed “Superpave” traffic level at the different binder contents. At the 4.5 percent binder content, for example, the Marshall VIM were 7.1 percent which corresponds to the gyratory VIM of 7.3 percent for traffic class B (i.e. 0.1 – 1 million ESALs). Likewise, for the 5 percent binder content, the Marshall compaction also corresponds to the B traffic class. At the 5.5 percent binder content, however, the Marshall VIM was 2.7 percent, which is comparable to the gyratory VIM of 2.8 percent for the C traffic level. At a binder content of 6 percent, the Marshall compaction corresponds to the gyratory D traffic class.

The Superpave mix design system was designed to accommodate different traffic levels. From Table 3-8 can be seen that for each binder content, the VIM decrease with in as the expected level of traffic increase (from class A to D). Also, for heavier traffic, the optimum binder content (for 4 percent VIM) is lower than for lighter traffic. For example, an optimum binder content of 5.5 percent would be appropriate for traffic class B, while for the heavier traffic class C, an optimum binder content of 5.0 percent would be appropriate.

Hence it appears that at the higher binder contents, Marshall compaction is more severe and perhaps misleading as to the compactibility of the mix at these higher binder contents. As a consequence, optimum binder contents based on Marshall mix designs may be lower or higher than those based on gyratory compaction mix designs. This is because with Marshall compaction, a fixed amount of energy is applied to the specimen through impact compaction. Thus, the stiffness of the mix will have a significant effect on the compaction. On the other hand, the SGC applies a constant shear strain to the specimen and the energy will increase as the mix stiffness increases.

Brown *et al* (1993) found that the mechanical Marshall hammer provides highest optimum binder content of all compaction methods. They concluded that this compaction method would result in an asphalt mix that is more susceptible to rutting. They also found that gyratory specimens have lower stability than Marshall compacted specimens. This is attributed to the re-orientation of particles from the gyrating compaction mechanism. D'Angelo *et al* (1995) also found that SGC specimens had lower VMA than Marshall specimens. This difference in VMA is as a result of the difference in aggregate structure between the SGC and Marshall specimens. This is the reason why the Hugo hammer was developed (Hugo, 1969; 1970). Hugo found that the structure of specimens compacted with this hammer are more closely related to those of gyratory compacted specimens as well as final insitu conditions in an asphalt pavement.



When only the VIM was evaluated, D'Angelo *et al* (1995) found that the SGC yielded similar results to the Marshall. Hence, it leads to the conclusion that VMA is more an indication of the aggregate structure of the mix than the VIM. D'Angelo *et al* concluded that VMA values determined from SGC specimens do not react to changes in binder content the same as VMA from Marshall specimens. The SGC specimens indicate that addition of binder has filled the void space between the aggregate and is forcing the aggregate apart. The Marshall specimens indicate the addition of binder is lubricating the aggregate to allow it to be compacted more densely. This provides some indication of differences between impact and kneading compaction. The SGC uses a shear compaction effort, while the Marshall compaction uses impact energy. The kneading-type compaction allows aggregate particles to move, as a result of which air voids are more readily filled than is the case with impact compaction. The aggregate orientation, and consequently the development of density, is different for specimens compacted using these two compaction processes.

### 3.4.2 Gradation

Figure 3-11 illustrates the influence of the gradation exponent,  $n$ , on the compactibility of the different mixes. The figure shows this influence at the different Superpave gyratory compaction levels for traffic class D (i.e. very heavy traffic, refer to Table 3-7). Only those mixes with a binder content of 4.5 percent and a filler content of 6.5 percent are shown. The figure illustrates that the lowest VIM is achieved using gradation exponents less than 0.4. Above 0.4, the VIM of the mixes increases significantly.

The use of very low  $n$ -values for gradations results in mixes with a higher percentage of finer materials, particularly within the sand fraction i.e. material between the 0.075 mm and 2.36 mm sieves. A greater percentage of finer material may assist in filling the voids in the stone-sand skeleton of the mix. Mixes with low  $n$ -values may have questionable skid resistance at higher speeds due to low macro texture, particularly mixes having an  $n$ -value of 0.2.

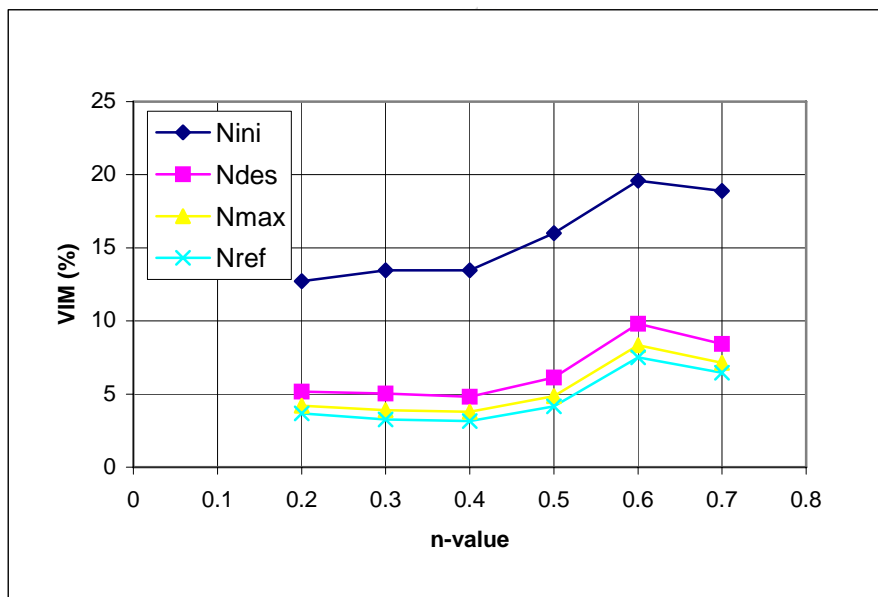


**Figure 3-11: The influence of the gradation exponent  $n$  on compactibility of 19mm COLTO Coarse mix**

The second investigation (Jenkins and Douries, 2001 (a)) comprised the gyratory compaction of three different gradations with different binders. The influence of the binder type and the addition of Gilsonite on the compactibility of these mixes were also investigated. Details on the gradation and specimen preparation are given in Section 3.3.1.

For each of the nine mixes, 18 samples were compacted. Two samples were compacted to 300 gyrations to determine the refusal density. The remainder of the 18 samples were compacted to approximately 7 % voids for MMLS3 testing (see Section 4.5). The average voids results at specific gyration levels are given in Table 3-9 through Table 3-11.

From these tables, it is evident that the LAMBS mixes compacted very easily compared to the other two mixes. The BTB mixes exhibited the highest resistance to compaction. The mixes with the harder binder (40/50 pen) were more difficult to compact than those with the 60/70-pen binder. The addition of Gilsonite also decreased the compactibility. The inclusion of sand in the LAMBS also aided the compactibility of those mixes. The gyratory compaction data indicate that the LAMBS mixes (with sand) will have a lower rut resistance. The refusal density (after 300 gyrations) is at 98% Rice density (2% voids).

**Table 3-9: Gyratory compaction results - COLTO Medium**

Number Of Gyrations	40/50		60/70		60/70 + Gilsonite	
	% VOIDS					
	$\bar{x}$	<i>s</i>	$\bar{x}$	<i>s</i>	$\bar{x}$	<i>s</i>
<b>8</b>	17.8	0.41	16.4	0.64	17.5	0.28
<b>50</b>	10.5	0.51	9.5	0.22	10.1	0.11
<b>100</b>	8.2	0.47	7.2	0.16	7.8	0.15
<b>300</b>	5.0	0.00	4.6	0.14	5.7	0.71
<b>Marshall voids</b>	5.0		4.4		5.0	
<b>*N<sub>MMLS</sub></b>	<b>140</b>		<b>100</b>		<b>120</b>	
<b>(7% voids)</b>	7.2	0.45	7.2	0.16	7.1	0.37

**Note:** \*N<sub>MMLS</sub> = number of gyrations to prepare MMLS specimens

**Table 3-10: Gyrotory compaction results - BTB**

Number Of Gyrations	40/50		40/50 + Gilsonite		60/70 + Gilsonite	
	% VOIDS					
	$\bar{x}$	$s$	$\bar{x}$	$s$	$\bar{x}$	$s$
<b>8</b>	18.2	0.43	17.8	0.29	17.8	0.57
<b>50</b>	11.3	0.41	10.8	0.39	11.2	0.61
<b>100</b>	9.1	0.39	8.5	0.42	9.1	0.64
<b>300</b>	5.6	0.19	5.1	1.13	6.0	0.28
<b>Marshall voids</b>	5.4		5.3		5.7	
<b>*N<sub>MMLS</sub></b>	<b>200</b>		<b>180</b>		<b>200</b>	
<b>(7% voids)</b>	7.2	0.40	6.9	0.42	7.2	0.69

**Note:** \*N<sub>MMLS</sub> = number of gyrations to prepare MMLS specimens

**Table 3-11: Gyrotory compaction results - LAMBS**

Number Of Gyrations	40/50		60/70		40/50 NO SAND	
	% VOIDS					
	$\bar{x}$	$s$	$\bar{x}$	$s$	$\bar{x}$	$s$
<b>8</b>	12.7	0.92	12.8	0.59	16.4	0.93
<b>50</b>	6.4	0.20	6.7	0.36	9.0	0.82
<b>100</b>	4.9	0.21	4.7	0.50	6.7	0.23
<b>300</b>	1.9	0.57	2.1	0.42	3.7	0.23
<b>Marshall voids</b>	3.4		4.0			
<b>*N<sub>MMLS</sub></b>	<b>60</b>		<b>60</b>		<b>130</b>	
<b>(6% voids)</b>	5.9	0.19	6.2	0.35	6.2	0.65

**Note:** \*N<sub>MMLS</sub> = number of gyrations to prepare MMLS specimens

### 3.4.3 Nature of the filler

Figure 3-6 shows the particle size distributions of the different fillers. Fillers M1 (Contermanskloof) and M3 (Eerste River) have a high percentage (35 percent) of material smaller than 0.01 mm (10 micron). It has been found that the stiffening effect of fillers tends to increase with decreasing particle sizes below 10 micron (Shashidhar and Romero, 1998). This high percentage of material smaller than 10 micron is almost twice that of the M2 and M4 fillers used in other parts of the country, and justified the investigation of stiffening potential.

### 3.4.4 Binder content

The influence of binder content on the compactibility of the 19mm COLTO Coarse mix is shown in Figure 3-12. As expected, an increase in binder content facilitates compaction. The figure shows this influence at each of the Superpave gyratory levels for traffic class D.

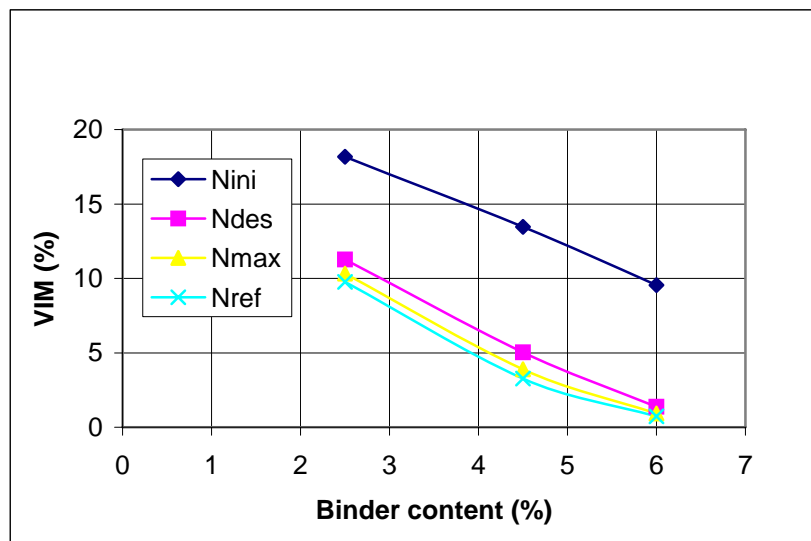


**Figure 3-12: The influence of binder content on compactibility of 19mm COLTO Coarse Mix ( $n = 0.3$  and filler content = 6.5%)**

The optimum binder contents to achieve 4 percent VIM at  $N_{des}$  was determined for each of the mixes having different  $n$ -values and a filler content of 6.5 percent. These are shown in Figure 3-13 for the different traffic classes. From this figure it can be seen that the design traffic has a significant influence on the optimum binder content. Furthermore, for mixes having  $n$ -values greater than 0.4, the optimum binder content increases (refer Figure 3-11). It should also be

noted that the optimum binder content selected for the 19mm COLTO Coarse mix is lower than the binder content required to achieve 4 percent VIM at  $N_{des}$  for very high design traffic.

### 3.4.5 Filler content

The influence of the filler content on the compactibility of the 19mm COLTO Coarse mix is shown in Figure 3-14. An increase in filler content appears to improve the compactibility of the mixes slightly. The influence is insignificant. The figure shows this influence at each of the Superpave gyratory levels for traffic class D. Mixes having a binder content of 4.5 percent and an  $n$ -value of 0.3 are shown.

It should be pointed out that the nature of the filler can also influence compactibility. When the filler particles are  $< 20 \mu\text{m}$ , it can act as an extender rather than creating stiffening. Thus even though higher filler contents may be beneficial in terms of bitumen extenders and/or void reducers, their benefit reduces when the optimum filler/binder ratio is exceeded due to excessive stiffening of the mix.

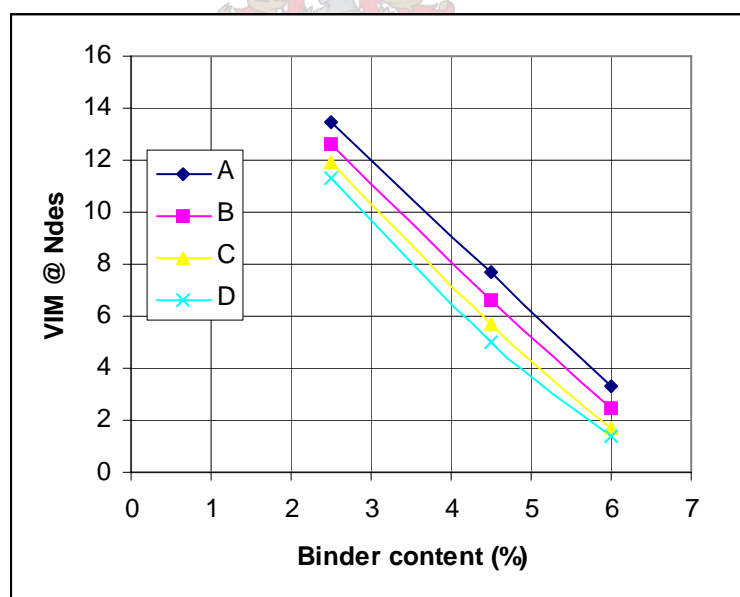


**Figure 3-13: Mix design chart for  $N_{des}$  VIM for 19mm COLTO Coarse mixes having an  $n$ -value of 0.3**

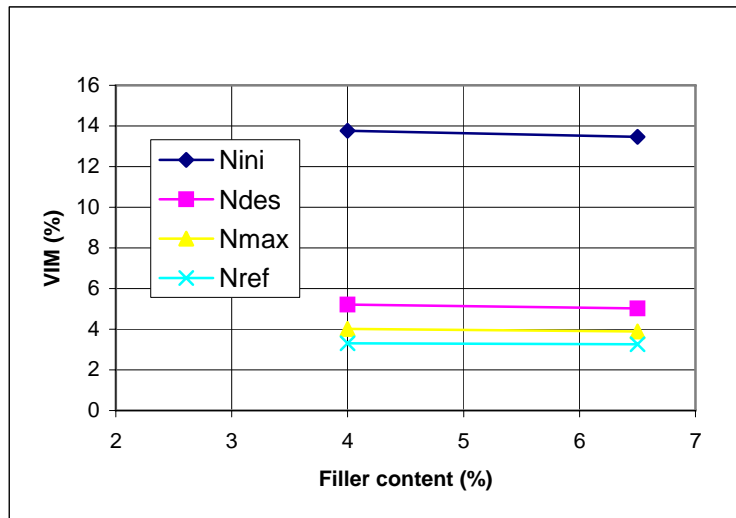


**Figure 3-14: The influence of filler content on compactibility of 19mm COLTO Coarse mix ( $P_b = 4.5\%$ ;  $n$ -value = 0.3)**

### 3.4.6 Filler/binder ratio

The air voids in the compacted fillers were determined and is summarised in Table 3-12.

**Table 3-12: Rigden voids of fillers**

Filler	Rigden Voids (%)
M1	42
M2	46
M3	39
M4	40

Softening point tests were done on the CALREF 60/70 bitumen at different percentages of bulk volume of filler. The softening point of the pure bitumen was 48 °C. The M1 filler was chosen as the reference filler. Figure 3-15 shows the results of the softening point tests. It is evident that an increase in the filler content has a stiffening effect on the mastic, resulting in an increase in the softening point of the mastic. The M1 has the lowest stiffening effect and the M4 the highest.

As mentioned previously, the Belgium mix design method allows an increase in softening point temperature of the mastic of between 12 °C and 16 °C. Kandhal (1981) concluded that the

lower limit is applicable and suggested limiting criteria on changes in softening point temperature of 12 °C. Values above this may result in mastics that are too stiff.

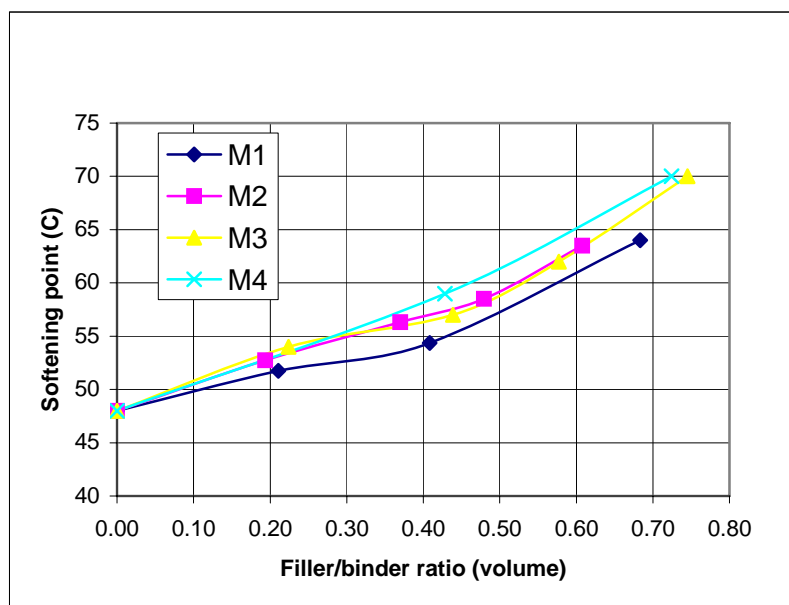


**Figure 3-15: Softening point test results on different fillers**

Based on this, an increase in softening point of 12 °C was used to determine the optimum filler/binder ratio to optimise the stiffening influence of the filler (and still provide good rut resistance). From Figure 3-16, the optimum filler/binder ratio for M1 fillers is in the order of 0.57 (on a volume basis). This is the highest ratio for all the fillers investigated. Assuming a filler bulk relative density of 2.75 and a bitumen bulk density of 1.025 this relates to a filler/binder ratio of about 1.5 (on a mass basis). The filler binder ratio of the 19mm COLTO Coarse mix at an optimum binder content of 4.7 percent was 1.6, which is slightly higher than the maximum of 1.5 to optimise the stiffening effect. Note that for the M4 filler, a maximum filler/binder ratio of 0.46 (volume basis) may be appropriate.

Considering the upper limit of 16 °C as used in the Belgium mix design method, a filler/binder ratio (volume) of about 0.7 or 1.9 (on a mass basis) would result (see Figure 3-16). Using this filler/binder ratio would result in a stiff mastic, which may be appropriate for rut resistant mixes although workability of the mix will decrease.

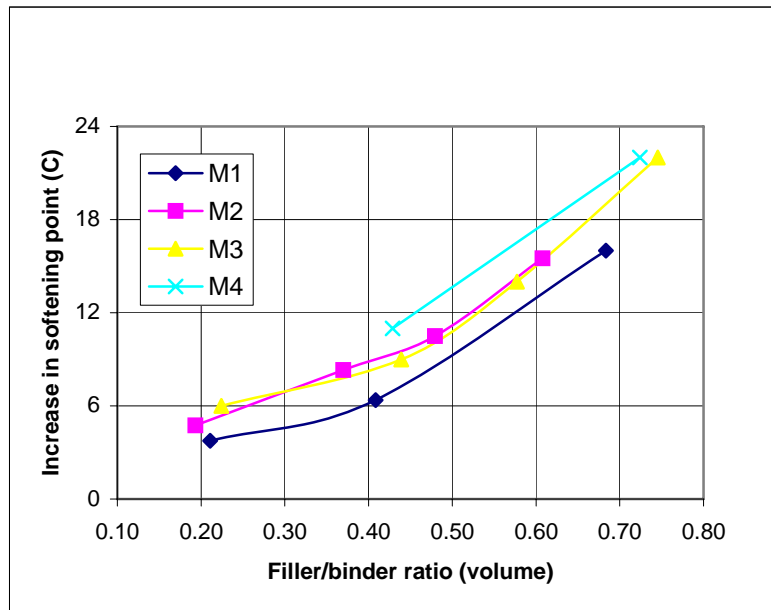


**Figure 3-16: Increase in softening point of mastic (in terms of filler/binder ratio)**

Comparing the filler/binder results to the findings of Cooley *et al* (1998), the stiffening effect with increase in percentage bulk volume of filler follows the same trend (see Figure 3-18), although correlation is not as good. This can be attributed to the fact that fillers were assumed to be of the same density. However, from the results it appears that the use of percentage bulk volume of filler as a unique parameter to predict stiffening is useful. Also, for the results of this study, there appears to be a certain percentage bulk volume of filler above which the stiffening increase, as also found by Kandhal (1981) and Cooley *et al* (1998).

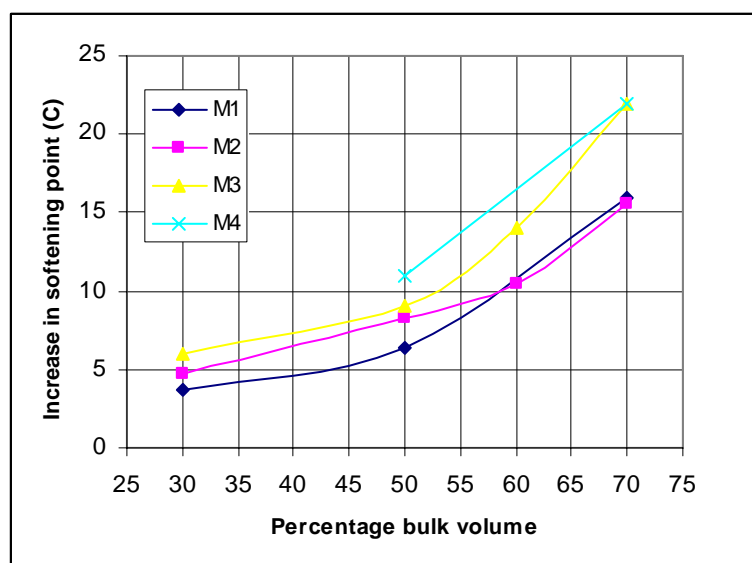


**Figure 3-17: Increase in softening point of mastic (in terms of % bulk volume of filler)**

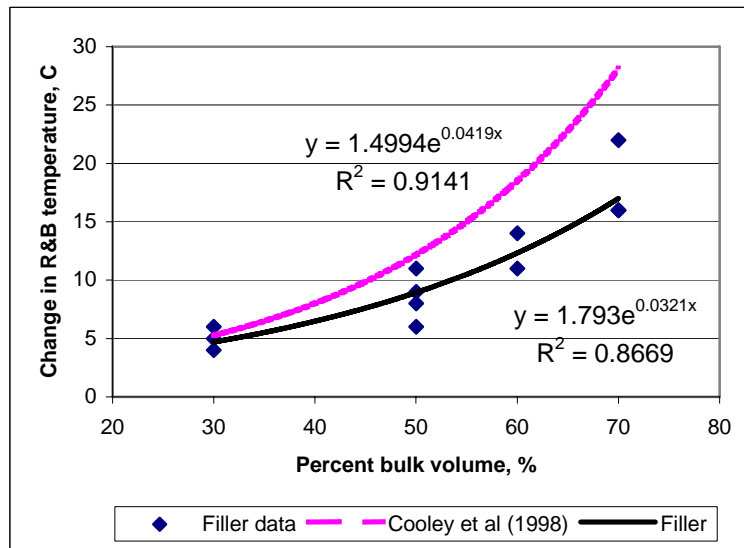


**Figure 3-18: Stiffening of study filler/binder mortars**

Based on the work done by Shashidar and Romero (1999), it was expected that the two finer fillers (M1 and M3) would create the highest stiffening. Figure 3-16 does not validate the findings of Shashidar and Romero, as because fillers M1 and M3 did not create the highest stiffening. Shashidar and Romero, however, based their conclusion on the stiffening potential of different average sizes of the same sand.

Anderson (1982) also tested fillers from various sources and he found in his study that the finer fillers, which he expected to cause the highest stiffening, did in fact not. He concluded that fineness alone is not always a measure of the amount of stiffening that will result when a filler is added to a binder. He also stated that for a given filler source, the finer the filler, the greater the stiffening effect. However, when the filler is  $< 20 \mu\text{m}$ , it can act as an extender rather than creating stiffening. This may explain why the finer fillers investigated in this thesis did not create the highest stiffening.

Based on the findings of the filler/binder characterisation, a filler/binder ratio of between 1.3 and 1.5 (by mass) was selected as optimum for the Contermanskloof material and CALREF binder in question. Figure 3-4 shows the gradation of the experimental mix compared to the 19mm COLTO Coarse mix. Essentially, the filler content of the new mix was reduced to 5.5 percent. A mix with a filler content of 6.5 percent was also investigated.

Gyratory compaction tests were done on the experimental mixes at binder contents of 4.5, 5, 5.5 and 6 percent. Table 3-13 shows the VIM at the Superpave  $N_{des}$  level for the mix with a filler content of 5.5 percent and Table 3-14 the VIM at  $N_{des}$  for the mix with a filler content of 6.5 percent.

**Table 3-13: Gyratory VIM @  $N_{des}$  for different binder contents and traffic levels  
(Experimental mix with filler content of 5.5 %)**

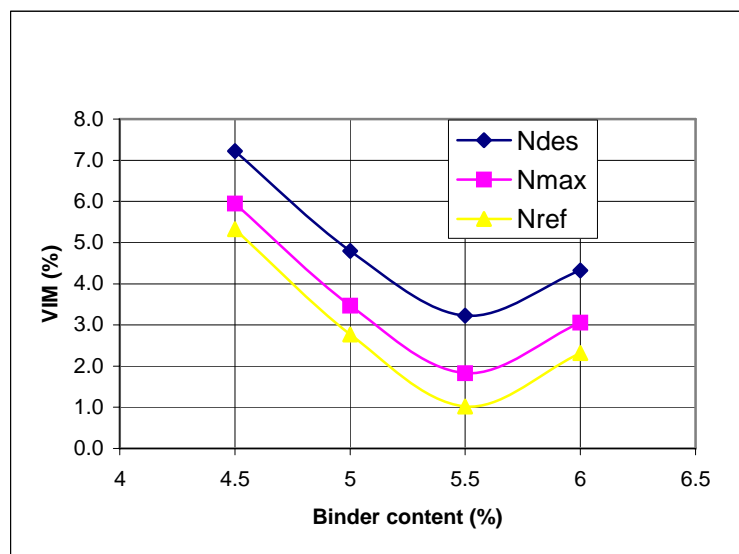
Traffic class	Binder content			
	4.50%	5%	5.50%	6%
<b>A</b>	10.1	7.8	6.4	7.3
<b>B</b>	9.0	6.7	5.2	6.2
<b>C</b>	7.9	5.6	4.0	5.1
<b>D</b>	7.2	4.8	3.2	4.3

**Table 3-14: Gyratory VIM @  $N_{des}$  for different binder contents and traffic levels  
(Experimental mix with filler content of 6.5 %)**

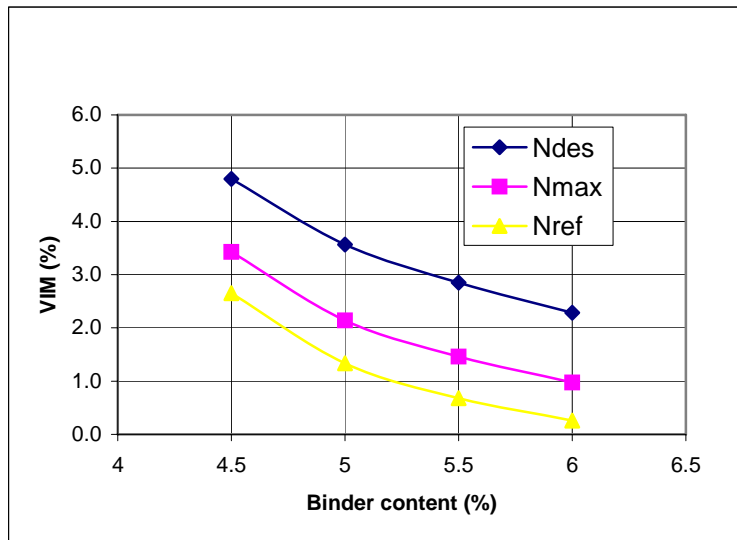
Traffic class	Binder content			
	4.50%	5%	5.50%	6%
<b>A</b>	7.9	6.8	6.1	5.5
<b>B</b>	6.7	5.6	4.9	4.3
<b>C</b>	5.6	4.4	3.7	3.1
<b>D</b>	4.8	3.6	2.9	2.3

Table 3-13 and Table 3-14 may be compared with the gyratory compaction test results for the 19mm COLTO Coarse mix (filler content of 7.7 percent) shown in Table 3-8. A number of observations can be made. The experimental mixes were established by coarsening the 19mm COLTO Coarse mix. For the experimental mix at the lower filler content (5.5 percent), the compactibility at the different binder contents and traffic levels is lower than that of the 19mm COLTO Coarse mix at corresponding binder contents and traffic levels. For the experimental mix with a filler content of 6.5 percent, the compactibility at a binder content of 4.5 percent is higher than the 19mm COLTO Coarse mix for the different traffic levels but is lower at higher binder contents for the different traffic levels. This illustrates the complexity of asphalt mix design and indicates that the compactibility of a mix may be sensitive to even small deviations in gradation.

Figure 3-19 summarises the gyratory compaction test results for the experimental mix at a filler content of 5.5 percent and Figure 3-20 for the experimental mix at a filler content of 6.5 percent. For both cases, the Superpave compaction indices are shown for design traffic level D (see Table 3-7). Based on these results, optimum binder contents of 5.2 and 5.0 percent were chosen for the experimental mixes at filler contents of 5.5 and 6.5 percent respectively. At these binder contents, the VIM at  $N_{max}$  is greater than 2 percent. Mixes with lower filler/binder ratios were then selected for analysis in terms of rutting so that the comparison of compaction and rutting could be made.



**Figure 3-19: Gyratory compaction summary for experimental mix with Filler @ 5.5 %**



**Figure 3-20: Gyrotory compaction summary for experimental mix with Filler @ 6.5 %**

### 3.4.7 Compaction temperature

To evaluate the influence of temperature on the compactibility the mix, specimens were mixed at the design optimum binder content of 4.7 percent and compacted at temperatures of 100 °C and 160 °C. Two specimens were compacted at each of these temperatures. The average curves for these two temperatures are shown in Figure 3-21.

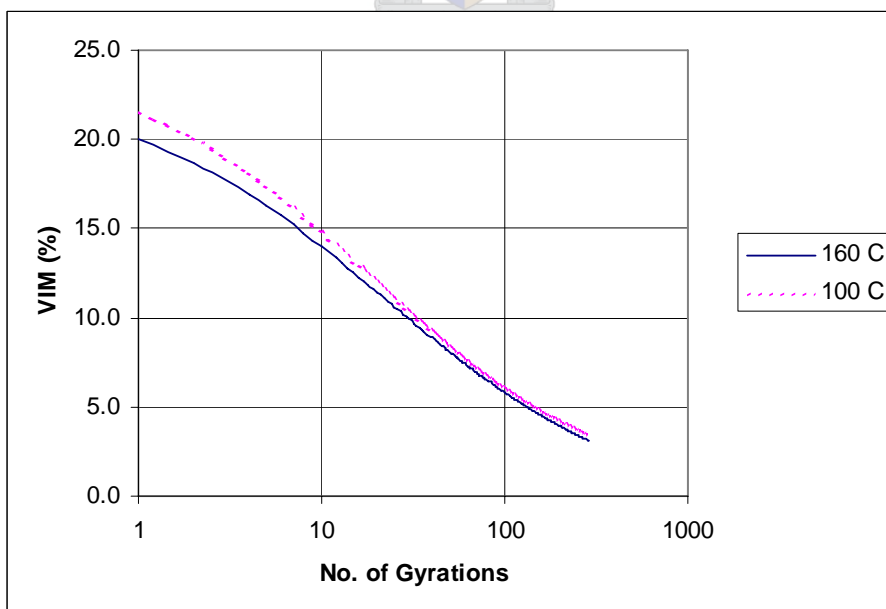


**Figure 3-21: The influence of temperature on the compactibility of the 19mm COLTO Coarse mix**

The compaction results did not indicate a significant influence of compaction temperature on compactibility. Although only the average curves are shown in Figure 3-21, the compaction characteristics for the two specimens at 100 °C varied indicating a likelihood of pronounced variability in compactibility compared to the specimens compacted at 160 °C. Typically one would expect asphalt to have improved compactibility at higher compaction temperatures. The fact that the mean compaction density of the specimens compacted at 160 °C is only slightly higher than that of the specimens compacted at 100 °C may be specific to gyratory compaction and the result at these temperatures is therefore inconclusive. It may also indicate that, with the SGC, as found by Huner and Brown (2001), mixes at lower temperatures are compacted with higher compaction effort since the strain is the same and the load is higher.

### 3.4.8 Mechanical testing

Mechanical tests were done on the 19mm COLTO Coarse mix at binder contents of 4.7 and 5.0 percent to determine the performance properties of this mix. The tests included dynamic creep modulus (at 40 °C), indirect tensile strength and stiffness tests in the indirect tensile mode (at 25 °C).

Two specimens were tested in each case. Table 3-15 shows the mean results for the different tests. The properties satisfy the respective criteria typically established for wearing course mixes. The low indirect tensile strength (ITS) obtained for the specimens at a binder content of 5 percent is contrary to what one would expect since tensile strength typically increases with an increase in binder content on the left of the optimum curve (where this would be expected to be).

**Table 3-15: Mechanical test results on 19mm COLTO Coarse mix**

Test/Binder content	4.7 %	5 %
Dynamic Creep (MPa)	20	46
ITS (kPa)	1193	802
Stiffness (MPa)	1097	1620

Dynamic creep tests were done on the experimental mixes with relatively high binder contents at 40 °C and 60 °C. Binder contents of 5.2 and 5.0 percent were chosen for the experimental

mixes at filler contents of 5.5 and 6 percent respectively. The binder contents of these mixes, although much higher than the binder content of the 19mm COLTO Coarse mix (4.7 percent), still provided satisfactory gyratory compaction results.

Having established the optimum binder contents for the experimental mixes, dynamic creep tests were done on these mixes at temperatures of 40 °C and 60 °C. Table 3-16 shows the results of the dynamic creep tests. Specimens for the dynamic creep tests were gyratory compacted to a 4 percent VIM level.

**Table 3-16: Dynamic creep test results on experimental mixes**

<b>Sample</b>	<b>Filler content</b>	<b>Binder content</b>	<b>F/B ratio</b>	<b>Temp (°C)</b>	<b>Dynamic creep (MPa)</b>
5-1	5.5 %	5.2 %	0.95	60	Failed
5-2	5.5 %	5.2 %	0.95	60	2.2
6-1	6.5 %	5.0 %	0.77	60	4.2
6-2	6.5 %	5.0 %	0.77	60	6.9
5-3	5.5 %	5.2 %	0.95	40	15
5-4	5.5 %	5.2 %	0.95	40	11.8
6-3	6.5 %	5.0 %	0.77	40	16
6-4	6.5 %	5.0 %	0.77	40	10.4

The dynamic creep test results indicate that the mixes appear to have adequate stability at a temperature of 40 °C. At 60 °C, however, one of the specimens failed under repeated loading and the dynamic creep results of the other specimen are well below the experimental limiting value of 10 MPa. The higher binder contents of these mixes have resulted in lower dynamic creep values (Table 3-16) compared with those of the 19mm COLTO Coarse mix shown in Table 3-15. It is however believed by Brown *et al* (2001) that the dynamic creep test’s ability to relate to performance is questionable. They found that for testing above 40EC, samples tend to fail prematurely. Also, the test configuration does not allow for lateral support, while in the field, asphalt always has some form of lateral confinement.

### 3.5 Conclusions

Based on the findings of this chapter, it is evident that the critical factors influencing the compactibility of the wearing course mix investigated include the binder content and the filler/binder interaction.

It was confirmed that the filler has a stiffening effect on the binder. The softening point tests indicated that the reference filler, Contermanskloof (M1), although the second finest filler, had the lowest stiffening effect at the different percentages of percent bulk volume of filler for the four fillers tested. This should be viewed in the light of Anderson's work which shown that fineness of a filler is not always an indicator of its stiffening potential. The relationship established between percent bulk volume of filler and increase in softening point for the fillers investigated was similar to that found by other researchers. The use of percentage bulk volume of filler as a unique parameter to predict stiffening appears useful.

A significant difference in the volumetric properties of the 19mm COLTO Coarse mix was found between the plant and laboratory Marshall mix designs. The difference in the designs must be attributed to the fact that the one Marshall design was based on plant mixes whereas the other Marshall design was done on laboratory mixes using sieved aggregate fractions. The newer Marshall mix design, at the design binder content of 4.7 percent had VIM after Marshall compaction in excess of 5 percent indicating that the mix is relatively harsh and difficult to compact at this binder content. The minimum VMA occurred at a binder content of 5.5 percent and there was a definite increase in the VFB with the addition of binder beyond 5.5 percent.

A comparison of volumetric data from the Marshall and gyratory compaction tests indicated that Marshall compaction does not necessarily correspond with a fixed Superpave traffic level at the different binder contents. It appeared that at the higher binder contents, Marshall compaction is more "punishing" and perhaps misleads the mix designer as to the compactibility of the mix at these higher binder contents. As a consequence, optimum binder contents based on Marshall mix designs may be lower or higher than those based on gyratory compaction mix designs.

The influence of compaction temperature on compactibility at the test temperatures was inconclusive. The mean compaction density of the specimens compacted at 160 °C was only slightly higher than that of the specimens compacted at 100 °C, although the variability in the

compaction at 100 °C was greater. The results could also mean that, in terms of the SGC, there is at least a window (100 °C – 160 °C) in which compactibility seems to stay more or less constant.

It was found that the lowest VIM is achieved using gradation exponents less than 0.4. Above 0.4, the VIM of the mixes evaluated increased significantly. The use of very low  $n$ -values for gradations results in mixes with a higher percentage of finer materials, particularly within the sand fraction. This fine material may act as a bitumen extender and thereby aid compaction. A greater percentage of finer material will also assist in filling the voids in the stone skeleton of the mix. These fine mixes may have questionable skid resistance, particularly mixes having an  $n$ -value of 0.2.

As expected, increases in binder content facilitated compaction. The Superpave  $N_{des}$  and  $N_{max}$  criteria were used to establish acceptable binder contents for the continuously graded mixes.

An increase in filler content from 4 to 6.5 percent improved the compactibility of the 19mm COLTO Coarse mix slightly. The use of filler as a bitumen extender and void reducer appears to be beneficial but its benefit reduces when the optimum filler/binder ratio is exceeded due to excessive stiffening of the mix, as illustrated by the softening point tests.

It was found that at corresponding binder contents and traffic levels, the compactibility of the experimental mixes (with the exception of the experimental mix with a filler content of 6.5 percent and a binder content of 4.5 percent) was less than that of the 19mm COLTO Coarse mix. This indicated that the compactibility of a mix may be sensitive to even slight variations in gradation and emphasised the complexity of asphalt mix design.

It is recommended that softening point tests be done on filler/binder mastics at varying degrees of percent bulk volume of filler. An increase of 12 °C in the softening of the mastic compared to that of the base bitumen should be used to establish the maximum filler/binder ratios to optimise the stiffening effect of the filler. Binder contents should be established based on these ratios. Gyrotory compaction tests and mechanical tests should be done to validate the suitability of these binder contents.

# **4 INFLUENCE OF COMPACTABILITY ON PAVEMENT RUTTING PERFORMANCE: CASE STUDIES**

## **4.1 Introduction**

### ***4.1.1 Background***

This chapter presents five case studies in which some of the factors influencing the rut resistance and moisture damage of an asphalt mix are evaluated by means of APT. The relationship between compactability and rut resistance is also highlighted. APT was performed using the MMLS3. MMLS3 testing was performed on laboratory compacted briquettes and slabs, as well as full-scale field pavements. Tests were performed as hot/wet (trafficking with water at high temperature) and hot/dry (trafficking without water at high temperature).

Most of the laboratory compacted specimens were at 7 percent voids before MMLS3 trafficking. Generally, the level of compaction after construction in the field is specified at 93 % Rice density. So the laboratory tests are representative of trafficking during the early life of the layer.

Selected fatigue and SASW testing were performed on specimens after trafficking to gauge the relative damage due to MMLS3 trafficking.

### ***4.1.2 Influence of compaction on asphalt properties and influence on rutting performance***

As an asphalt layer is compacted the amount of air voids is reduced. Various researchers have reported that on the importance of proper compaction on the ultimate performance of an asphalt pavement under traffic. Compaction increases the mixture stability by forcing the aggregate particles closer together and achieving greater particle-to-particle contact (Asphalt

Institute, 2002). Both particle interlock and inter-particle friction will normally increase as mix density increases, up to a point (Semmelink, 2000).

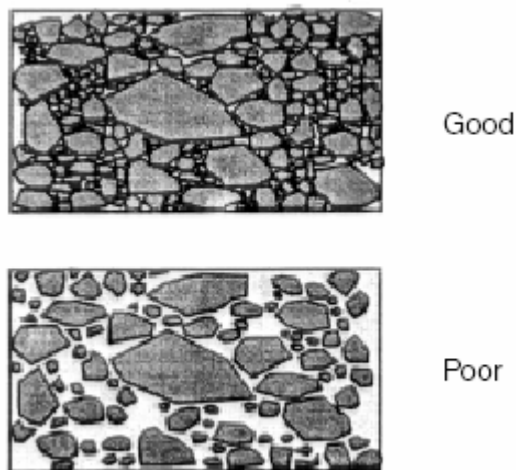


**Figure 4-1: Impact of Compaction on the Orientation and Interlock of Aggregate Particles in an Asphalt Mix (Santucci, 2001)**

Linden and van der Heide (1987) reported that a well-compacted mix has better durability and better mechanical properties, which, at a lower binder content will deliver a high resistance against permanent deformation. They also reported that a higher degree of compaction will improve durability and will result in a higher dynamic resilient modulus.

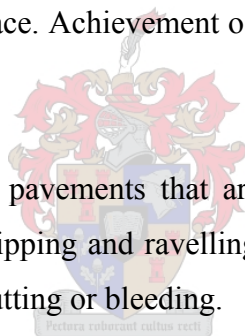
Santucci (2001) reported that the primary benefit of increased compaction is to pack and orient the aggregate particles in the asphalt mix into an interlocking mass of material that resists shear deformations. Bissada (1983) found that increased compaction results in a relative increase in the volume of mineral aggregates, which improves the strength of the asphalt mix by increasing the components of its frictional resistance. This appears to be valid only as long as the VIM does not reach a critical end value. As soon as the percentage of VIM drops below this critical value, due to further traffic densification, significant losses in the component of frictional resistance start to occur, which results in low stiffness values and excessive permanent deformation.

Too many voids may cause instability because of a lower degree of particle interlock, and the layer will also be more permeable, allowing air and water to enter more freely

(Simmelink, 2000). This shortens its life on account of greater oxidation and stripping of the binder. On the other hand, if all inter-particle voids are filled with binder, the asphalt layer will also not perform properly because of the reduction in particle interlock and loss in stability. The layer will then tend to fat up, and may even rut in severe cases as a result of the loss in stability. This is emphasized by Cross and Brown (1991), who pointed out the importance of in-place air void contents above three percent to decrease the probability of premature rutting throughout the life of the pavement.

As the asphalt mix is laid, the aggregate particles in the mix may or may not be in contact; however, their respective binder films will be in contact (Rickards *et al*, 1999). As compaction proceeds, reorientation of the aggregate particles suspended in the bitumen phase will occur as the binder flows under the external compaction force. The final reorientation will involve rotation or sliding, until all the forces – internal and external – at the aggregate contact points are in equilibrium. As the aggregate particles move and rotate, shearing of the bitumen will occur at the binder-aggregate interface. Achievement of inter-particle contact relies on binder shear flow.

De Sombre *et al* (1998) stated that pavements that are under-compacted might experience problems such as rutting, fatigue, stripping and ravelling. Pavements that are over-compacted may also experience problems with rutting or bleeding.

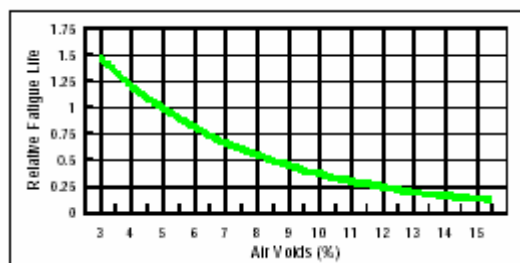


The fatigue life of an asphalt mix is directly related to the air void content of the asphalt mix (Scherocman and Acott, 1989). Environmental variables that increase the time available for compaction can decrease the air void content of the mix and thus increase the fatigue life of the mix. The air void content also has a significant effect on the hardening of the binder in an asphalt mix (Finn *et al*, 1990).

Mixes that are not compacted properly will have less resistance to rutting due to a weaker structure and secondary consolidation under traffic (AAPA, 1999). Figure 2-17 gives an indication of relative rutting rate of a mix designed for 5 percent voids and compacted to different voids levels.

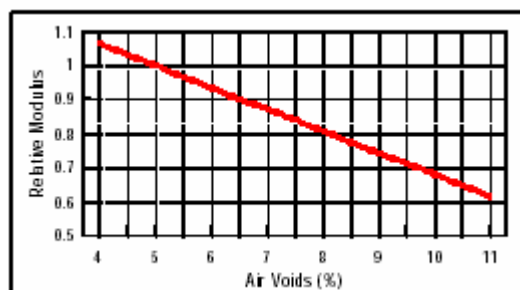
Compaction density will also affect the fatigue life of an asphalt pavement. Figure 4-2 shows results of fatigue testing of the same mix relative to compaction at 5 percent voids. In this

figure it is illustrated how an increase of air voids from 5 percent to 8 percent can result in a 50 percent reduction in fatigue life.



**Figure 4-2: Relative fatigue life vs. air voids (AAPA, 1999)**

The structural strength of an asphalt mix, as measured by its stiffness, is also related to compaction level. Figure 4-3 shows stiffness modulus relative to 5 percent air void content. In this case an increase in voids from 5 percent to 8 percent has resulted in a 20 percent reduction in stiffness or load carrying capacity.



**Figure 4-3: Relative stiffness modulus vs. air voids (AAPA, 1999)**

Hunter *et al* (2000) stated that over-compaction may have adverse affect on the performance of the layer. An increase in the density of an asphalt mix improves the resistance to permanent deformation and to fatigue cracking along with an increase in elastic stiffness.

Rickards *et al* (1999) concluded that low compaction could result in low tensile strength of the asphalt mix. This is also echoed by Haddock *et al* (1999), which stated that higher compaction produces higher strength.

The performance of asphalt mixtures is influenced by its internal structure, which refers to the arrangement of aggregates and their associated air voids (Masad *et al*, 1999). This internal structure is mainly affect by the method of compaction, such that specimens with the same average percent voids may have a different distribution of air voids, and are thus expected to respond differently under loading and yield distinct mechanical properties in laboratory testing. These differences in mechanical properties have also been observed by Sousa *et al* (1991). They found that rolling wheel compaction results in mixes with higher stiffness. The orientation of aggregates and aggregate contact points may also be different and can have an influence on the shear strength properties of the mix (Masad *et al*, 1999). A higher number of coarse aggregate contacts will result in higher shear strength.

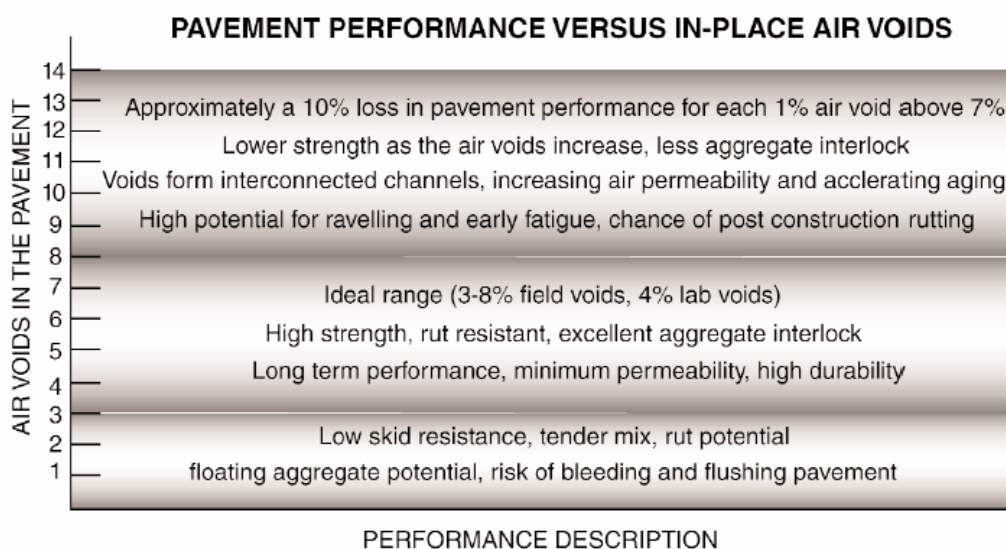


**Figure 4-4: Chart showing the relationship between density (expressed in terms of air voids remaining) and performance (NETTCP, 2002).**

### ***4.1.3 Accelerated pavement testing (APT)***

Metcalf (1998) defined full scale APT as “ ... the controlled application of prototype wheel loading, at or above the appropriate legal load limit to a prototype or actual, layered, structural pavement system to determine pavement response and performance under controlled, accelerated, accumulation of damage in a compressed time period.”

For small scale APT, the definition must include wheel loadings below the legal load limit (Hugo, 2000). APT is a tool that can be used for the evaluation of performance of new pavement materials (e.g. reinforced asphalt, cement treated bases, etc.), distress mechanisms such as impact of water, pavement distress and selection of rehabilitation strategies. Evaluation is often done to determine the present condition of a pavement in terms of remaining life and mechanisms of failure, and enable future performance to be predicted and/or for implementation of maintenance and rehabilitation strategies.

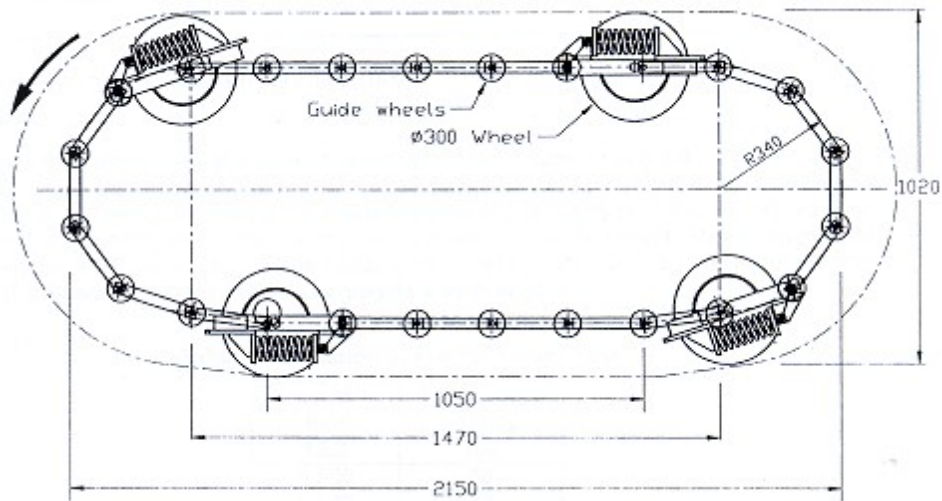
The immediate benefit of scaled APT is that testing can be done at a fraction of the cost of full-scale APT. Furthermore, testing can be done either in the laboratory or in the field under controlled environmental and testing conditions. This allows many of the variables impacting pavement systems to be controlled directly. Examples are the control of pavement temperature and trafficking speed. These factors have a direct influence on the stiffness of asphalt layers and hence the response of the pavement under loading.

Figure 4-5 shows a schematic of the MMLS3 wheel configuration. The main advantages of this type of scaled APT device are that:

1. The load is always moving in one direction
2. Many repetitions are possible in a short period
3. A relative high trafficking speed is possible

A further advantage of the MMLS3 is that it can be used to carry out field tests on conventional pavement mixtures (provided that the maximum particles size is less than 25mm). The device has four wheels (300 mm diameter and 80 mm wide) and these can be laterally displaced across 150 mm in a triangular distribution about the centre-line. The MMLS Mk.3 is able to apply 7200 wheel loads per hour. The wheel load can be set to 1.9 kN up to 2.7 kN and tyre pressures may be varied up to 800 kPa. The MMLS 3 has been used extensively to evaluate both the rutting and fatigue characteristics of asphalt mixtures. It has also been used to

test the effectiveness of steel reinforcement in a wearing course layer. Operating instructions and other technical information are available in the MMLS3 Operators Manual (Müller, 1999).



**Figure 4-5: Wheel Configuration of the MMLS Mk.3**

A. Epps *et al* (2001) conducted research to relate the rut depth under MMLS3 loading to a terminal rut depth under full-scale traffic loading. The MMLS3 tyre pressure was 690 kPa (at 25 °C) with a wheel load of 2.1 kN. For the full-scale truck, with dual wheels, the tyre pressure was 700 kPa (at 25 °C) and the load 20 kN per single wheel. Comparative tests were done on a full-scale pavement under full scale truck trafficking and MMLS3 trafficking at a temperature of 60 °C. This temperature is regarded as the critical temperature for permanent deformation over an extremely hot period during the summer. At this temperature, a rut depth of 10mm was set as failure criterion under full scale truck trafficking. A. Epps *et al* developed rut depth criteria with a maximum average of 3.5 mm under the MMLS3 for three transverse profiles after 100 000 MMLS3 load repetitions at the critical temperature for permanent deformation over a hot summer period.

## 4.2 CASE STUDY 1: Influence of filler/binder ratios on rut resistance

In Chapter 2 the stiffening effect of filler on the viscosity of a binder was highlighted. It has been found that an optimum filler/binder ratio for compaction exists, but too high filler/binder ratios may result in mixes that are difficult to compact. Tayebali *et al* (1996) also found that increase in filler content may enhance rutting performance, but at a higher filler content, the binder content is reduced which may have a detrimental effect on other mixture properties such as fatigue, thermal cracking, and ravelling.

In Chapter 3, optimum filler/binder ratios were established for the 19 mm COLTO Coarse mix to optimise the stiffening effect. Based on the findings of Chapter 3, it was decided to investigate alternative (experimental) continuously graded asphalt mixes, with lower filler/binder ratios. This was done by the author (Jenkins and Douries, 2001(c)) to ascertain whether improving the compactibility of these mixes have compromised their resistance to permanent deformation. APT of laboratory compacted slabs were done under the MMLS3 to evaluate the rut resistance of these mixes.

Four different asphalt wearing course mixes were tested. A total of two rutting tests with the MMLS3 were to be done at an average temperature of 55 °C. Slabs were manufactured at the University of Stellenbosch using retained samples (at room temperature) obtained from Much Asphalt (Pty) Ltd. in paper bags. These mixes were slowly reheated in a draft oven to 150 °C. The asphalt was compacted at  $\pm 135$  °C as described in section 4.2.2.

### 4.2.1 Materials

In total, four different continuously graded wearing course mixes were tested. The gradation and the properties of the different mixes, as received from Much Asphalt (Pty) Ltd is shown in Figure 4-6 and Table 4-1 respectively. Two MMLS3 tests were performed and three mixes were tested in one test as shown in Table 4-2.

**Table 4-1: Properties of mixes with adjusted filler/binder ratios**

Properties	Mixes			
	19mm	13 mm A	13 mm B	9 mm
Binder content (%)	4.6	5.3	5.5	5.7
Rice density	2.534	2.513	2.504	2.507
Bulk relative density	2.433	2.398	2.358	2.402
Marshall VIM (%)	4.0	4.6	5.8	4.2
Stability (kN)	13.4	13.8	12.3	13.9
Flow (mm)	3.6	3.5	2.7	3.6
Filler/binder ratio (m/m)	1.2	1.4	1.1	1.3

To distinguish between the two 13 mm mixes, they designated Mix A and Mix B respectively (refer Table 4-1). The aggregate was Hornfels from the Eerste River quarry. The binder was 60/70-penetration grade bitumen from the CALREF refinery.

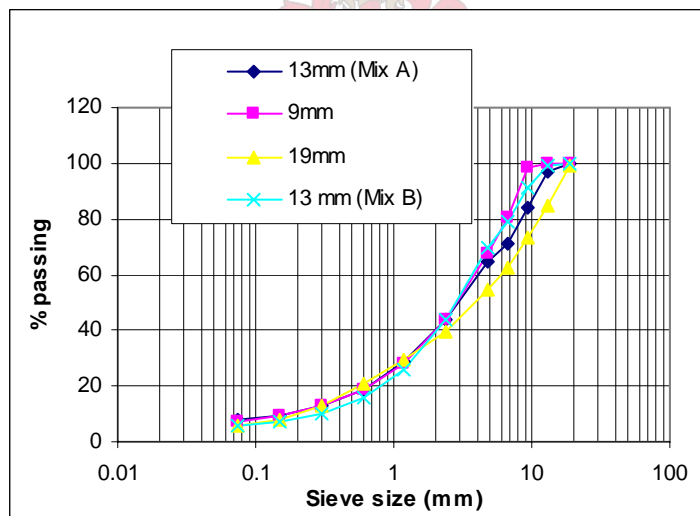


**Figure 4-6: Gradations of mixes with adjusted filler/binder ratios**

**Table 4-2: MMLS3 Test sequence for mixes with adjusted filler/binder ratios**

MMLS Test No.	Mixes			
	19mm	13 mm A	13 mm B	9 mm
1	<input type="checkbox"/>	<input type="checkbox"/>		<input type="checkbox"/>
2	<input type="checkbox"/>	<input type="checkbox"/>	<input type="checkbox"/>	

### 4.2.2 Specimen preparation

The asphalt slabs were compacted in steel moulds at  $\pm 135\text{ }^{\circ}\text{C}$  using a Kango hammer. The head of the Kango hammer was modified by welding a square base plate (150 mm x 150 mm) onto the existing circular head. The slabs were compacted attempting to obtain 7 percent VIM. The compaction was controlled using a steel mould of known volume (300mm x 300mm x 60 mm). It should be noted that no actual density measurements were carried out on the slabs.

### 4.2.3 Set up

A wooden mould was used to hold and confine the slabs (see Figure 4-7). The slabs were placed on a 5 mm masonite board overlying a concrete base. The masonite was stiff so as not to deflect or deform under the loading. It was just used to ensure the slabs didn't stick to the concrete floor. The setup consisted of five slabs. The three slabs in the middle are the actual test slabs, and two dummy asphalt slabs were used on either side for the on- and off-ramps. The reason for the position of the slabs must be related to the load distribution under the MMLS3. Loading occurs when the MMLS3 wheels strike the pavement on the on-ramp slab. The load is then maintained over the middle one metre of the test section before the wheels are lifted on the off-ramp slab.

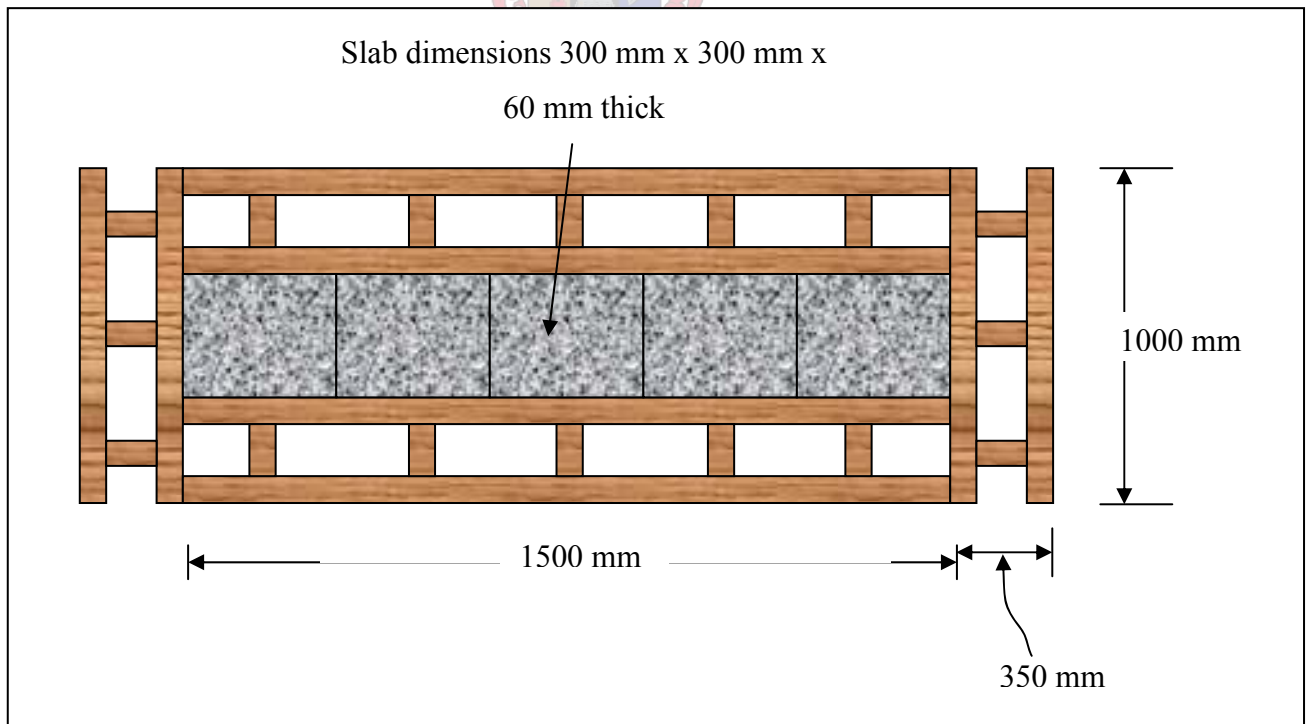


**Figure 4-7: MMLS3 Wooden mould and slab configuration**

#### 4.2.4 Temperature control and measurements

The heating process entailed blowing hot air across the test slabs from both sides. The direction of the heat flow changed every six minutes. The heating process was regulated by an automatic control in the heating unit. Thermocouples were placed within the asphalt at mid-depth to monitor the asphalt temperature during testing. After profile measurements it was necessary to reheat the slabs for a period before commencing with MMLS3 trafficking.

#### 4.2.5 Rut profile measurements

Transverse profile measurements were taken after specific intervals to obtain the rut depths and rate of rutting during MMLS3 trafficking i.e. after 0, 1000, 10 000, 25 000, 50 000, 100 000 and 150 000 axles. These are measurements of the vertical deformation of the asphalt under trafficking. The profilometer measure the change in height relative to a position with fixed coordinates with accuracy of 10  $\mu\text{m}$  (Müller, 2001). The positions at which these measurements were taken are indicated on Figure 4-8 as dotted lines from position 1 through 13 in the direction of trafficking. These positions were chosen to have transverse profiles across each tested slabs as follows:

- 1) Three profiles in the middle third of each slab, 50 mm apart
- 2) Four profiles 50 mm from the interface of the slabs to provide information regarding transition of the MMLS3 wheel from one slab to another.

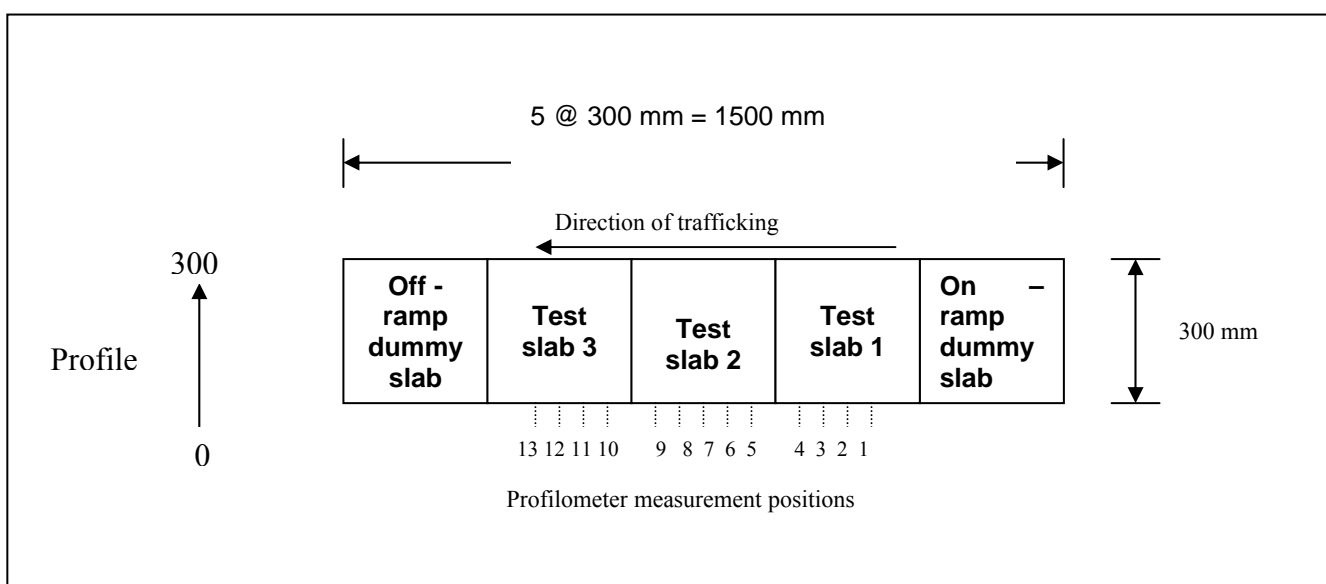


Figure 4-8: Slab configuration with transverse profile positions

### 4.2.6 MMLS3 Rutting results

The test temperature for the MMLS3 testing was determined from the seven hottest days according to the method set out by Huber (1994). The test conditions were as follows:

- Number of load repetitions 150 000
- Tyre pressure 690 kPa
- Scaled wheel load 2.5 kN
- Test temperature (asphalt) 55 °C
- Load rate 7200 repetitions per hour

The target average asphalt temperature for both tests was 55 °C, but due to technical difficulties the average mid-depth asphalt temperature for test 1 was  $53 \pm 2$  °C and  $50 \pm 1$  °C for test 2.

The cumulative rutting curves for test 1 are shown in Figure 4-9.

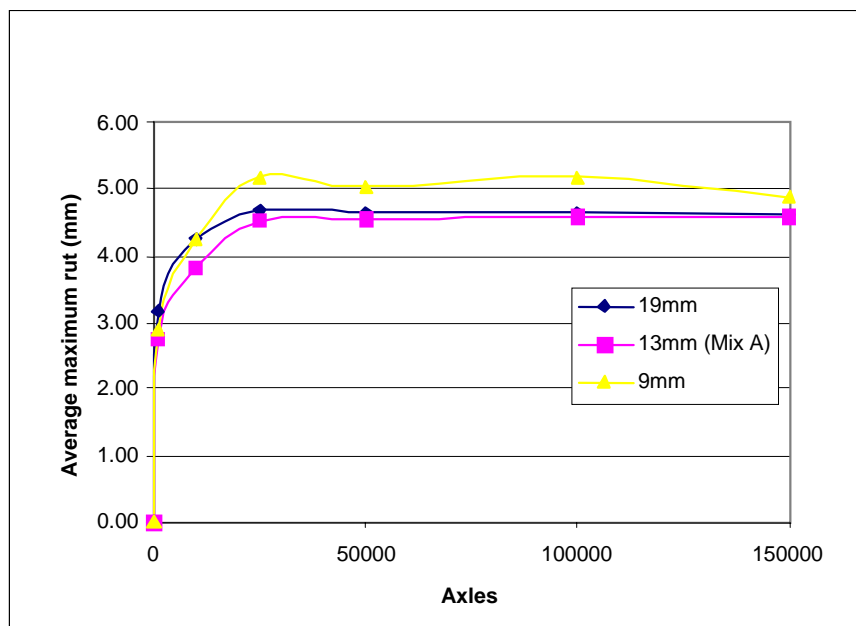


**Figure 4-9: Cumulative rutting curves for Test 1**

From Figure 4-9 it is evident that the 9mm mix had the largest maximum rut. The 19 mm and 13 mm (Mix A) mixes performed fairly the same except for a larger initial settlement for the 19 mm mix. The rate of rutting decreased after 25 000 axles for all three mixes. It shows there is little increase in the rutting after 25 000 axles. No gyratory compaction was performed on these mixes, but when looking at the available Marshall compaction data (Table 4-3); the 13 mm (Mix A) specimens with the lowest compactibility ranking performed best in terms of rut resistance.

The results for the second test are shown in Figure 4-10. From this figure, it can be seen that Mix B has the largest initial settlement (1.6 mm) followed by Mix A (1.4 mm). The rut progression of the 19 mm and Mix A is fairly the same up to 50 000 axles, thereafter the rutting rate of the Mix A is larger. Although Mix B deformed faster initially, the rutting rate decreased with little deformation thereafter. Compared to Mix A, with a larger increase in rutting over time, Mix B had a smaller maximum rut at the end of the test. The behaviour of Mix B after 100 000 axles can possibly be related to an improved aggregate interlock. It appears that after 100 000 axles, the binder did not play considerable role in the rut resistance. The improved aggregate interlock now provides better shear resistance and subsequent rut resistance.

Sousa (1994) stated that as an asphalt mix densifies under traffic, it steadily develops better aggregate interlock and resistance to shear stresses. However, the mix might lose stability when the reduction of the air void content causes the binder to prevent point-to-point contact in the aggregate structure.

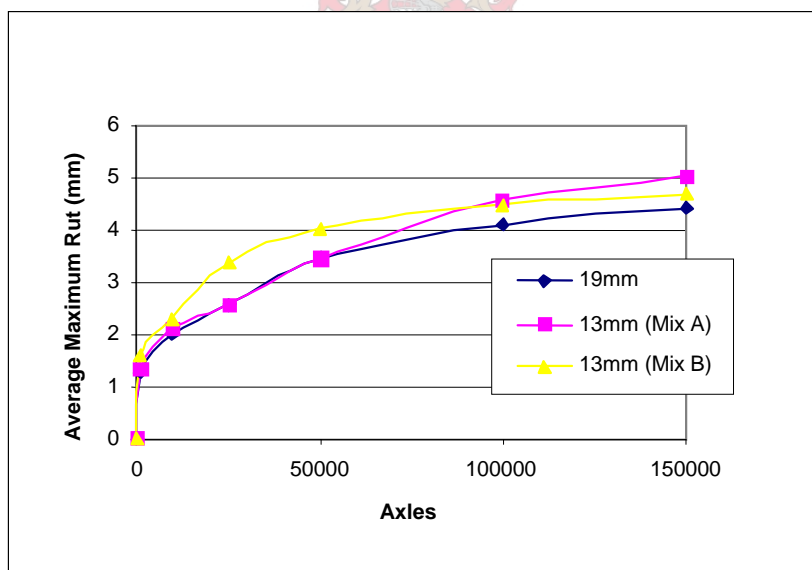


**Figure 4-10: Cumulative rutting curves for Test 2**

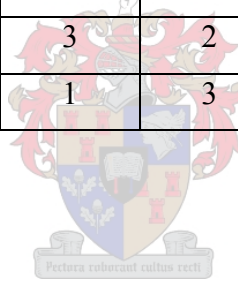
An important aspect between the two tests is the influence of the temperature. Inadvertently, test 1 was carried out at 53 °C and test 2 at 50 °C. Nevertheless, the results of the 19 mm and Mix A are comparable.

**Table 4-3: Summary of results**

Property	TEST 1			TEST 2		
	19 mm	Mix A	9mm	19 mm	Mix A	Mix B
Marshall VIM (%)	4.0	4.6	4.2	4.0	4.6	5.8
F/B ratio (m/m)	1.2	1.4	1.3	1.2	1.4	1.1
$\Delta T_{r\&b}$ (°C)	9.1	12.4	10.0	9.1	12.4	8.5
Rut @ 50 °C @ 150000 MMLS3 reps	4.7	4.6	5.8	4.4	5.0	4.7

**Table 4-4: Ranking of mixes**

Property	TEST 1			TEST 2		
	19 mm	Mix A	9mm	19 mm	Mix A	Mix B
Compactibility	1	3	2	1	2	3
F/B ratio	1	3	2	2	3	1
Rut resistance	2	1	3	1	3	2



#### 4.2.7 Conclusions of CASE STUDY 1

When ranking the mixes in terms of compactibility (based on Marshall compaction), the best compactable mix does not necessarily exhibit the best rut resistance. This conclusion may be specific to Marshall compaction.

It appears that compactibility alone is not necessarily the only indicator of whether a mix will perform good or bad in permanent deformation response. Compaction energy and stresses are different than those present in permanent shear deformation. Also, compaction is achieved at lower viscosities than is the case with permanent deformation.

The 9mm mix was the least rut resistant. This could be related to a slightly higher binder content.

The 13mm mix (Mix B), with lower filler/binder ratio for improved compactibility, showed better rut resistance at the end of the test than the 13mm mix (Mix A), although it had a larger initial deformation. This behaviour of Mix B to the end of the test can possibly be related to an improved aggregate interlock. It appears that after 100 000 axles, the binder did not play considerable role in the rut resistance. The improved aggregate interlock now provides better shear resistance and subsequent rut resistance. It can be concluded that reduction of the filler/binder ratios in order to improve compactibility does not significantly increase rutting under APT.

It is recommended that in the test setup of five slabs in series, at least three slabs of the same mix be tested during one test to reduce the variability of the test results.

### **4.3 CASE STUDY 2: Influence of Polymer Modified Binders (PMBs) on rut resistance of intersections**

Rutting is a common problem encountered at busy intersections. A survey of different intersections in the Cape Town Central Business District (CBD) showed major deformations in the wearing course and bituminous base. These higher incidents of rutting at intersections can partly be explained by the increased loading time and braking and acceleration forces (Dawley *et al*, 1990). Slow-moving or standing loads subject the pavement to higher stress condition (starting and stopping movements, increased temperatures, turning movements, etc.), which may be enough to induce rutting or shoving. In addition, the increase in the number of trucks and heavier wheel loads also can play a significant role in the premature failure of some pavements.

This case study reports on the performance testing of a standard wearing course mix typically used in the Cape Town Central Business District (Jenkins and Douries, 2002). APT testing was done using the MMLS3. Different modified asphalt mixes were tested and compared to determine the influence of the modifiers on improving the rutting performance of the standard mix. The influence of different filler/binder ratios on the rutting performance of these modified mixes was also investigated. Because this study included limited laboratory compaction results

and APT results, the link of compaction and rut resistance could be analysed for PMB mixes.

Three variations on CTCC's standard mix were analysed:

- 1) STD - no modified binder
- 2) LD - Gilsonite / Loadas modifier
- 3) EVA - EVA modifier

For each of these three binders, the binder and filler contents were varied as in Table 4-5.

**Table 4-5: Binder and filler contents of PMB mixes**

<b>Designation</b>	<b>Binder content (%)</b>	<b>Filler content (%)</b>	<b>F/B ratio (m/m)</b>	<b>F/B percentage [F/(F+B)x100]</b>
<b>4A</b>	4.0	4.0	1.0	50
<b>4C</b>	4.0	7.4	1.9	65
<b>5D</b>	5.0	5.0	1.0	50
<b>5E</b>	5.0	6.8	1.4	57.5
<b>5F</b>	5.0	9.3	1.9	65

**Table 4-6: Test sequence for PMB mixes**

<b>Test No.</b>	<b>Mix</b>		
<b>1</b>	EVA 4A	STD 4A	LD 4A
<b>2</b>	EVA 4C	STD 4C	LD 4C
<b>3</b>	EVA 5D	STD 5D	LD 5D
<b>4</b>	EVA 5E	STD 5E	LD 5E
<b>5</b>	EVA 5F	STD 5F	LD 5F

### 4.3.1 Materials and testing

A total of 5 tests were carried out. For each test, the set up consisted of three test slabs plus two dummy slabs at each end (see Figure 4-8). A total of 25 slabs were compacted; the 15 test slabs plus 10 dummy slabs. The materials were mixed at temperatures of 150 °C to 170 °C and compacted at 140 °C to 155 °C, depending on the modifier used (see Table 4-7). The compaction and setup were the same as in section 4.2.2 through 4.2.5.

No gyratory compaction was performed on these mixes to assess their compactibility, but by observing Table 4-7, it can be seen that the modified mixes requires higher mixing and compaction temperatures.

**Table 4-7: Mixing and Compaction temperatures for different modifiers (Distin, 2002)**

Modifier	Mixing Temperature (°C)	Compaction Temperature (°C)
No Modifier	150	140
Gilsonite/Loadas	160	150
EVA	170	155

The test conditions were as follows:

- Number of load repetitions 150 000
- Tyre pressure 690 kPa
- Scaled wheel load 2.5 kN
- Test temperature (asphalt) 50 °C
- Load rate 6 000 repetitions per hour

### 4.3.2 Test results

All five tests were done at an average asphalt temperature of 50 °C (at mid-depth). Transverse profile measurements were taken every 4 mm across the slabs after 0, 1000, 10 000, 25 000, 100 000 and 150 000 axles. Figure 4-11 through Figure 4-13 give a comparison of the cumulative rutting of the different mixes.

As expected, the maximum rut increase with an increase in the total number of load repetitions. In Figure 4-11, all five mixes exceeded 8 mm rutting after 100 000 axles. The mixes with the lower binder content (4percent) showed better rut resistance, as expected. At 4 percent binder content, there was no significant difference between the rut resistances for the two different filler/binder ratios. Comparing the filler/binder ratios of the mixes with 5 percent binder, the mixes with a filler/binder ratio in percentage of 57.5 percent showed the best rut resistance. The ranking of rut resistance for filler/binder ratio percentages were 57.5 percent, 65 percent and then 50 percent from best to poorest performance.

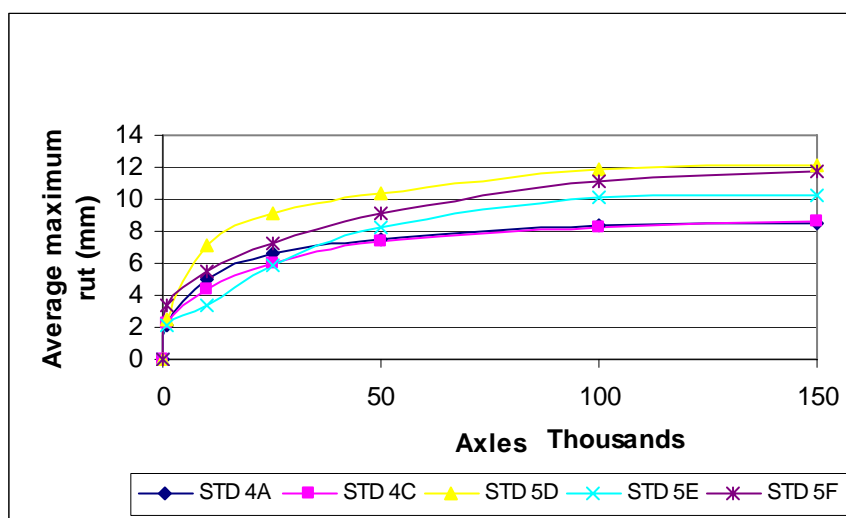


**Figure 4-11: Cumulative rutting curves – STD mix**

The rutting results for the EVA modified mix (Figure 4-12) indicate an improvement of more than 50percent in rut resistance, compared to the standard mix. For the 4percent binder content mixes, there appear to be a significant difference between the different filler/binder ratios, but EVA 4C mix (65 percent filler/binder) show a substantially large initial settlement, but this could be as a result of possible differences in the initial compaction. It appears that the VIM for this particular mix might have been higher than 7percent at the start of the test.

After the large initial settlement, the rate of rutting for this particular mix was similar to that of the other 4percent binder mix (EVA 4A). As for the 5percent binder mixes, the filler/binder ratio in percentage of 57.5 percent showed the best rut resistance. The ranking of rut resistance was also the same as for the standard mix.

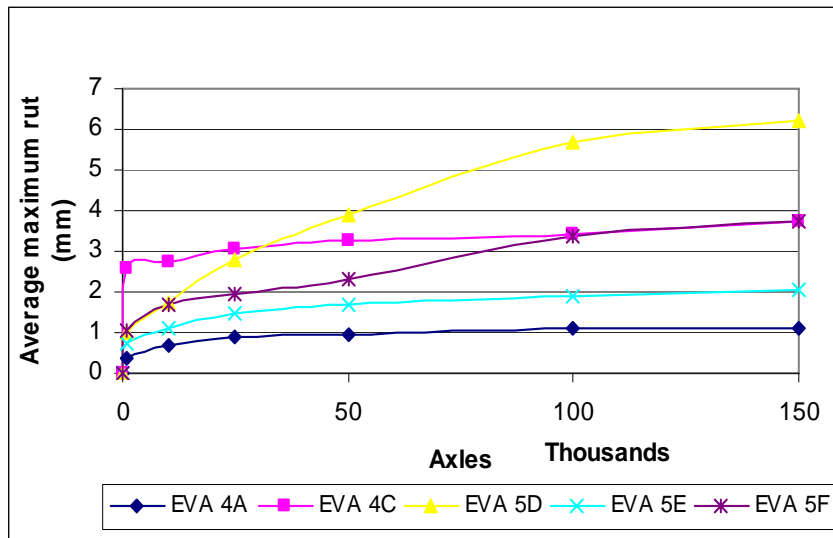


**Figure 4-12: Cumulative rutting curves – EVA mix**

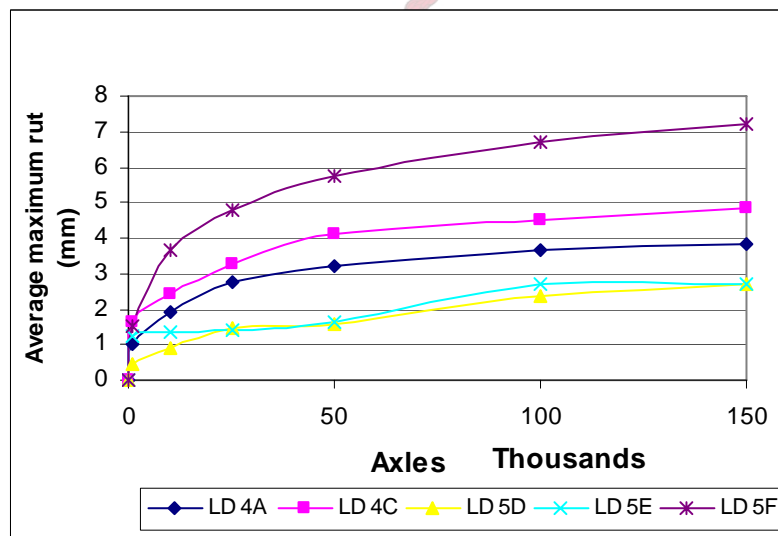


**Figure 4-13: Cumulative rutting curves – LD mix**

As in test1 and test 2, the EVA mix showed better rut resistance than the other two mixes. The ranking of rut resistance was EVA 5E, LD 5E and then STD 5E.

The only available compaction data was for the mixes shown in Table 4-8. The filler/binder ratios for the STD mixes were the same, but they had different binder contents. The difference in binder contents can be seen in the compaction data. The mix with 5% binder contents was compacted to significantly lower air void contents with both the Marshall and gyratory

compactor. It is therefore expected that this mix would show higher rutting, as can be seen in Table 4-8. Comparing the STD mixes with the corresponding PMB mixes in terms of binder content, it can be seen that EVA 4A had better compaction than STD 4A and the void contents of LD 5C and STD 5C were comparable. One would expect the STD mixes to compact better. Since the binder properties of these mixes are totally different, it is not justified to make a comparison between compaction and rutting solely based on same binder content and same filler/binder ratio. Because of the properties of the PMB, one would expect it to perform better than an unmodified binder in terms of rutting. This is in fact shown in Table 4-8.

**Table 4-8: Compaction and Rutting results for PMB mixes**

Property	Mix			
	STD 4A	STD 5D	LD 5D	EVA 4A
<b>Binder content (%)</b>	4.0	5.0	5.0	4.0
<b>Filler content (%)</b>	4.0	5.0	5.0	4.0
<b>F/(F+B)x100 (%)</b>	50	50	50	50
<b>Marshall voids (%)</b>	9.7	6.4	6.5	8.0
<b>SGC voids @ 288 gyr (%)</b>	6.5	4.3	3.9	4.3
<b>Rut @50 °C @ 100000 MMLS3 reps</b>	8.3	11.8	2.4	1.1
<b>Rut @50 °C @ 150000 MMLS3 reps</b>	8.5	12.2	2.7	1.1

### 4.3.3 Conclusions of CASE STUDY 2

Based on the results of this section, it is evident that with polymer modification i.e. EVA, less than half of the rutting of a standard mix will occur, under the same loading conditions. Also, the effect of filler/binder ratio on rut resistance is also observed.

## **4.4 CASE STUDY 3: Influence of antistripping agent on rutting and stripping**

Stripping is a failure mechanism on asphalt road pavements that may lead to premature failure. Extreme cases such as disintegration of the asphalt layer and formation of potholes are evident on some of our roads in South Africa.

Numerous research projects have been launched to identify the mechanisms of asphalt stripping. The term “stripping” is applied to HMA mixtures that generally exhibit separation and removal of binder film from aggregate surfaces due primarily to the action of moisture and/or moisture vapour (Kandhal & Rickards, 2001).

External factors and/or in-place properties of the HMA pavements can induce premature stripping in HMA pavements (Kandhal 1992, Kandhal & Rickards, 2001). These factors have been highlighted in Chapter 2.

Different test methods are being used to evaluate the moisture susceptibility of HMA mixes, but a definite need for the development of a reliable, realistic laboratory test method has been identified (Du Preez, 2001). This led to the construction of an apparatus to evaluate the rutting and stripping performance of laboratory compacted asphalt specimens under water using accelerated testing at Stellenbosch University.

During the pilot testing phase, two studies were conducted. The first study by Du Preez (2001) included the evaluation of a LAMBS mix at two different void levels (4 and 7 percent). In the follow-up study by the author (Jenkins and Douries, 2001 (d)), the same mix was tested at 7 percent air voids with the addition of an anti-stripping agent GripperL. The results of these two studies will be combined to illustrate the effect of the anti-stripping agent on the performance of this particular mix.

The particular aggregate type and grading was selected due to its known susceptibility to moisture and stripping. The mix without anti-stripping agent was used as the reference mix. For the reference mix, two sets of specimens were compacted to different densities; one set at 7 percent voids and the other at 4 percent voids. The lower density specimens (7 percent voids) should be more susceptible to stripping because of the higher permeability. The higher density

specimens (4 percent voids) should exhibit minimal stripping, because of the lower permeability. It means that the water will not be able to penetrate the specimens. Subsequent compaction due to MMLS3 trafficking will seal the specimens further and no pore pressure will be created. Another set of specimens with the antistripping agent Gripper L was compacted to 7 percent air voids. Referring to the literature study (section 2.5.1) and Figure 2-19, it can be concluded that 7 percent air void specimens falls within the “pessimum” void range.

#### 4.4.1 Materials

The LAMBS mix is mainly used for heavily loaded asphalt bases, steep gradients and slow moving traffic. Because of its gradation, the mix has a relatively high permeability and the mix is subjected to water-induced damage.

The aggregate used was Port Elizabeth quartzite obtained from Lafarge Moregrove quarry. The Port Elizabeth quartzite has a history of stripping and polishing and is used in the Eastern Cape for pavement construction. The binder used was 60/70-penetration grade bitumen from CALREF. The gradation of the LAMBS mix is shown in Figure 4-14.

After mixing at  $\pm 140$  °C, the mixes were aged in a draft oven for 2-3 hours, and then compacted at  $\pm 135$  °C in the SGC. Each compacted specimen consisted of 4.5kg aggregate and 4.8 percent binder.

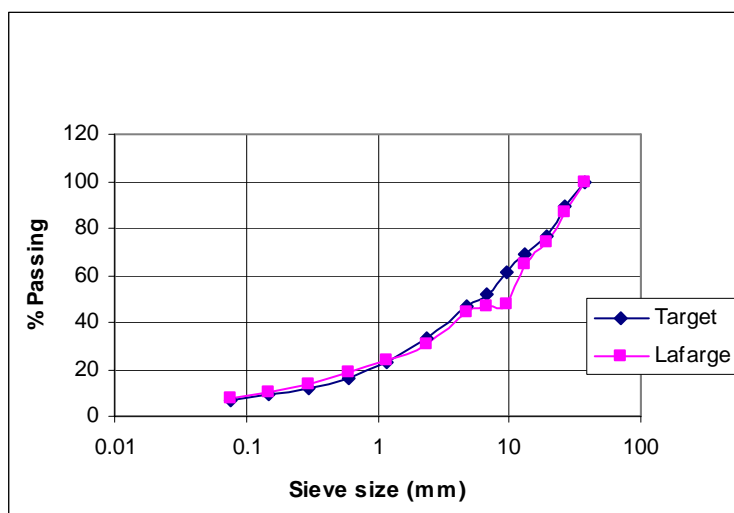
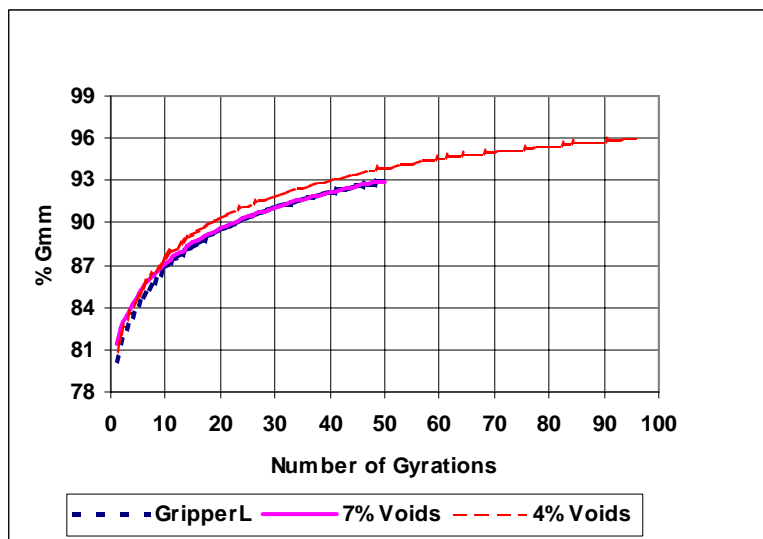


Figure 4-14: Gradation of Quartzite LAMBS mix

The specimens were compacted for 50 gyrations to approximately 7 percent air voids and the second set at 96 gyrations to approximately 4 percent voids (see Figure 4-15). For the specimens with anti-stripping agent, GripperL was added in amount of 0.4 percent of the binder mass. The specimens were also compacted for 50 gyrations to approximately 7 percent air voids (see Figure 4-15).



**Figure 4-15: Gyratory compaction of Quartzite LAMBS mixes**

Generally, the level of compaction after construction in the field is specified at 93 percent Rice density. So the laboratory tests are representative of trafficking during the early life of the layer. The 96 percent Rice density level is the ideal after further compaction by traffic.

Gripper L is an adhesive agent between aggregates and bitumen, mainly used for hot mixes application, and is specially designed for the applications where very high performance is needed. Due to its composition, Gripper L does not decompose after storage at high temperature, thus it is an antistripping agent resistant to heat effects.

**Table 4-9: Characteristics of GripperL (Kao Corporation S.A., 2001)**

<b>Aspect at room temperature</b>	Liquid
<b>Colour</b>	Yellowish
<b>Freezing point (°C)</b>	< - 10 °C
<b>-Viscosity at 20°C</b>	Approx. 2500 cps
<b>Active ingredient</b>	100 percent
<b>Density at 20°C</b>	1.05

#### **4.4.2 Test setup**

A total of eight 150 mm diameter specimens were used for each test. The specimens were cut to a height of  $60 \pm 1$  mm, and the side were trimmed to fit against each other (see Figure 4-16). A water bath was constructed with heating elements and a pump to circulate the water, to immerse specimens during trafficking. The specimens were cut to fit into a water bath on a steel platform (see Figure 4-17). The specimens were confined in both directions by clamps.

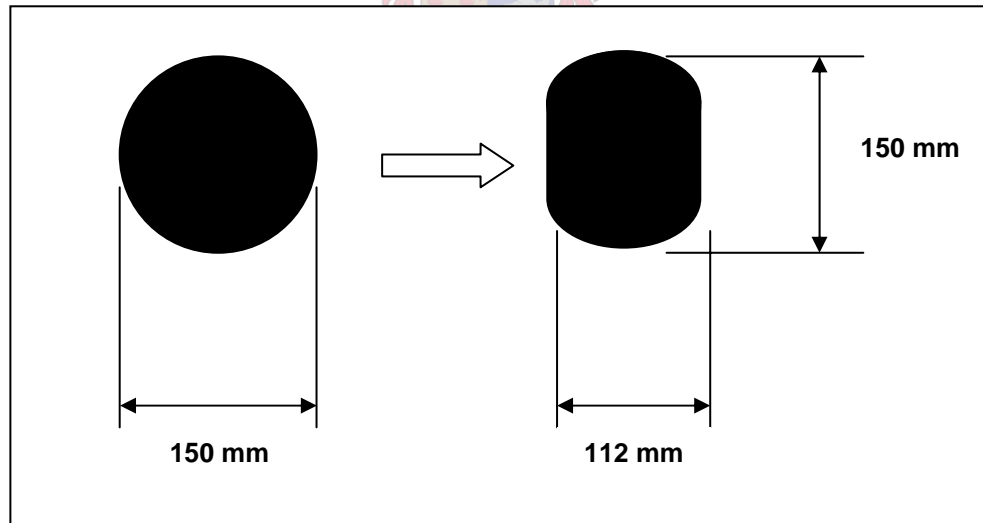


**Figure 4-16: Specimens cut to fit in water bath: Plan view**

The specimens were conditioned for 2 hours at a water temperature of 50 °C before commencement of MMLS3 trafficking. Water was added to the system during trafficking to account for water loss due to evaporation and splashing. During testing, the specimens remained fully submerged with the water level at least 1mm above the specimens. A sheet of water 1mm thick is equivalent to about 5 mm rain per hour (Smit *et al*, 1999).

It is important to test for stripping in water because the presence of water is essential for evaluation of stripping. In this test set up, it is important to load the samples to create pore pressures. Due to the pore pressure, the water is forced between the binder film and the aggregate that can lead to loss of adhesion and stripping.

#### 4.4.2.1 Temperature control and measurements

The water temperature was regulated with a thermostat and the asphalt temperature with thermocouples in the specimens at mid-depth. Water was added to the system during trafficking to account for water loss due to evaporation and splashing. In correlation tests done on this specific set up, the temperature difference between the water and the specimens at mid depth was found to be 10 °C (Jenkins and Douries, 2001(b)). This means that for a specimen temperature of 50 °C, the water temperature needs to be at 60 °C. This temperature difference was due to the insulation of the specimens by the clamps. This can be overcome by using clamps that are more heat conductive.

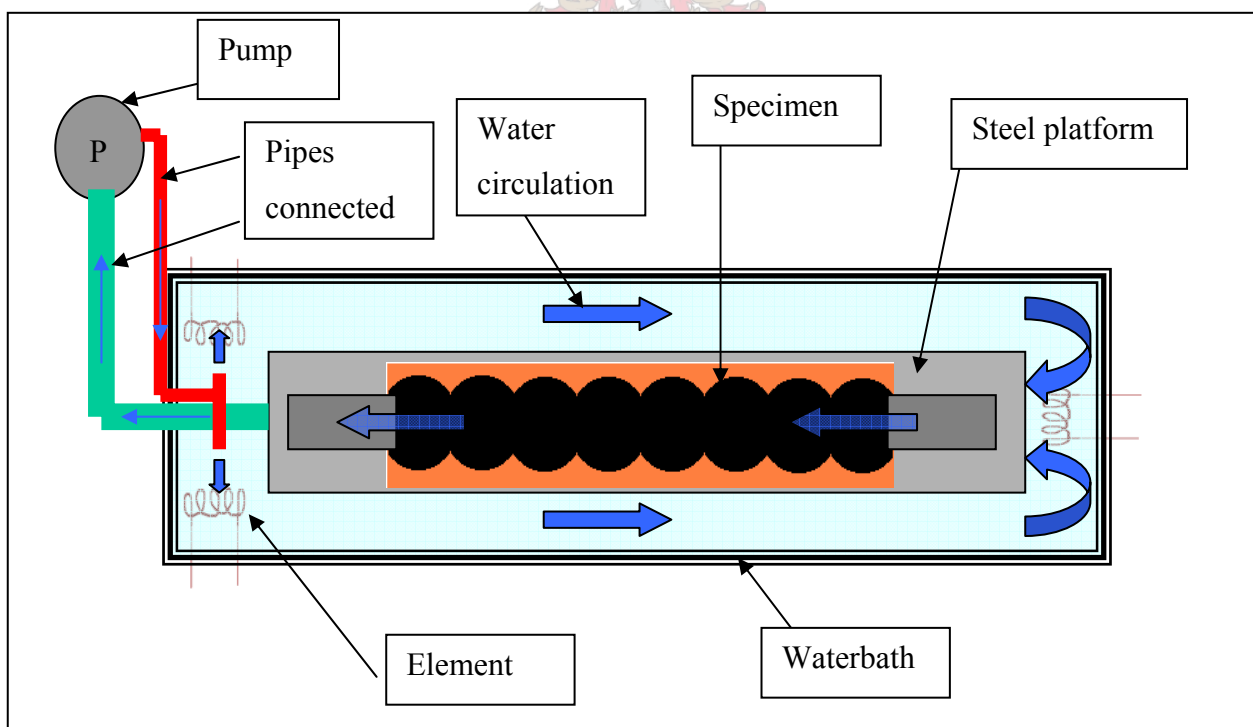


Figure 4-17: Plan view of MMLS3 testing under water: Diagrammatical

#### 4.4.2.2 Rut profile measurements

Transverse profile measurements were taken after specific intervals to obtain the rut depths and rate of rutting during MMLS3 trafficking. These readings were typically taken after 0, 100, 500, 1000, 5000, 10000, 50000, 100000 and 200000 MMLS3 load repetitions. These intervals may differ between any two tests. A maximum of two profile readings (10 mm apart; in 2 mm increments) were taken on each briquette on the centreline perpendicular to the trafficking direction (see Figure 4-18). The profilometer measure the change in height relative to a position with fixed coordinates with accuracy of 10  $\mu\text{m}$  (Müller, 2001). This gives an indication of the vertical deformation of the asphalt specimens under MMLS3 trafficking.



**Figure 4-18: Rut profile measurements**

It was necessary to apply corrections to the rut data for rotation of the specimens during clamping and individual particle influence. This rotation, however, is confined to the first 100 axles. Most of the consolidation occurs during the first 100 axles, thereafter the specimens stabilise. This can be overcome by using clamps that do not allow rotation of specimens during testing.

### 4.4.3 MMLS3 Rutting results

The testing was performed at an asphalt temperature of 40 °C. Smit *et al* (2002) concluded that limiting value of 40 °C below which no significant increase in rutting damage occurs.

The cumulative rutting curves are shown in Figure 4-19. For the lower density (7 percent air voids) specimens, slight binder stripping from the surface was observed after 1000 axles. After 5000 axles, the aggregate at the surface became clearly visible. Aggregate stripping was noticed after 50000 axles and somewhere between 50000 and 100000 the aggregate stripping increased considerably. The test was stopped at 140000 axles to prevent possible damage to the MMLS3. From Figure 4-19 can be seen how the rutting increases considerably after 100000 axles.

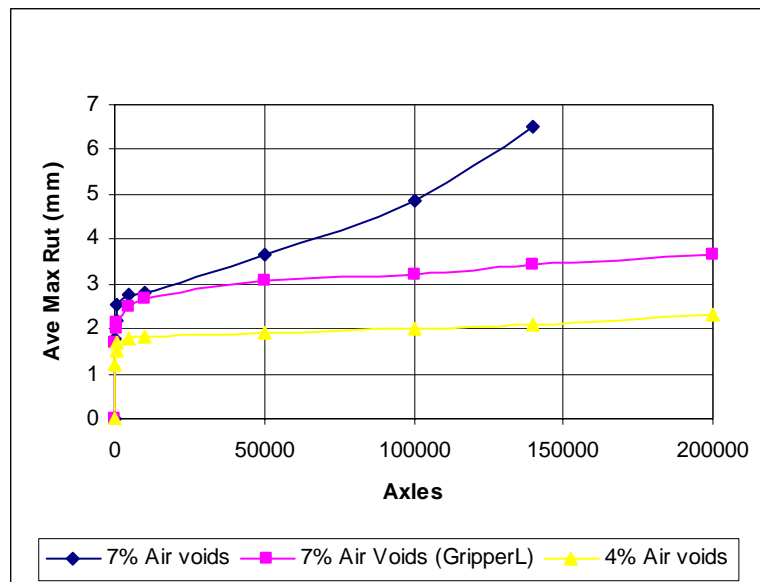


**Figure 4-19: Cumulative rutting for Quartzite LAMBS**

With the addition of GripperL, after 5000 axles, the aggregate surface became slightly visible as binder stripped from the surface. After 100000 axles, a slight stripping of the finer aggregate became visible. The test was stopped after 200000 axles. From Figure 4-19, it is evident that there is a slight increase in the rutting after 140000 axles. This increase is significantly smaller than in the previous test (without GripperL).

With the higher density (4 percent air voids) specimens, no stripping occurred. Between 0 and 100 axles, a significant amount of rutting was observed due to consolidation. After 5000 axles,

slight polishing of the aggregate was observed, which increased until the end of the test. Bleeding of the binder was observed after 100000 axles. The effect of the higher density is evident, as the 4 percent void specimens performed significantly better than the 7 percent void specimens with and without Gripper L. The rate of rutting of the 4 percent void specimens and the 7 percent void specimens (with Gripper L) were similar.

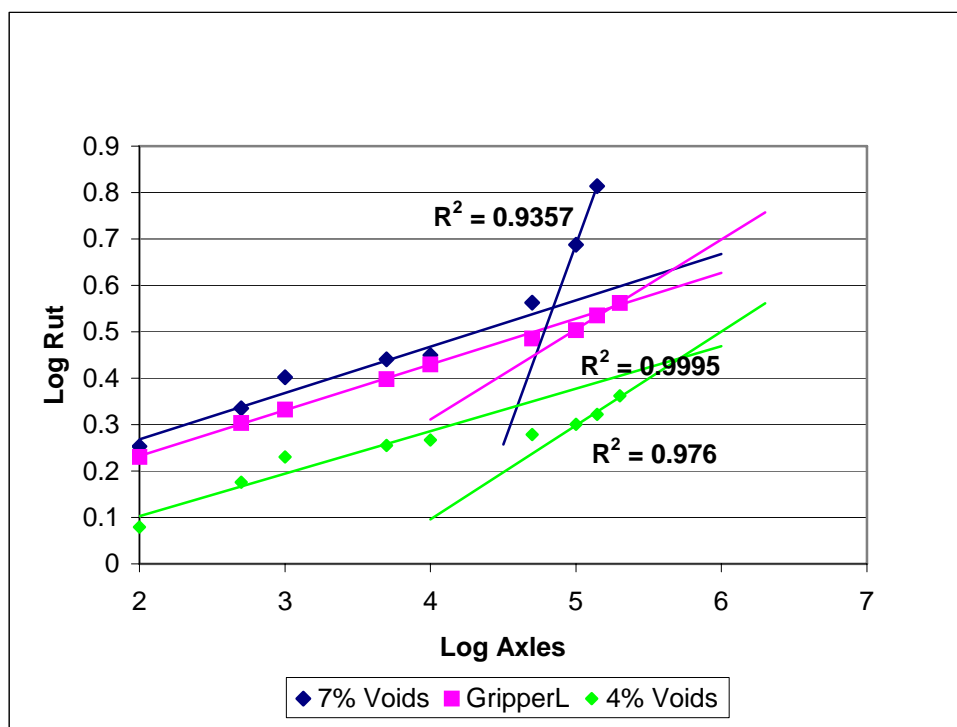


**Figure 4-20: Linear relation of log plot – Quartzite LAMBS**

Observing the log-log plot of the rutting curve, two different gradients can be identified. Extending those two lines, such as in Figure 4-20, where they intersect, a point where rutting becomes stripping can be identified, called the “stripping inflection point”. For the 7 percent void specimens, this point corresponds to 70000 axles (4.85 log axles). The gradient of the second line gives also an idea of the rate at which stripping would occur.

For the 7percent void specimens with Gripper L the “stripping inflection point” corresponds to 160000 axles (5.2 log axles). For the 4 percent void specimens, the “stripping inflection point” is approximately 500000 axles (5.7 log axles).

The results show clearly the effect of the degree of compaction on the stripping and rutting performance of the Quartzite LAMBS mix as tested under the MMLS3. Although the gradation and binder contents were virtually the same, the one was compacted to 4 percent voids and the other to 7 percent voids. The 7 percent voids specimens exhibited significant stripping whilst the 4 percent voids specimens only exhibited rutting. Figure 4-21 shows the specimens after trafficking (the 7 percent void specimens is to the right).



**Figure 4-21: Quartzite LAMBS specimens after MMLS3 trafficking**

When comparing the 7 percent void specimens, it can be seen that the addition of the antistripping agent Gripper L has a significant effect on the reduction of permanent deformation and stripping of the Quartzite LAMBS mixes.



**Figure 4-22: Quartzite LAMBS specimens (with Gripper L) after MMLS3 trafficking**

#### ***4.4.4 Conclusions of CASE STUDY 3***

Based on the results presented in this section it may be concluded that the testing of asphalt specimens under water with the MMLS3 can be useful as it gives an insight into the rutting and stripping performance of a particular mix.

For this particular mix and the aggregate used, it is concluded that at 4 percent air voids content, the moisture susceptibility of the mix is significantly decreased. This can be related to the fact that at this void level, the mix is sealed to moisture ingress. Thus, there is a reduction in pore pressures as a result of reduced permeability.

The addition of Gripper L decreases the rutting and also the rate of rutting of the Quartzite LAMBS mix that result from the stripping failure mechanism. The amount of aggregate stripping is also visibly decreased.

Recommendations for future research in this direction include:

- 1) The same tests are repeated at a higher asphalt temperature, say 50 °C (which requires a water temperature of 60 °C). Due to the thermal conduction of the polypropylene moulds, the specimen temperature is about 10 °C lower than the water temperature.
- 2) Clamps be used that are more heat conductive and that does not allow rotation of the specimens which could influence the rutting profiles
- 3) The mix be evaluated in terms of tensile and fatigue strength prior to and after MMLS3 trafficking, to gauge the relative damage of wet trafficking

It should be noted that during the course of publication of this thesis, the first two recommendations have been implemented. The number of briquettes has been increased to nine and the width of the briquettes cores changed to 105 mm to increase the width through which the asphalt has to flow when extruded. The polypropylene mould has also been replaced by an aluminium test bed comprising three moulds each capable of holding three briquettes.

## 4.5 CASE STUDY 4: Influence of binder type and gradation on rut resistance

This section covers the performance testing of asphalt wearing course and base course mixes as candidate mixes for use in the CTIA taxiway rehabilitation project (Jenkins and Douries, 2001(a)). The test matrix is shown in Table 4-10.

The same mixes were used as described in section 3.3.1. In section 3.4.2, it was shown that the LAMBS mix compacted very easily compared to the other two mixes. The BTB mixes exhibited the highest resistance to compaction. It was also emphasized that the LAMBS mixes would be more susceptible to rutting. The harder binder (40/50 pen) and the addition of Gilsonite also decreased the compactibility. The inclusion of sand in the LAMBS also reduced the compactibility of those mixes.

**Table 4-10: Test matrix for the effect of binder type and gradation on rut resistance**

<b>Gradation</b>	<b>Binder Type</b>		
<b>COLTO Medium</b>	60/70	60/70 + Gilsonite	40/50
<b>LAMBS</b>	60/70	40/50	40/50 (no sand)
<b>BTB</b>	60/70 + Gilsonite	40/50	40/50 + Gilsonite
<b>TEST SEQUENCE</b>		<b>CONDITIONS</b>	
Gyratory Compaction (Chapter 3)		Temp.135 - 145 °C; voids 7%	
Indirect tensile strength and fatigue		Temperature 20 °C; Fatigue at 20% ITS	
MMLS3 testing (under water)		40 & 50 °C, 2.1 kN, 690 kPa , 200 000 load reps	
Indirect tensile strength and fatigue		Temperature 20 °C; Fatigue at 20% ITS	

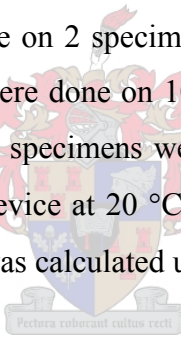
The rutting tests with the MMLS3 were done at an average asphalt temperature of 40 °C. Two additional tests were done on the BTB 40/50 and the COLTO Medium 40/50 mixes at an average asphalt temperature of 50 °C.

### 4.5.1 Indirect tensile fatigue testing

Under wet trafficking with water, moisture leads to a reduction in asphalt stiffness, stripping, cracking, degradation and loss in fatigue life. Walubita (2000) found that the fatigue life expectancy of asphalt materials susceptible to moisture damage is significantly reduced by wet trafficking, so that even light axle loads with high tyre pressures (690 kPa), as the case with the MMLS3, cause substantial damage.

Selected fatigue tests in indirect tensile mode were performed on trafficked and untrafficked specimens to gauge the relative damage due to MMLS3 trafficking. The difference in fatigue life of the trafficked specimens compared to that of the untrafficked specimens was assumed to be indicative of the distress caused by the MMLS3 trafficking under different environmental conditions, at high temperature, specimens submerged under water during trafficking and with water on the pavement surface during trafficking.

Indirect tensile splitting tests were done on 2 specimens per material to determine the tensile strength of the materials. These tests were done on 100mm diameter cores extracted from the specimens. Trafficked and untrafficked specimens were cored wet. Testing was performed in the MTS (Materials Testing System) device at 20 °C with a displacement-loading rate of 50-mm/min. The indirect tensile strength was calculated using equation 4-1 (Sabita, 1997):



$$\sigma_{ITS} = \frac{2 \times 10^3 P}{\pi D t} \quad \text{Equation 4-1}$$

Where;

- $\sigma_{ITS}$  = indirect tensile strength in kPa,
- P = maximum failure load at break in N,
- t = thickness of specimen in mm,
- D = diameter of specimen in mm.

The indirect tensile fatigue tests were done as in previous case studies i.e. at a temperature of 20 °C and a frequency of 10 Hz with sinusoidal (haversine) loading under controlled stress conditions at stress levels in the order of 20 percent of the maximum tensile strengths of the

materials determined using indirect tensile strength testing. All the specimens were conditioned at 20 °C for three hours before testing.

### 4.5.2 MMLS3 Results

Nine MMLS3 tests were performed and each mix was tested once. A series of eight briquettes were tested during one test. For all the tests, profile measurements were done at nine intervals during the test. These were at: 0, 100, 500, 1000, 10000, 50000, 100000 and 200000 axles.

The average maximum ruts are shown in Figure 4-23 through Figure 4-25.

With respect to the COLTO Medium mixes, the COLTO Medium 60/70 had the largest rut after 200 000 repetitions, followed by the COLTO Medium 40/50. The COLTO Medium 60/70 with Gilsonite had the least maximum rut. The rate of rutting is fairly similar for the three mixes. From these results it can be concluded that the addition of Gilsonite decreases the amount of rutting. Between the two binders, the mix with the 40/50-pen grade binder showed less rutting than mix with the 60/70-pen grade binder.

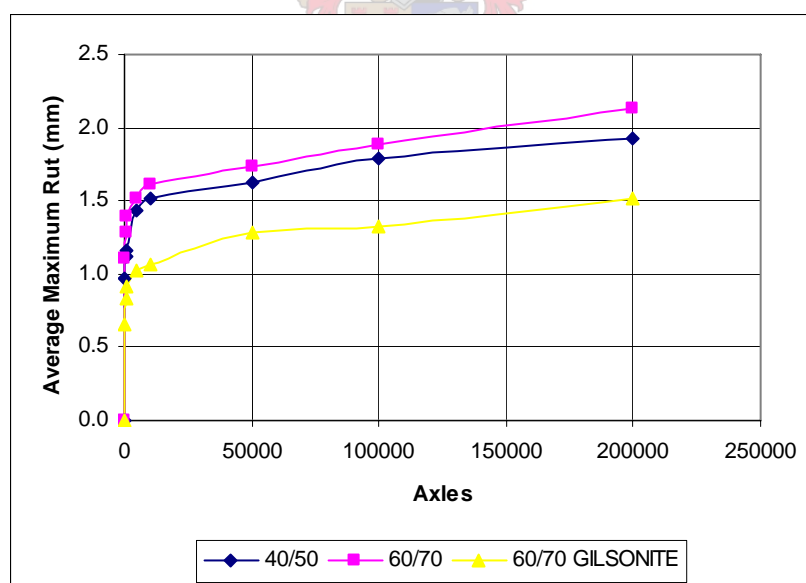
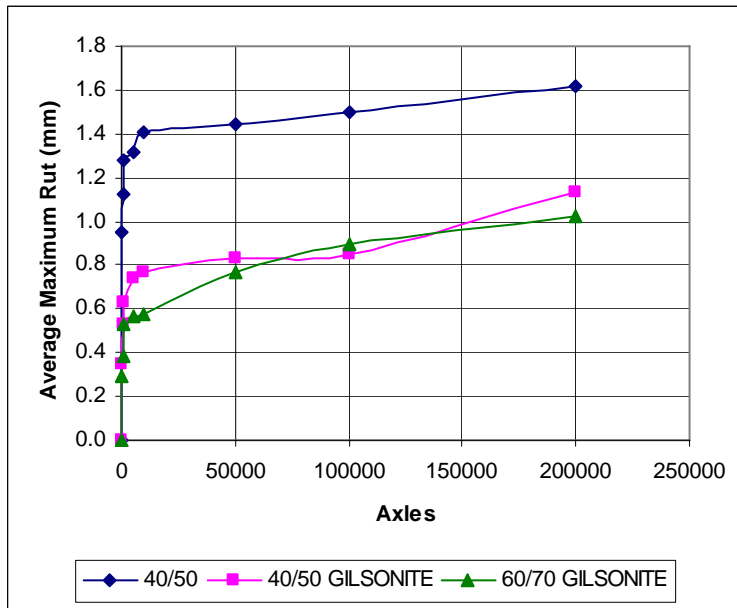


Figure 4-23: Cumulative rutting for COLTO Medium mixes

The BTB 60/70 with Gilsonite had a smaller initial settlement than the BTB 40/50 with Gilsonite, but a larger maximum rut.



**Figure 4-24: Cumulative rutting for BTB mixes**

The results of the LAMBS mixes show that the LAMBS 60/70 had a larger rut after 200 000 axles than the LAMBS 40/50. The absence of sand in the LAMBS 40/50 mix leads to a higher rut, although the initial settlement for the two LAMBS 40/50 mixes is approximately the same.

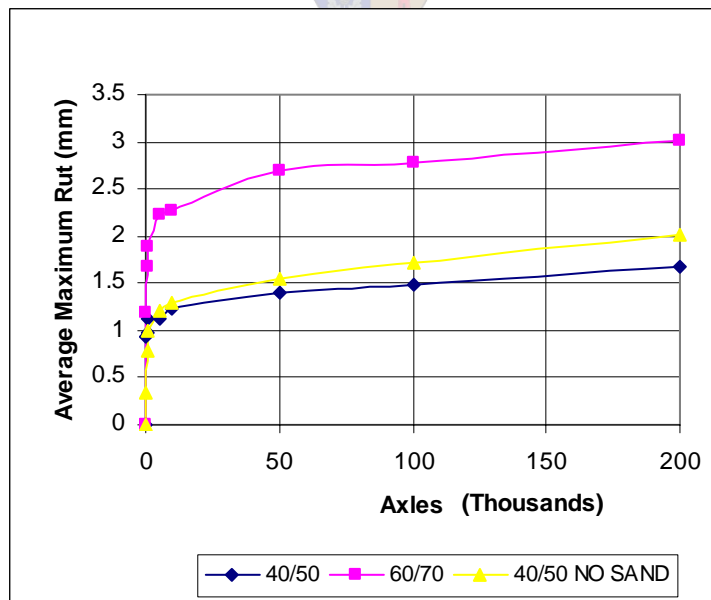


**Figure 4-25: Cumulative rutting for LAMBS mixes**

When comparing the results presented in Figure 4-23 and Figure 4-25 it is interesting to note that the effect of binder type (40/50 and 60/70) on rutting is more pronounced for the LAMBS mix. For the COLTO Medium mix the effect is minimal.

From Figure 4-26 and Figure 4-27, it is evident that the increase in test temperature increases the amount of rutting significantly. Although the BTB 40/50 at 40 °C had a larger initial settlement, it had a smaller maximum rut. The rutting rate at 50 °C was also higher (increased by a factor of 2.3). For the COLTO Medium 40/50, the initial settlement was the same, but at 50 °C, the rate of rutting was higher (increased by a factor of 1.3). Other APT research using the MMLS3 has shown that a 4 °C in asphalt temperature can double the rate of permanent deformation (Hugo, 2004).

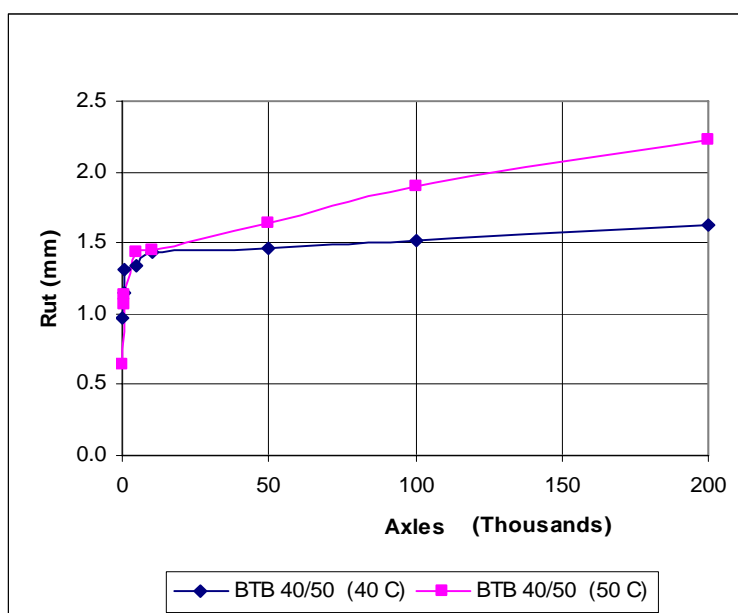


**Figure 4-26: Cumulative rutting at different temperatures for BTB 40/50**

From Figure 4-26 and Figure 4-27, it can be seen how an increase in specimen temperature has an influence on the rutting performance. A 10 °C increase in the temperature results in a 25 percent increase in the rutting. It shows that rutting is very dependent on temperature. This can be related to asphalt’s viscoelastic behaviour. At very low temperatures, asphalt behaviour is almost elastic, i.e. the phase angle approaches zero and no significant viscous deformation occurs. As the temperature increases, so do the phase angle and the amount of viscous deformation. In this particular case, the phase angle is greater for 50 °C than for 40 °C and thus the viscous component of the deformation is larger at 50 °C than at 40 °C.

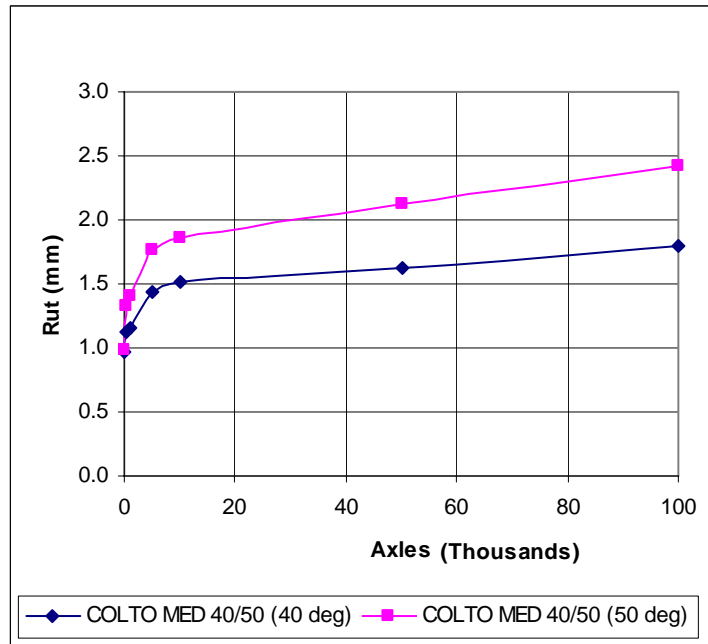


**Figure 4-27: Cumulative rutting for COLTO Medium 40/50 at different temperatures**

By looking at the log-log plot of the rutting curve, one can identify two different gradients. Extending those two lines, like in Figure 4-28, where they intersect, a point where rutting goes into stripping can be identified, called the “stripping inflection point”. The gradient of the second line gives also an idea of what the rate of stripping would be. Although for most of these tests, such an inflection point between 100 000 and 200 000 axles could be found graphically, only the LAMBS 60/70 showed minor stripping. One reason for this graphical misinterpretation could be the number of data points for the second gradient. Just two data points were used for the gradient of the second line. If more data points were used on the second gradient line, a different inflection point could have been found which might, based on the visual assessments, have plotted beyond 200 000 axles.

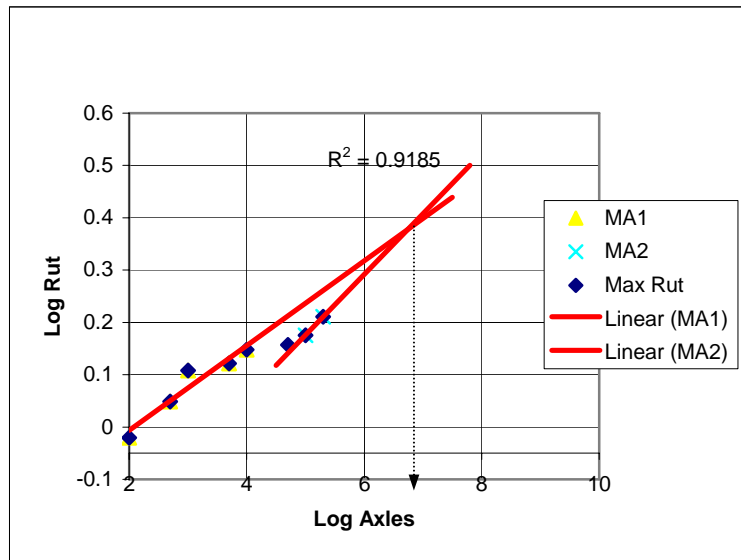


**Figure 4-28: Slope of rutting curve BTB 40/50**

### 4.5.3 Indirect tensile strength and fatigue results

Table 4-11 shows the indirect tensile strength test results and Table 4-12 the indirect tensile fatigue test results for the two materials evaluated (LAMBS 40/50 and BTB 40/50). The results are average values obtained on both strength and fatigue tests; in each case a minimum of two trafficked specimens and two untrafficked specimens were tested.

**Table 4-11: Indirect tensile strength test results (in kPa)**

Material	Trafficked	Untrafficked	Strength ratio
BTB	1700	1747	0.97
LAMBS	1567	1574	0.99

**Table 4-12: Indirect tensile fatigue test results (in cycles to failure)**

Material	Trafficked	Untrafficked	Fatigue ratio
BTB	55 000	68 000	0.81
LAMBS	111 000	154 000	0.72

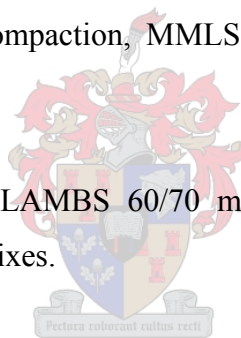
In previous research (Walubita, 2000), the indirect tensile fatigue ratio was used to evaluate the relative damage of trafficked specimens. This ratio was defined as the indirect tensile fatigue life after trafficking compared to the indirect tensile fatigue life before trafficking. The same approach was used here.

For both the materials evaluated, the fatigue ratio is lower than the strength ratio. As with previous research using this approach, the difference in fatigue life between trafficked and untrafficked specimens is greater than the difference in strengths. At the 20 percent stress levels, the LAMBS mix appears to have marginally better fatigue resistance than the BTB, although the results are comparable.

#### ***4.5.4 Conclusions of CASE STUDY 4***

From the results of the gyratory compaction, MMLS3 testing and the fatigue testing, the following conclusions can be drawn:

Except for minor stripping of the LAMBS 60/70 mix, no stripping occurred during the MMLS3 testing of any of the other mixes.



The LAMBS mixes exhibit a significantly lower rut resistance compared to the BTB mixes. This confirms the results of the gyratory compaction. The LAMBS showed significantly better compactibility and it was anticipated that this mix would exhibit lower rut resistance.

The BTB mixes with Gilsonite mixes (both 60/70 and 40/50 pen binder) appears to have better rut resistance compared to those without the Gilsonite. This is also evident in the compactibility results. It appears that while the Gilsonite decreases compactibility, it increase the rut resistance. No significant difference in rut resistance was observed between the 40/50 and 60/70 pen binder types (with Gilsonite). The COLTO Medium 60/70 with Gilsonite also showed better rut resistance if compared to those without Gilsonite. The improvement in rut resistance with the addition of Gilsonite is generally in the order of 30%. It can thus be concluded that the addition Gilsonite results in a substantial improvement in the rut resistance of the mixes in question.

When comparing these results, it should be taken into account that the Gilsonite mixes might exhibit brittle ageing and high stiffness, which may result in reduced fatigue resistance. Anderson *et al* (1999) reported that although Gilsonite modification produced stiffer mixture and an improvement in rut resistance, these mixes were observed to show signs of raveling, surface cracking, and general deterioration associated with the stiffness and brittleness of these mixtures and the binders with which they have been made.

The loss in fatigue life is more significant than the loss in tensile strength. Thus, the loss in fatigue life appears to be a better indicator of moisture susceptibility than strength loss especially for quantitative evaluation of damage. At the 20 percent stress levels, the LAMBS mix appears to have marginally better fatigue resistance than the BTB, although the results are comparable. However, it appears that the LAMBS mix is slightly more affected by wet trafficking as indicated by the loss in fatigue life.

#### **4.6 CASE STUDY 5: Influence of wet trafficking on rutting and fatigue life**

This case study reports on the performance testing of four different asphalt mixes from Texas (Jenkins and Douries, 2001 (b)). Rutting tests were done on asphalt briquettes under water using the MMLS3. SASW (Spectral Analysis of Surface Waves) testing was performed on specimens before and after MMLS3 trafficking. Indirect tensile fatigue tests were carried out on trafficked and untrafficked specimens. These tests were done at stress levels of 20 percent of the maximum tensile strengths of the materials determined using indirect tensile strength (ITS) testing.

Four HMA mixtures were selected in order to get mixtures of different quality from best to worst. The materials tested were:

- 1) Type C Texas mixture with limestone aggregate, (LS),
- 2) Tender mixture with rounded natural gravel, (RG),
- 3) 12.5-mm SMA mixture with granite aggregate, (SMA) and
- 4) 19-mm Superpave mixture with granite aggregate, (SUP).

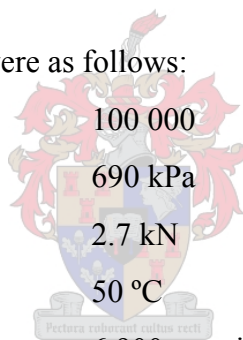
Rutting tests were done on asphalt briquettes under water at an average specimen temperature of 50 °C. Details of this test setup can be found in section 4.6.2. SASW testing was performed on specimens before and after MMLS3 trafficking. Indirect tensile fatigue tests were also carried out on trafficked and untrafficked specimens.

Two MMLS3 tests were performed, using eight specimens for each test. In the first test, four specimens each of materials 2 (RG) and 4 (SUP) were tested. Four specimens each of materials 1 (LS) and 3 (SMA) were tested in the second test. All of these specimens, as received, were compacted to 7 percent air voids.

Profilometer measurements were taken after six intervals, i.e. after 0, 1000, 10000, 25000, 50000, 100000. One profile reading was taken on each briquette on the centreline perpendicular to the trafficking direction. Visual assessments were done on the surface of the briquettes to check for stripping.

The test conditions for the MMLS3 were as follows:

- Number of load repetitions 100 000
- Tyre pressure 690 kPa
- Scaled wheel load 2.7 kN
- Test temperature (asphalt) 50 °C
- Load rate 6 900 repetitions per hour



It should be noted that some of the specimens were received with both faces sawed and others with just one face sawed. It is preferred to run the MMLS3 on specimens with compacted faces. Table 4-13 illustrates how the specimens were set up in a specific sequence so that those with compacted faces took up the middle four places (shaded in Table 4-13).

**Table 4-13: MMLS3 specimen sequence**

	Direction of trafficking →							
Test1	SUP 3-1	SUP4-1	SUP3-2	SUP4-2	RG4-2	RG3-2	RG4-1	RG3-1
Test2	SMA4-1	SMA3-1	SMA4-2	SMA3-2	LS 3-2	LS 4-2	LS 4-1	LS 3-1

A second batch of 16 samples, 4 per material, was received for indirect tensile splitting and fatigue tests. Indirect tensile splitting tests were done on 2 specimens per material to determine the tensile strength of the materials. These tests were done on 100mm diameter cores extracted from the specimens. The indirect tensile and indirect tensile fatigue testing was performed as described in Section 4.5.1. A total number of 16 trafficked and 8 trafficked specimens were tested. All of the tested specimens were 100 mm in diameter.

#### ***4.6.1 Stiffness testing (SASW)***

SASW (Spectral Analysis of Surface Waves) measurements were done on specimens before and after MMLS3 trafficking to estimate the stiffness moduli of the specimens. A Poisson's ratio of 0.35 was assumed for all.

The SASW method uses the dispersive characteristics of surface waves to determine the variation of the shear wave velocity (stiffness) of layered systems with depth. This process involves generating a signal (surface wave) and measuring the velocities at which that signal travels through the pavement. The speed at which the wave travels through a certain material is directly proportional to the modulus of that material.

The SASW testing is applied from the surface, which makes the method nondestructive. Once the shear wave velocity profiles are determined, shear and stiffness (Young's) moduli of the materials can be calculated through the use of simple mathematical equations. The shear wave velocity profiles are determined from the experimental dispersion curves (surface wave velocity versus wavelength) obtained from SASW measurements through a process called forward modeling or through an inversion process.

More on the practical and theoretical aspects of SASW testing are available in the literature (Nazarian and Stokoe, 1985 & 1986).

#### 4.6.2 Materials

The mixtures (and the order in which they were tested with the MMLS3) are shown in Table 4-14.

**Table 4-14: Mix types tested with the MMLS3**

Mix type	MMLS Test
19 mm Superpave mixture with granite aggregate	1
Tender mixture with rounded natural river gravel	1
25 mm SMA mixture with granite aggregate	2
Type C Texas mixture with limestone aggregate	2

TxDOT provided the mix designs for the limestone and river gravel mixes (designed using the Texas gyratory compactor). Georgia DOT provided both the SMA and Superpave mixture designs using granite. Koch Materials, Inc. supplied the binder for the mixtures (PG 64-22, and PG 76-22). The following is a description of the different materials.

1) Type C limestone mix

Limestone aggregate was received from Colorado Materials, Texas. The field sand for this mixture was collected from Brazos Valley, Texas.

2) River gravel mix

The river gravel aggregate was collected from Brazos Valley, Texas. It is uncrushed and mostly rounded.

3) SMA granite mix

The aggregate was supplied by Vulcan Materials from their Lithia Springs, GA quarry. The filler was composed of 9 percent fly ash and 1 percent hydrated lime. The fly ash was provided by Boral Materials Technology, Inc. This mixture also included 0.4 percent mineral fibre.

#### 4) Superpave granite mix

The aggregate was supplied by Vulcan Materials from their Lithia Springs, GA quarry. The filler includes 1 percent hydrated lime. Georgia DOT designates this mixture as “Level B”.

Table 4-15 shows the fine aggregate angularity (FAA) and coarse aggregate angularity (CAA) for the different aggregates used in the study. For CAA, a sample retained on the 4.75 mm sieve is collected and the number of particles with fractured faces is compared to the number of particles without fractured faces. A fractured face is defined as an "angular, rough, or broken surface of an aggregate particle created by crushing, by other artificial means, or by nature" In order for a face to be considered fractured it must constitute at least 25 percent of the maximum cross-sectional area of the rock particle. This test is performed according ASTM D 5821. CAA is necessary in asphalt to assist in resisting shoving and rutting under traffic. The internal friction among the crushed aggregate particles prevents them from being moved past each other and provides for a stable mix.

FAA is a Superpave test used to determine the uncompacted void content of fine aggregate, which gives some indication of fine aggregate particle shape and surface texture. The test involves filling a 100 mL cylinder with fine aggregate defined as that aggregate passing the 2.36 mm sieve, by pouring it from a funnel at a fixed height. After filling, the amount of aggregate in the cylinder is measured and a void content is calculated. The assumption is that this void content is related to the aggregate angularity and surface texture (e.g., more smooth rounded particles will result in a lower void content). The key disadvantage to this test is that inclusion of flat and elongated particles, which are known to cause mix problems, will cause the fine aggregate angularity test results to appear more favourable. Finally, surface texture may have a larger effect on mix performance than fine aggregate angularity values. This test is done according ASTM C 1252.

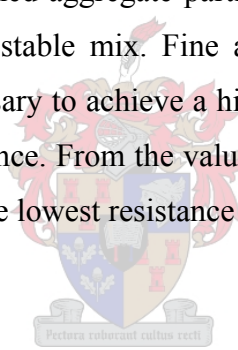
**Table 4-15: FAA and CAA of aggregate**

Aggregate Type	FAA	CAA	
		percent 1* Fractured faces	percent 2** Fractured faces
Limestone	45.18	100	100
River gravel	40.23	30	19
Granite (SMA)	47.16	100	100
Granite (Superpave)	47.16	100	100

Note: \* -- the percentage of the coarse aggregate that has one or more fractured faces

\*\* -- the percentage of the coarse aggregate that has two or more fractured faces

Coarse aggregate angularity is necessary to assist in resisting shoving and rutting under traffic. The internal friction among the crushed aggregate particles prevents them from being moved past each other and provides for a stable mix. Fine aggregate angularity, like the crushed content of coarse aggregate, is necessary to achieve a high degree of internal friction and thus, high shear strength for rutting resistance. From the values in Table 4-15, it is apparent that the river gravel specimens would have the lowest resistance to rutting.



### 4.6.3 Mix designs

Figure 4-29 shows the gradation of the different mixes tested using the MMLS3. Table 4-16 shows the mix design information. The gyrations used for the Superpave mix design were 7 ( $N_{ini}$ ), 86 ( $N_{des}$ ), and 134 ( $N_{max}$ ).

**Table 4-16: Mix design information**

Mixture Type	Binder content, percent	Binder Type	Rice density	Design Method
Limestone	4.4	PG 64-22	2.428	Texas Gyrotory
River Gravel	5.5	PG 64-22	2.416	Texas Gyrotory
Granite (SMA)	5.9	PG 76-22	2.396	Marshall 50-blow
Granite (Superpave)	4.0	PG 64-22	2.481	Superpave

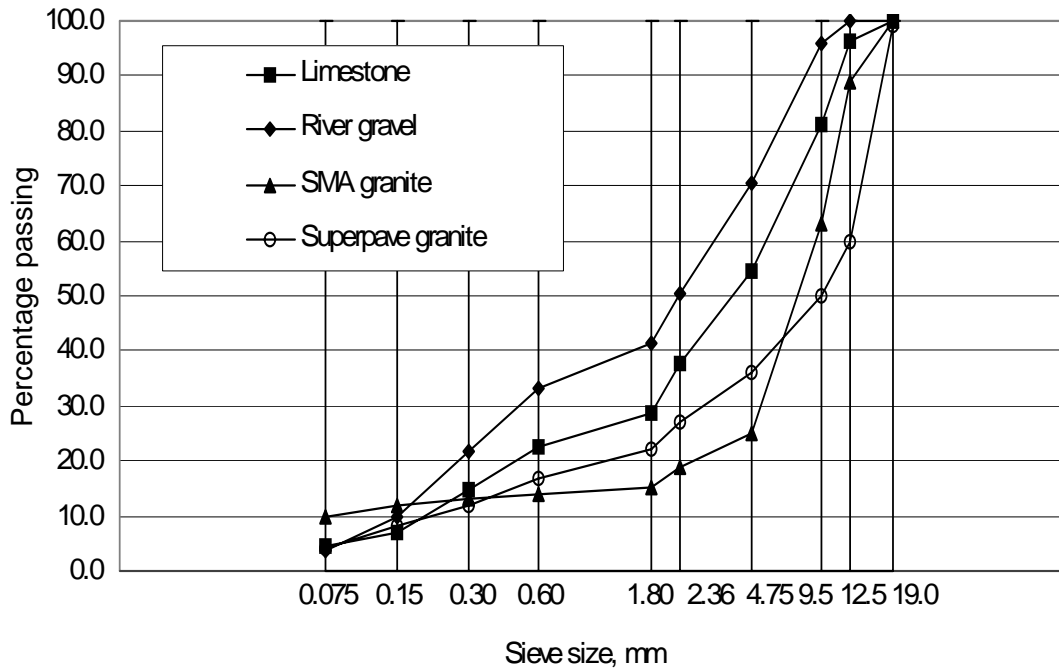
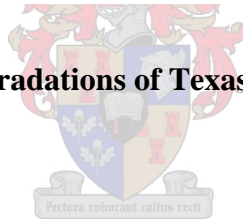


**Figure 4-29: Gradations of Texas study mixtures**



The mixing and compaction temperatures for the binder study are shown in Table 4-17.

**Table 4-17: Mixing and compaction temperatures of Texas study binders**

Binder	Temperature, °C	
	Mixing	Compaction
PG 64-22	160	146
PG 76-22	166	154

#### 4.6.4 Test results

##### 4.6.4.1 Indirect Tensile Strength

All the 100 mm diameter specimens used for indirect tensile testing were cored wet. For the SMA and SUP specimens, only one specimen each could be tested due to:

- 1) SMA --- specimen got stuck in coring drill and broke when tried to remove it. It should be noted that all the SMA specimens were difficult to remove from coring drill.
- 2) SUP --- “strange” data retrieved from computer and could not be used.

After the loss of these two specimens, it was decided not to use any more of the remaining specimens for ITS, but rather have at least two specimens per material for the untrafficked indirect tensile fatigue tests. The indirect tensile strength results are summarised in Table 4-18. From these results it can be seen that the ITS values of the RG specimens were more than 50 percent less than those of the other materials.

**Table 4-18: ITS results**

Specimen	Thickness (mm)	ITS (kPa)	Max Load (N)	Air Voids before trafficking (%)
<b>RG 3</b>	64	<b>792</b>	7961	7.4
<b>RG 4</b>	64	<b>684</b>	6878	6.6
<b>SUP 1</b>	64	<b>1733</b>	17426	7.1
<b>SUP 4</b>	64	*	*	6.7
<b>SMA 3</b>	64	**	**	6.7
<b>SMA 4</b>	64	<b>1545</b>	15529	6.8
<b>LS 1</b>	64	<b>1723</b>	17321	6.5
<b>LS 2</b>	64	<b>1630</b>	16382	6.7

\* "Strange" data

\*\* Specimen broken

#### 4.6.4.2 MMLS3 Results

The MMLS3 tests were conducted at a water temperature of 60 °C to obtain a specimen temperature of 50 °C at mid depth (Jenkins and Douries, 2001(a)). The average water temperature for Test 1 was 60 ±4 °C and for Test 2 it was 61 ±2 °C.

In the first test, all the specimens except SUP 3-2 and SUP 4-2 were tested up to 25 000 axles. After 25 000 axles, aggregate loss was observed for specimens SUP 3-1 and SUP 4-1. Specimens SUP 3-2 and SUP 4-2 were tested further up to 100 000 axles along with 6 dummy specimens. At the end of the test, a crack (<1mm) was noticed in specimen SUP 4-2.

In the second test, all the specimens were tested up to 100 000 axles. The LS specimens exhibited better rut resistance than the SMA specimens. After 25 000, the aggregate on the surface became slightly visible, due to the binder film being removed. At the end of the test, minor stripping of the finer aggregate was visible on the LS specimens, whilst the stripping on the SMA specimens was mainly binder stripping from the surface. The rutting results of the two tests are summarised in Table 4-19.

**Table 4-19: MMLS3 test summary**

TEST 1	Max Rut (mm)		TEST 2	Max Rut (mm)		
	Specimen	25k		100k	Specimen	25k
	SUP 3-1	3.69	x	SMA 4-1	2.41	3.30
	SUP 4-1	4.86	x	SMA 3-1	2.46	2.71
	SUP 3-2	4.28	5.70	SMA 4-2	3.22	3.45
	SUP 4-2	4.80	6.79	SMA 3-2	2.21	2.83
	RG 4-2	11.92	x	LS 3-2	1.58	2.86
	RG 3-2	6.52	x	LS 4-2	1.38	1.95
	RG 4-1	6.49	x	LS 4-1	1.23	1.50
	RG 3-1	4.53	x	LS 3-1	1.54	1.97

x = test stopped after 25 000 axles

As expected, the RG (river gravel) specimens showed the least resistance to rutting. It was mainly due to the smooth rounded aggregates, which does not possess high enough internal

friction to develop high shear strength necessary to resist rutting. This lower coarse and fine aggregate angularity is shown in Table 4-15.

Tayebali *et al* (1996) reported that asphalt mixtures containing natural aggregates (especially the natural river sands) are generally more susceptible to rutting, shoving and bleeding than mixtures containing 100 percent crushed fine aggregate. These round and smooth aggregate particles would allow for easy compaction, which is evident in the significant increase in density (from 7 percent voids to 4.5 percent voids) under MMLS3 trafficking.

The LS specimens showed the best resistance to permanent deformation, followed by the SMA specimens. After 25000 axles, the SUP and RG specimens already had rutting of higher than 4mm, with the RG specimen the highest.

#### **4.6.4.3 Indirect tensile fatigue tests**

The analysis was based on comparison of the indirect tensile fatigue life of the trafficked specimens relative to the untrafficked specimens. As mentioned earlier, this was assumed to be indicative of the distress caused by the MMLS3 trafficking.

The indirect tensile fatigue tests were conducted at stress levels of 20 percent of the untrafficked ITS values for the respective materials (as described in Section 4.5.1). Trafficked and untrafficked specimens were cored wet. In total, 8 untrafficked specimens and 16 trafficked specimens were tested. The temperature during testing varied between 18 °C and 21 °C. The results of the indirect tensile fatigue tests are summarised in Table 4-20 and Table 4-21

**Table 4-20: Indirect tensile fatigue results – Untrafficked**

Specimen	Thickness (mm)	Air voids (%)	Cycles to failure
<b>RG 1</b>	64	7.3	29000
<b>RG 2</b>	64	6.9	29500
<b>SUP 2</b>	64	7.1	23000
<b>SUP 3</b>	64	6.7	14500
<b>SMA 1</b>	64	7.1	95500
<b>SMA 2</b>	63	7.0	118500
<b>LS 3</b>	64	6.8	59000
<b>LS 4</b>	64	6.9	38500

**Table 4-21: Indirect tensile fatigue results - Trafficked**

Specimen	Cycles to failure			
	LS	SUP	SMA	RG
<b>3-1</b>	6000	5300	211000	516000
<b>3-2</b>	12500	7900	136000	171500
<b>4-1</b>	82500	1800	104000	396000
<b>4-2</b>	29000	1700	148000	265500

From these results it is evident that the fatigue life of the RG and SMA specimens increased generally. The SUP specimens experienced a loss in fatigue life in the range of 58 percent to 91 percent. A loss of fatigue life in the range of 41 percent to 88 percent was evident in the LS specimens, with the exception of one specimen, which gained 69 percent. The gain in the fatigue life of the RG specimens was considerably high, which can be as a direct result of the densification (reduction in air voids) under MMLS3 trafficking.

**Table 4-22: Average indirect tensile fatigue values**

Material	Average cycles to failure		Gain (%)
	Untrafficked	Trafficked	
RG	29250	337250	1053
SUP	18750	4175	(-) 78
SMA	107000	149750	40
LS	48750	32500	(-) 33

#### 4.6.4.4 Discussion

With regard to rutting, the LS specimens showed better resistance to permanent deformation, followed by the SMA specimens. After 25k, the SUP and RG specimens already had rutting of higher than 4mm, with the RG specimen the highest. These levels of MMLS3 rutting would convert to ruts of well in excess of 15mm on a full scale pavement after 100 000 repetitions (A. Epps *et al*, 2001).

All of the specimens showed minor stripping from the surface. The SUP specimens showed some aggregate fracturing underneath. The SUP specimens yielded the highest indirect tensile strength (1733 kPa), followed by LS (1677 kPa) and SMA (1545 kPa). The ITS of the RG specimens (738 kPa) were less than half the ITS of the other three materials.

Walubita *et al* (2002) studied the indirect tensile fatigue performance of asphalt after MMLS3 trafficking. They used, amongst others, the indirect tensile fatigue ratio to evaluate the relative damage of trafficked specimens. This ratio was defined as the indirect tensile fatigue life after trafficking compared to the indirect tensile fatigue life before trafficking. The same approach was used here.

The relative ratios (RR) of the properties measured before and after MLS3 trafficking, and the rutting results are summarised in Table 4-23. The  $RR_x$  values this table are explained through equation 4-2.

$$RR_x = \frac{X_{trafficked}}{X_{untrafficked}}$$

**Equation 4-2**

with X =  $\left\{ \begin{array}{ll} N_f & = \text{Indirect tensile fatigue life} \\ \text{BRD} & = \text{Bulk Relative Density} \\ \text{SASW} & = \text{SASW modulus} \end{array} \right.$

The results in Table 4-23 show that on average, all four materials had a reduction in SASW stiffness, with the SUP specimens the highest (almost 60 percent reduction on average). This could be related to the effect of moisture damage during MMLS3 trafficking.

The RG specimens yielded a considerable gain in fatigue life after MMLS3 trafficking. The SMA specimens also gained some fatigue life. This gain in fatigue life could be due consolidation and healing of the asphalt. The SUP and LS specimens showed a loss in fatigue life, which indicates micro fracturing during MMLS3 loading. In general, all four material experienced some increase in density.



**Table 4-23: Summary of test results**

Sample	20 % ITS	RR <sub>Nf</sub>	RR <sub>BRD</sub>	RR <sub>SASW</sub>	Max rut	Max rut
	Stress (kPa)				25k (mm)	100k (mm)
<b>RG 3-1</b>	148	17.64	1.03	0.58	4.53	x
<b>RG 3-2</b>	148	5.86	1.03	0.86	6.52	x
<b>RG 4-1</b>	148	13.54	1.03	0.71	6.49	x
<b>RG 4-2</b>	148	9.08	1.02	0.91	11.92	x
<b>SUP 3-1</b>	347	0.28	1.00	0.47	3.69	x
<b>SUP 3-2</b>	347	0.42	1.01	1.42	4.28	5.70
<b>SUP 4-1</b>	347	0.10	1.00	0.24	4.86	x
<b>SUP 4-2</b>	347	0.09	1.02	0.51	4.80	6.79
<b>SMA 3-1</b>	309	1.97	1.01	0.77	2.46	2.71
<b>SMA 3-2</b>	309	1.27	1.01	1.01	2.21	2.83
<b>SMA 4-1</b>	309	0.97	1.00	0.34	2.41	3.30
<b>SMA 4-2</b>	309	1.38	1.01	0.50	3.22	3.45
<b>LS 3-1</b>	335	0.12	1.01	0.80	1.54	1.97
<b>LS 3-2</b>	335	0.26	1.00	0.78	1.58	2.86
<b>LS 4-1</b>	335	1.69	1.02	0.70	1.23	1.50
<b>LS 4-2</b>	335	0.59	1.01	1.16	1.38	1.95

#### **4.6.5 Conclusions of CASE STUDY 5**

The performance of the four different mixes was evaluated in terms of surface rutting, loss of stiffness in pavement layers, loss in fatigue life and permanent deformation of the specimens. This provided information regarding the progressive changes due to distress caused by trafficking or the moisture. Based on the findings of this section, the following conclusions may be drawn:

The tender mixture with rounded natural river gravel (RG) exhibited the lowest indirect tensile strength, lower than 50 percent of the ITS of the other materials. In terms of stiffness, the RG mixture showed the highest SASW stiffness on average, both before and after MMLS3 trafficking. The RG specimens were least resistant to rutting. The maximum rut after 25k axles ranged between 4.5 mm and 12 mm. The low rut resistance was anticipated due to the aggregate gradation.

The indirect tensile strengths of the other three materials (LS, SUP and SMA) were comparable. It should be noted that the air voids of the specimens ranged between 6.5 percent and 7.4 percent.

The 19 mm Superpave mixture with granite aggregate (SUP) had an average maximum rut of 25 000 axles. Two of these specimens failed after 25 000 axles, with aggregate breaking loose of the specimens. Aggregate fracturing was also observed. On average, the Superpave mixture exhibited the lowest indirect tensile fatigue life, before and after MMLS3 trafficking. The Superpave mixture also experienced the highest loss in fatigue life (78 percent on average), which can be related to the aggregate fracturing.

The Type C Texas mixture with limestone aggregate (LS) showed the best rut resistance with an average maximum rut of 2.1 mm after 100 000 axles, followed by the 12.5 mm SMA mixture with granite aggregate (SMA) with 3.1 mm after 100 000 axles.

In general, the Type C Texas (LS) and Superpave (SUP) mixture experienced a loss in fatigue life after MMLS3 trafficking.

The SMA and river gravel (RG) mixtures gained fatigue life after MMLS3 trafficking. This considerable increase in fatigue life could be as a direct result of the densification under MMLS3 trafficking. The air voids were reduced to 4.5 percent, compared to the 6.2 percent to 6.3 percent of the other materials.

All the materials tested showed an overall decrease in SASW stiffness after MMLS3 trafficking, with the Superpave mixture the largest decrease on average.

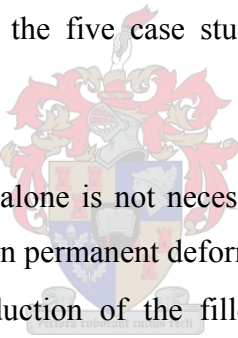
Although the river gravel (RG) mixture showed least resistance to permanent deformation, the Superpave mixture seems to be worst affected by the trafficking under water.

The indirect tensile fatigue testing and SASW testing used in this study proved to be valuable as a tool for monitoring progressive distress of asphalt owing to traffic and to environmental factors as water, as also found by Walubita (2000).

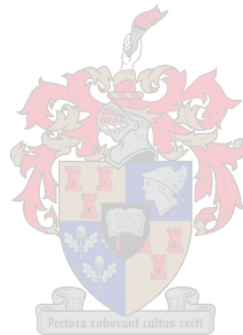
It can thus be concluded that moisture has a significant effect on reducing the indirect tensile fatigue resistance of moisture susceptible mixtures such as the Superpave (SUP) and Limestone (LS) tested in this study.

## 4.7 Overall Conclusions

Based on the results and finding of the five case studies presented, the following overall conclusions may be drawn:

- 
- It appears that compactibility alone is not necessarily the only indicator of whether a mix will perform good or bad in permanent deformation response.
  - It can be concluded that reduction of the filler/binder ratios in order to improve compactibility does not significantly increase rutting under APT
  - With polymer modification such as EVA, less than half of the rutting of a standard mix will occur, under the same loading conditions.
  - The testing of asphalt briquettes under water with the MMLS3 can give an insight into the rutting and stripping performance of a particular mix.
  - For the particular mix and the aggregate concerned, it is concluded that a reduction in air voids from 7 to 4 percent can decrease the moisture susceptibility of the mix significantly.
  - The addition of the anti-stripping agent Gripper L decreases the rutting and also the rate of rutting of the Quartzite LAMBS mix that result from the stripping failure mechanism. The amount of aggregate stripping is also visibly decreased.

- It appears that while the Gilsonite decreases compactibility, it increase the rut resistance. However, it should be taken into account that the Gilsonite mixes might exhibit brittle ageing and high stiffness, which may result in reduced fatigue resistance.
- Moisture has a significant effect on reducing the indirect tensile fatigue resistance of moisture susceptible mixtures such as the Superpave granite and Limestone tested in this study



# 5 RELATING LABORATORY TO FIELD PERFORMANCE

## 5.1 Introduction

The purpose of laboratory testing of an asphalt mix is to estimate the performance of the mix as it will be compacted in the field, both compared with other asphalt mixes and in terms of field conditions such as traffic and environment. Empirical tests and predicting models are frequently used to predict the rutting performance of an asphalt pavement. However, these tests determine only certain properties of the asphalt and cannot always relate to the actual asphalt field performance.

It is important however that, when predicting or testing permanent deformation response, the mechanisms of permanent deformation are understood. Also, to characterise asphalt for permanent deformation response in the laboratory, two factors are important. Firstly, the appropriate laboratory test should be used; secondly, the test configuration must allow accurate determination of the required properties. Specimen dimensions need to be sufficient to enable representative results to be obtained and the aspect ratio of the specimens should be adequate to minimise test imperfections. Sousa and Weissman (1994) suggested that due to the plastic nature of asphalt mixes, rut testing should be performed:

- At the temperature representative of the highest temperature encountered in the pavement
- At shear stresses representative of the highest applied to the pavement; and
- Under repetitive conditions not only to simulate traffic but also because if creep loads were applied, underestimation of the rutting propensity of a mix would occur.
- Furthermore, specimens should be subjected to ageing and moisture conditioning standards corresponding to the region where the mixes will be placed.

Epps *et al* (2001) recommended that the testing temperature be selected as the critical temperature for permanent deformation over the hottest week in the summer of a 30-year period. In addition, they suggested a minimum of 100 000 MMLS3 load repetitions and three rut depth measurements along the length of an MMLS3 test section. Deacon *et al* (1994) defined the critical temperature for permanent deformation as that temperature at which the largest amount of damage (rutting) would occur in service. They consider this critical

temperature (appropriate to the geographical location and structural section), or a standard temperature near the critical temperature, as the optimal temperature for laboratory testing because it minimises error associated with variations in mixture temperature sensitivity and because of its accelerated rate of damage accumulation. According to Smit *et al* (2002), there appears to be a threshold pavement surface temperature (about 40 °C) below, which no significant increase in rutting damage occurs.

Laboratory testing does not entirely simulate field conditions, and therefore differences in the results may be expected. However, it can provide useful information. Differences between laboratory and field conditions may include:

- Specimen preparation that fails to reproduce the material matrix encountered in the field (density, particle orientation, etc.)
- Differences in testing conditions such as support conditions, temperature, moisture, etc., and
- Differences in loading conditions such as magnitude, time and especially the way in which the load is applied to the specimen

There is a growing tendency to develop performance-related specifications, and thus the need for performance related testing. Nowadays, APT forms an integral part of performance related research. APT devices are designed to simulate the effect of traffic on an asphalt pavement and to induce permanent deformation. The advantages of APT in the laboratory include (Sousa and Weissman, 1994; Hugo, 2000):

- Testing can be done at a fraction of the cost of full-scale APT
- Variables impacting pavement systems can be better controlled
- Laboratory tests can be done on compacted asphalt slabs, laboratory prepared briquettes and field cores.
- Specimens of sufficient size can be tested
- The specimens are produced in the laboratory to the compaction level expected in the field

Thus, laboratory tests can give an indication and trend in behaviour and is a good tool to rank different mixes.

This chapter presents the analysis of relating laboratory-rutting results to field rutting results under the MMLS3, as outlined in Figure 5-1.

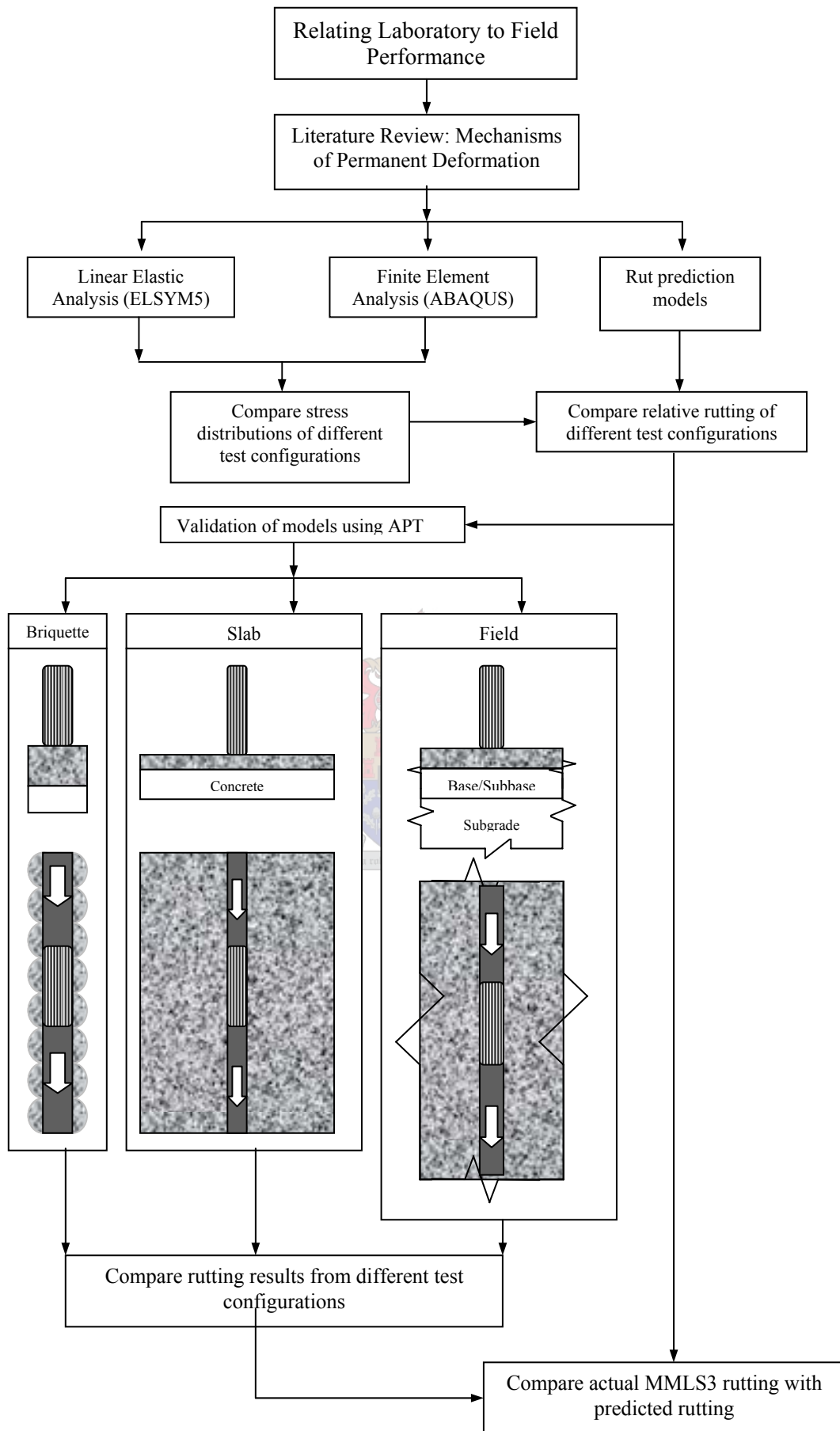


**Figure 5-1: Outline for Chapter 5**

## 5.2 Mechanisms of permanent deformation

In order to predict the rutting performance of an asphalt mix with regard to permanent deformation, one needs to understand the mechanisms and factors that govern the permanent deformation properties. Permanent deformation of asphalt is a complex phenomenon, which depends on the properties and proportions of the components of the mixture, construction quality, environmental conditions and the applied loading. Asphalt permanent deformation consists of elastic, viscoelastic, plastic and viscoplastic components. The plastic and viscoplastic components constitute the permanent deformation and their accumulation results in rutting in asphalt pavements. The rate of accumulation of permanent deformation changes with the number of load repetitions (Von Quintus, 1994).

The well-known Burgers' model can be used to describe a viscoelastic material response (Figure 5-2). The elastic component is described by a linear elastic spring, in which the stress ( $\sigma = E\varepsilon$ ) is directly proportional to the deformation ( $\varepsilon$ ) of the spring and the magnitude of the resistance is determined by the stiffness ( $E$ ) of the spring. The viscous element is described by a dashpot, in which stress is directly proportional to the rate of strain ( $\sigma = \eta d\varepsilon/dt$ ). The magnitude of the resistance is determined by the viscosity ( $\eta$ ) of the material. When the combination in Figure 5-2 is subjected to a stress, the resulting strain is composed of three components namely (Figure 5-3):

1. An instantaneous elastic component ( $E_1$ )
2. A delayed elastic component ( $E_2$  and  $\eta_2$ )
3. A viscous component ( $\eta_1$ )

From Figure 5-3 it can be seen that when the stress is applied, an instantaneous elastic deformation occurs due to the spring in series ( $E_1$ ). With time, viscous deformation occurs in the dashpot in series ( $\eta_1$ ), together with delayed elastic deformation due to the spring and dashpot in parallel ( $E_2$  and  $\eta_2$ ). When the stress is removed, instantaneous elastic recovery occurs followed by a delayed elastic recovery which tends towards an asymptotic value. The value of the asymptote is the amount of permanent deformation accumulated due to viscous deformation (dashpot  $\eta_1$ )

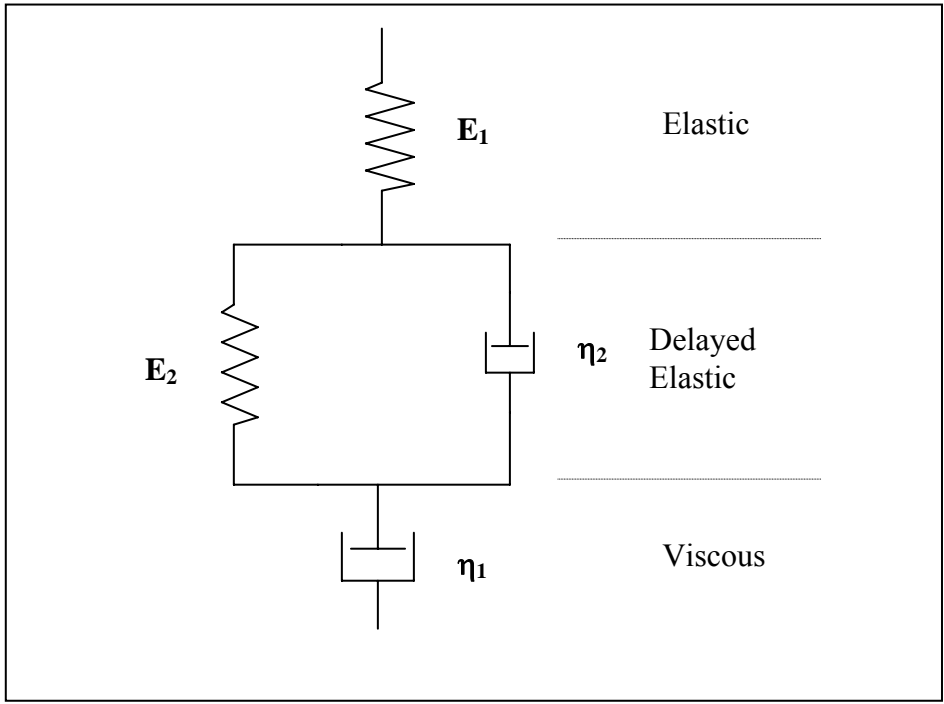


**Figure 5-2: Burgers' model**

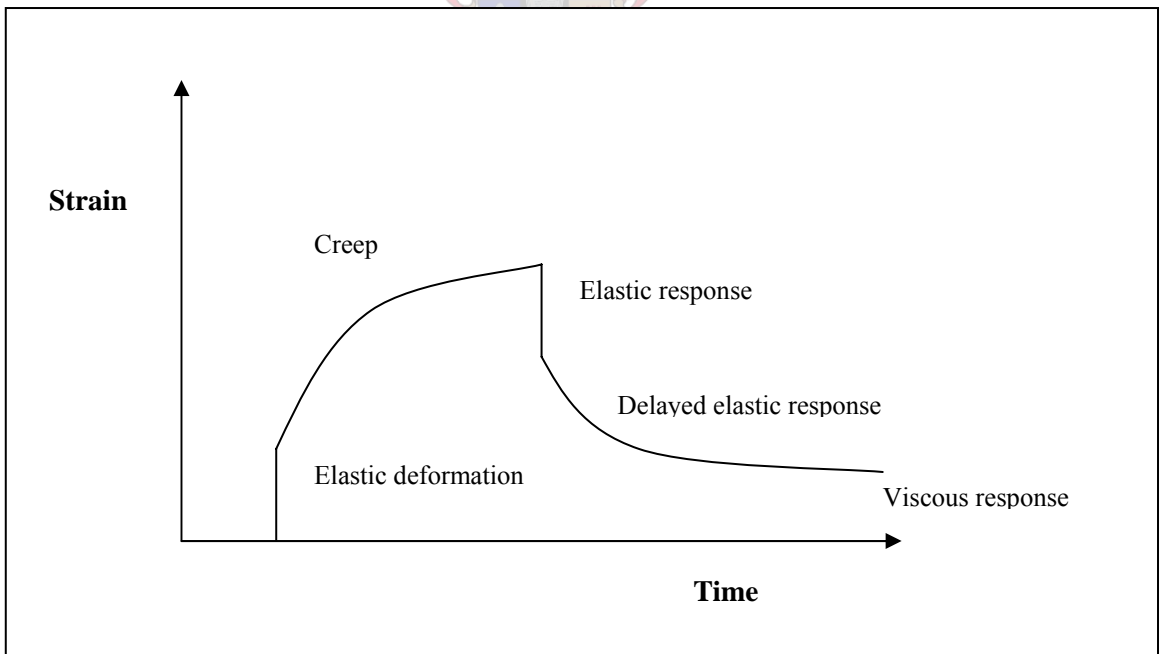


**Figure 5-3: Deformation response of a viscoelastic material under constant load**

In rheology, elastic behaviour is defined as an in-phase strain response to an applied load; this means the phase angle is 0°. Viscous behaviour is defined as a strain response that is 90° out of phase from the applied load. Viscoelastic behaviour occurs when the phase angle is between 0° and 90°. The viscoelastic behaviour of asphalt can be explained by means of Figure 5-4. When an asphalt mixture or specimen is subjected to a cyclic load (like traffic loading on the pavement), the resulting deformation does not occur immediately. The lag in time between stress application and the resulting strain is the phase angle ( $\delta$ ). Part of the strain is also not recovered completely.

At low temperatures and high loading frequencies, the bitumen and asphalt mix behave purely elastic. At high temperatures and long loading times the bitumen and asphalt mix will behave viscous (Figure 5-5). The complex shear modulus ( $G^*$ ) quantifies the total resistance to binder deformation when shear loads are repeatedly applied. Recoverable (elastic) and non-recoverable (viscous) parts constitute  $G^*$ . The equation used to determine  $G^*$  is the maximum shear stress divided by maximum shear strain. The phase angle denotes quantities of recoverable and non-recoverable deformation. It can be seen that material 1 behaves more viscous and material 2 more elastic.

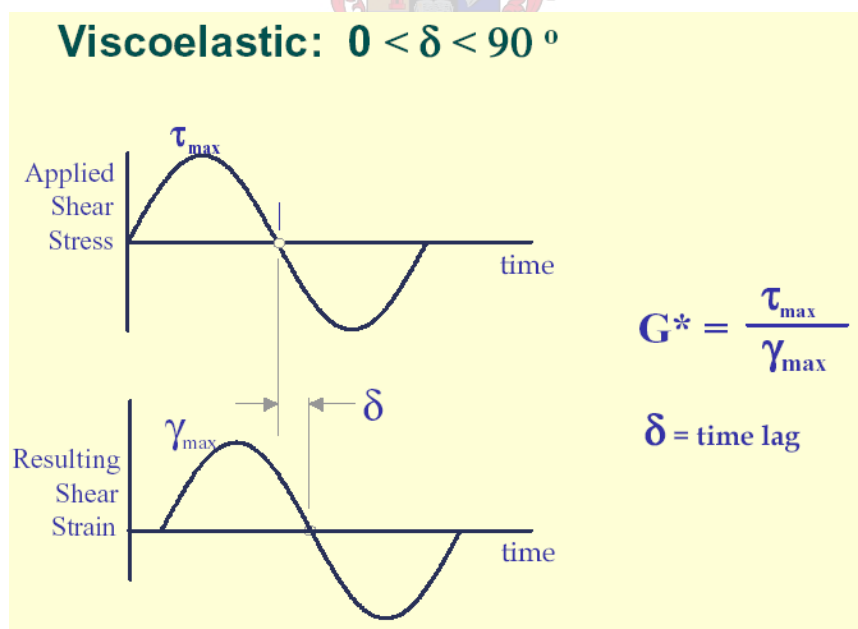


**Figure 5-4: Viscoelastic behaviour**

For rutting resistance, a high complex shear modulus,  $G^*$  and a low phase angle  $\delta$  are desirable. The higher the  $G^*$  value, the stiffer and thus the more resistant to rutting the binder

will be. The lower the  $\delta$  value, the more elastic the binder. These two values are combined to develop the parameter of  $G^*/\sin \delta$  or high temperature stiffness. It has been shown that the higher the high temperature stiffness the lower the rutting. Increasing  $G^*$  for same phase angle indicates more elasticity. Decreasing phase angle for same  $G^*$  indicates more elasticity.

At most service temperatures, binders and asphalt mixes are viscoelastic materials

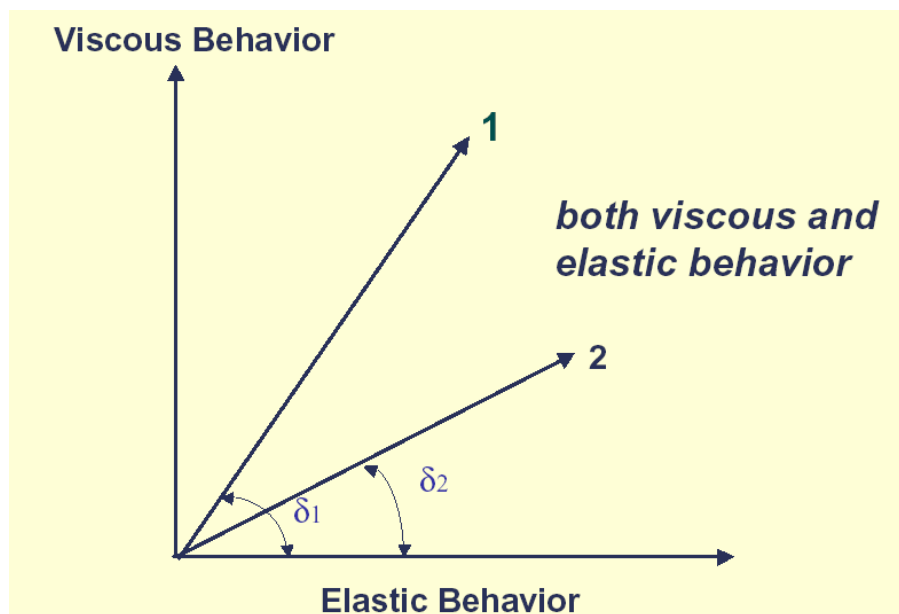


**Figure 5-5: Elastic and Viscous behaviour**

Permanent deformation is caused by a combination of densification and shear flow. The initial rut is caused by densification of the pavement under the wheel. However, the subsequent rut is a result of shear flow of the mix. This can be seen in the upheaval of the pavement in between the wheel paths. In properly compacted pavements, however, shear flow in asphalt is thought to be the primary rutting mechanism. Shear deformation can be a result of inadequate aggregate (well-rounded and/or weak) in the asphalt mixture. This leads to irrecoverable movement of the material along the shear plane during heavy trafficking. Material is forced out from under the tyres causing a depression in the wheel path and upheaval on the edges (Figure 2-15). Plastic flow due to excessive binder may lead to a decrease in aggregate interlock and the load carried by the binder itself. This produces similar effects as shear deformation in that there is a lateral movement of material from under the loading area to the outer edge.

The rut caused by further compaction due to traffic is the result of a reduction in volume. Compaction after construction occurs in almost every pavement. After construction there is

typically 6 to 8 percent air voids. After about a year of traffic exposure, 3 to 5 percent air voids is common in wheel paths. This decrease in the amount of air voids means less volume and a small rut is formed. In excessive cases, the air voids can be reduced to zero resulting in significant rutting.

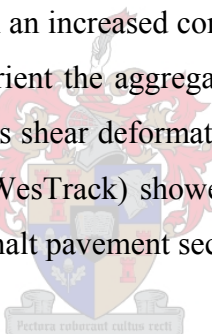
Three phases can be identified in the development of permanent deformation. In the initial phase, the material is considered to experience additional compaction and/or rearrangement of the aggregate skeleton (see Figure 2-16). Without the aggregate skeleton resisting the shear stresses that appear near the edge of the tyres, the mix rapidly develops large permanent shear strains, which, in turn, cause the development of the rut. The relatively high local pressures results in the reorientation, which ultimately leads to an improved aggregate interlock. Consequently, the slope (or rut rate) reduces as the modulus of the mixture increases. In the second phase, the linear phase, the rate of deformation is slower. As the mixture densifies, it steadily develops better aggregate interlock and resistance to shear stresses. In some cases no significant linear phase occurs because the material is very unstable or the loading conditions are so severe that it reaches the tertiary phase before reaching a constant slope. The tertiary or catastrophic phase is reached when the rut rate begins to increase again. In this phase, large-scale aggregate movements are observed, accompanied by significant volumetric effects, i.e., the material exhibits dilatancy. The mix loses stability only when the reduction of the air void content causes the binder to prevent point-to-point contact in the aggregate.

The extent to which permanent deformation will occur in the pavement depends on the stress level, which is influenced by the load and the geometry of the structure and the materials in the structure, as well as the materials' resistance to permanent deformation. With regard to the influence of the stresses it is noted that especially the magnitude of the shear stresses are of importance (Molenaar, 2001).

Asphalt pavement layers transfer the traffic-induced load from the surface to underlying layers through interparticle contact and resistance to flow of the binder matrix; therefore, high shear resistance must be developed in the asphalt to withstand the high shear stresses. If the shear stress created by repeated wheel load applications exceeds the shear strength of the mix, then rutting will occur.

The shear resistance of an asphalt mix depends on the resistance of the aggregate structure and the cohesion of the binder or viscous shear resistance. The effect of these components can vary with different conditions. At high temperatures, and longer loading times, the apparent cohesion of the binder is much lower and deformation will take place due to the shearing resistance being exceeded. The performance of the material, at high temperatures, will therefore depend on the shear strength of the material.

With asphalt, the amount and nature of the binder and filler used, and the temperature of the mix influence the cohesion of the mix. The angle of internal friction is influenced by the binder content, temperature and the aggregate properties. Softer binders at higher temperatures or longer loading times have less cohesion, thus the shear strength of the mix is lower. Higher binder contents also decrease the cohesion. More rounded particles and fewer angular particles, or an increased binder content can reduce the angle of internal friction and therefore reduce the shear strength of the mix (De Sombre *et al*, 1998). Improvements in the rutting resistance of asphalt pavements can be expected with an increased compactive effort. The primary benefit of increased compaction is to pack and orient the aggregate particles in the asphalt mix into an interlocking mass of material that resists shear deformation. An analysis of results from a full-scale pavement test track in Nevada (WesTrack) showed that a reduction in air void content improved the rut resistance of most asphalt pavement sections (J. Epps *et al*, 1999).



Rutting in an asphalt mix normally occurs in the early stages of a pavement's life when the binder is relatively low in viscosity. As the mix ages, the binder stiffens and the elastic strains decrease and the permanent deformation accumulated at each load application decreases.

Tyre-pavement contact stress distribution plays an important role in the development of permanent deformation in the asphalt layer. Rutting increases slightly with inflation pressure. Rutting is also dependent on load and contact area. For a given load, rut depth is higher when it is carried on single tyres, although the rut volume differs little between single and dual tyres. Speed interacts with rutting through its influence on the time for which a point on the pavement is exposed to wheel loads. Thus, deformation will be proportional to wheel load and inversely proportional to speed. A substantial amount of rutting can also occur if very thick asphalt layers are consolidated by traffic (Roberts *et al*, 1991).

In addition, construction factors, such as cold weather paving leading to low density, affect the rutting of asphalt pavements. Some asphalt mixes that have a good history of resisting rutting in posted speed applications may not perform well in intersections, climbing lanes, truck weigh stations, and other slow speed areas. The slow moving or standing loads occurring at these sites subject the pavement to higher stress conditions that can be enough to induce rutting and shoving. Braking, accelerating and turning movements generate shear stresses at the pavement surface. In addition, load repetitions at intersections are sometimes double than that of mainline pavement due to the cross flow of traffic.

One of the factors affecting rutting is ageing. As the mix ages the binder stiffens, the elastic strains decrease and the permanent deformation accumulated at each load application decreases. Short-term oven ageing (four hours at 135 °C on the loose mix) is supposed to simulate ageing effects occurring during the mixing process in the plant (Sousa, 1994). It is therefore likely that a specimen prepared in this fashion might not be representative of a specimen that was three or four years in the field. The long-term oven ageing might be a more appropriate procedure. The relative effects of long term and short-term ageing are quite different. This will significantly affect the number of ESALs predicted by the procedure and emphasizes the need to establish a criterion of laboratory specimen fabrication that will produce specimens with characteristics similar to those encountered in the field. Before this procedure can be used to its fullest extent, research has to determine the best test protocol in laboratory to account for ageing affects.

The compaction method also has an influence on the rutting resistance of asphalt mixes. Test results (Sousa *et al*, 1991) using a repetitive direct simple shear device had shown that the kneading compactor produces specimens more resistant to shear deformation and with greater dilation under shear load than do rolling wheel or gyratory specimens, with rolling wheel specimens exhibiting properties between those of kneading and gyratory specimens. The effects of compaction are much more pronounced in well-compacted specimens in whom each compaction method produces its own distinct aggregate structure. In poorly compacted specimens, the lack of compaction results in a poor aggregate structure regardless of the method used. It shows that specimens with the same average percent voids may have a different distribution of air voids, and are thus expected to respond differently under loading and yield distinct mechanical properties in laboratory testing.

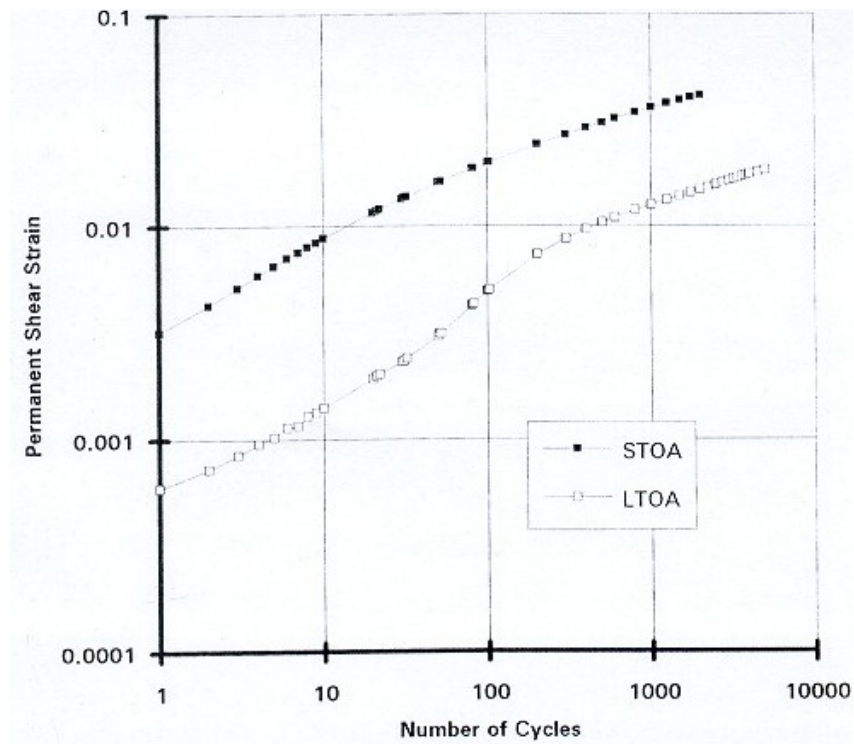


**Figure 5-6: Variation of Permanent Shear Strain in RSST-CH on Specimens of the Same Mix Subjected to Short-Term and Long-Term Ageing (Sousa, 1994)**

The orientation of aggregates and aggregate contact points may also be different and can have an influence on the shear strength properties of the mix (Masad *et al*, 1999). A higher number of coarse aggregate contacts will result in higher shear strength.

Bissada (1983) found that increased compaction results in a relative increase in the volume of mineral aggregates, which improves the strength of the asphalt mix by increasing the components of its frictional resistance. This appears to be valid only as long as the VIM does not reach a critical end value. As soon as the percentage of VIM drops below this critical value, due to further traffic densification, significant losses in the component of frictional resistance start to occur, which results in low stiffness values and excessive permanent deformation.

Bitumen shows a lower modulus when measured at low frequency than it does at high frequency. This explains why asphalt pavements can be susceptible to permanent deformation when subjected to slow moving (i.e. low frequency) traffic (Hunter *et al* 2000) Although temperature has the greatest effect on the properties of the bitumen, it is also important to consider the effects of time.

Air void content affects permanent deformation characteristics of asphalt aggregate mixes. With increase in confining pressure the permanent deformation is reduced (Sousa *et al*, 1994). Dilation is a phenomenon that accounts for the tendency of the development of confining stresses when the mix is subjected to relatively large shear strains. These confining stresses will in turn provide an increase in shear stiffness that reduces permanent deformation. Dilatency occurs in coarse-graded mixes with large aggregate and is due to the aggregate particles trying to slide past each other during shear.

### **5.3 Effect of specimen geometry on stress distribution**

The development of permanent deformation at any point inside asphalt layers is related to the prevailing state of stress and temperature conditions (Eckmann, 1987). These, in turn depend on the applied loads, climatic conditions, geometry of the structure and the material characteristics (stiffness). Using elastic layer theory, it is possible to compute the state of stress developed at any depth under any given loading and temperature condition.

When testing for permanent deformation in the laboratory, the testing should be performed at realistic temperature and stress conditions. One could not, for example, use a tyre width that is the same as the specimen width, because this would not really allow shear stresses to generate and get movement of the material due to shear. Laboratory testing specimens do not always have proper boundary conditions. In the laboratory, the specimens are confined in a mould and are resting on steel or very stiff base. This is however not the case in an asphalt pavement in the field.

Two types of specimens are typically used in the laboratory at Stellenbosch University for MMLS3 testing. These are briquettes and slabs (refer Chapter 4). During MMLS3 trafficking, the briquette specimens are constantly subjected to increasing vertical stresses during MMLS3 trafficking. This causes the material to tend to displace horizontally. The clamps used to confine the specimens resist this displacement, which lead to an increase in horizontal stresses. In asphalt pavements horizontal displacement does occur due to the applied vertical stresses. To make this test more representative, Du Preez (2001) recommended that the clamps confining the specimens horizontally should be able to allow some horizontal displacement. Concern has been raised that the confinement and specimen geometry may

influence the rutting results. Analysis has been performed with ELSYM5 and ABAQUS (HKS, 2002) to ascertain whether different specimen geometries would influence the stress distribution within the specimen, and subsequently the rutting results. These was done by estimating the stresses in the asphalt specimens at 50 °C under an MMLS3 load and then use these stresses as input parameters in rut prediction models to predict the rutting for the different specimen geometries.

Figure 5-7 shows the different variables considered in the stress analysis. The analysis is summarised in section 5.3.1 through section 5.3.3. For a comprehensive account of the sensitivity analysis and stress distributions, the reader is referred to Appendix A.

### ***5.3.1 Linear Elastic Analysis with ELSYM5***

Semi-infinite two layer systems have been analysed using ELSYM5. ELSYM5 is a linear elastic program capable of computing stresses in strain in a multilayer pavement structure. The variables considered are shown in Figure 5-7. The variation in thickness was to estimate the stresses in a slab (40 mm thick), briquette (60 mm thick) and very deep asphalt layer 1000 mm asphalt. For each case, the asphalt was analysed on top of a semi-infinite concrete subgrade with an elastic modulus of 28 GPa and Poisson's ratio of 0.18. Poisson's ratio for the asphalt was assumed 0.45 and the elastic modulus was varied between 500 MPa and 1500 MPa, to determine the influence of the stiffness on the stress distribution. A wheel pressure of 690 kPa was applied over a wheel width of 80 mm. Appendix A gives a comprehensive account of the sensitivity analysis.

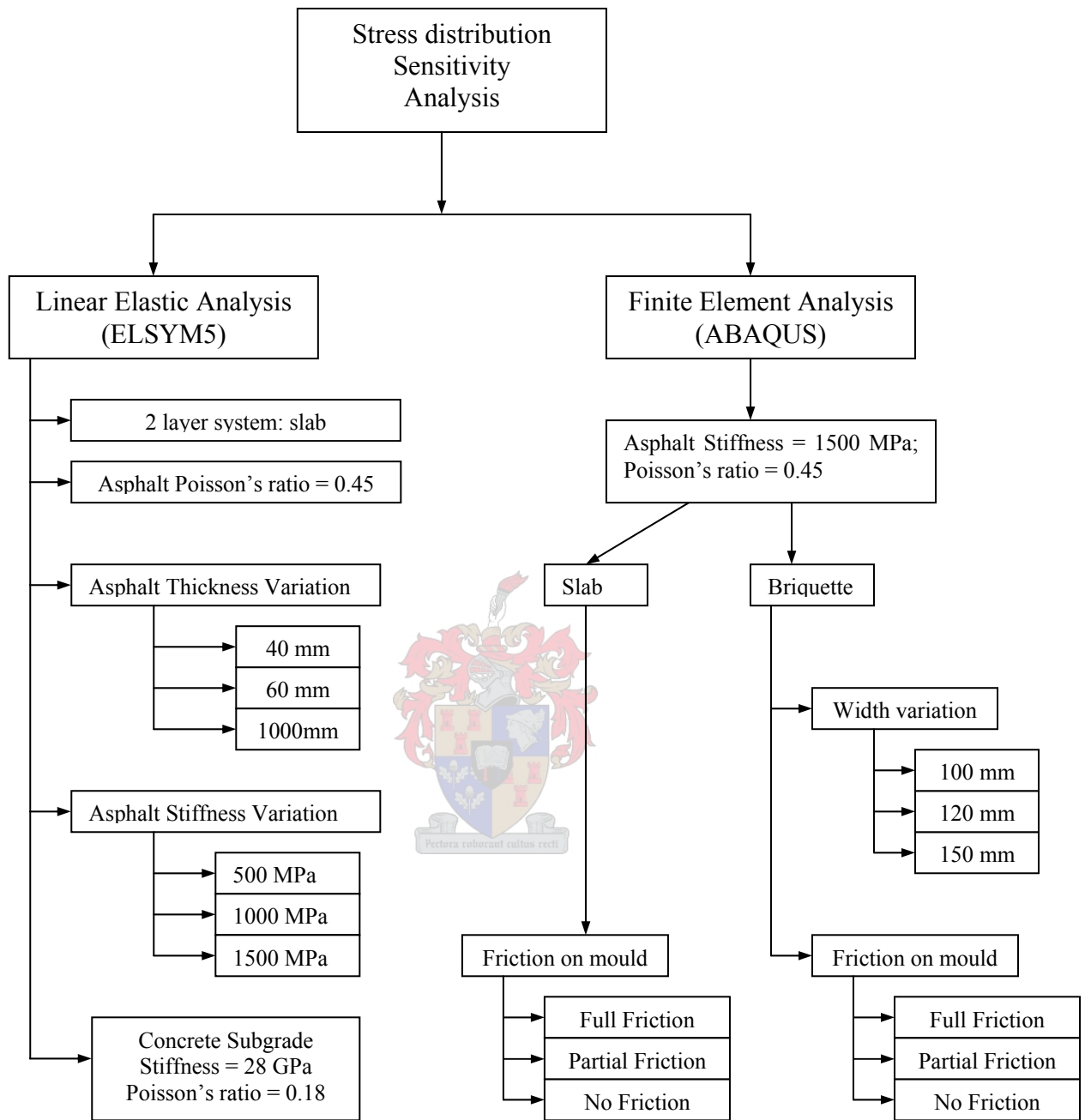


**Figure 5-7: Diagram illustrating the stress analysis for different specimen geometries**

### **5.3.2 Finite Element Analysis with ABAQUS**

ELSYM5 is not able to model horizontal confinement. A finite element program ABAQUS was used to obtain a better approximation of the stress conditions in the slab en brique specimen respectively, due to confinement. A two dimensional linear elastic analysis was performed. For the geometrical model, 8-noded quadrilateral plane strain finite elements (5 x 5 mm) were used, formulated according to the linear elastic theory. Since there was a plane of symmetry, only half of the specimen was analysed. The following cases were analysed:

- Briquette 60 mm height and widths of 100, 120 and 150 mm
- Slab 40 mm height and width 600 mm

The specimens were subjected to an equivalent static loading of 690 kPa over a width of 80 mm. The bottom boundaries were fixed. The symmetry boundary was only constrained from horizontal displacement. For the outside boundary no horizontal displacement was allowed and with regard to vertical displacement, three conditions were considered:

1. Fixed boundary (simulating full friction between specimen and mould)
2. Vertical roller support (simulating no friction between specimen and mould)
3. Prescribed displacement; 50 percent of the resulting displacement from case 2 (simulating partial friction between specimen and mould)

The results from ELSYM5 and ABAQUS were stored in a spreadsheet and contours were plotted in MATLAB. Some of these results can be seen in Figure 5-11 and Figure 5-12. More contour plots can be found in Appendix A.

The ABAQUS input files can be seen in Appendix B. Figure 5-8 and Figure 5-9 illustrate the meshes of the briquette and slabs with typical deformation under the wheel.

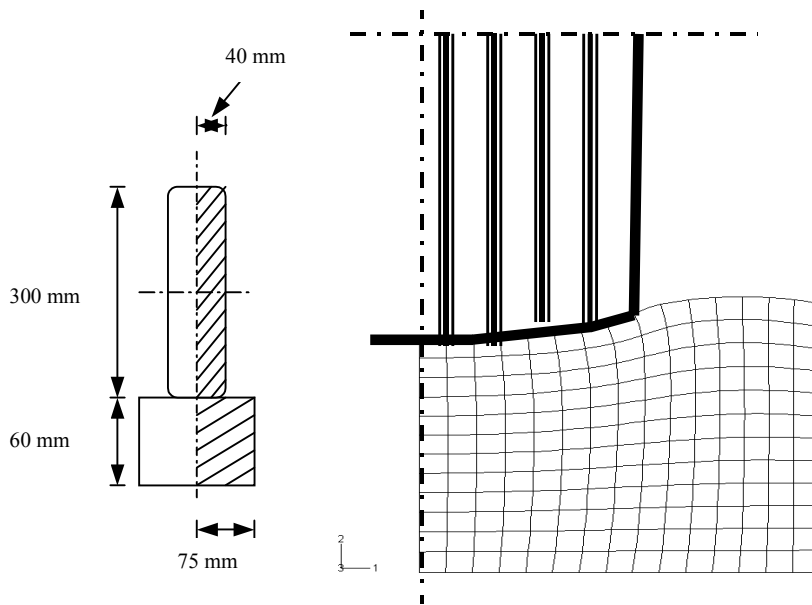


**Figure 5-8: Illustration of briquette deformation (not to scale)**

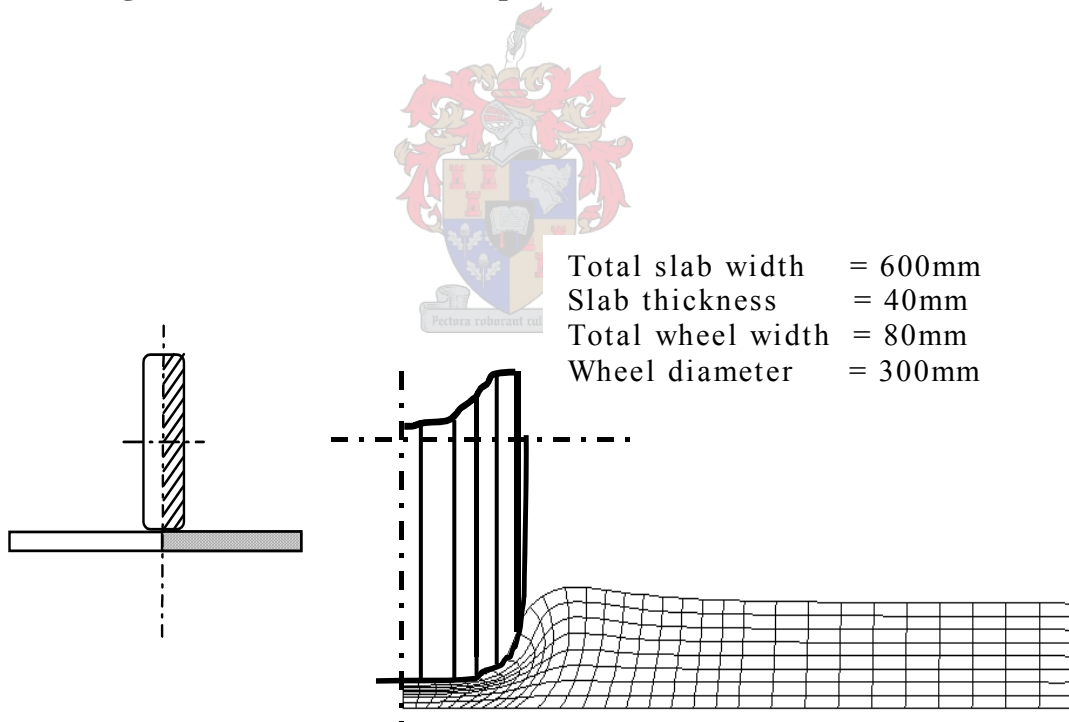


**Figure 5-9: Illustration of slab deformation (not to scale)**

For the analysis, the axes have been selected as shown in Figure 5-10.

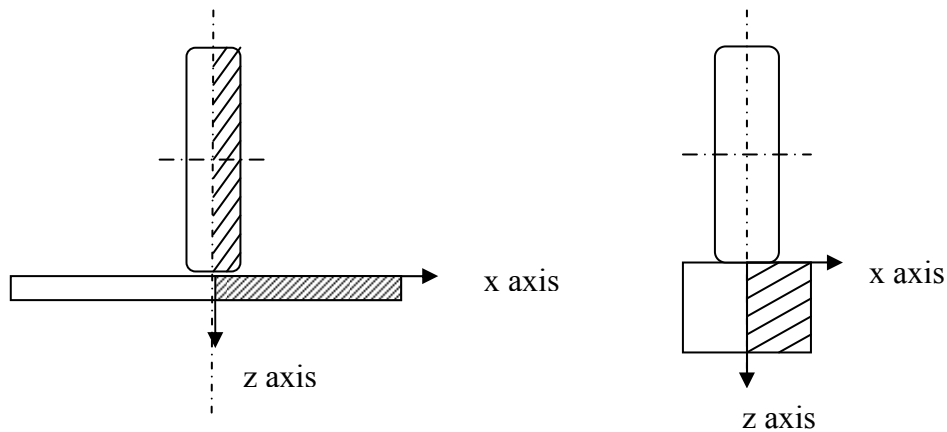


**Figure 5-10: The coordinate system for the stress distribution analysis**

### **5.3.3 Summary of stress distribution analysis**

From the ELSYM5 analysis, it appears that the asphalt elastic modulus does not have a significant influence on the stress distribution. Table 5-1 and Table 5-2 give the horizontal ( $\sigma_h$ ) and deviator stress ( $\sigma_d$ ) values for different stiffness moduli at selected positions for the 40 mm and 60 mm asphalt respectively. From these tables it can be seen that the corresponding stresses are comparable, only differing by as much as 5 percent.

The thickness of the asphalt layer did influence the stress distribution, as was expected. Comparing Table 5-1 and Table 5-2, it can be seen that the horizontal stresses in the thinner layer (40mm) were generally higher than in the thicker layer (60mm), except for the upper 5 – 10 mm where the stresses for the 60mm layer were higher. When comparing the deviator stresses, it is evident that the stress in the upper 20mm is higher for the 40mm layer than for the 60mm layer. Since ELSYM5 treated the layers as semi-infinite in the horizontal direction, the influence of the specimen size and confinement could not be determined.

**Table 5-1: Influence of asphalt modulus on stress distribution (asphalt thickness 40mm)**

Position		ELSYM5 40mm 1500 MPa		ELSYM5 40mm 1000 MPa		ELSYM5 40mm 500 MPa	
z(mm)	x(mm)	$\sigma_h$ (kPa)	$\sigma_d$ (kPa)	$\sigma_h$ (kPa)	$\sigma_d$ (kPa)	$\sigma_h$ (kPa)	$\sigma_d$ (kPa)
0	0	412	278	406	284	400	290
0	20	461	246	456	250	451	256
0	40	295	140	293	143	291	147
0	60	10	42	10	44	10	46
20	0	273	425	272	427	272	429
20	20	234	411	234	412	233	414
20	40	200	287	200	287	199	286
20	60	133	124	132	124	132	124
40	0	448	110	454	108	460	106
40	20	386	248	391	248	395	247
40	40	210	335	211	335	213	335
40	60	60	210	58	209	57	208

From the above and Appendix A it can be concluded that the variation in stiffness for a particular thickness does not have a significant influence on the stress distribution. Only when comparing the same stiffness at different thicknesses, the influence of the thickness becomes apparent.

**When comparing the ELSYM5 and ABAQUS results, it can be seen from**

Table 5-3 when horizontal boundaries are introduced, the stresses increases. The ABAQUS vertical stress results for the 150mm briquette showed that the case with no friction is comparable to the ELSYM5 distribution, except that the higher stresses occur slightly deeper in the specimen. The amount of friction does only appear to influence the stresses in the outer 25mm of the specimen. As the briquette width decreases, the vertical stresses in the region

between the wheel and the mould increase. The amount of friction also plays an increasing role in that region, with the most interference observed in the full friction case.

**Table 5-2: Influence of asphalt modulus on stress distribution (asphalt thickness 60mm)**

Position		ELSYM5 60mm 1500 MPa		ELSYM5 60mm 1000 MPa		ELSYM5 60mm 500 MPa	
z(mm)	x(mm)	$\sigma_h$ (kPa)	$\sigma_d$ (kPa)	$\sigma_h$ (kPa)	$\sigma_d$ (kPa)	$\sigma_h$ (kPa)	$\sigma_d$ (kPa)
0	0	504	186	500	190	496	194
0	20	525	173	522	177	518	180
0	40	297	119	295	121	293	123
0	60	49	50	49	52	50	54
20	0	210	452	209	454	208	456
20	20	182	445	181	446	179	447
20	40	168	328	167	328	166	328
20	60	122	133	121	133	121	133
40	0	151	388	152	390	153	391
40	20	147	348	145	348	149	349
40	40	145	238	146	237	146	237
40	60	121	132	121	131	121	130
60	0	318	81	324	79	329	77
60	20	277	178	281	178	286	178
60	40	177	240	179	240	181	241
60	60	81	195	81	195	81	195

**Table 5-3: Influence of asphalt thickness on stress distribution**

Position		ELSYM5 40mm		ABAQUS 40mm		ELSYM5 60mm		ABAQUS 60mm	
z(mm)	x(mm)	$\sigma_h$ (kPa)	$\sigma_d$ (kPa)	$\sigma_h$ (kPa)	$\sigma_d$ (kPa)	$\sigma_h$ (kPa)	$\sigma_d$ (kPa)	$\sigma_h$ (kPa)	$\sigma_d$ (kPa)
0	0	412	287	349	338	504	186	515	173
0	40	295	140	213	285	297	119	289	260
0	50	54	70	90	61	77	80	55	32
0	60	10	43	6	16	49	50	17	21
0	75	24	39	68	65	15	32	41	40
20	0	273	425	324	379	210	452	327	365
20	40	200	287	236	293	168	328	298	300
20	50	182	190	244	222	161	215	325	274
20	60	133	124	197	185	122	140	302	272
20	75	54	77	118	134	72	75	281	273
40	0	448	110	517	115	151	388	293	351
40	40	210	335	271	426	150	238	300	197
40	50	121	288	163	398	148	179	312	189
40	60	60	210	84	318	127	132	317	215
40	75	20	113	27	197	87	89	317	240
60	0	-	-	-	-	318	81	468	104
60	40	-	-	-	-	177	240	286	281
60	50	-	-	-	-	125	227	216	245
60	60	-	-	-	-	81	195	162	167
60	75	-	-	-	-	39	136	129	29

**Table 5-4: Influence of friction on the 150mm briquette specimen (ABAQUS)**

Position		Briquette 150 No Friction		Briquette 150 Partial Friction		Briquette 150 Full Friction	
z(mm)	x(mm)	$\sigma_h$ (kPa)	$\sigma_d$ (kPa)	$\sigma_h$ (kPa)	$\sigma_d$ (kPa)	$\sigma_h$ (kPa)	$\sigma_d$ (kPa)
0	40	289	260	293	260	257	270
0	60	17	21	29	16	40	12
0	75	41	40	31	30	757	487
40	40	300	197	295	195	345	165
40	60	317	215	312	220	363	142
40	75	317	240	302	306	342	63

For the various briquette widths, the maximum shear stresses decrease as the width decreases (Figure A - 29 through Figure A - 32). This can be expected, because the narrower specimens do not allow that much horizontal displacement within the material as the wider specimen. This gives an indication that the wider specimens may exhibit more vertical deformation. For all the 150mm briquette width, only the full friction case appears to have a significant influence on the shear stresses between the wheel and the mould. The shear stresses right under the side of the wheel are higher for the slab than the briquettes, with the highest shear stresses occurring at the bottom of the slab. As for the vertical stresses, the shear stresses from the applied wheel load do not extend significantly beyond 100mm from the center of the wheel.

The horizontal stresses within the briquettes increases with a decrease in briquette widths. This can be expected due to the confinement that resists horizontal movement. The horizontal stresses between the wheel and the mould are also higher for the 100mm briquette. The horizontal stresses in the slab are generally lower than in the briquettes. There is not any significant difference in horizontal stress distributions for the different slab results. Also, the friction does not influence the stress distributions. Table 5-5 and Figure 5-11 summarizes some of the horizontal and deviator stresses for the different specimen widths.

**Table 5-5: Influence of specimen width on stress distribution**

Position		Briquette 100		Briquette 120		Briquette 150		Slab	
z(mm)	x(mm)	$\sigma_h$ (kPa)	$\sigma_d$ (kPa)	$\sigma_h$ (kPa)	$\sigma_d$ (kPa)	$\sigma_h$ (kPa)	$\sigma_d$ (kPa)	$\sigma_h$ (kPa)	$\sigma_d$ (kPa)
0	0	577	120	561	128	515	173	349	338
0	40	251	274	284	263	289	260	213	285
0	50	172	97	87	55	55	32	90	61
0	60	-	-	47	38	17	21	6	16
0	75	-	-	-	-	41	40	68	65
0	100	-	-	-	-	-	-	9	75
20	0	449	231	384	301	327	365	324	379
20	40	475	222	373	303	298	300	236	293
20	50	528	210	415	307	325	274	244	222
20	60	-	-	416	309	302	272	197	185
20	75	-	-	-	-	281	273	118	134
20	100	-	-	-	-	-	-	56	74
40	0	427	210	348	287	293	351	517	115
40	40	479	79	391	145	300	197	271	426
40	50	492	66	417	157	312	189	163	398
40	60	-	-	428	171	317	215	84	318
40	75	-	-	-	-	317	240	27	197

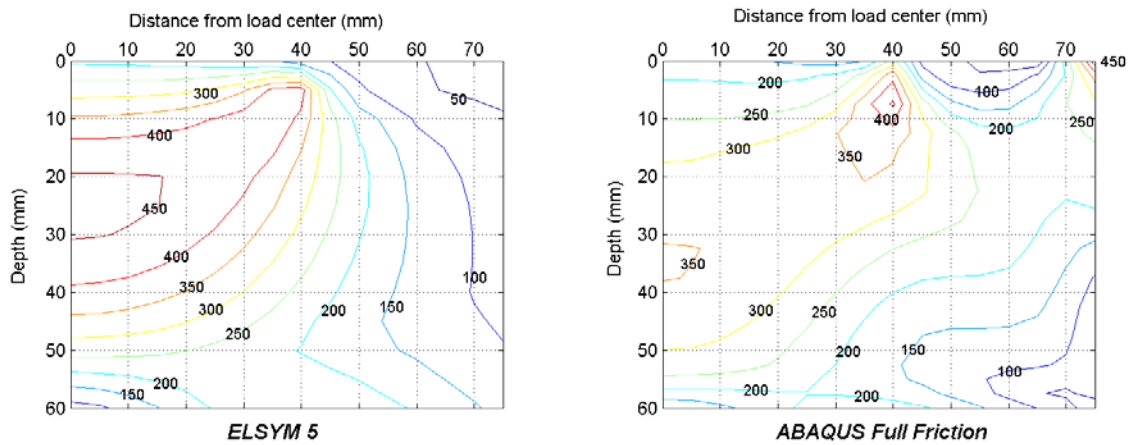


**Figure 5-11: Deviator stress ( $\sigma_1 - \sigma_3$ ) contours (kPa) for Briquette width 150 mm**

The deviator stress distributions for the different briquette thicknesses (Table 5-5) showed that the higher deviator stresses occur in the 150 mm briquette. This indicates that this specimen will yield higher rutting, followed by the 120mm and then the 100mm briquette. The deviator stresses for the slab are generally higher than for the briquettes. For the slab, it is once again seen that the deviator stresses does not extend beyond 100mm from the wheel center. This and the other slab stress distributions indicate that the slab is wide enough not to have border effects influence the stress distribution.

As expected, the highest vertical, horizontal deviator stresses occur under the wheel. The highest shear stresses occur under the side of the wheel, also as expected. For the briquettes, the deviator stress decreases and the horizontal stress increases with a decrease in width. The horizontal stress on the outside of the wheel is generally higher for the briquettes than was the case for the slab. It appears that the width of the briquette does influence the stress distribution within the specimen. The amount of friction may also play a role especially in the region between the wheel and the mould.

Based on the analysis for the slab, it can be derived that there is no significant difference in the stress distribution for the slab specimen as determined by ELSYM5 and ABAQUS. Since ELSYM5 consider layers as having semi-infinite width, it can therefore concluded from the ABAQUS results that the slab is wide enough so that the sides of the mould does not interfere with the stress distribution. It also appear that the amount of friction between the sides of the mould and the slab specimen do not influence the stress distribution. The highest deviator

stress is experienced under the wheel, as expected. This is also the case for the horizontal and vertical stresses. The highest shear stresses occur under the side of the wheel.

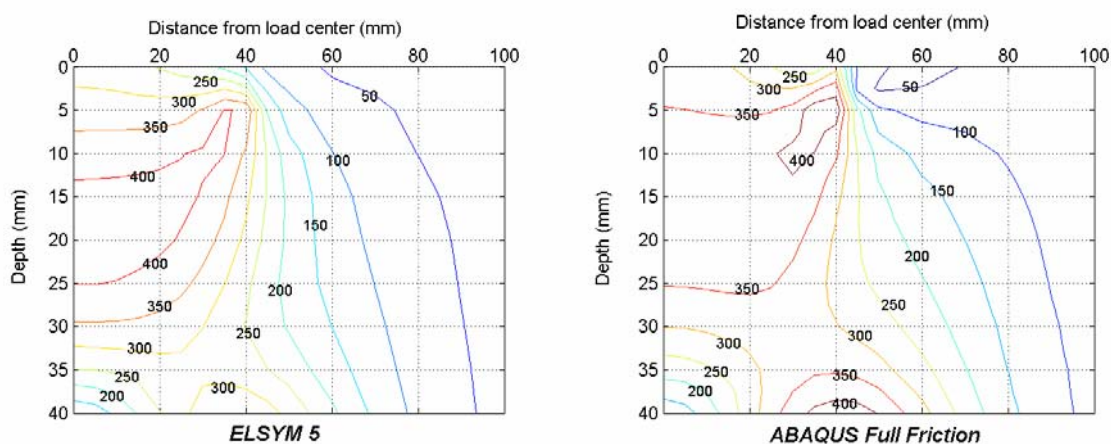


**Figure 5-12: Deviator stress ( $\sigma_1 - \sigma_3$ ) contours (kPa) for slab**

## 5.4 Rut prediction models

As mentioned in section 5.2, the stresses are one of the factors influencing rutting. The stresses in the different test configurations were estimated in section 5.3. These stresses from ELSYM5 and ABAQUS will be used to compare rutting estimation for the two methods and different test configurations (slab vs. briquette), and then analyse the order of difference.

Leahy and Witczak (1991), May and Witczak (1992) developed models for relating permanent strain to temperature, deviator stress and load repetitions from triaxial experiments.

$$\log \varepsilon_p = -15.83 + 7.132 \log T + 1.1505 \log \sigma_d - 0.118 \log \eta + 2.155 \log Vb_{eff} + 1.117 \log V_a + 0.986 [T^{-0.102} VMA^{-0.158}] \log N$$

**Equation 5-1**

$$\log \varepsilon_p = -11.86 + 6.129 \log T + 1.117 \log \sigma_d - 0.113 \log \eta + 0.716 \log Vb_{eff} + 0.285 \log V_a + (0.0015T \times 0.01736VMA) \log N$$

**Equation 5-2**

$$\log \varepsilon_p = -14.97 + 6.865 \log T + 1.1107 \log \sigma_d - 0.117 \log \eta + 1.908 \log Vb_{eff} + 0.971 \log V_a + 0.408 \log N$$

**Equation 5-3**

where

$\varepsilon_p$	= plastic strain (microstrain)
T	= test temperature (°F)
$\sigma_d$	= deviator stress (psi)
$\eta$	= viscosity at 70 °F ( $10^6$ poise)
$Vb_{eff}$	= effective binder volume (%)
$V_a$	= air voids (%)
VMA	= voids in the mineral aggregate (%)
N	= number of load repetitions

These models were based on 251 repeated load triaxial tests done by Leahy (1989). In these tests, 100mm x 200mm specimens were subjected to 30 000 repetitions at a constant load frequency of 60 cycles/min. Two aggregate types (rounded gravel & crushed stone) and two binder types (AC-5 & AC-20) were considered. These models are not applicable to the case of extremely low air voids (< 3%), where plastic flow dominates the behaviour of the mix.

Deacon *et al* (1994) used layered strain procedures to estimate permanent surface deformation as follows:

$$\sum \varepsilon_p \cdot (thickness)$$

**Equation 5-4**

where:

$\varepsilon_p$	= vertical permanent strain in a layer increment,
thickness	= thickness of the increment, and
$\Sigma$	= summation over all of the increments within the asphalt layer

In this approach, multiplayer elastic analysis (ELSYM) is used to estimate the stress and strain within hypothetical pavement structures. These are used together with the models in equations 5-1 through 5-3 to estimate the effect of load repetitions on permanent surface deformation.

To properly account for temperature effects, the asphalt layer was subdivided into four sublayers of varying temperature and, hence varying stiffnesses. The deviator stress was computed at 25 mm deep increments throughout the asphalt layer. Because failure was associated with a permanent surface deformation of 12.7 mm (0.5 in.), a trial-and-error process was necessary to determine the appropriate permanent deformation life.

Monismith *et al* (1977) reported that the estimation of permanent deformation occurring in a pavement structure requires determination of some relationship between plastic (permanent) strain and applied stress, i.e.  $\epsilon_p = f(\sigma_{ij})$ , for each of the components susceptible to rutting. They estimated the permanent strain at a point in the pavement structure in the vertical direction is estimated using the following form of equation:

$$\epsilon_z^p = R[\sigma_z - \frac{1}{2}(\sigma_x + \sigma_y)] \tag{Equation 5-5}$$

with Poisson's ratio assumed 0.5

where:

$\sigma_x$ ,  $\sigma_y$  and  $\sigma_z$  = stresses in tangential, radial and vertical directions respectively

$\sigma_x$  = positive in tension

$\sigma_y$  = positive in tension

$\sigma_z$  = positive in compression

R = ratio of total “effective strain” to the “equivalent stress”

For triaxial conditions the equivalent stress =  $(\sigma_1 - \sigma_3)$  and the total effective strain =  $\frac{2}{3}(\epsilon_1 - \epsilon_3)$

These values were then used for a number of load repetitions to compute permanent strains, which, in turn permitted permanent deformation in the layer to be obtained from the relation:

$$\delta^p = \sum_{i=1}^n (\epsilon_i^p \Delta z_i) \tag{Equation 5-6}$$

where:

- $\delta^p$  = rut depth in asphalt layer  
 $\varepsilon_i^p$  = permanent strain in subdivided layer

For asphalt materials, temperature and loading time effects must also be incorporated. The total permanent strain becomes time dependent, as does the relationship for R. For asphalt, this equation becomes:

$$\varepsilon_z^p = \delta(T) \cdot N^\alpha \left(\bar{\sigma}\right)^{n-1} \cdot t \left[ \sigma_z - \frac{1}{2}(\sigma_x + \sigma_y) \right] \quad \text{Equation 5-7}$$

where:

- $\bar{\sigma}$  =  $\frac{1}{2}[(\sigma_1 - \sigma_3)^2 + (\sigma_2 - \sigma_3)^2 + (\sigma_3 - \sigma_1)^2]$ ,  
 N = Number of load repetitions,  
 $\delta(T)$  = function of temperature, T (absolute), with one form as  
 $\delta(T) = T e^{-A/T}$ , and  
 $\alpha, n, A$  = experimentally determined coefficients

While there are some limitations to this approach, e.g., the effects of lateral road placement are not considered nor are the reversal of shear stresses which may take place with load passage and lateral distribution, the methodology produce results which are “reasonable” in form. Moreover, a limited comparison indicates that the procedure can predict permanent deformations of the right order of magnitude. Accordingly, it is suggested by Monismith *et al* (1977) that such methodology can be used for special situations to check whether or not rutting will be of sufficient magnitude to cause concern.

Francken (1977), Francken and Clauwert (1987) described permanent deformation by means of:

$$\varepsilon_p(t) = At^B + C(\exp Dt - 1) \quad \text{Equation 5-8}$$

in which A,B,C and D are experimentally determined coefficients.

This law was to be fed into a structural design method directed towards the limitation of rutting. Cylindrical specimens of 5 different asphalt mixes (see Figure 5-13) were subjected to dynamic triaxial tests at different temperatures, frequencies and stress conditions; in these tests the vertical stress is a sinusoidal function of time and the lateral stress is a static one. The confining stress ( $\sigma_3$ ) was in the range of 0 to 5 MPa, and the vertical stress ( $\sigma_1$ ) in the range of 0 to 0.5 MPa. The test frequencies were between 1 and 50 Hz and the temperatures between 15 °C and 50 °C. The results obtained have been interpreted by considering two important mechanical characteristics: the dynamic stiffness modulus  $|E^*|$  and the creep curve.

Mix Number	56	59	66	67	68	
Max. size ( $\phi$ mm)	32	32	32	32	16	
Composition by weight	% stones	55	55	60	76	40
	% sand	38	38	31	18.5	48
	% filler	7	7	9	5.5	12
	% binder	6.1	6.1	4.7	3.8	6
Composition by volume	$V_A$	81.6	81.6	82.1	76.2	82.8
	$V_L$	13.4	13.4	10.1	7.8	11.2
	$v$	5	5	7.8	16	6
	$V_A/V_L$	6.08	6.08	7.91	9.77	7.39
Bitumen	penetration	57	97	97	97	42
	coefficient J	0.349	0.429	0.429	0.429	0.321

Note :  $J = \frac{d \log \text{pen}}{d \log t}$ , loading time susceptibility.

**Figure 5-13: Composition and characteristics of Francken mixes (Francken, 1977)**

If there is no plastic failure, then  $C = 0$ . It has been shown that  $A$  is related to a mean deviator stress level  $\sigma_0$ , where

$$\sigma_0 = \frac{\sigma_1 - \sigma_3}{2} + \sigma_3 \quad \text{Equation 5-9}$$

where:

$\sigma_1$  = total vertical pressure

$\sigma_3$  = cell pressure

A so-called plastic deformation modulus  $E_p$  was then defined using

$$E_p = \frac{\sigma_0 - \sigma_3}{A} \quad \text{Equation 5-10}$$

Equation 5-8 then becomes

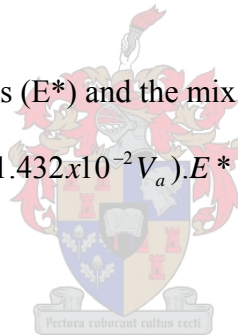
$$\varepsilon_p = \left( \frac{\sigma - \sigma_3}{E_p} \right)^B \quad \text{Equation 5-11}$$

The parameter B seems to be less dependent on the physical conditions and ranges from 0.1 to 0.3. A mean value close to 0.25 is a realistic value. The particular values of parameters C and D have not been investigated and are of little practical interests provided that the failure criterion is satisfied (Francken, 1977).

$E_p$  was related to the dynamic modulus ( $E^*$ ) and the mix composition such that:

$$E_p = (2.716 \times 10^{-3} + 1.432 \times 10^{-2} V_a) \cdot E^* \quad \text{Equation 5-12}$$

where  $V_a$  = void content



## 5.5 Rut prediction results

The aforementioned models were to be used to estimate the difference in rutting between the slab and briquette specimens. The models were set up in Microsoft Excel, and the permanent deformation were calculated for every 5mm sublayer and then summarised over the whole thickness. Transverse profiles were plotted to see what the amount of rutting was further away from the wheel load. It should be noted that although some of the models use imperial units, the spreadsheet was organised such that the input values could be entered in SI units, which were then converted to imperial units, and the final results were given in SI units.

Although these models may be derived for different mixes and conditions, the idea is to compare the output of these models for the different briquette and slab setup; i.e. then the stresses will be the only variable between the different geometries. Two of the rut prediction models, i.e. equation 5-1 and equation 5-3, yielded unrealistic rut estimations (in the order of 100 – 200 mm). These two models were excluded from subsequent analyses.

The models that were chosen for comparative rut estimation will be, for convenience, from here on referred to as the Witczak, Monismith and Francken models respectively:

Where,

- Witczak – equation 5-2
- Monismith – equation 5-7
- Francken – equation 5-11

The predicted rutting profiles for the 150mm briquette specimen for some of the models are given in Figure 5-14 and Figure 5-15.

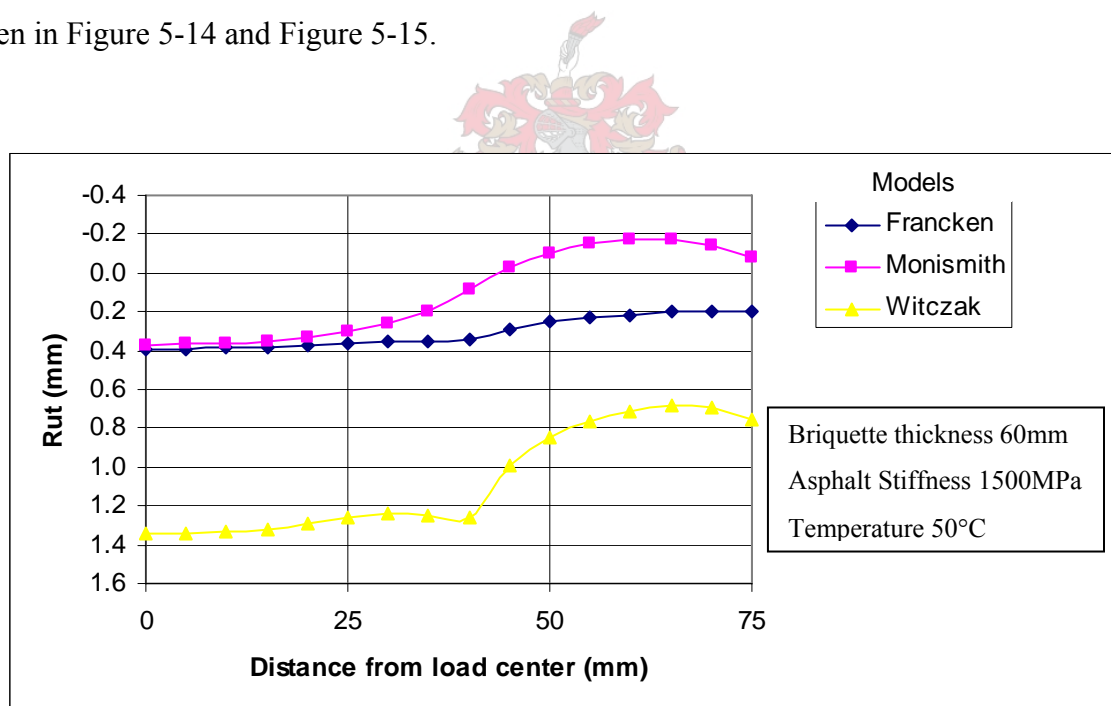
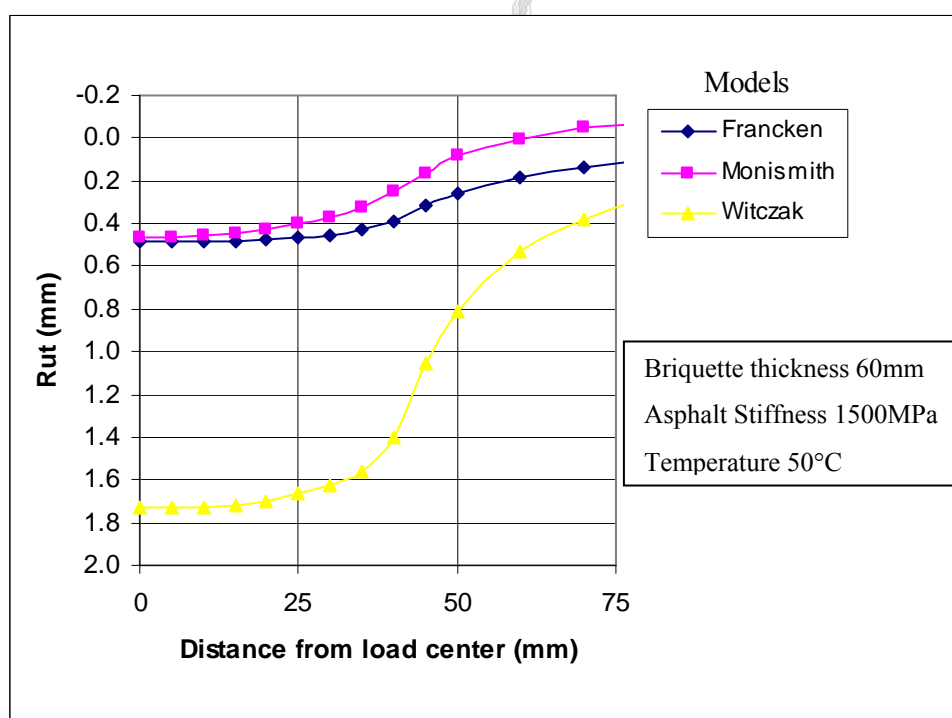


**Figure 5-14: Rut prediction profiles for 150mm briquette – ELSYM5**

An interesting observation is that only the Monismith-model gives a more realistic rutting profile across the briquette in that the rutting under the wheel is accompanied by an upheaval, which starts just outside the wheel path. An explanation could be that from equation 5-7, it is evident that this model takes into account the three-dimensional stress situation. For the other

two models, the deviator stress is the only input parameter that varies across the width of the briquette. Also, these two models were only developed to predict the maximum amount of rutting under the centre of the wheel, since it was derived from triaxial tests. The triaxial test is used to simulate the stress conditions on the symmetry axis of a wheel load (Brown and Bell, 1977).

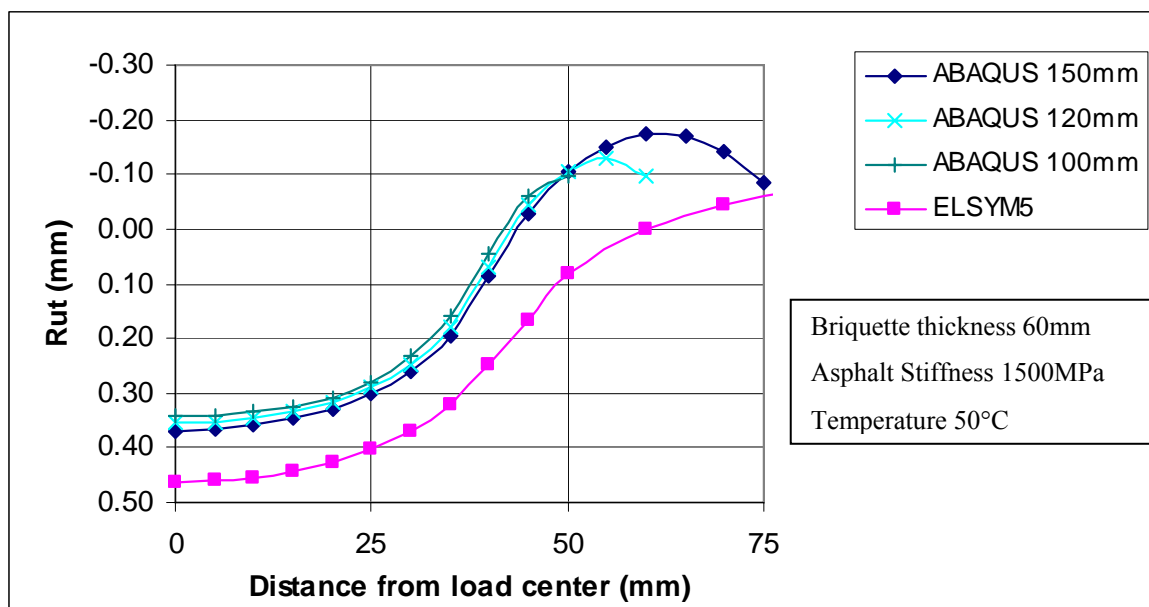
The slight increase in deviator stress on the side of the briquette can be observed by looking at the Witczak model in Figure 5-14. In the ELSYM5 analysis, there was no confinement (this linear elastic tool does not allow for horizontal boundaries being incorporated), thus the deviator stresses decrease all the way further from the wheel. This effect can be observed in Figure 5-15. As in Figure 5-14, the Francken and Monismith models yielded similar maximum rutting under the centre of the wheel. Also, the rutting prediction was higher for ELSYM 5 than was the case for ABAQUS. This was expected, since the ELSYM 5 stress outputs were higher than the ABAQUS outputs.



**Figure 5-15: Rut prediction profiles for 150mm briquette – ELSYM5**

Figure 5-16 gives the prediction for the briquettes calculated from the Monismith-model. This is given for different widths. As expected, the highest rutting is experienced with the highest width. This is due to the fact that the deviator stresses increases with increasing width. Thus,

the model yields higher rut for higher width. In actual testing, however, this was also the case, since in the middle of the briquette (150mm width) the rutting was higher than closer to the end of the briquette (100mm width).



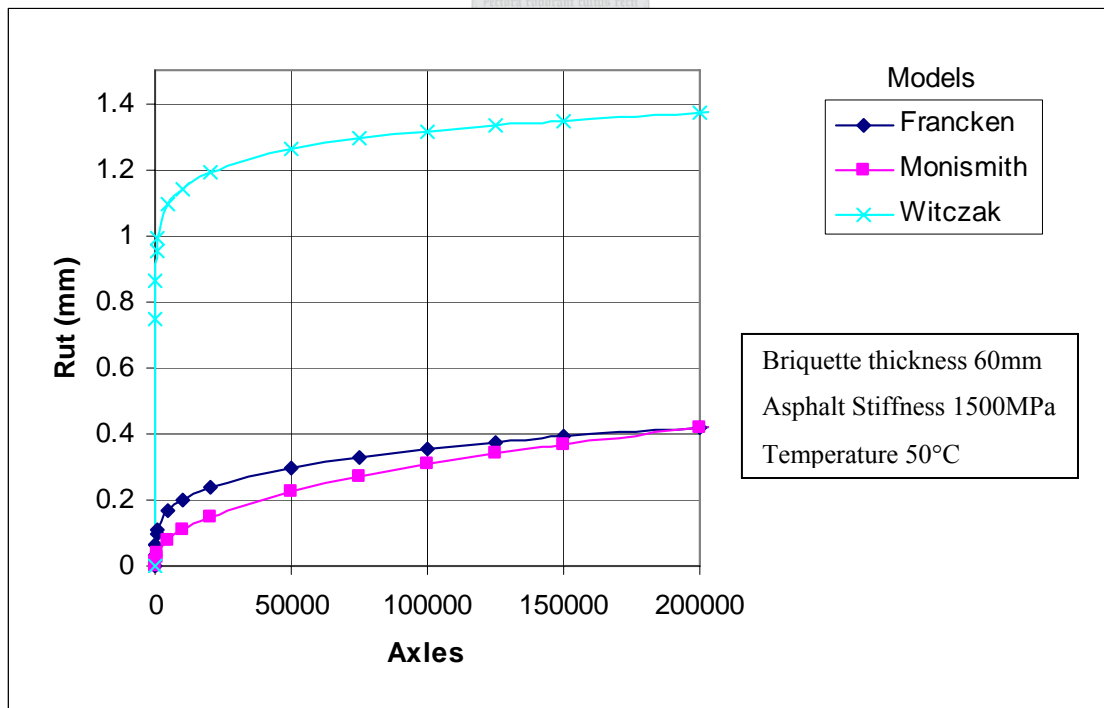
**Figure 5-16: Briquette full friction rut prediction profiles for Monismith-model**

Table 5-6 gives a summary of the rut prediction after 150 000 axles. The order of magnitude of these results is reasonable. The rut predictions for the slab are also lower than those for the briquettes, as expected. The results also indicate that would full friction exist between the briquettes and the mould; the rutting would be less that in the case of partial or even no friction. This could be expected.

Figure 5-17 gives the rut predictions with time. The rut development can be clearly observed, as there is a primary and secondary curve. It compares well with rutting curve of actual tests. However, none of the models of these models make provision for a tertiary curve, which marks the onset of shear failure.

**Table 5-6: Rut prediction after 150 000 axles**

	Width	Friction	Predicted Rut (mm)		
			Francken	Monismith	Witczak
Briq	150	Full	0.391	0.370	1.347
Briq	150	Partial	0.425	0.377	1.470
Briq	150	None	0.423	0.377	1.463
Briq	120	Full	0.322	0.354	1.078
Briq	120	Partial	0.356	0.362	1.195
Briq	120	None	0.350	0.361	1.177
Briq	100	Full	0.273	0.342	0.883
Briq	100	Partial	0.280	0.344	0.912
Briq	100	None	0.271	0.342	0.889
Briq	Elsym 5		0.484	0.463	1.731
Slab	600	Full	0.284	0.223	1.044
Slab	600	Partial	0.284	0.223	1.044
Slab	600	None	0.284	0.223	1.044
Slab	Elsym 5		0.287	0.255	1.395



**Figure 5-17: Rut prediction with time for briquette specimens**

## 5.6 Validation of Prediction Models with MMLS3 Tests

In the previous sections, the stress distributions of the different test configurations were analysed. These stresses were then used as in rut prediction models to compare the relative rutting of the different test configurations. From these models it was estimated that the briquettes specimens would yield higher rutting relative to the slab. It is the objective of this section to validate these estimates with MMLS3 testing. The MMLS3 tests will be analysed as follows:

- Firstly, the actual MMLS3 tests will be compared with each other
- Secondly, the actual MMLS3 tests will be compared with the estimated rutting to validate the rut prediction models

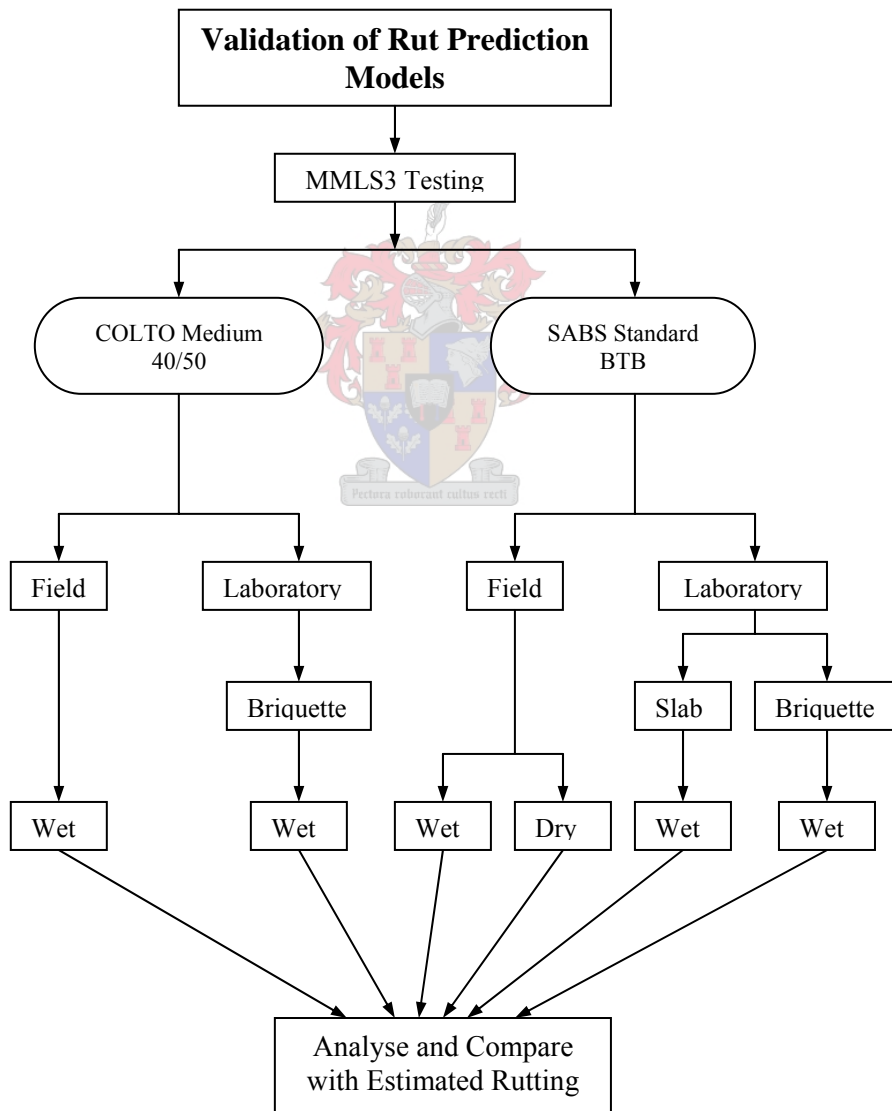


Figure 5-18: Validation of rutting models

### 5.6.1 Materials

Two different mixes were tested:

- SABS standard BTB mix (with sand) with 60/70 pen binder
- COLTO Medium wearing course mix with 40/50 pen binder

#### 5.6.1.1 SABS BTB

The SABS BTB mix comprised Malmesbury Hornfels from the Lafarge Peak Quarry and CALREF 60/70 binder. The gradation of the mix is given in Figure 5-19.

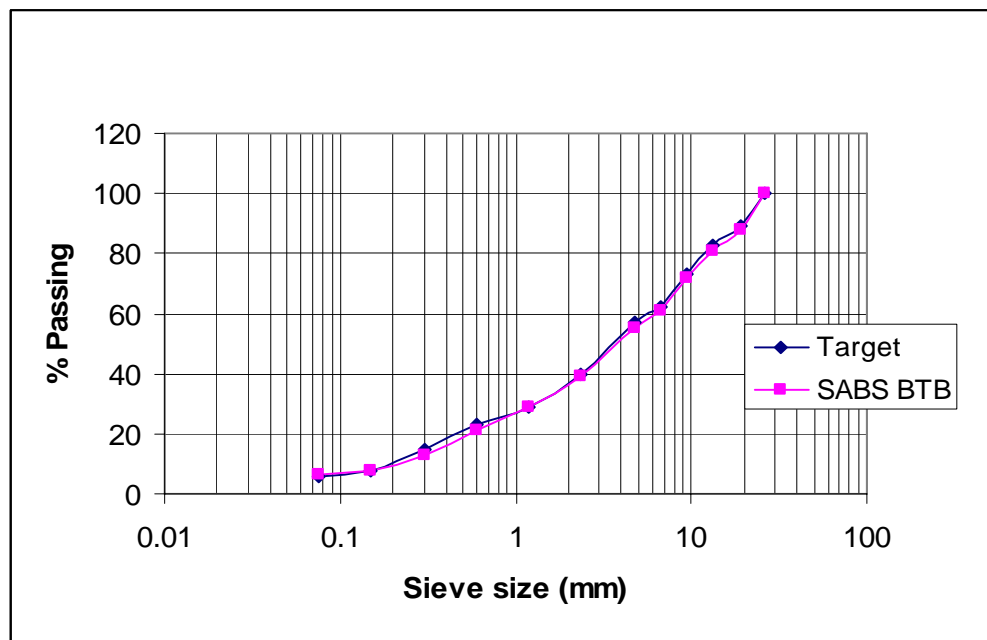


**Figure 5-19: Gradation for SABS BTB**

#### 5.6.1.2 COLTO Medium

The COLTO Medium mix was used for constructing the surface wearing course layer. The mix comprises Hornfels from the Eerste River quarry, and 40/50-pen grade binder from the SAPREF refinery. The laboratory specimens were compacted in the SGC to approximately 7% VIM at a temperature of 145 °C. The gradation for this mix is shown in Figure 5-20.

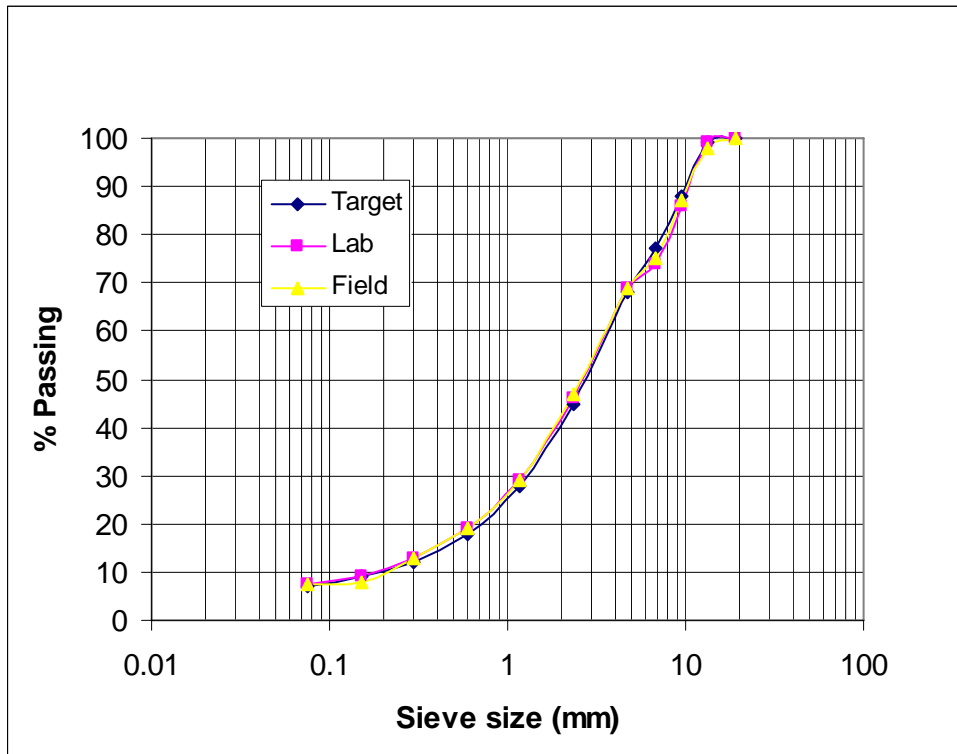


**Figure 5-20: Gradations for COLTO Medium 40/50**

## 5.6.2 MMLS3 Testing

The testing consisted of 3 tests in the laboratory and 5 tests in the field. The laboratory testing was performed on 150 mm briquette specimens either gyratory compacted or cores from field pavement section.

### 5.6.2.1 Laboratory testing

The testing was performed on 150 mm diameter briquettes as described in section 4.4.2. Two tests were performed on the COLTO Medium mix, at 40 °C and 50 °C respectively. These specimens were gyratory compacted. The test conditions for the MMLS3 were as follows:

- Number of load repetitions                      200 000
- Tyre pressure                                        690 kPa
- Scaled wheel load                                 2.1 kN
- Test temperature (asphalt)                    40 °C and 50 °C
- Load rate    6 900 repetitions per hour

Profiles were measured after 0, 100, 500, 1000, 10 000, 50 000, 100 000 and 200 000 repetitions.

Two laboratory test were performed on the SABS BTB mix. One test was performed on 150 mm diameter cored specimens extracted from the field. These were cut to fit in the setup as described in section 4.4.2. The second test was performed on a laboratory compacted slab with dimensions 1200 mm x 600 mm wide x 40 mm thick. This slab was compacted with a laboratory drum roller. The test was performed at an average temperature of 50 °C. The conditions for this test were as follows:

- Number of load repetitions                    250 000 (briquettes) / 150 000 (slab)
- Tyre pressure                                    690 kPa
- Scaled wheel load                            2.1 kN
- Test temperature (asphalt)                50 °C
- Load rate                                        7200 repetitions per hour

Profiles were measured after 0, 100, 500, 1000, 10 000, 50 000, 100 000, 200 000 and 250 000 axles.

### 5.6.2.2 Field testing

A total of 5 tests were performed at Cape Town International Airport in 2002. The author was actively involved in all these tests. For the COLTO Medium mix, only one wet test was performed at an average temperature of 50 °C. The MMLS3 load and tyre pressure for this test was 2.1 kN and 690 kPa respectively. A total number of 150 000 axles were applied.

The tests on the SABS mix consisted of 2 wet tests and 2 dry tests at an average temperature of 50 °C. The dry and wet tests were performed at two different tyre pressures, i.e. 690 kPa and 800 kPa. These were tested up to 100 000 MMLS3 axles. No lateral wander of the wheel was applied during both wet and dry testing.

For the dry tests, the heating process entailed blowing hot air across the test section from both sides. The direction of the heat flow changed every six minutes. The heating process was regulated by an automatic control in the heating unit.

For the wet test, heat was applied with an approximately 1 mm sheet of water flowing across the pavement surface. Figure 5-21 and Figure 5-22 give a view of the test setup.

Thermocouples were placed within the asphalt at 25 mm depths to monitor the asphalt temperature during testing. To capture the development of the rutting during the test,

profilometer measurements were taken after the following number of axles: 0, 5000, 20 000, 50 000 and 100 000. The COLTO Medium test included a profile after 150 000. Three transverse profile measurements, 250 mm apart, were taken after each interval. After profile measurements it was necessary to reheat the pavement for a period before commencing with MMLS3 trafficking.



**Figure 5-21: Pictorial View of Setup for Typical Wet Trafficking Test**



**Figure 5-22: Typical Wet Trafficking Test in Progress**

### 5.6.3 MMLS3 Test results

#### 5.6.3.1 COLTO Medium 40/50

The two laboratory tests on the COLTO Medium mix were done at average specimen temperatures of 40 °C and 50 °C respectively. The field test was done at an average temperature of 48 °C. The control temperatures measured on either side of the trafficked section varied between 46 °C and 53 °C on average. This gradient was as a result of the hot water flowing from one side to the other. The cumulative rutting curves for these tests are shown in Figure 5-23.

As expected, the 10 °C increase in temperature result in an increase in rutting in the laboratory results. An increase of 35 percent after 100 000 axles is observed. There is a relatively large initial settlement for both 40 °C and 50 °C followed by a relatively small increase with increasing axles. This increase is slightly higher at 50 °C. This can be due to the lower viscosity of the binder at the higher temperature.

Comparing the laboratory and field results, there is a 1.5 mm difference in the rutting after 100 000 axles. It also appears that there is a change in the rutting rate after 100 000 axles. This marks the start of a tertiary rutting curve.

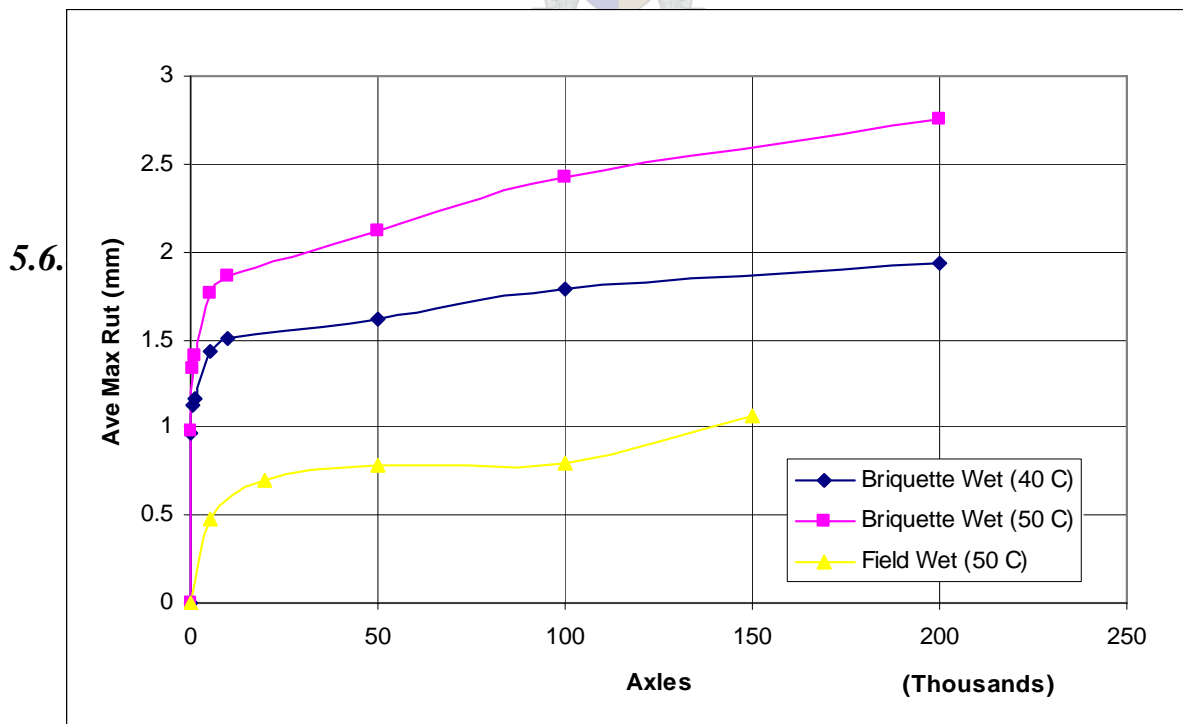


Figure 5-23: Cumulative Rutting Curves –COLTO Medium 40/50

### 5.6.4.1 SABS BTB

The cumulative rutting curves for the SABS BTB Mix are shown in Figure 5-24. The temperature for the laboratory test varied between 50 °C and 51 °C. The temperatures for the field tests are summarized in Table 5-7.

**Table 5-7: Average temperatures for SABS BTB Field tests (60mm from centerline)**

Test	Average	Left	Right
Wet 690 kPa	47	51	44
Wet 800 kPa	49	52	46
Dry 690 kPa	49	53	45
Dry 800 kPa	46	50	44

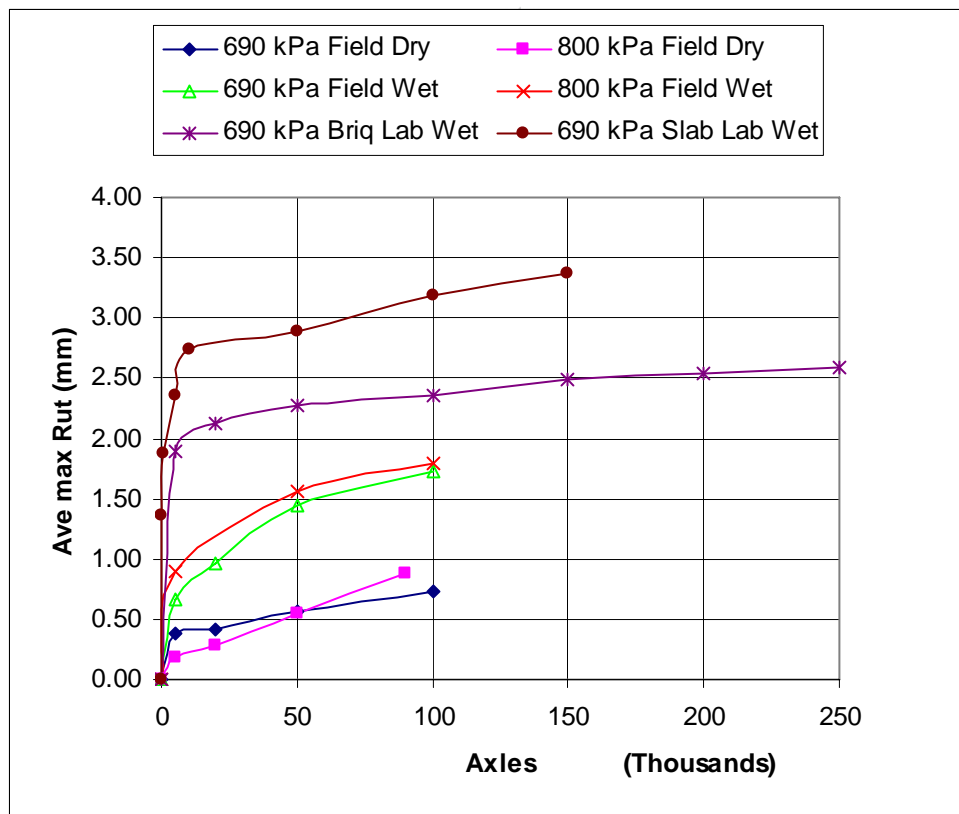


**Figure 5-24: Cumulative Rutting Curves –SABS BTB**

From Figure 5-24, it is evident that the water has a significant effect on the rutting performance. Higher ruts are observed for the wet tests than for the dry tests. It can also be

seen that an increase in tyre pressure does increase the rutting. The briquette specimens tested in the laboratory also yielded higher rutting results for the same mix tested in the field. This could be due to the fact that the confinement in the laboratory specimens is different than in the field. Also, in the laboratory, the specimens are fully submerged in the water, whilst this is not the case in the field. The temperature in the laboratory can also better controlled. In the field, there is more temperature variation, especially during the evening. This variation is more frequently below the desired test temperature.

The ageing of the specimens may also have contributed to the differences in the results. The laboratory specimens were tested soon after compaction, whilst the mix in the field has been subject to weather influences.

The slab tested in the laboratory yielded higher rutting than the briquettes. In the briquette setup, horizontal movement of the asphalt material upon loading is somewhat restricted by the moulds. In the slab specimen, one would expect more horizontal deformation displacement with accompanied vertical deformation. This could be one of the reasons why the slab rutting was higher. The difference in compaction method could also have influenced the results. The slab was compacted using a laboratory drum roller and the briquettes were cores extracted from the field, thus compacted by field rollers. The slab was compacted attempting to obtain 7 percent VIM. The compaction was controlled by using a known quantity of material and a steel mould of known volume. It should be noted that no actual density measurements were taken on the slab to confirm whether the desired density was achieved and also whether a uniform density was achieved over the test section. However, the three transverse rut profiles taken over the slab did not indicate significant variation.

### 5.6.5 Model vs. MMLS3 rutting

In this section, the actual MMLS3 rutting results will be compared to the rutting model results.

The rutting results for both the models and the MMLS3 are shown in Figure 5-25. It can be seen that the Francken and Monismith models yield rutting below 0.5 mm. The rutting for the Witczak model is higher (1.0 – 1.5 mm). This is significantly lower than the actual slab and briquette ruts. Further, the slab rutting for all three models is lower than the briquette rutting. For the MMLS3, the slab showed higher rutting compared to the briquettes. Thus, the models did not correctly “rank” the two different configurations in terms of rutting.

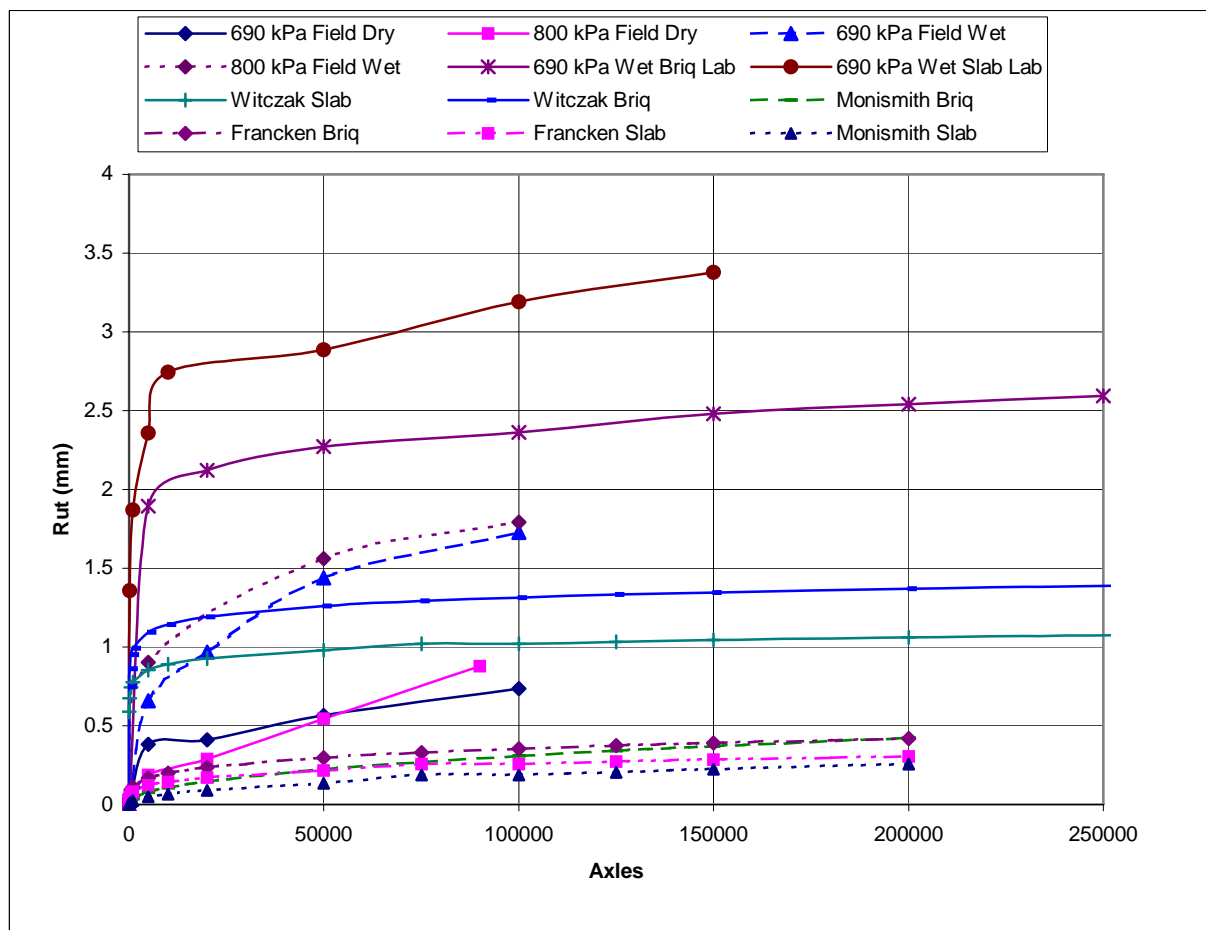


Figure 5-25: Results of actual and predicted rutting

The higher briquette rutting from the models can be related to the deviator stresses and the thickness of the asphalt. Referring to section 5.4, the permanent deformation is a function of

stress and layer thickness. Permanent deformation is the product of the permanent strain and the sublayer increment, accumulated over the whole layer. The permanent strain is the result of the stress in the layer, in this case the deviator stress. In these models, all other parameters being equal, the deviator stress is the only variable between the slab and briquette.

Referring to the stress analysis in Appendix A, the briquette specimen has higher deviator stresses direct under the center of the wheel. This would result in larger permanent strains (as calculated in these models) for the briquette compared to the slab. Above that, the briquette is thicker than the slab, thus a summation over the thickness would yield higher rutting for the briquette. It is clear that, with these specific models and the difference in thickness between the slab and briquette, larger rutting would always be predicted for the briquette.

The fact that the models yielded significantly lower results than the actual can be related to the conditions for which these models were developed. These models were developed for temperatures between 18 and 35 °C and deviator stress levels of between 70 – 210 kPa. The stresses calculated using ELSYM5 and ABAQUS were for conditions of 50 °C, and also the resulting deviator stresses were in the majority of the cases higher than 210 kPa.



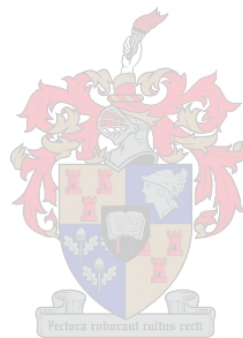
## 5.7 Conclusions

The importance of the influence of temperature on permanent deformation is once again highlighted. The control of the temperature during testing cannot be over-emphasised when meaningful comparisons between different mixes with regard to rutting performance are to be made.

The geometry of test specimens has an influence on the stress distribution within the specimens and it appears that the confining and deviator stresses might influence the permanent deformation results. It is therefore important to use specimens that are most representative of field conditions.

An increase in contact pressure leads to an increase in rutting, as also found by other researchers. The presence of water also has a significant effect on rutting. The wet tests yielded larger ruts than the dry tests.

The briquette specimens tested in the laboratory yielded lower rutting than the slab tested in the laboratory for the same mix. This could be due to the fact that the confinement of the briquette specimens is different than in the slab. However, contrary to expectations, the field tests yield lower rutting than both briquettes and slabs tested in the laboratory. This may be related to the fact that the laboratory specimens are fully submerged in the water, whilst this is not the case in the field (which would influence temperature distribution with depth). The ageing of the specimens may also have contributed to the differences in the results. The laboratory specimens were tested soon after compaction, whilst the mix in the field has been subject to weather influences.



## 6 CONCLUSIONS AND RECOMMENDATIONS

From the findings of this thesis, the following conclusions can be drawn.

### 6.1 Conclusions

It is evident that the critical factors influencing the compactibility of the wearing course mix investigated include the binder content and the filler/binder interaction.

The addition of filler to a binder does stiffen up the filler/binder mastic as indicated by the increase in the softening point of the mastics. The relationship established between percent bulk volume of filler and increase in softening point for the fillers investigated was similar to that found by other researchers. The use of filler as a bitumen extender and void reducer appears to be beneficial but its benefit reduces when the optimum filler/binder ratio is exceeded due to excessive stiffening of the mix.

It was found that gradation has a significant influence on compaction as well as rutting performance.

As expected, the binder type has a significant influence on the rutting resistance as well as compactibility. In addition, an increase in binder content facilitated compaction, but decreased rutting resistance.

The binder type does influence the compactibility. As expected, the higher penetration binder mixes was easier to compact. The binder type also has a significant influence on the rutting resistance. Mixes with 40/50-penetration grade binder showed better rut resistance compared to the mixes with 60/70-penetration grade binder.

Based on the limited tests performed, the reduction of the filler/binder ratios in order to improve compactibility does not significantly increase rutting under APT.

It was found that with polymer modification i.e. EVA, less than half of the rutting of a standard mix would occur, under the same loading conditions. An improvement in the rutting resistance using PMB was expected.

The addition of the antistripping agent Gripper L decreased the rutting and also the rate of rutting of the Quartzite LAMBS mix that results from the stripping failure mechanism. The amount of aggregate stripping is also visibly decreased. For this particular mix and the aggregate used, it is concluded that at 4 percent air voids content, the moisture susceptibility of the mix is significantly decreased, as compared to 7 percent air voids.

In terms of compactibility, it appears that there exists a temperature window in which compaction can be achieved, but in terms of rutting; even a small deviation in temperature can influence rutting results significantly.

The importance of influence of temperature on permanent deformation is once again highlighted. The control of the temperature during testing is important to make meaningful comparisons between different mixes with regard to rutting performance.

The geometry of test specimens has an influence on the stress distribution within the specimens. Confining and deviator stresses influence the permanent deformation results. It is therefore important to use applicable performance criteria for APT type tests e.g. MMLS3, depending on the geometry of the test specimen.

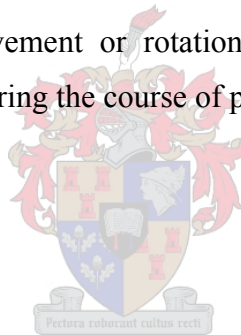
An increase in contact pressure leads to an increase in rutting, as noted for the mix analysed. This trend was also found by other researchers. However, it was verified for only one additional mix type in this study. The presence of water also has a significant effect on rutting. For the one mix tested under both wet and dry conditions, the wet tests yielded larger ruts than the dry tests.

## 6.2 Recommendations

It is recommended that more softening point tests be done on filler/binder mastics at varying degrees of percent bulk volume of filler. An increase of 12 °C in the softening of the mastic compared to that of the bitumen should be used to establish the maximum filler/binder ratios to optimise the stiffening effect of the filler. Binder contents should be established based on these ratios. Gyrotory compaction tests and mechanical tests should then be done to validate the suitability of these binder contents.

When using the test setup of five slabs in series, it is recommended that at least two slabs of the same mix be tested during one test to reduce the variability of the test results.

For the briquette testing, clamps should be used that are more heat conductive and these clamps should not allow movement or rotation of specimens during testing. These measures were implemented during the course of publication of this thesis.



## REFERENCES

- ABAQUS User's Manual, Version 6.3-1, Hibbitt, Karlsson & Sorensen Inc., Rhode Island, 2002
- Anderson D.A., *Guidelines for Use of Dust in Hot Mix Asphalt Concrete Mixtures*, Proceedings of the Association of Asphalt Paving Technologists, Vol. 56, 1987, p. 492
- Anderson D.A., Maurer D., Ramirez T., Christensen D.W., Marasteanu M.O. and Mehta Y., *Field Performance of Modified Asphalt Binders Evaluated with Superpave Test methods: I-80 Test Project*, Transportation Research Record 1661, Transportation Research Board, National Research Council, Washington DC, 1999
- Anderson D.A., Tarris J.P. and Brock J.D., *Dust Collector Fines and their Influence on Mixture design*, Proceedings of the Association of Asphalt Paving Technologists, Vol. 51, 1982, p. 363
- ASTM D4123-82, *Standard Test Method for Indirect Tension Test for Resilient Modulus of Bituminous Mixtures*, Annual Book of ASTM Standards, Vol 04.03, American Society for Testing and Materials, Philadelphia
- ASTM D422-63, *Standard Test Method for Particle Size Analysis of Soils*, American Society for Testing and Materials, Vol. 04.08, Philadelphia, Revised Annually.
- Australian Asphalt Pavement Association, *Air Voids in Asphalt*, Pavement Work Tips No.17, June 1999
- Australian Asphalt Pavement Association, *Polymer Modified Binders*, Pavement Work Tips No.6, May 1998(a)
- Australian Asphalt Pavement Association, *Temperature Characteristics of Binders in Asphalt*, Pavement Work Tips No.13, November 1998(b)
- Bahia H.U. and Anderson D.A., *The New Proposed Rheological Properties of Asphalt Binders: Why are They Required and how do They Compare to Conventional*

**Properties**, Physical Properties of Asphalt Cement Binders, ASTM STP 1241, John C. Hardin, Ed., 1995, p. 1-27

Bahia H.U. and Hanson D.I., **A Project NCHRP 9-10 Superpave Protocols for Modified Asphalt Binders**”, Draft Topical Report (Task 9), Prepared for: The National Cooperative Highway Research Program, Transportation Research Board, National Research Council, May 2000.

Bahia H.U., Friemel T.P., Peterson P.A., Russell J.S. and Poehnelt B., **Optimization of Constructability and Resistance to Traffic: A New Design Approach for HMA Using the Superpave Compactor**, Proceedings Association of Asphalt Paving Technologists, Vol. 67, 1998, p.189

Bahia H.U., Zhai H., Zeng M., Hu Y., and Turner P., **Development of Binder Specification Parameters Based on Characterization of Damage Behavior**, Proceedings Association of Asphalt Paving Technologists, Vol. 70, 2001

Bissada A.F., **Compactability of Asphalt Paving Mixtures and Relation to Permanent Deformation**, Transportation Research Record 911, Transportation Research Board, National Research Council, Washington DC, 1983

Blankenship P.B., C. K. Mahboub and G. A. Huber, **Rational method for laboratory compaction of hot mix asphalt**, Transportation Research Record 1454, Transportation Research Board, National Research Council, Washington DC, 1994.

Bolk N.J.N.A., van der Heide J.P.J. and van Zantvliet M.C., **Basic Research into the Effect of Filler on the Mechanical Properties of Dense Asphaltic Concrete**, Proceedings of the Association of Asphalt Paving Technologists, Vol. 51, 1982, p. 398

Bouldin M.G. and Collins J.H., **Influence of Binder Rheology on Rut Resistance of Polymer Modified and Unmodified HMA**, Polymer Modified Asphalt Binders, ASTM STP 1108, K.R. Wardlaw and S. Shuler (editors), Philadelphia, 1992

- Bouldin M.G., Rowe G.M., Sousa J.B. and Sharrock M.J., ***Mix Rheology – a Tool for predicting the High Temperature Performance of HMA***, Proceedings of the Association of Asphalt Paving Technologists, Vol. 63, 1994, p. 182
- Brown E.R. and Cross S.A., ***A Study of in-place Rutting of Asphalt***, NCAT Report No. 89-02, National Center for Asphalt Technology, Auburn University, Alabama, 1989
- Brown E.R., Gabrielson J. and Adettiwar S., ***Variation in Hot Mix Asphalt Mix Design Properties***, Proceedings of the Association of Asphalt Paving Technologists, Vol. 62, 1993, p.708
- Brown E.R., Kandhal P.S. and Zhang J., ***Performance Testing for HMA***, NCAT Report No. 2001- 05, National Center for Asphalt Technology, Auburn University, Alabama, November 2001
- Button J.W., Little D.N., Jagadam V. and Pendleton O.J., ***Correlation of Selected Laboratory Compaction Methods with Field Compaction***, Transportation Research Record 1454, Transportation Research Board, National Research Council, Washington, D.C., 1994.
- Chadbourn B.A., Skok, Jr. E.L., Newcomb D.E., Crow B.L. and Spindler S., ***The Effect of Voids in Mineral Aggregate (VMA) on Hot-Mix Asphalt Pavements***, Report No. MN/RC - 2000-13, Prepared for Minnesota Department of Transportation, 2000
- Cheng D., Little D.N., Lytton R.L. and Holste J.C., ***Use of Surface Free Energy Properties of the Asphalt-Aggregate System to Predict Moisture Damage Potential***, Proceedings Association of Asphalt Paving Technologists, Vol. 71, 2002
- Collop A., ***Presentation on “Functions & Properties”***, University of Nottingham, 2002, [www.civeng.nottingham.ac.uk/p&g/functionsproperties.pdf](http://www.civeng.nottingham.ac.uk/p&g/functionsproperties.pdf)
- COLTO, ***Standard specifications for road and bridge works for state road authorities***, Committee for Land Transport Officials, Department of Transport, Johannesburg, South Africa, 1998.

- Cook R.D., Malkus D.S., Plata M.E. and Witt R.J., ***“Concepts and Applications of Finite Element Analysis”***, 4<sup>th</sup> Edition, 2002, John Wiley & Sons Inc.
- Cooley Jr. L.A., Kandhal P.S., Buchanan M.S., Fee F. and Epps A., ***Loaded Wheel Testers in the United States: State of the Practice***, NCAT Report No. 2000-4, National Center for Asphalt Technology, Auburn University, Alabama, July 2000
- Cooley Jr. L.A., Stroup-Gardiner M., Brown E.R., Hanson D. and Fletcher M., ***Characterization of asphalt-filler mortars with Superpave binder tests***, Proceedings of the Association of Asphalt Paving Technologists, Vol. 67, 1998.
- Cooper K.E., Brown S.F. and Pooley G.R., ***The Design of Aggregate Gradings for Asphalt Basecourses***, Proceedings of the Association of Asphalt Paving Technologists, Vol. 54, 1985, p. 324
- Coree B.J. and Hislop W.P., ***A Laboratory Investigation into the Effects of Aggregate-Related Factors of Critical VMA in Asphalt Paving Mixtures***, Iowa DOT Project TR-415, Center for Transportation Research and Education (CTRE), Iowa State University, June 2000
- Craus J., Ishai I. and Sides A., ***Some Physico-Chemical Aspects of the Effect and the Role of the Filler in Bituminous Paving Mixtures***, Proceedings of the Association of Asphalt Paving Technologists, Vol. 47, 1978, p. 558
- Cross S.A. and Brown E.R., ***A National Study of Rutting in Asphalt Pavements***, NCAT Report No. 91-8, National Center for Asphalt Technology, Auburn University, Alabama, 1991.
- D'Angelo, J.A., Paugh C., Harman T.P. and Bukowski J., ***Comparison of the Superpave Gyrotory Compactor to the Marshall for Field Quality Control***, Proceedings of the Association of Asphalt Paving Technologists, Vol. 64, 1995, p. 611
- Dawley C.B., Hogewiede B.L. and Anderson K.O., ***Mitigation of Instability Rutting of Asphalt Concrete Pavements in Lethbridge, Alberta, Canada***, Proceedings of the Association of Asphalt Paving Technologists, Vol. 59, 1990, p. 481

- De Sombre R., Newcomb D.E. Chadbourn B. and Voller V., ***Parameters to Define the Laboratory Compaction Temperature Range of Hot-Mix Asphalt***, Proceedings Association of Asphalt Paving Technologists, Vol. 67, 1998, p.125
- Deacon J.A., Coplantz J.S., Tayebali A.A. and Monismith C.L., ***Temperature Considerations in Asphalt-Aggregate Mixture Analysis and Design***, Transportation Research Record 1454, Transportation Research Board, National Research Council, Washington DC, 1994
- Distin T., ***Telephonic Communication***, April 2002
- Du Preez H., ***Development of a Method for the Testing of Cylindrical Asphalt Specimens under water with the MMLS Mk3*** (in Afrikaans), Undergraduate Project (BEng), University of Stellenbosch, Stellenbosch, 2001
- Dukatz E.L. and Anderson D.A., ***The Effect of Various Fillers on the Mechanical Behavior of Asphalt and Asphaltic Concrete***, Proceedings of the Association of Asphalt Paving Technologists, Vol. 49, 1980, p. 530
- Eckmann B., ***Rut Depth Prediction: A Practical Verification***, Sixth International Conference on the Structural Design of Asphalt Pavements, University of Michigan, Ann Arbor - July 13-17, 1987
- Epps A.L., Ahmed T., Little D.C., and Mikhail M., ***Performance Assessment with the MMLS3 at WesTrack***, Proceedings Association of Asphalt Paving Technologists, Vol. 70, 2001, p. 509
- Finn F.N., Yapp M.T., Coplantz J.S. and Durrani A.Z., ***Asphalt Properties and Relationship to Pavement Performance: Literature Review***, SHRP-A/IR-90-015, Strategic Highway Research Program, National Research Council, 1990
- Flexible Pavements Council of West Virginia, ***Centerline***, Volume V, Issue 1, Spring 2000
- Francken L. and Clauwert C., ***Characterization and Structural Assessment of Bound Materials for Flexible Road Constructions***, 6<sup>th</sup> International Conference on Structural Design of Asphalt Pavements, Ann Arbor, Michigan, 1987

- Francken L., *Permanent Deformation Law of Bituminous Road Mixes in Repeated Triaxial Compression*, 4<sup>th</sup> International Conference on Structural Design of Asphalt Pavements, Ann Arbor, Michigan, August 22-26, 1977
- Goodrich J.L., *Asphaltic Binder Rheology, Asphalt Concrete Rheology and Asphalt Concrete Mix Properties*, Proceedings Association of Asphalt Paving Technologists, Vol. 60, 1991, p.80
- Hesp S.A.M., Smith B.J. and Hoare T.R., *Effect of the Filler Particle Size on the Low and High Temperature Performance in Asphalt Mastic and Concrete*, Proceedings of the Association of Asphalt Paving Technologists, Vol. 70, 2001, p. 492
- Huber G.A. and Heiman G.H., *Effect of Asphalt Concrete Parameters on Rutting Performance: A Field Investigation*, Proceedings Association of Asphalt Paving Technologists, Vol. 56, 1987, p.33
- Huber G.A., *Weather Database for the Superpave Mix Design System*, Strategic Highway Research Program, SHRP-A-648A: 139pp, 1994
- Hughes C.S. et al, *Compaction of Asphalt Pavement*, NCHRP Synthesis 152, National Cooperative Highway Research Program, Transportation Research Board, National Research Council, Washington D.C., 1989
- Hugo F., *APT as a Tool for Evaluation and Rehabilitation*, Presentation at the Advanced Course on Flexible Pavement Evaluation and Rehabilitation, University of Stellenbosch, November 2000, Stellenbosch
- Hugo, F., 1969: *A critical review of asphalt paving in current use with proposals for a new mix*. Proc. First Conf. Asp. Pav. for Southern Africa, Durban.
- Hugo, F., 1970: *A critical review of bituminous mixtures at present being used for surfacing pavements, with proposals for the composition and design of mixtures suitable for SA conditions*. MSc (CE) Thesis, Univ. of Natal.
- Hugo, F., De Witt, R., Helmich A., 2004, *Application of the MMLS3 as APT tool for evaluating asphalt performance in Namibia*, Synopsis accepted for preparation

of a paper for presentation at 8<sup>th</sup> Conference on Asphalt Pavements for Southern Africa

Hugo, F., *Personal Communication*, Stellenbosch, 2004

Huner M.H. and Brown E.R., *Effects of Re-heating and Compaction temperature on HMA Volumetrics*, NCAT Report No. 01-04, National Center for Asphalt Technology, Auburn University, Alabama, November 2001

Hunter R.N. *et al*, *Asphalts in Road Construction*, edited by Hunter R.N., 2000, Thomas Telford, London

Huschek S. and Angst C.H., *Mechanical Properties of Filler-Bitumen Mixes at High and Low Service Temperatures*, Proceedings of the Association of Asphalt Paving Technologists, Vol. 49, 1980, p. 440

Izzo R.P. and Stuart K.D., *Correlation of SUPRPAVE™  $G^*/\sin\delta$  with Rutting Susceptibility from Laboratory Mixture Tests*, Prepared for Presentation at 1995 Annual Meeting of the Transportation Research Board, Washington, DC, 1995

Jenkins K.J. and Douries W.J., *Accelerated Pavement Testing of Polymer Modified Asphalt Mixes*, ITT Report 1/2002, University of Stellenbosch, Stellenbosch, 2002

Jenkins K.J. and Douries W.J., *Gyratory Compaction and MMLS3 Testing of Asphalt Wearing- and Base-Course Mixes for Cape Town International Airport Taxiway Rehabilitation*, ITT Report 1/2001, University of Stellenbosch, Stellenbosch, 2001(a)

Jenkins K.J. and Douries W.J., *MMLS3 and Fatigue Testing of Four Different Materials from Texas*, ITT Report 4/2001, University of Stellenbosch, Stellenbosch, 2001(b)

Jenkins K.J. and Douries W.J., *MMLS3 Testing of asphalt wearing course mixes*, ITT Report 3/2001, University of Stellenbosch, Stellenbosch, 2001(c)

- Jenkins K.J. and Douries W.J.,  *Rutting and Stripping Evaluation of a LAMBs mix*, ITT Report 5/2001, University of Stellenbosch, Stellenbosch, 2001(d)
- Kandhal P.S. & Rickards I.J., *Premature Failure of Asphalt Overlays from Stripping: Case Histories*, NCAT Report No. 01-01, National Center for Asphalt Technology, Auburn University, Alabama, April 2001
- Kandhal P.S. and Mallick R.B., *Potential of asphalt Pavement Analyzer (APA) to Predict Rutting of HMA*, Paper No. CS6-2), Paper prepared for presentation at the International Conference on Accelerated Pavement Testing to be held in Reno, Nevada (October 18-20, 1999)
- Kandhal P.S. and Maqbool K., *Evaluation of Asphalt Absorption by Mineral Aggregates*, Proceedings of the Association of Asphalt Paving Technologists, Vol. 60, 1991, p. 207
- Kandhal P.S., Cross S.A. and Brown E.R., *Evaluation of Bituminous Pavements for High Pressure Truck Tires*, FHWA Report No. FHWA-PA-90-O08 + 87-01, National Center for Asphalt Technology, Auburn University, Alabama, December 1990
- Kandhal P.S., *Evaluation of baghouse fines in bituminous paving mixtures*, Proceedings of the Association of Asphalt Paving Technologists, Vol. 50, 1981, p. 150
- Kandhal P.S., Lubold Jr. C.W. and Roberts F.L., *Water Damage To Asphalt Overlays: Case Histories*, NCAT Report No. 89-1, National Center for Asphalt Technology, Auburn University, Alabama, 1989.
- Kandhal P.S., Lynn C.Y. and Parker Jr. F., *Tests for Plastic Fines in Aggregates Related to Stripping in Asphalt Paving Mixtures*, NCAT Report No. 98-3, National Center for Asphalt Technology, Auburn University, Alabama, March 1998(a)
- Kandhal P.S., Mallick R.B. and Brown E.R., *HMA for Intersections in Hot Climates*, NCAT Report No. 98-6, National Center for Asphalt Technology, Auburn University, Alabama, March 1998(b)

- Kandhal P.S., *Moisture Susceptibility of HMA mixes: Identification of Problem and Recommended Solutions*, NCAT Report No. 92-1, National Center for Asphalt Technology, Auburn University, Alabama, May 1992
- Kao Corporation, *Kao Additives for the Road Making Industry*, Kao Corporation S.A., Barcelona, Spain, 2001
- Kavussi A. and Hicks R.G., *Properties of Bituminous Mixtures containing Different Fillers*, Proceedings of the Association of Asphalt Paving Technologists, Vol. 66, 1997, p. 153
- Kennedy T.W., Roberts F.L., McGennis R.B. & Anagnos J.N., *Compaction of Asphalt Mixtures and the Use of Vibratory Rollers*, Research Report 317-1, Center for Transportation Research, Austin, Texas, 1984
- Khatri A, Bahia H.U. and Hanson D., *Mixing and Compaction Temperatures for Modified Binders using the Superpave Gyrotory Compactor*, Proceedings of the Association of Asphalt Paving Technologists, Vol. 70, 2001, p. 368
- Kiggundu B.M. and Roberts F.L., *Stripping in HMA Mixtures: State-of-the-Art and Critical Review of Test Methods*, NCAT Report No. 88-2, National Center for Asphalt Technology, September 1988
- King G.N., King H.W. Harders O., Chavenot P. and Planche J-P, *Influence of Asphalt Grade and Polymer Concentration on the High Temperature Performance of Polymer Modified Asphalt*, Proceedings Association of Asphalt Paving Technologists, Vol. 61, 1992, p.28
- King G.N., Muncy H.W. and Prudhomme J.B., *Polymer Modification: Binder's Effect on Mix Properties*, Proceedings of the Association of Asphalt Paving Technologists, Vol. 55, 1986, p. 519
- Leahy R.B. and Witczak M.W., *The Influence of Tests Conditions and Asphalt Concrete Mix Parameters on Permanent Deformation Coefficients Alpha and Mu*, Proceedings of the Association of Asphalt Paving Technologists, Vol. 60, 1991, p. 333

- Leahy R.B., Harrigan E.T. and Von Quintus H., *Validation of Relationships Between Specification Properties and Performance*, SHRP-A-409, Strategic Highway Research program, National Research council, Washington, DC, 1994
- Leahy R.B., *Permanent Deformation Characteristics of Asphalt Concrete*, Ph.D. dissertation, University of Maryland, College Park, 1989
- Maccarrone S., Holleran G. and Gnanaseelan G.P., *Properties of polymer Modified Binders and Relationship to Mix and Pavement Performance*, Proceedings of the Association of Asphalt Paving Technologists, Vol. 64, 1995, p. 209
- Masad E., Muhunthan B., Shashidar N. and Harman T., *Quantifying Laboratory Compaction on the Internal Structure Asphalt Concrete*, Transportation Research Record 1681, Transportation Research Board, National Research Council, Washington DC, 1999
- May R.W. and Witczak M.W., *An Automated Asphalt Concrete Mix Analysis System*, Proceedings of the Association of Asphalt Paving Technologists, Vol. 61, 1992, p. 154
- Metcalf J.B., *Accelerated Pavement Testing, a Brief Review Directed Towards Asphalt Interests*, Proceedings of the Association of Asphalt Paving Technologists, Vol. 67, 1998, p. 553
- Molenaar A.A.A., *Road Materials Part III: Asphaltic Materials*, Lecture Notes on Flexible Pavement Design, University of Stellenbosch, October 2001
- Monismith C.L., Inkabi K., Freeme C.R. and McLean D.B., *A Subsystem to Predict Rutting in Asphalt Concrete Pavement Structures*, 4<sup>th</sup> International Conference on Structural Design of Asphalt Pavements, Ann Arbor, Michigan, August 22-26, 1977
- Müller F.P.J., *MMLS3 Operators Manual*, 1999, Stellenbosch
- Müller F.P.J., *Personal Communication*, Stellenbosch, June 2001
- National Asphalt Pavement Association, *Field Management of HMA*, NAPA Information Series 124, Lanham, Maryland, 1997

- Nazarian S. and Stokoe II K.H., *In situ Determination of Elastic Moduli of Pavement Systems by Spectral Analysis of Surface Waves method (Practical aspects)*, Research Report 368-1F, The University of Texas at Austin, 1985
- Nazarian S. and Stokoe II K.H., *In situ Determination of Elastic Moduli of Pavement Systems by Spectral Analysis of Surface Waves method (Theoretical aspects)*, Research Report 437 -2, The University of Texas at Austin, 1986
- OCW, *Handleiding voor de formulering van dichte bitumineuze mengsels*, Edition 2, Opzoekingscentrum voor de Wegenbouw, Brussels, Belgium, 1997.
- Parker F. and Hossain S., *Collection and Analysis of QC/QA Data for Superpave Mixes*, National Center for Asphalt Technology, April 1999
- Rickards I., Goodman S., Pagani J., El Halim A.O.A. and Haas R., *Practical Realization of a New Concept for Asphalt Compaction*, Transportation Research Record 1654, Transportation Research Board, National Research Council, Washington DC, 1999
- Roberts F.L., Kandhal P.S., Brown E.R., Lee D-Y, and Kennedy T.W., *HMA Materials, Mixture Design, and Construction*, 1<sup>st</sup> Ed, 1991, NAPA Research and Education Foundation, Maryland, USA
- Santucci L., *Rut Resistant Asphalt Mixes*, Institute for Transportation Studies, Tech Transfer Newsletter, Winter 2001
- Santucci L.E., Allen D.D. and Coats R.L., *The Effects of Moisture and Compaction on the Quality of Asphalt Pavements*, Proceedings of the Association of Asphalt Paving Technologists, Vol. 54, 1985, p. 168
- Scherochman J.A., *Compact Difficult Superpave mixes*, <http://www.asphalt.com/pavingpercent20tech/compact.html>, 2000
- Semmelink C.J., *Course Notes: Practical Compaction Guidelines*, Divisional Publication DP-2000/2, Transportek, CSIR, Pretoria, March 2000

- Shashidar N., Needham S.P., Chollar B.H. and Romero P., ***Prediction of the Performance of Mineral Fillers in Stone Matrix Asphalt***, Proceedings of the Association of Asphalt Paving Technologists, Vol. 68, 1999, p. 222
- Shell, ***The Shell Bitumen Handbook***, Shell Bitumen UK, 1991
- Smit A deF., ***Scaled “LAMB”- Performance with Bitumen Variation using MMLS testing and PPGS Application***, M.Eng Thesis, University of Stellenbosch, 1995
- Smit A. de F., Hugo F. and Epps A., ***Report on the First Jacksboro MMLS Tests***, Draft Report 1841-2 prepared for the Texas Department of Transportation by the Center for Transportation Research, The University of Texas at Austin, 1999.
- Smit AdeF, Hugo F., Rand D. and Powell B, ***MMLS3 Testing at the NCAT Test Track***, Paper submitted to the Transportation Research Board for Presentation and Publication at the 2003 Annual Meeting in Washington, D.C., 2002
- Smit AdeF, van de Ven M.F.C., Burger A.F, Weston C.T. and Douries W.J., ***Asphalt mix design and analysis towards improving compactibility of wearing course mixes in the Western Cape***. ITT Report 1/2000, University of Stellenbosch, 2000.
- Smit, A. dF., Hugo, F., Rand, D., and Powell, B. 2003, ***Model Mobile Load Simulator testing at the National Center for Asphalt Technology Test Track***, Transportation Research Record 1832, Transportation Research Board, National Research Council, Washington, D. C.
- Sousa J.B. and Weissman S.L., ***Modeling Permanent Deformation of Asphalt-Aggregate Mixes***, Proceedings of the Association of Asphalt Paving Technologists, Vol. 63, 1994, p. 224
- Sousa J.B., ***Asphalt – Aggregate Mix Design Using the Repetitive Simple Shear test (Constant Height)***, Proceedings of the Association of Asphalt Paving Technologists, Vol. 63, 1994, p. 298
- Sousa J.B., Deacon J.A. and Monismith C.L., ***Effect of Laboratory Compaction Method on Permanent Deformation Characteristics of Asphalt – Aggregate Mixtures***, Proceedings of the Association of Asphalt Paving Technologists, Vol. 60, 1991, p. 533

Southern African Bitumen Association, *Guidelines for the Manufacture and Construction of Hot-mix Asphalt*, SABITA Manual 5, Cape Town, June 1992

Southern African Bitumen Association, *LAMBS – The design and use of large aggregate mixes for bases*, Sabita Manual 13, 1997, Cape Town

Tayebali A.A., Khosla N.P. & Malpass G.A., *Impact of Fines on Asphalt Mix Design*, The Center for Transportation and the Environment, North Carolina State University, 1996

Terrel R.L. and Al-Swailmi S., *The Role of Pessimism Voids Concept in Understanding Moisture Damage to Asphalt Concrete Mixtures*, Transportation Research Record 1386, Transportation Research Board, National Research Council, Washington DC, 1993

The Asphalt Institute, *Density Specifications for Hot-Mix Asphalt (TB-9)*, 2002, <http://www.asphaltinstitute.org/faq/tb-9.html>

The Asphalt Institute, *Factors Affecting Compaction*, Educational Series 9 (ES-9), November 1980, Maryland

The Asphalt Institute, *Factors Affecting Compaction*, Educational Series No.9 (ES-9), November 1980

The Asphalt Institute, *Vibratory Compaction of Asphalt Paving Mixtures*, Educational Series No.2 (ES-2), June 1978

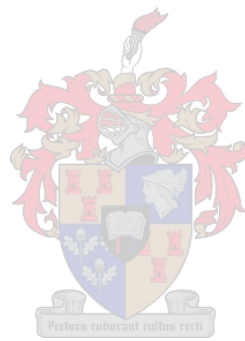
Tunncliff D.G., *The Binding Effect of Mineral Filler*, Proceedings Association of Asphalt Paving Technologists, Vol. 36, 1967

Valkering C.P., Lancon D.J.L., DeHilster E. and Stoker D.A., *Rutting Resistance of Asphalt Mixes Containing Non-Conventional and Polymer Modified Binders*, Proceedings of the Association of Asphalt Paving Technologists, Vol. 59, 1990, p. 590

Van de Ven M.F.C., Jenkins K.J. and Smit A. DeF., *Conceptualisation of Spatial Composition*, ITT Report 2-1999, University of Stellenbosch, Stellenbosch, 1999

- Verhaeghe B M J A, van de Ven M F C, Grobler J E and Smit A de F, 1995, *State-of-the-art review on volume-based asphalt mix design & provisional guidelines*, Volumetric design of asphalt, Phase 1, Report DPVT C-319-1F, Sabita
- Walubita L.F., *Accelerated Testing of an Asphalt Pavement with the Third-Scale Model Mobile Load Simulator (MMLS3)*, MSc.Eng Thesis, University of Stellenbosch, 2000
- Walubita L.F., Hugo F. and Epps A., *Indirect Tensile Fatigue Performance of Asphalt after MMLS3 trafficking under different environmental conditions*, Technical Paper 493 published in the Journal of the South African Institution of Civil Engineering, 44(3), 2002 , pp 2-11
- Walubita L.F., Hugo F. and Epps A., *Report on the Second Jacksboro MMLS Mk3 Tests*, Draft Report 1841-3 prepared for the Texas Department of Transportation by the Center for Transportation Research, The University of Texas at Austin, 2000
- Weissman S.L., Harvey J., Sackman J.L. and Long F., *Selection of Laboratory Test Specimen Dimension for Permanent Deformation of Asphalt Concrete Specimens*, Transportation Research Record 1681, Transportation Research Board, National Research Council, Washington DC, 1999
- Zhang X and Huber G., *Effect of Asphalt Binder on Pavement Performance: An Investigation Using the Superpave Mix Design System*, Proceedings of the Association of Asphalt Paving Technologists, Vol. 65, 1996, p. 449

# APPENDIX



# APPENDIX A

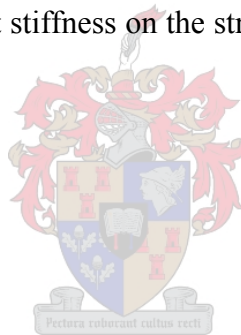
## Sensitivity Analysis of Stress Distribution between Different Specimen Geometries

This appendix covers the sensitivity analysis that was performed with ELSYM5 (linear elastic analysis) and ABAQUS (finite element analysis) to estimate the stresses in the asphalt specimens at 50 °C under an MMLS3 load for different specimen geometries.

### A1. Linear Elastic Analysis (ELSYM5)

ELSYM5 is a linear elastic program capable of computing stresses in strain in a multilayer pavement structure. Semi-infinite two layer systems have been analysed using ELSYM5. To determine the influence of the asphalt stiffness on the stress distribution, three different asphalt elastic moduli were considered:

- 500 MPa
- 1000 MPa
- 1500 MPa



The asphalt thickness was also varied as follows:

- 40 mm (modelling the thickness of slab)
- 60 mm (modelling the thickness of briquette)
- 1000 mm (modelling a very deep asphalt layer)

For each case, the asphalt was analysed on top of a semi-infinite concrete subgrade with an elastic modulus of 28 GPa and Poisson's ratio of 0.18. Poisson's ratio for the asphalt was assumed 0.45. A wheel load of 2.1 kN was applied. The tyre pressure was 690 kPa and the width of the wheel.

#### A1.1 Influence of stiffness and thickness on vertical stresses

From Figure A - 1 through Figure A - 4, it can be seen that there is not any significant difference in the vertical stress distributions with variation in stiffness as well as thickness. For

the same thickness and different stiffnesses, the vertical stress distribution is the same. When comparing the same stiffness at different thicknesses, there are also no significant differences in the vertical stress distributions, except that the corresponding stresses for the thinner layers occurs 5-10 mm deeper than for the 1000mm layer. The maximum vertical stress at a distance 75 mm from the wheel center (which would correspond to the outside of a briquette) is estimated at 50 kPa at a depth of about 40mm. At lesser depths, the vertical stress is between 0-50 kPa. The highest vertical stresses occur under the wheel, as one would expect.

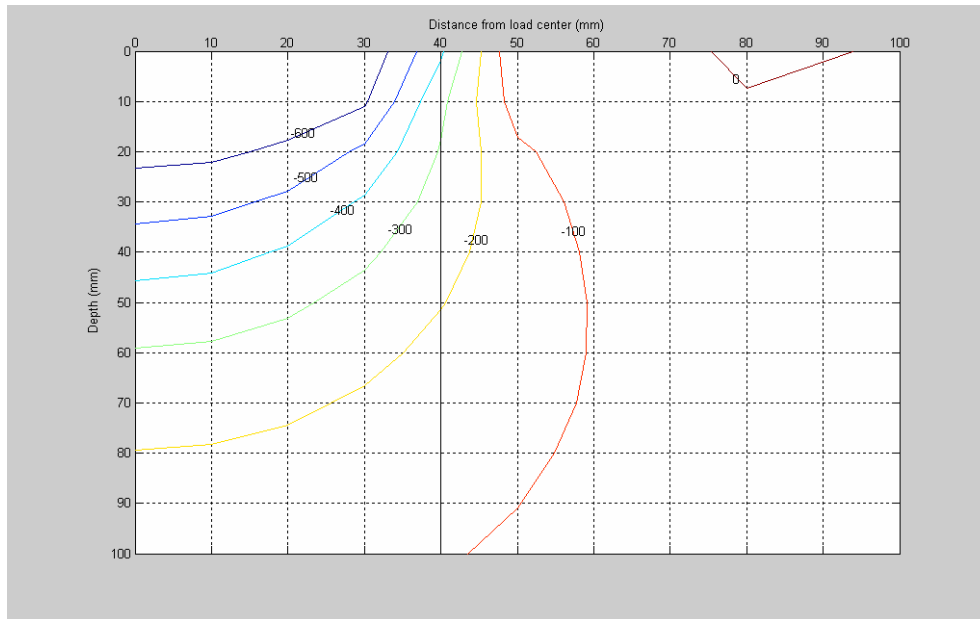


**Figure A - 1: ELSYM 5 Vertical Stress Contours (in kPa) for Asphalt thickness 1m;  
Stiffness 1000 MPa,  $\nu = 0.45$**

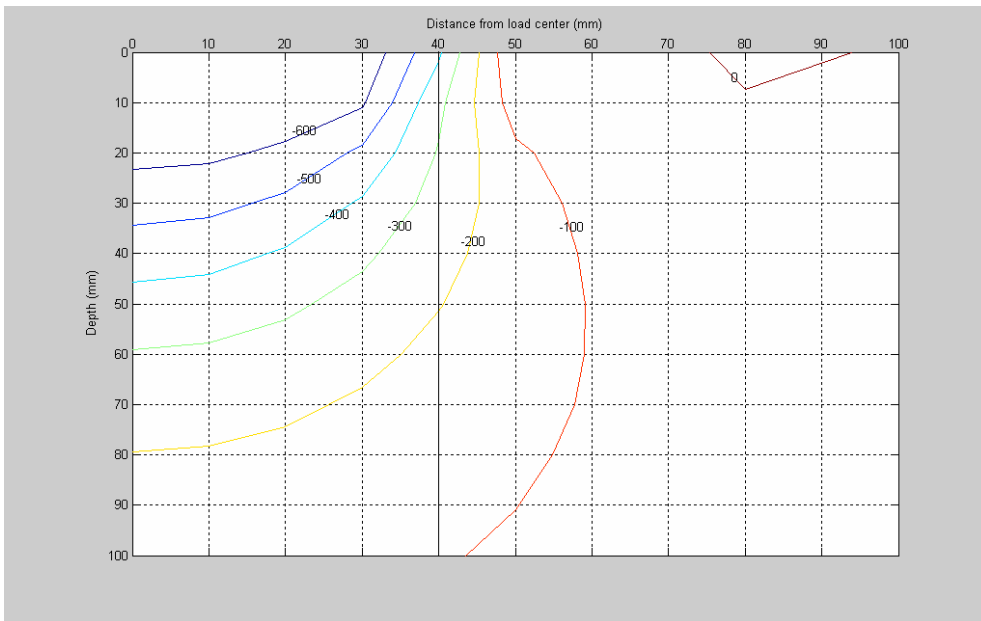


**Figure A - 2: ELSYM 5 Vertical Stress Contours (in kPa) for Asphalt thickness 1m;  
Stiffness 1500 MPa;  $\nu = 0.45$**

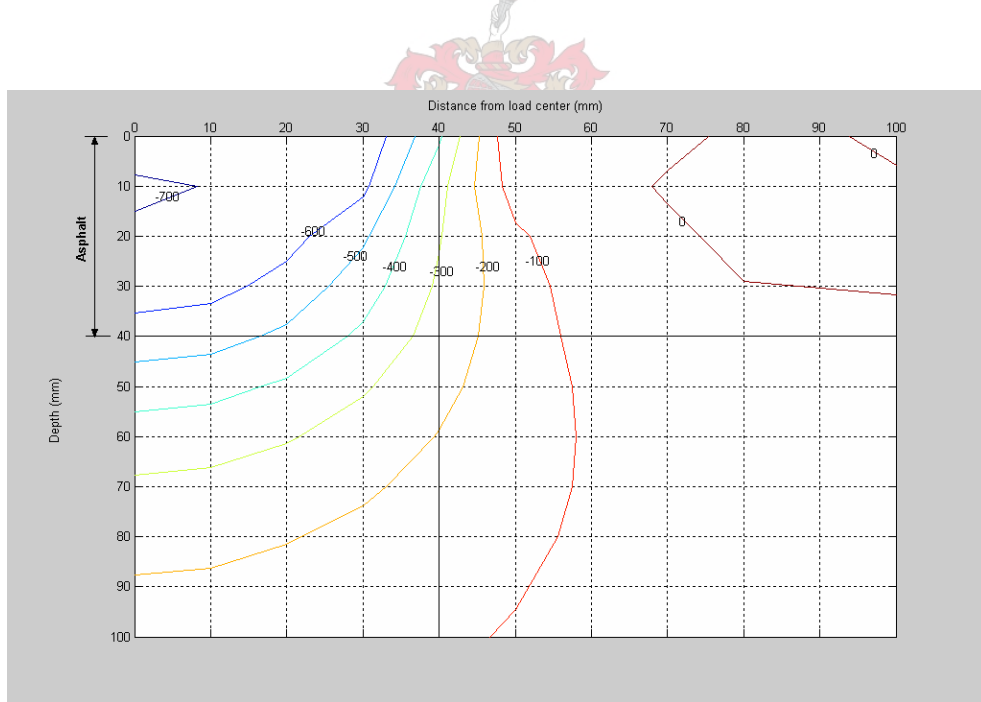


**Figure A - 3: ELSYM 5 Vertical Stress Contours (in kPa) for Asphalt thickness 40 mm;  
Stiffness 1500 MPa;  $\nu = 0.45$**

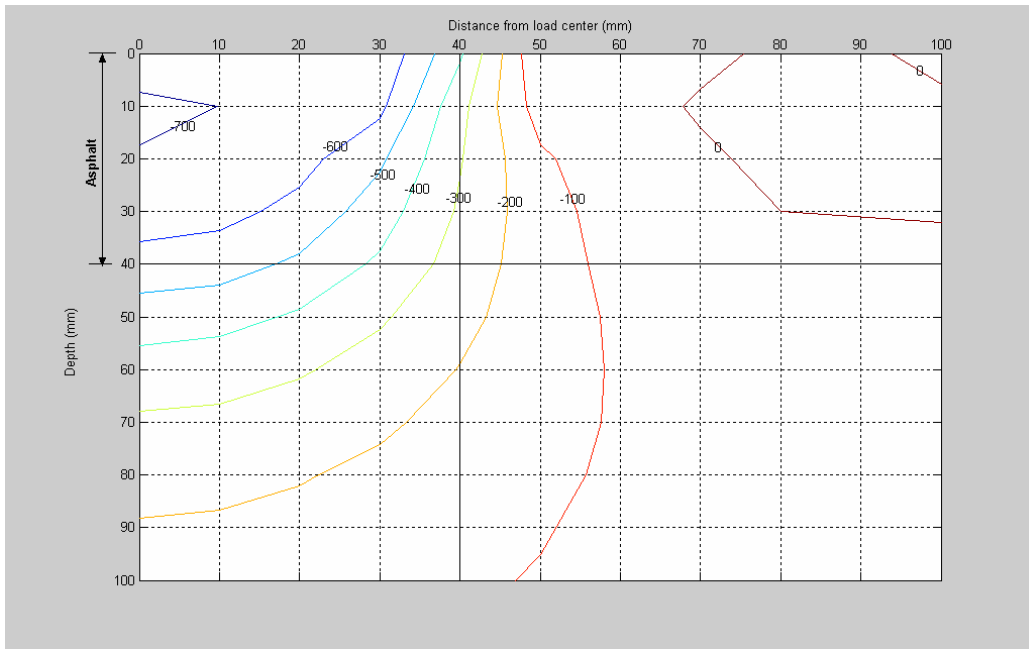


**Figure A - 4: ELSYM 5 Vertical Stress Contours (in kPa) for Asphalt thickness 40 mm;  
Stiffness 1000 MPa;  $\nu = 0.45$**



### **A1.2 Influence of stiffness and thickness on Shear stresses**

The shear stress distributions are given in Figure A - 5 through Figure A - 10. From these figures it is also clear that the variation in stiffness for a particular thickness does not have a significant influence on the shear stress distribution. These shear stresses are almost identical. Only when the thickness is varied, the differences in shear stresses become evident. For the 40mm thick layer, the highest shear stress at the bottom of the asphalt layer (150 kPa) is higher than at the bottom of the 60mm layer (100 kPa). The maximum shear stresses occur under the side of the wheel, as expected. The shear stress distributions indicate that the stiffness does not have a significant influence on the shear stress, but the thickness does. One would expect that because of the stiffer concrete layer underneath, the thinner layer will experience higher stresses.

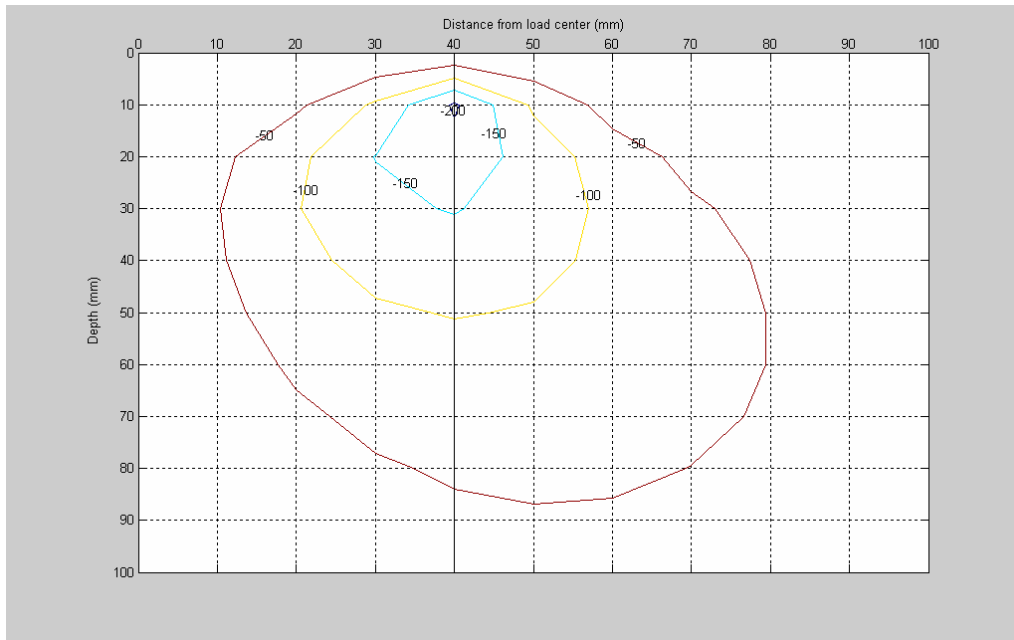


**Figure A - 5: ELSYM 5 Shear Stress Contours (in kPa) for Asphalt thickness 1m;  
Stiffness 1000 MPa;  $\nu = 0.45$**

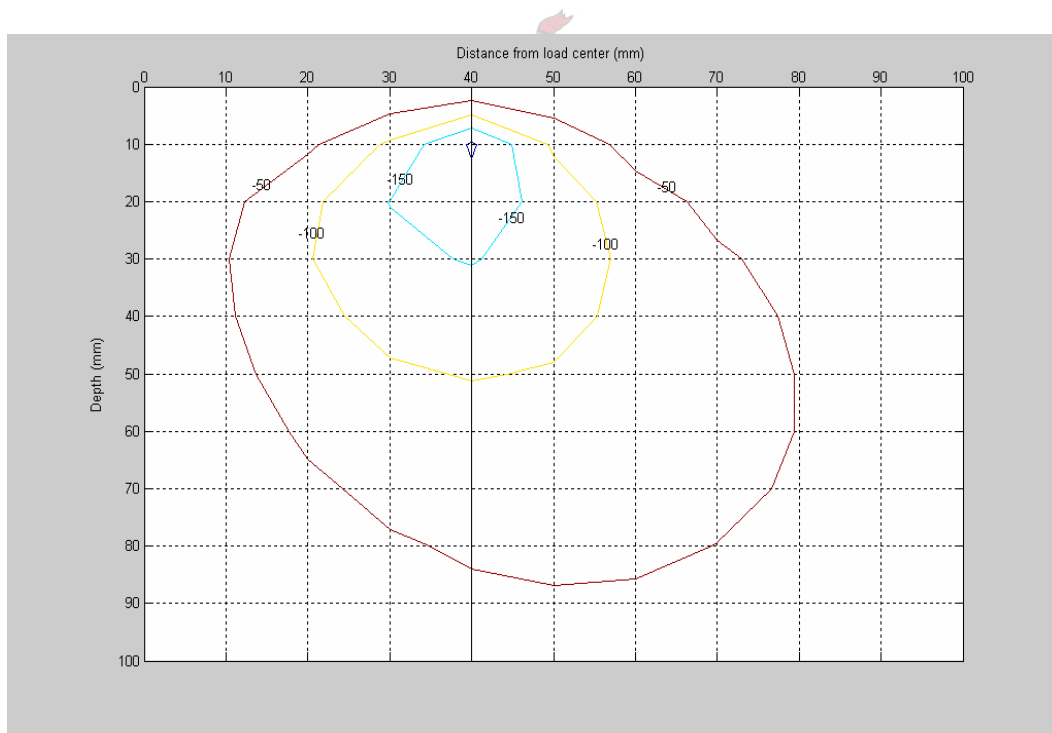


**Figure A - 6: ELSYM 5 Shear Stress Contours (in kPa) for Asphalt thickness 1m;  
Stiffness 1500 MPa;  $\nu = 0.45$**

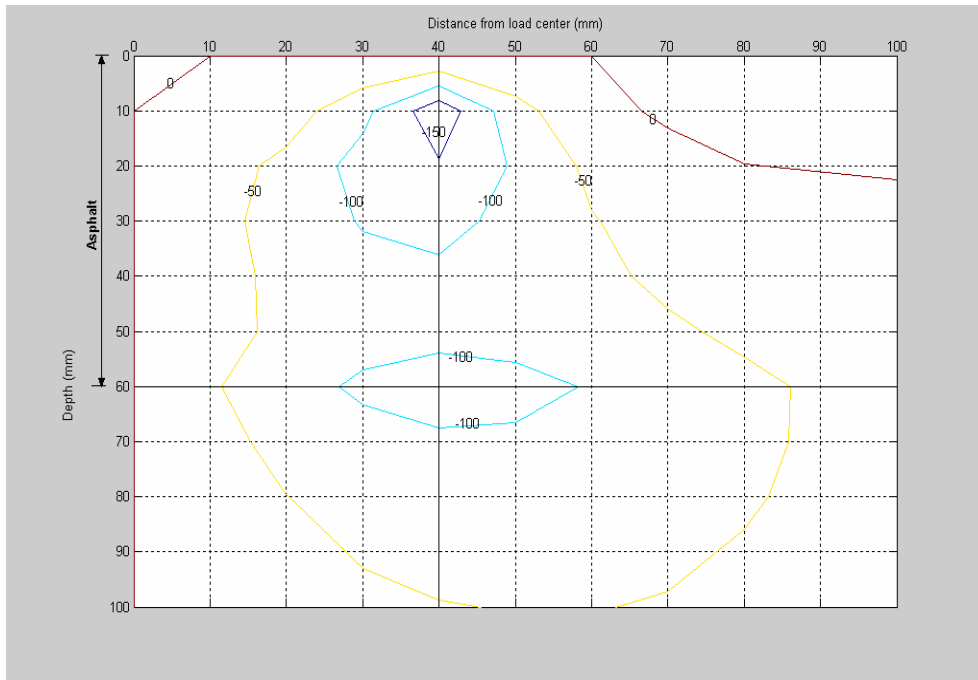


**Figure A - 7: ELSYM 5 Shear Stress Contours (in kPa) for Asphalt thickness 60 mm;  
Stiffness 1500 MPa;  $\nu = 0.45$**

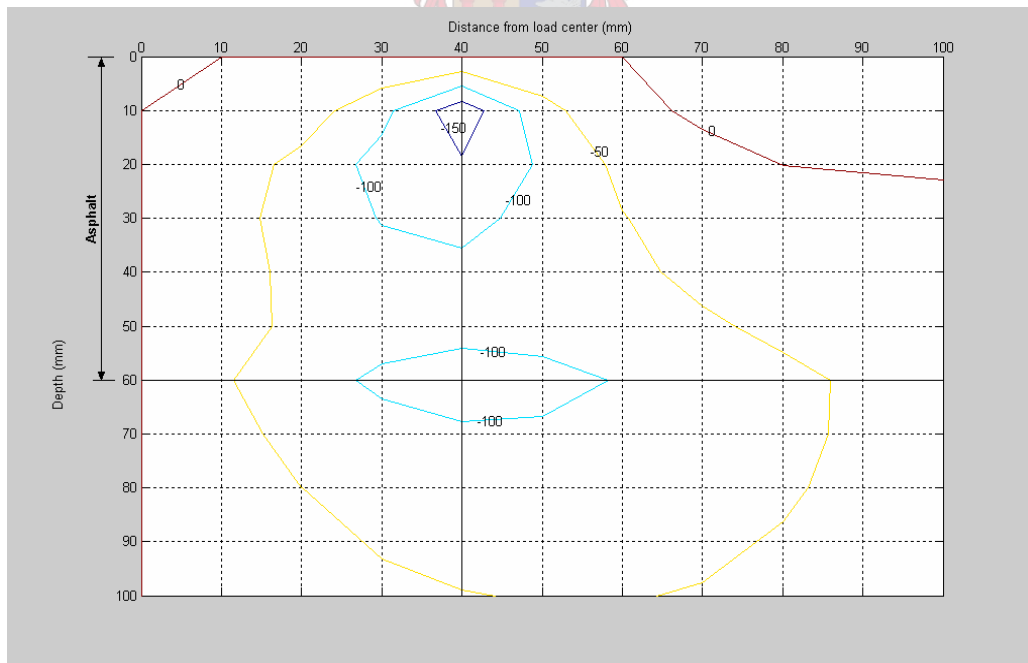


**Figure A - 8: ELSYM 5 Shear Stress Contours (in kPa) for Asphalt thickness 60 mm;  
Stiffness 1000 MPa;  $\nu = 0.45$**

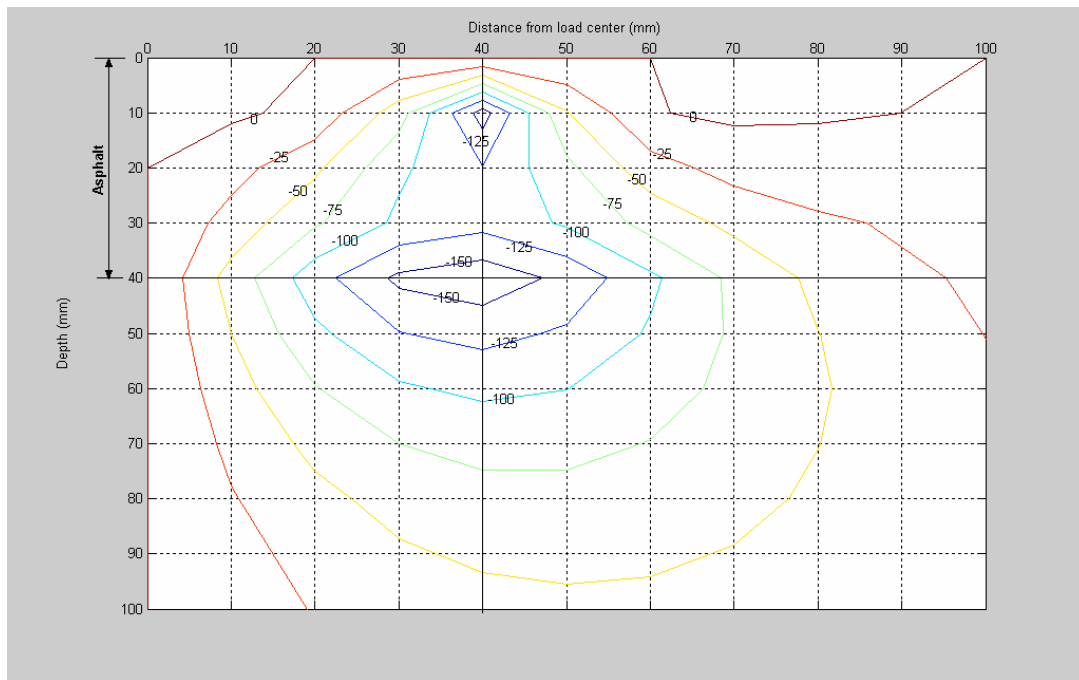


**Figure A - 9: ELSYM 5 Shear Stress Contours (in kPa) for Asphalt thickness 40 mm;  
Stiffness 1500 MPa;  $\nu = 0.45$**

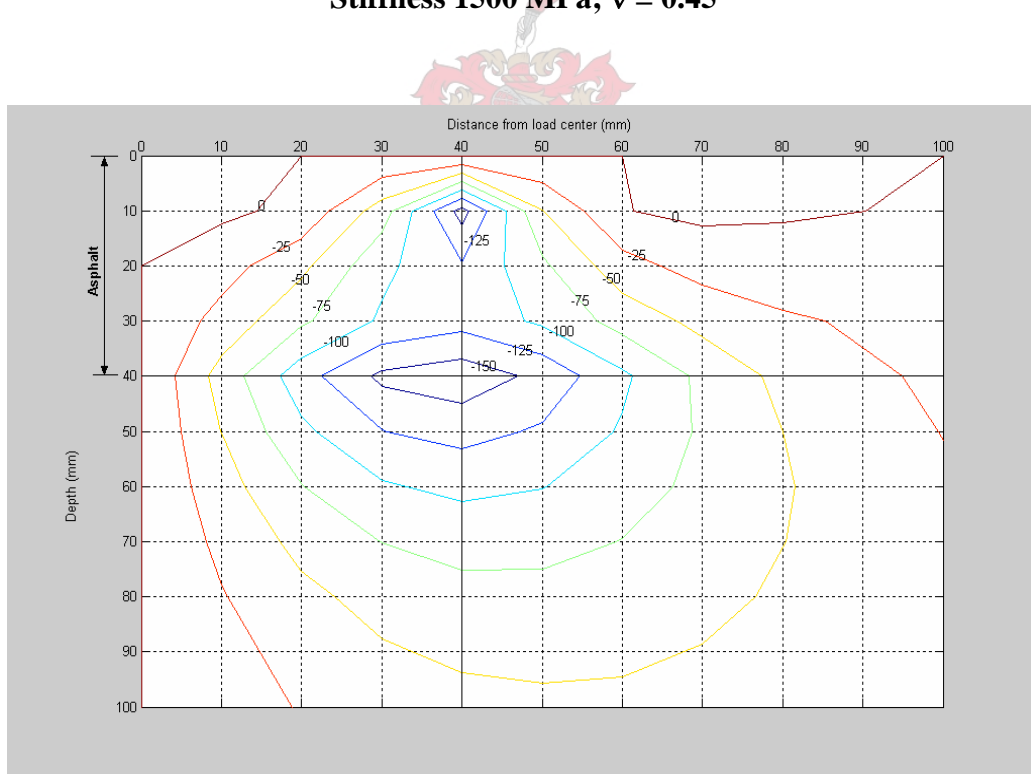


**Figure A - 10: ELSYM 5 Shear Stress Contours (in kPa) for Asphalt thickness 40 mm;  
Stiffness 1000 MPa;  $\nu = 0.45$**

### A1.3 Influence of stiffness and thickness on Horizontal stresses

The horizontal stress contours are given in Figure A - 11 through Figure A - 17. When comparing different stiffnesses for a particular thickness, the horizontal stress distributions are identical. The thickness, however, has a significant influence on the stress distributions. The horizontal stresses in the top of the asphalt layer decrease from the 1000mm to the 40mm layer. The horizontal stresses at the bottom are higher for the thinner layer than the thicker layer. The influence of the horizontal stresses outside the wheel (40 – 75 mm) is comparable for the 40mm and 60mm thickness.

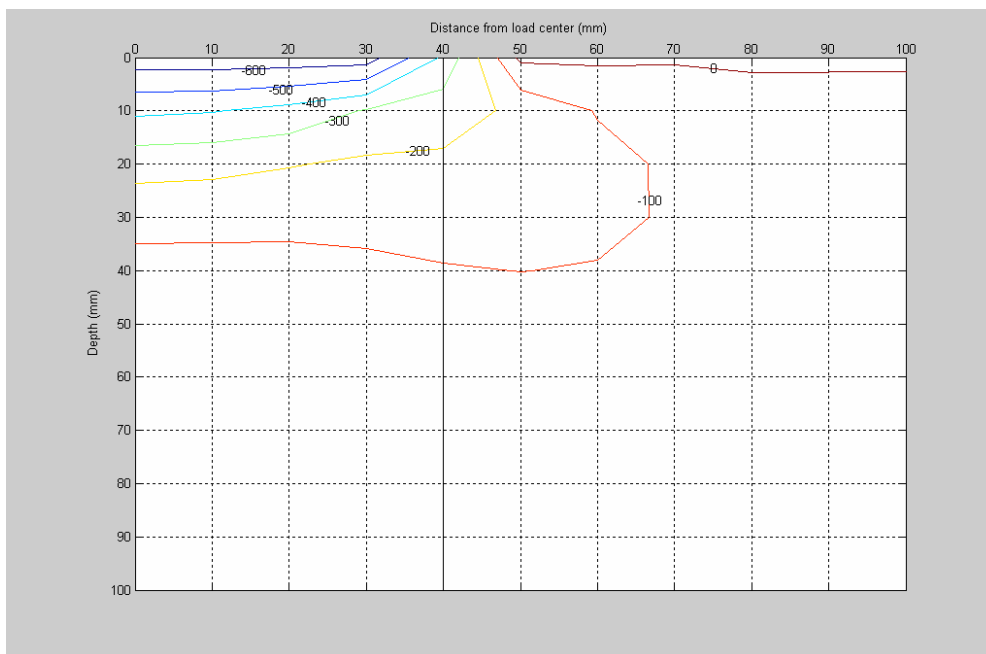


**Figure A - 11: ELSYM 5 Horizontal Stress Contours (in kPa) for Asphalt thickness 1m;  
Stiffness 1500 MPa;  $\nu = 0.45$**

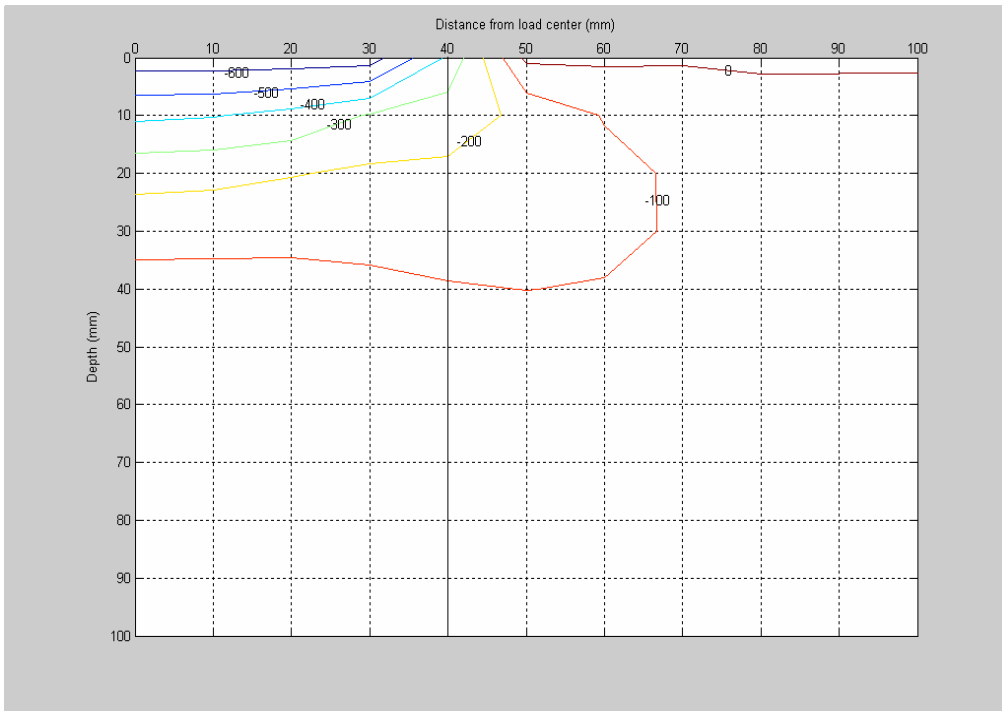


**Figure A - 12: ELSYM 5 Horizontal Stress Contours (in kPa) for Asphalt thickness 1m;  
Stiffness 1000 MPa;  $\nu = 0.45$**

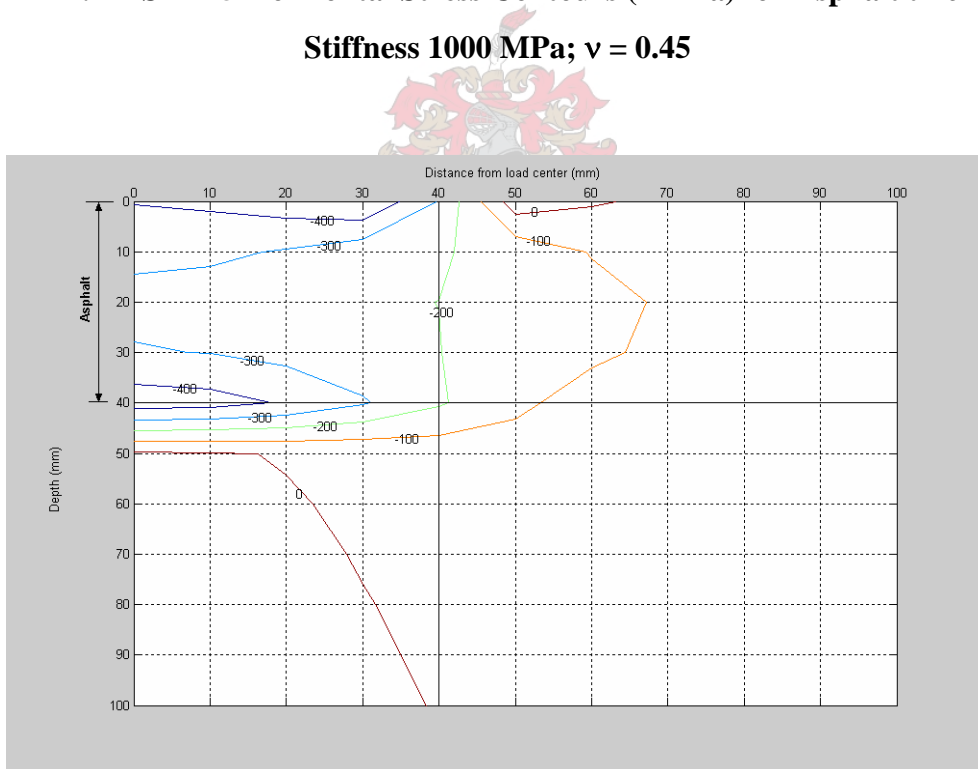


**Figure A - 13: ELSYM 5 Horizontal Stress Contours (in kPa) for Asphalt thickness 40  
mm; Stiffness 1000 MPa;  $\nu = 0.45$**

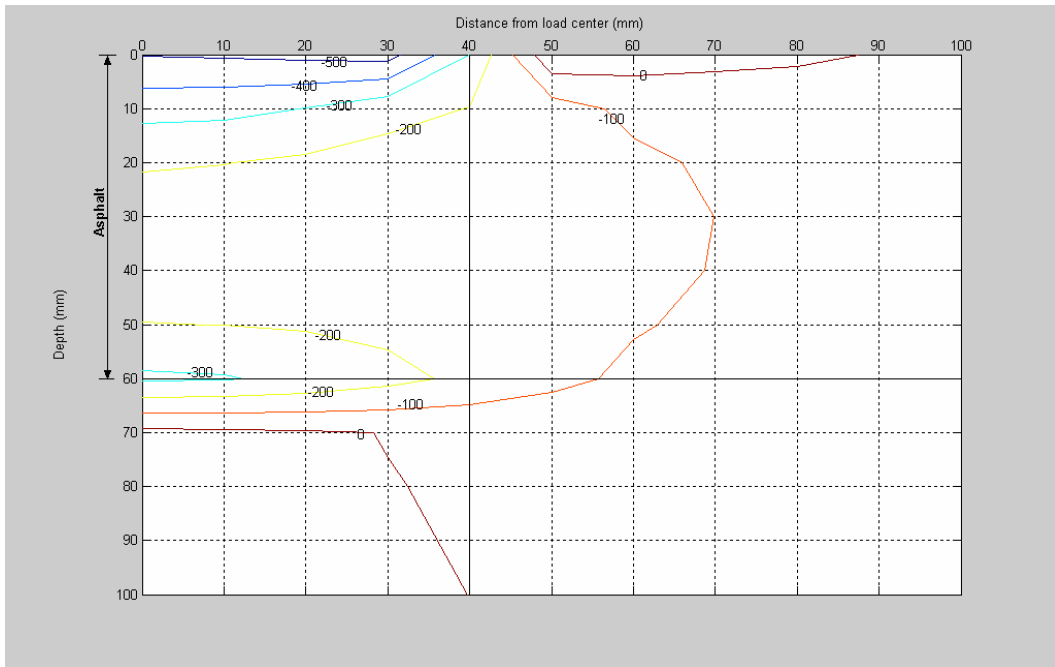


**Figure A - 14: ELSYM 5 Horizontal Stress Contours (in kPa) for Asphalt thickness 60 mm; Stiffness 1500 MPa;  $\nu = 0.45$**

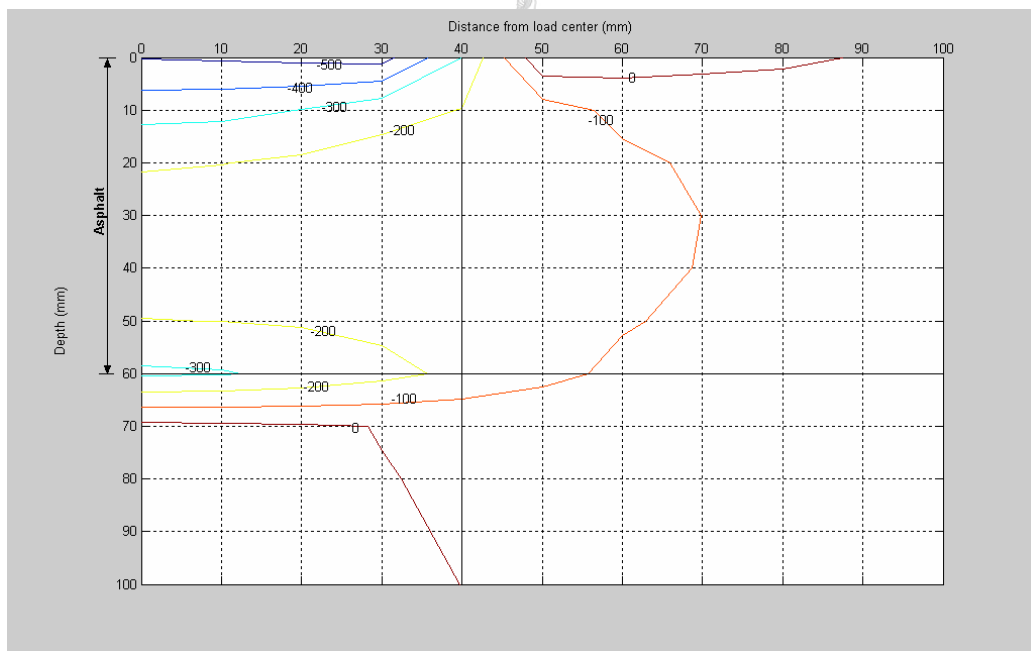


**Figure A - 15: ELSYM 5 Horizontal Stress Contours (in kPa) for Asphalt thickness 60 mm; Stiffness 1500 MPa;  $\nu = 0.45$**

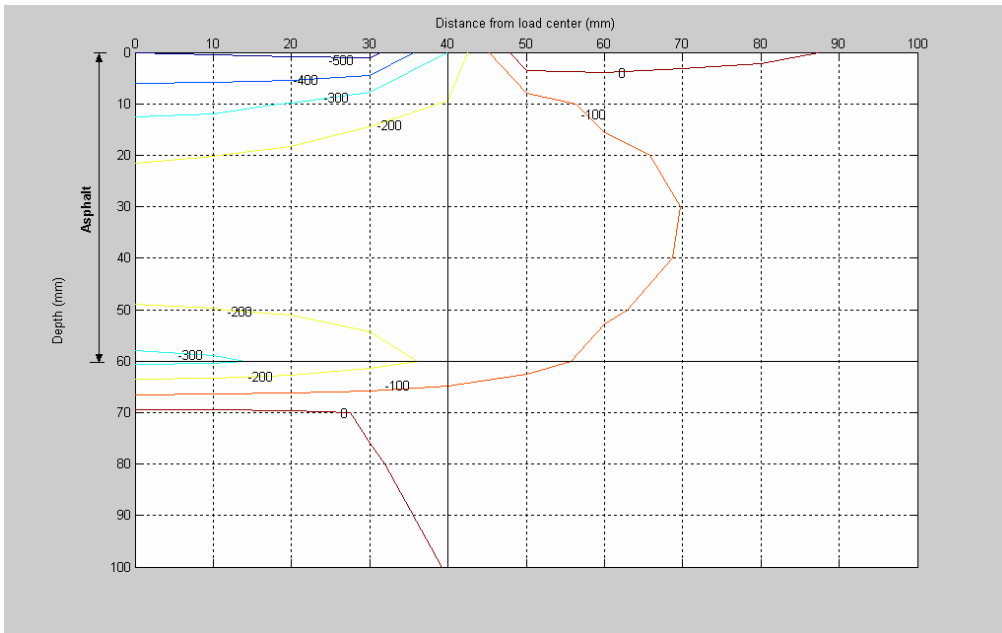


**Figure A - 16: ELSYM 5 Horizontal Stress Contours (in kPa) for Asphalt thickness 60 mm; Stiffness 1000 MPa;  $\nu = 0.45$**

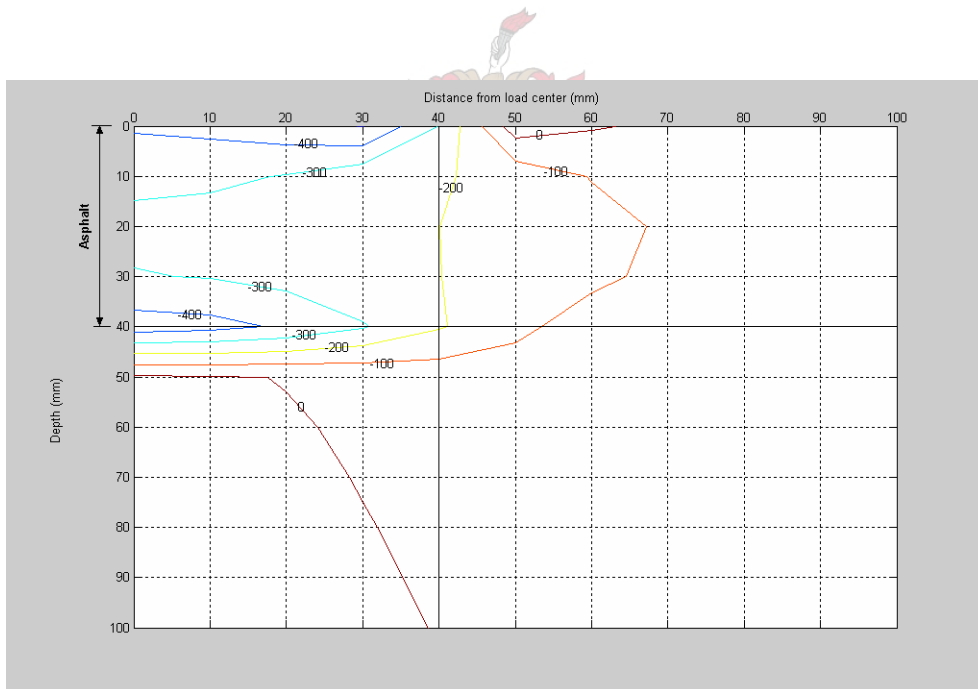


**Figure A - 17: ELSYM 5 Horizontal Stress Contours (in kPa) for Asphalt thickness 40 mm; Stiffness 1500 MPa;  $\nu = 0.45$**

### A1.4 Influence of stiffness and thickness on Deviator stresses ( $\sigma_1 - \sigma_3$ )

The deviator stress contours are given in Figure A - 18 through Figure A - 24. This figures also indicates that the stiffness does not have a significant influence on the stress distribution. The deviator stress distribution for the different thicknesses are also comparable under, as well as outside the wheel.

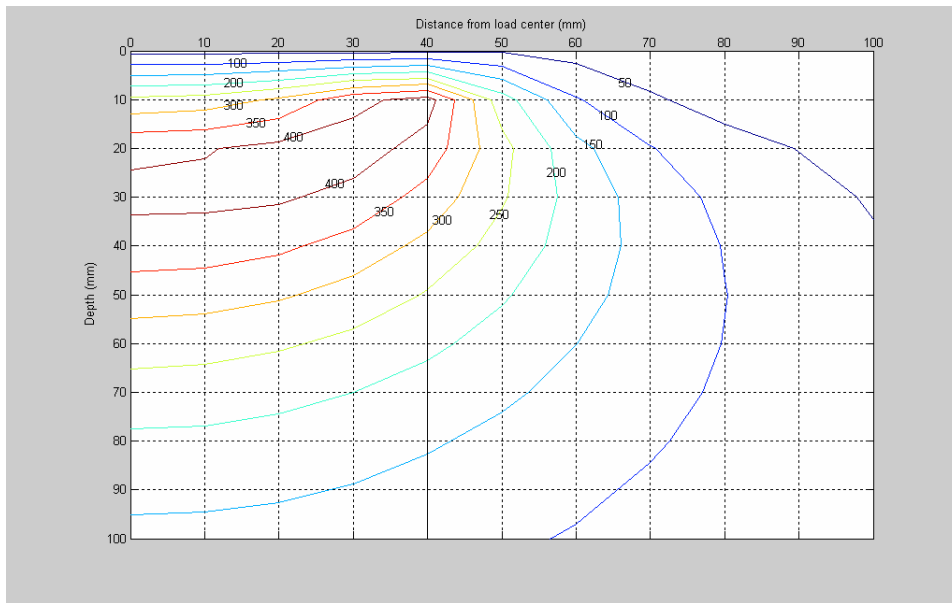


**Figure A - 18: ELSYM 5 Deviator Stress ( $\sigma_1 - \sigma_3$ ) Contours (in kPa) for Asphalt thickness 1m; Stiffness 1000 MPa;  $\nu = 0.45$**

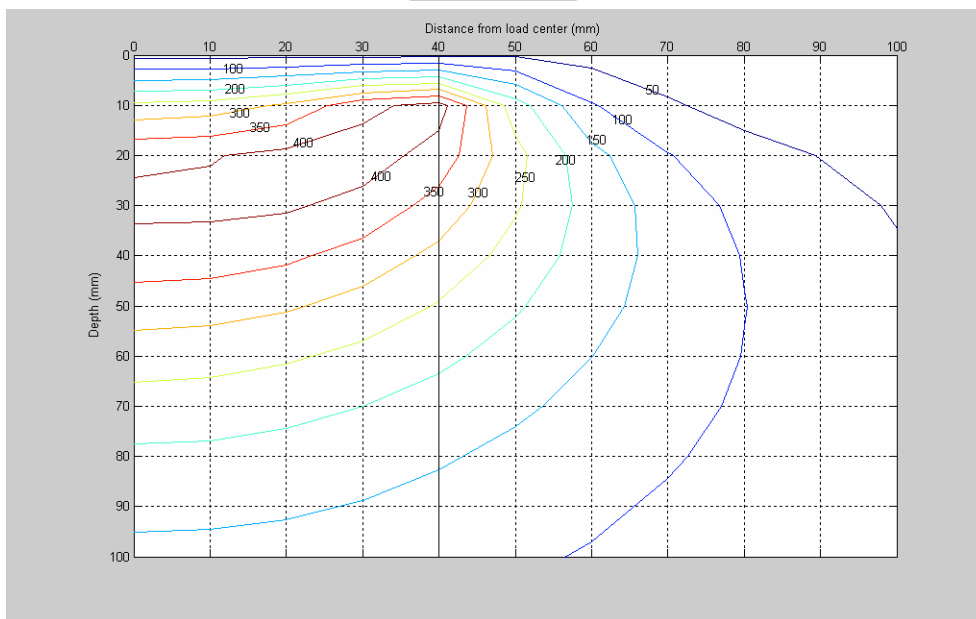


**Figure A - 19: ELSYM 5 Deviator Stress ( $\sigma_1 - \sigma_3$ ) Contours (in kPa) for Asphalt thickness 1m; Stiffness 1500 MPa;  $\nu = 0.45$**

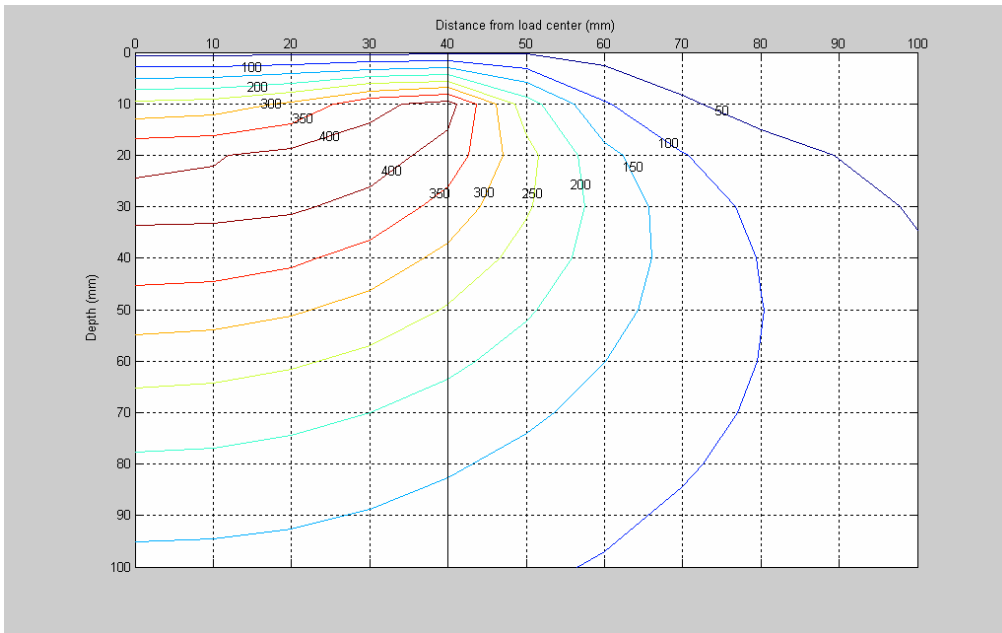


**Figure A - 20: ELSYM 5 Deviator Stress ( $\sigma_1 - \sigma_3$ ) Contours (in kPa) for Asphalt thickness 1m; Stiffness 500 MPa;  $\nu = 0.45$**

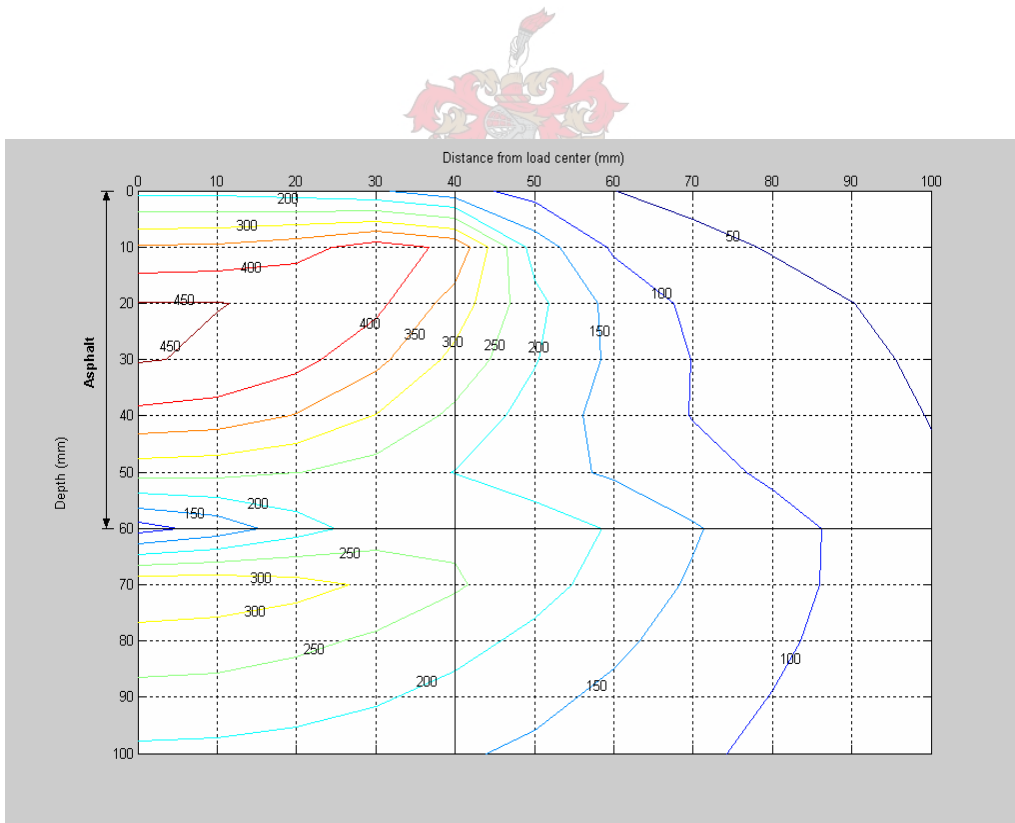


**Figure A - 21: ELSYM 5 Deviator Stress ( $\sigma_1 - \sigma_3$ ) Contours (in kPa) for Asphalt thickness 60 mm; Stiffness 1500 MPa;  $\nu = 0.45$**

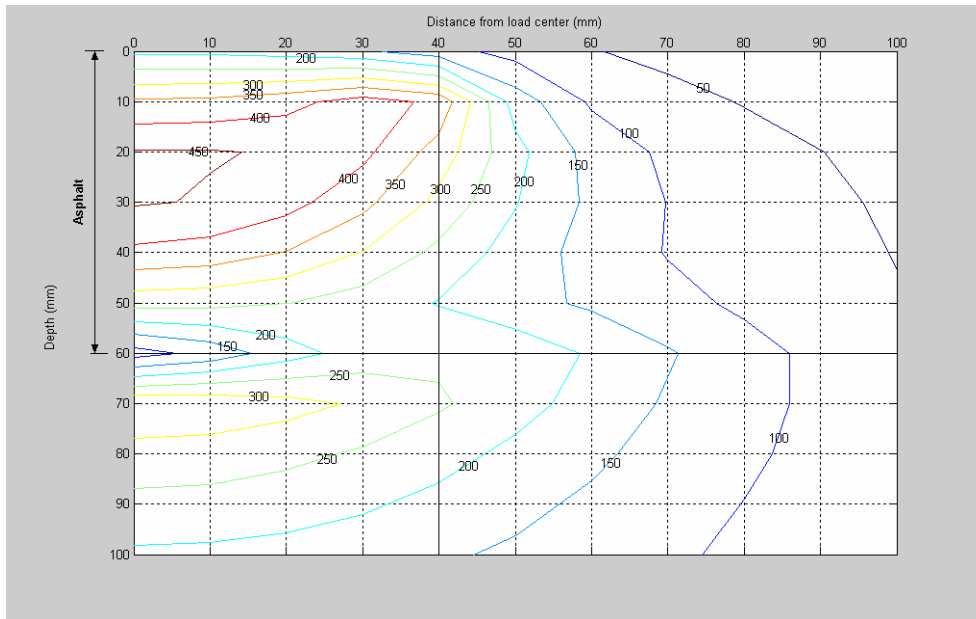


**Figure A - 22: ELSYM 5 Deviator Stress ( $\sigma_1 - \sigma_3$ ) Contours (in kPa) for Asphalt thickness 60 mm; Stiffness 1000 MPa;  $\nu = 0.45$**

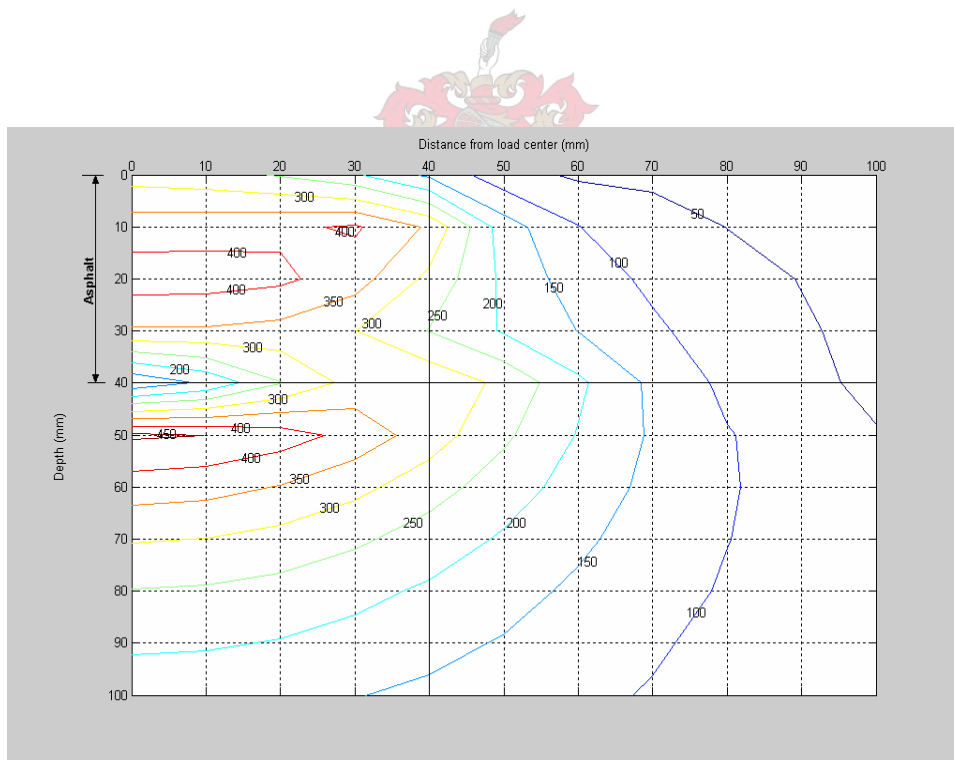


**Figure A - 23: ELSYM 5 Deviator Stress ( $\sigma_1 - \sigma_3$ ) Contours (in kPa) for Asphalt thickness 40 mm; Stiffness 1500 MPa;  $\nu = 0.45$**

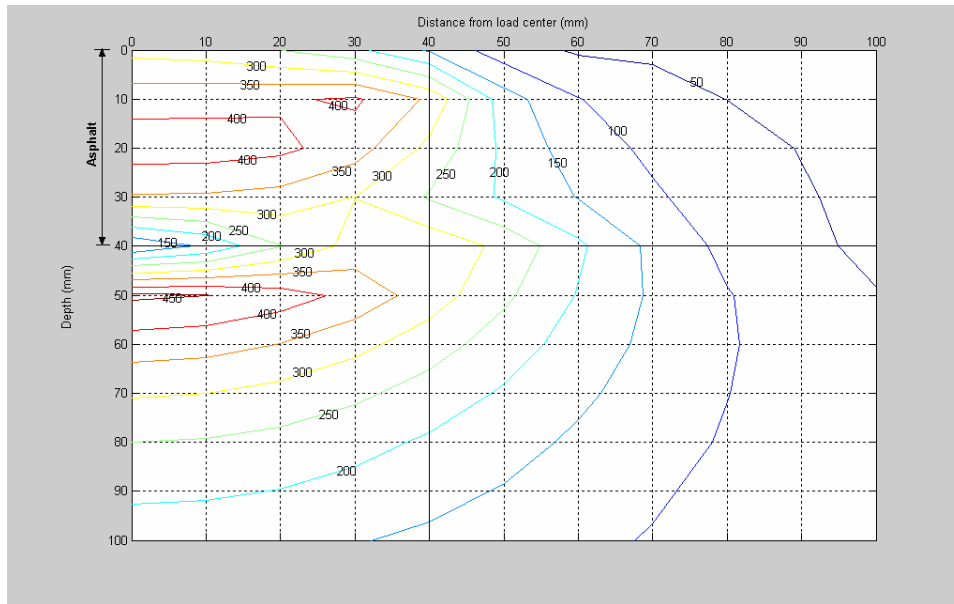


**Figure A - 24: ELSYM 5 Deviator Stress ( $\sigma_1 - \sigma_3$ ) Contours (in kPa) for Asphalt thickness 40 mm; Stiffness 1000 MPa;  $\nu = 0.45$**

In summary, for the ELSYM5 analysis, with the range of stiffnesses considered, the stiffness does not have a significant influence on the stress distributions in the asphalt layer. The thickness does however influence the stress distributions. The thinner layer experienced higher stresses than the thicker layers. The influence of the specimen size and confinement could not be evaluated, since ELSYM5 does not allow for horizontal boundaries being incorporated.

## **A2. Finite Element Analysis (ABAQUS)**

A finite element program ABAQUS was used to obtain a better approximation of the stress conditions in the slab en briquette specimen respectively, because ELSYM5 is not able to model horizontal confinement. A two dimensional linear elastic analysis was performed. Only the asphalt specimen were analysed with the appropriate boundary conditions. For the geometrical model, 8-noded quadrilateral plane strain finite elements (5 x 5 mm) were used, formulated according to the linear elastic theory. Since there was a plane of symmetry, only half of the specimen was analysed. The following cases were analysed:

- Briquette 60 mm height and widths of 100, 120 and 150 mm
- Slab 40 mm height and width 600 mm

The specimens were subjected to an equivalent static loading of 690 kPa over a width of 80 mm. The bottom boundaries were fixed. The symmetry boundary was only constrained from horizontal displacement. For the outside boundary no horizontal displacement was allowed and with regard to vertical displacement, three conditions were considered:

1. Fixed boundary (simulating full friction between specimen and mould)
2. Vertical roller support (simulating no friction between specimen and mould)
3. Prescribed displacement; 50 percent of the resulting displacement from case 2 (simulating partial friction between specimen and mould)



The ELSYM5 analysis showed that the stiffness does not have a significant influence on the stress distributions. In the finite element analysis, an asphalt stiffness of 1500 MPa and a Poisson's ratio of 0.45 were used.

### **A2.1 Vertical stress distributions**

Figure A - 25 gives the vertical stress contours for the 150mm briquette. The case with no friction is comparable to the ELSYM5 distribution, except that the higher stresses occur slightly deeper in the specimen. The amount of friction does only appear to influence the stresses in the outer 25mm of the specimen.

Observing Figure A - 26 through Figure A - 28, it is clear that as the briquette width decreases, the stresses in the region between the wheel and the mould increase. The amount of friction also plays an increasing role in that region, with the most interference observed in the full

friction case. The vertical stress distributions within the slab are identical for all cases. The side friction on the slab does not show any influence, in fact the vertical stresses (Figure A - 28) does not extend beyond a horizontal distance of about 70mm from the center of the wheel

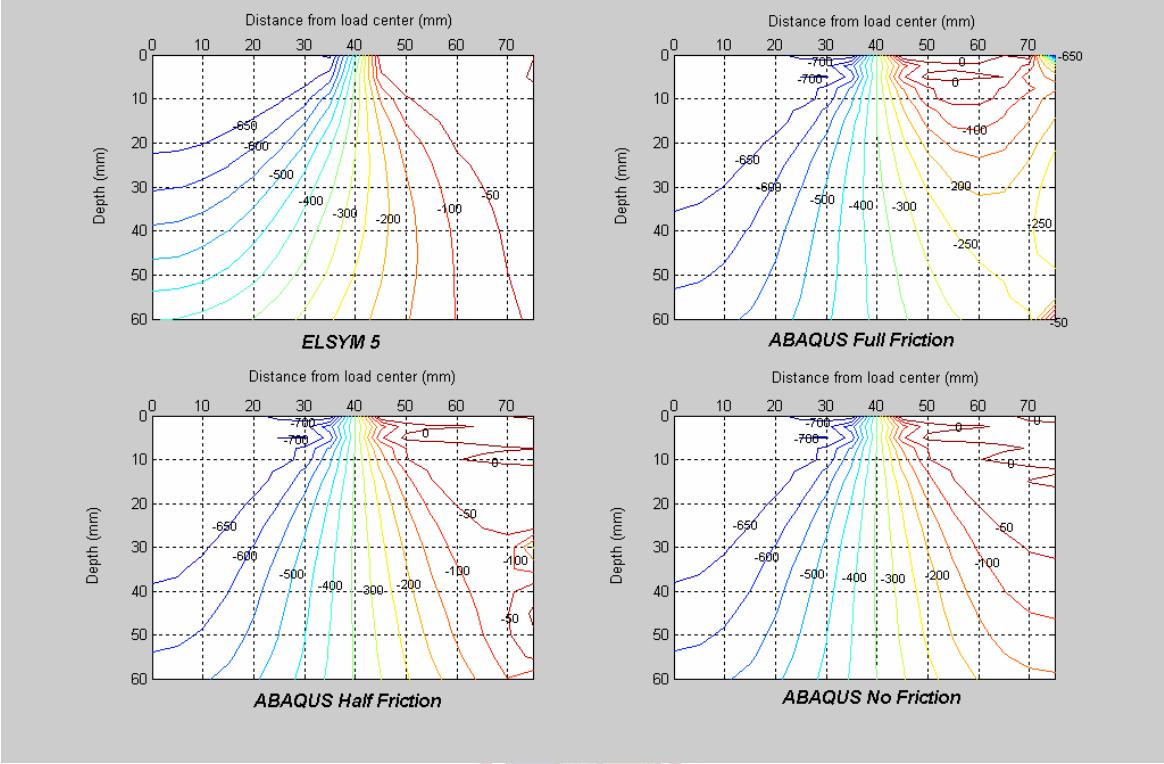


**Figure A - 25: ABAQUS Vertical Stress Contours (in kPa) for Briquette 150mm width; Thickness 60 mm; Stiffness 1500 MPa;  $\nu = 0.45$**

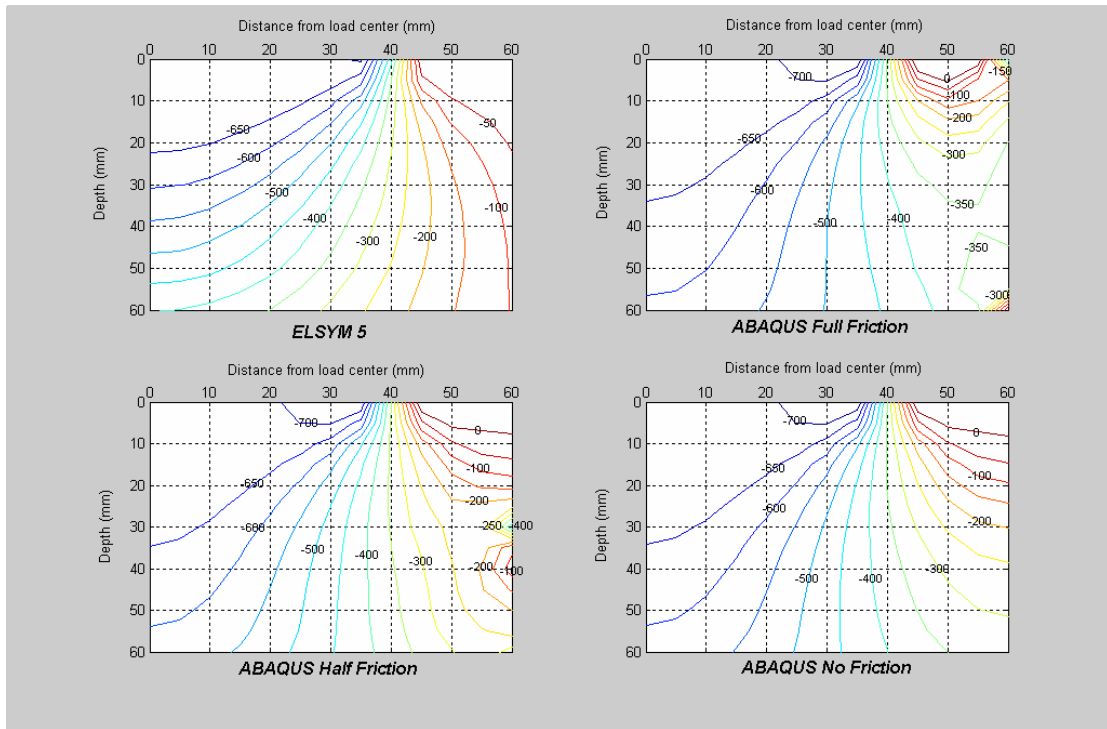


**Figure A - 26: ABAQUS Vertical Stress Contours (in kPa) for Briquette 120mm width;  
Thickness 60 mm; Stiffness 1500 MPa;  $\nu = 0.45$**

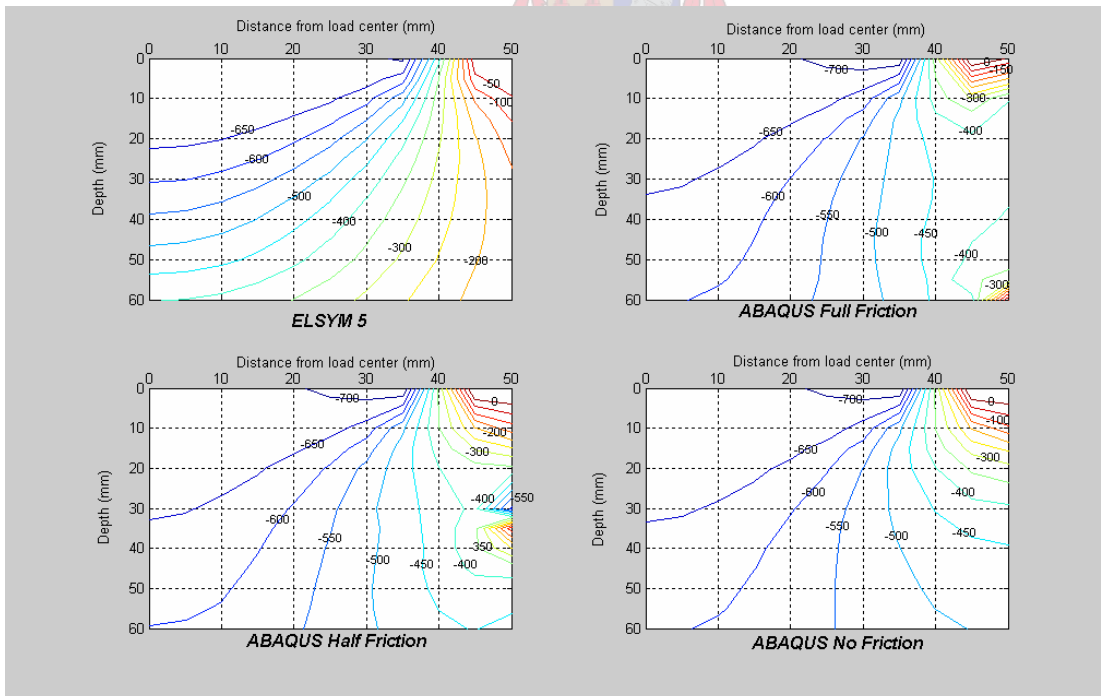


**Figure A - 27: ABAQUS Vertical Stress Contours (in kPa) for Briquette 100mm width;  
Thickness 60 mm; Stiffness 1500 MPa;  $\nu = 0.45$**

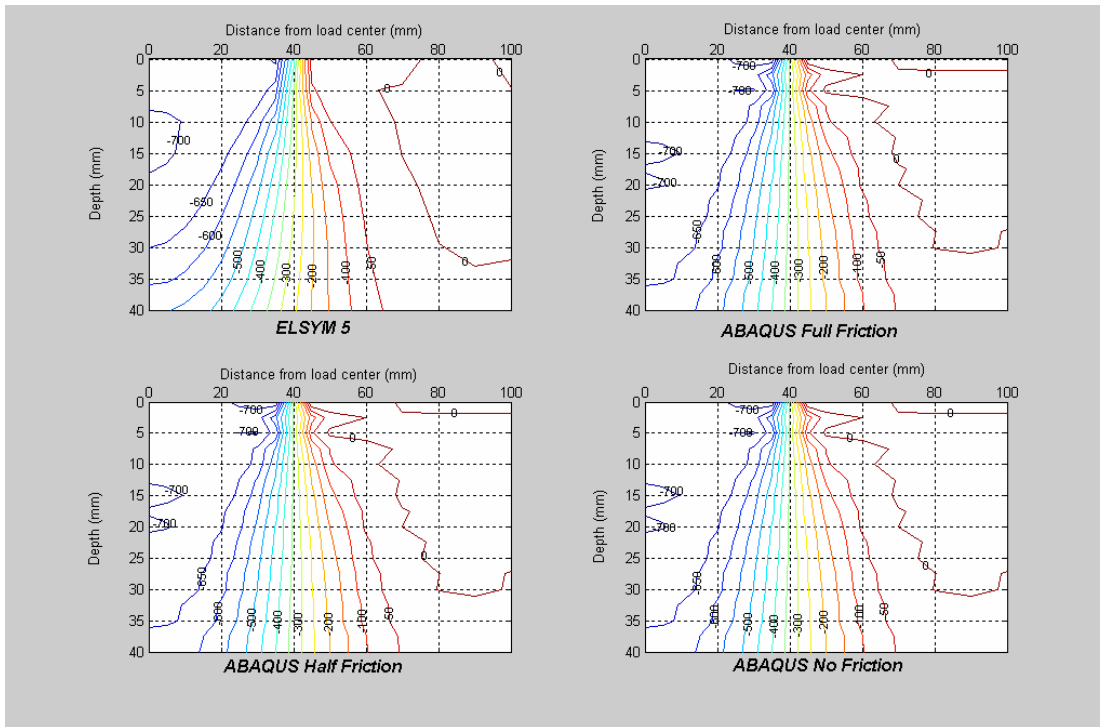


**Figure A - 28: ABAQUS Vertical Stress Contours (in kPa) for Slab 600 mm width;  
Thickness 40 mm; Stiffness 1500 MPa;  $\nu = 0.45$**

## A2.2 Shear stress distributions

The shear stress distributions are given in Figure A - 29 through Figure A - 32. For the various briquette widths, the maximum shear stresses decreases as the width decreases. This can be expected, because the narrower specimens do not allow that much horizontal displacement within the material as the wider specimen. This gives an indication that the wider specimens may exhibit more vertical deformation. For all the 150mm briquette width, only the full friction case appears to have a significant influence on the shear stresses between the wheel and the mould. The shear stresses right under the side of the wheel are higher for the slab than the briquettes, with the highest shear stresses occurring at the bottom of the slab. As for the vertical stresses, the shear stresses from the applied wheel load does not extend significantly beyond 100mm from the center of the wheel.

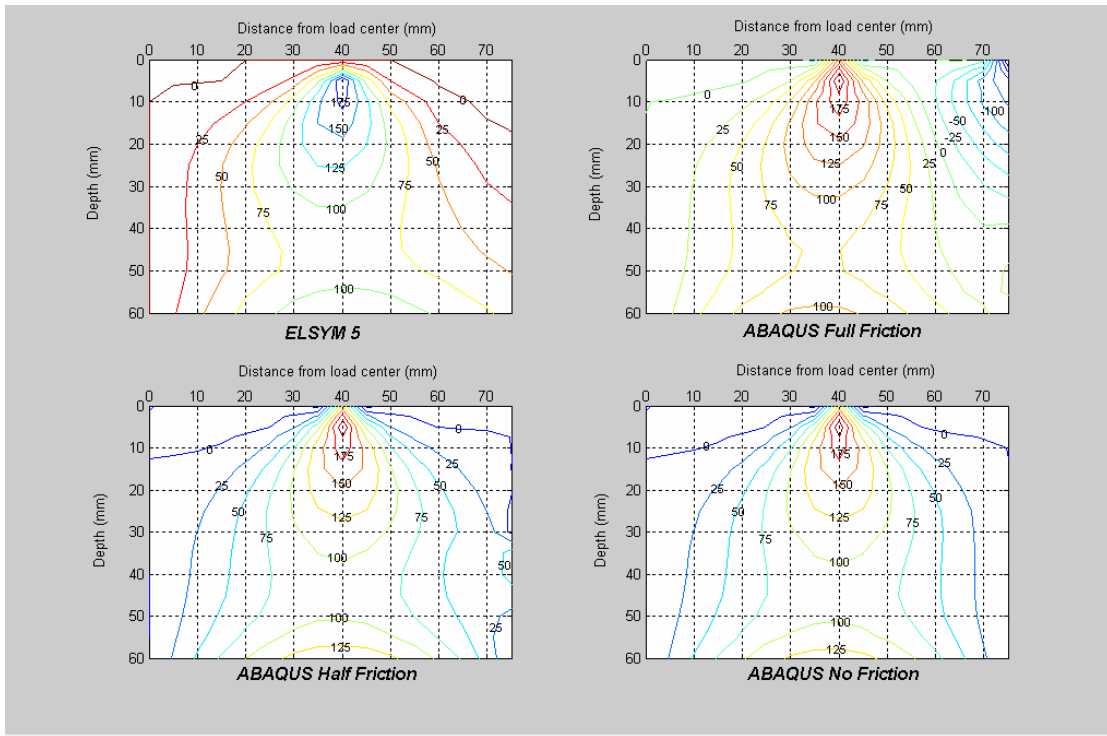


**Figure A - 29: ABAQUS Shear Stress Contours (in kPa) for Briquette 150mm width;  
Thickness 60 mm; Stiffness 1500 MPa;  $\nu = 0.45$**

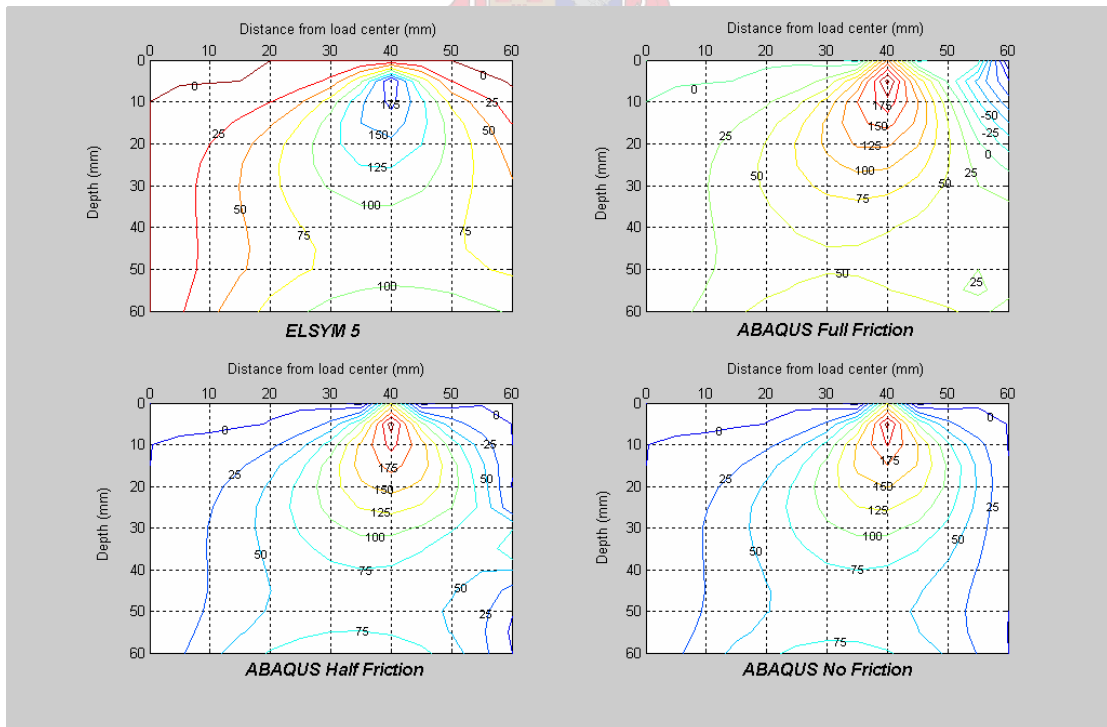


**Figure A - 30: ABAQUS Shear Stress Contours (in kPa) for Briquette 120mm width;  
Thickness 60 mm; Stiffness 1500 MPa;  $\nu = 0.45$**

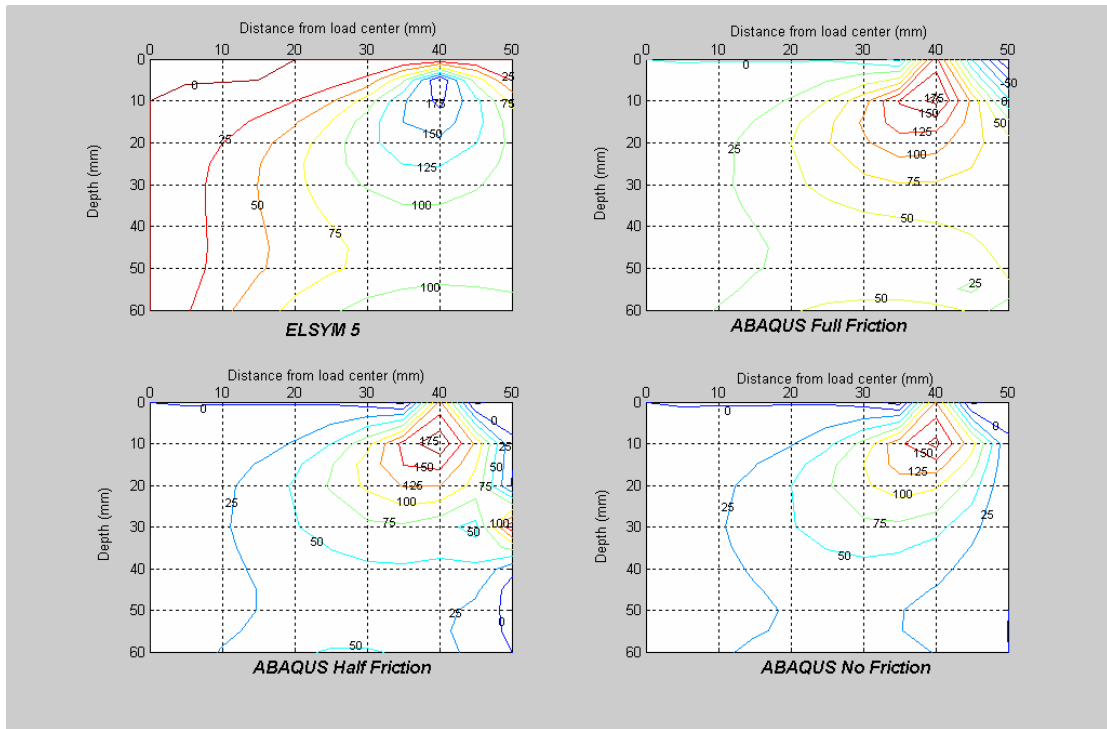


**Figure A - 31: ABAQUS Shear Stress Contours (in kPa) for Briquette 100mm width;  
Thickness 60 mm; Stiffness 1500 MPa;  $\nu = 0.45$**

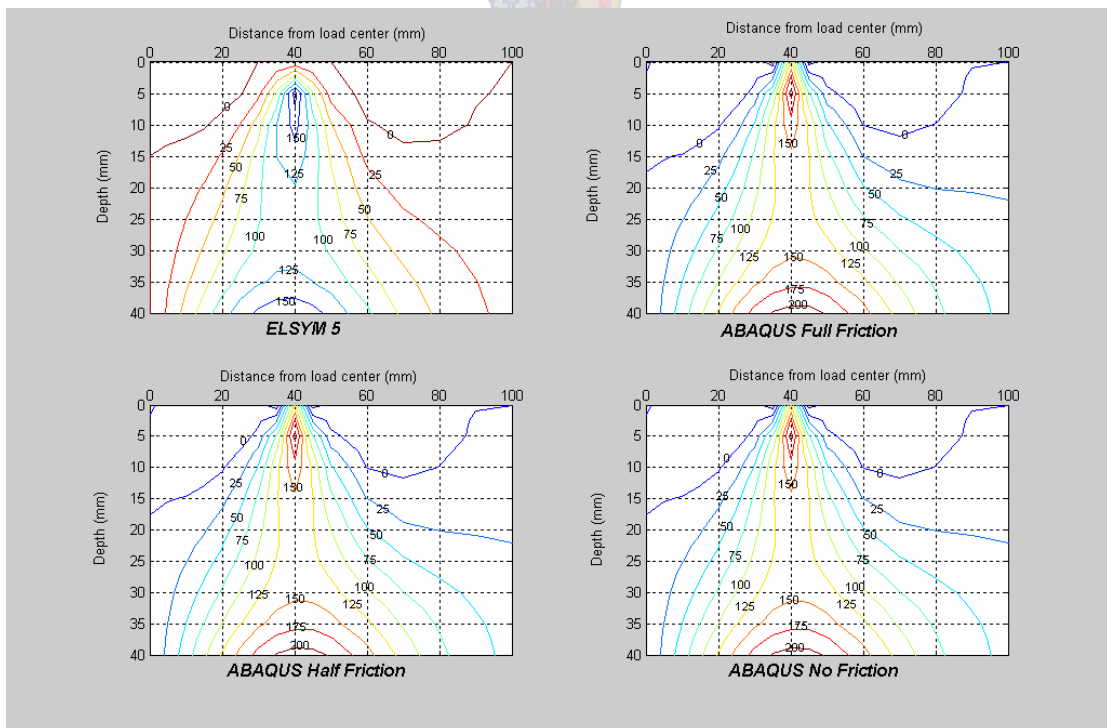


**Figure A - 32: ABAQUS Shear Stress Contours (in kPa) for Slab 600 mm width;  
Thickness 40 mm; Stiffness 1500 MPa;  $\nu = 0.45$**

### A2.3 Horizontal stress distributions

The horizontal stress distributions are given in Figure A - 33 through Figure A - 36. The horizontal stresses within the briquettes increase with a decrease in briquette widths. This can be expected due to the confinement that resists horizontal movement. The horizontal stresses between the wheel and the mould are also higher for the 100mm briquette. There is not any significant difference in horizontal stress distributions for the different slab results. Also, the friction does not influence the stress distributions.

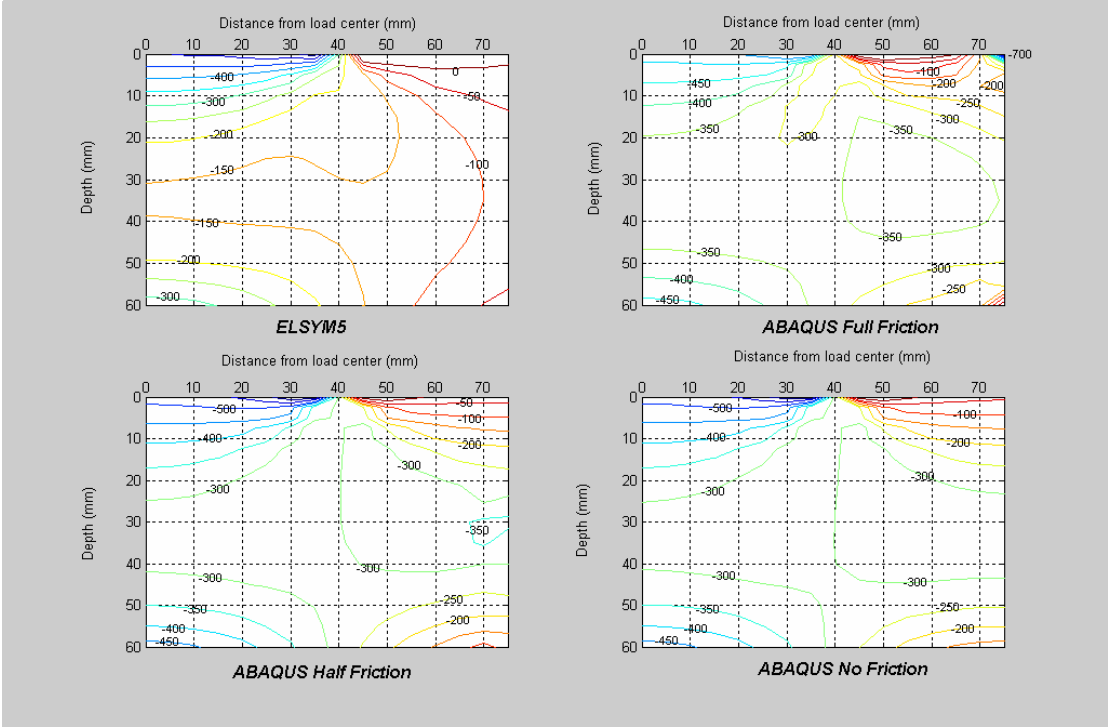


**Figure A - 33: ABAQUS Horizontal Stress Contours (in kPa) for Briquette 150mm width; Thickness 60 mm; Stiffness 1500 MPa;  $\nu = 0.45$**

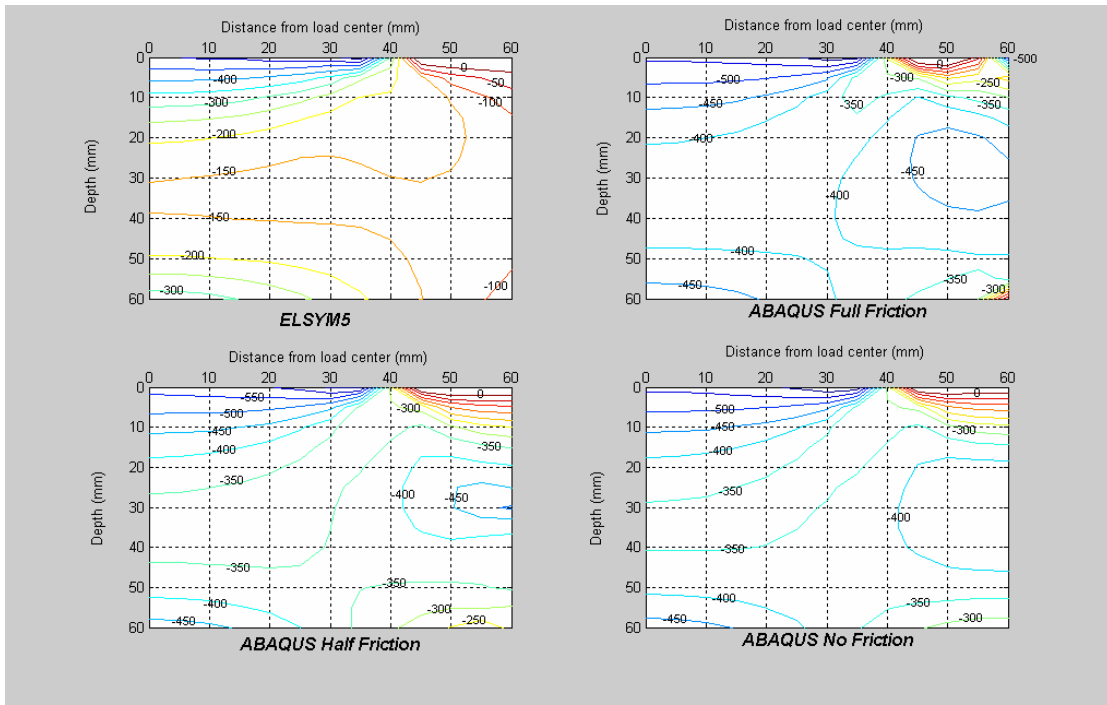


**Figure A - 34: ABAQUS Horizontal Stress Contours (in kPa) for Briquette 120mm width;  
Thickness 60 mm; Stiffness 1500 MPa;  $\nu = 0.45$**

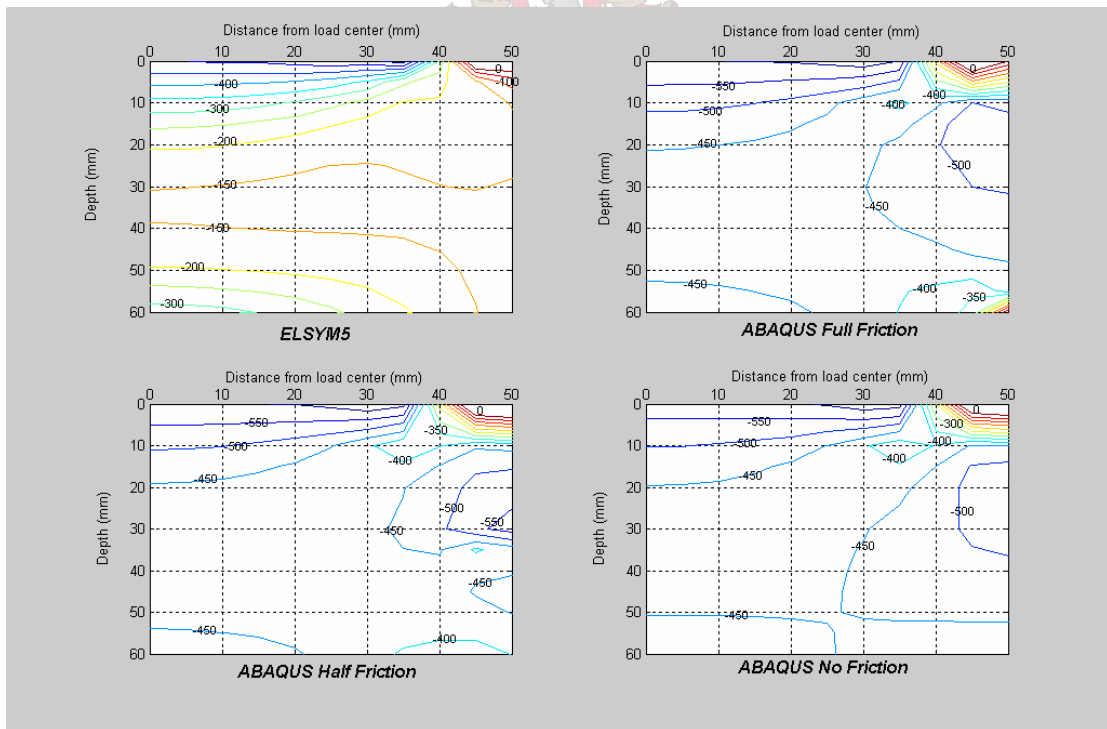


**Figure A - 35: ABAQUS Horizontal Stress Contours (in kPa) for Briquette 100mm width;  
Thickness 60 mm; Stiffness 1500 MPa;  $\nu = 0.45$**

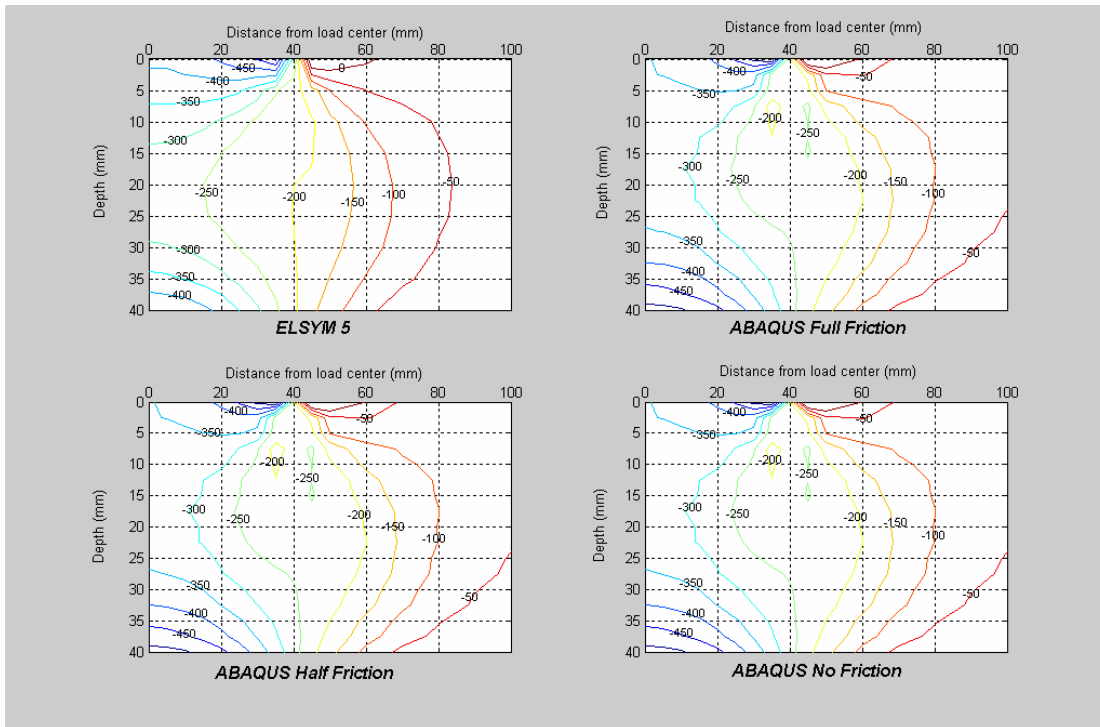


**Figure A - 36: ABAQUS Horizontal Stress Contours (in kPa) for Slab 600 mm width;  
Thickness 40 mm; Stiffness 1500 MPa;  $\nu = 0.45$**

## A2.4 Deviator stress ( $\sigma_1 - \sigma_3$ ) distributions

The deviator stress distributions are given in Figure A - 37 through Figure A - 40. It is evident that the higher deviator stresses occur in the 150 mm briquette. This indicates that this specimen will yield higher rutting, followed by the 120mm and then the 100mm briquette. For the slab, it is once again seen that the deviator stresses does not extend beyond 100mm from the wheel center. This, and the other slab stress distributions indicate that the slab is wide enough not to have border effects influence the stress distribution.

## A2.5 Summary

As expected, the highest vertical, horizontal deviator stresses occur under the wheel. The highest shear stresses occur under the side of the wheel, also as expected.

The stress distributions as determined from linear elastic and finite element analysis indicate that there is no significant difference in the stresses as determined by these two methods. It can

be concluded that the slab is wide enough so that the confinement and the amount of friction against the mould does not interfere with the stress distribution within the slab.

For the briquettes, the deviator stress decreases and the horizontal stress increases with a decrease in width. The horizontal stress on the outside of the wheel is fairly higher than was the case for the slab. It appears that the width of the briquette does influence the stress distribution within the specimen. The amount of friction may also play a role especially in the region between the wheel and the mould.

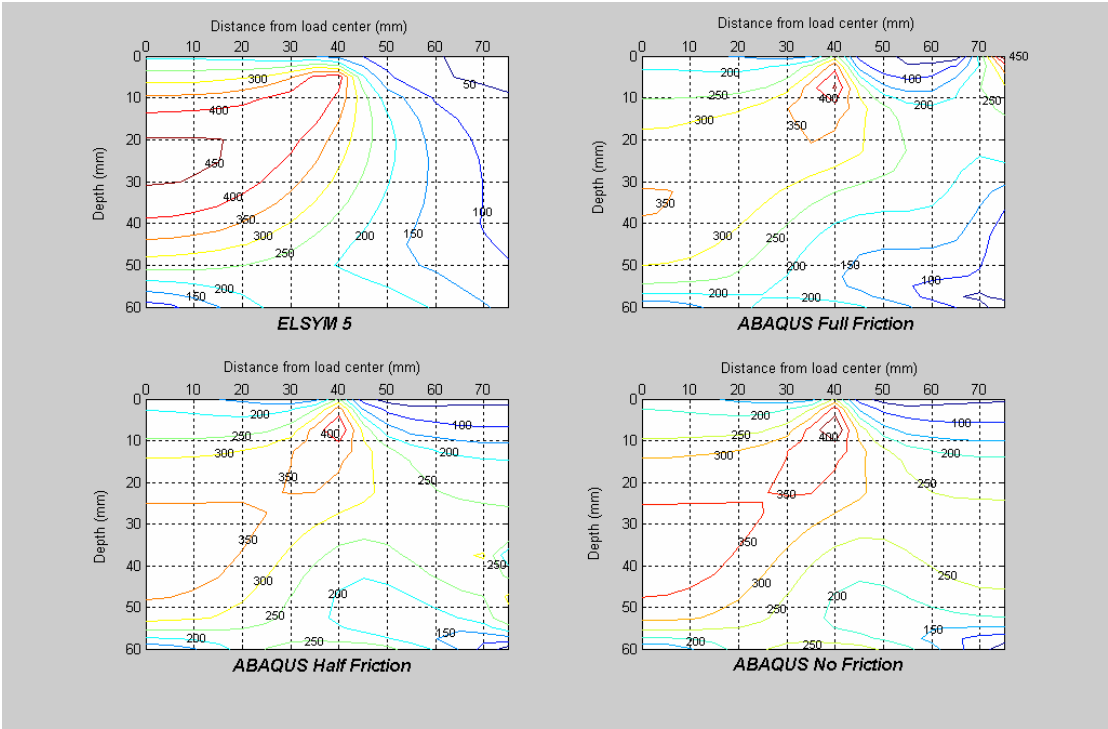


**Figure A - 37: ABAQUS Deviator Stress ( $\sigma_1 - \sigma_3$ ) Contours (in kPa) for Briquette 150mm width; Thickness 60 mm; Stiffness 1500 MPa;  $\nu = 0.45$**

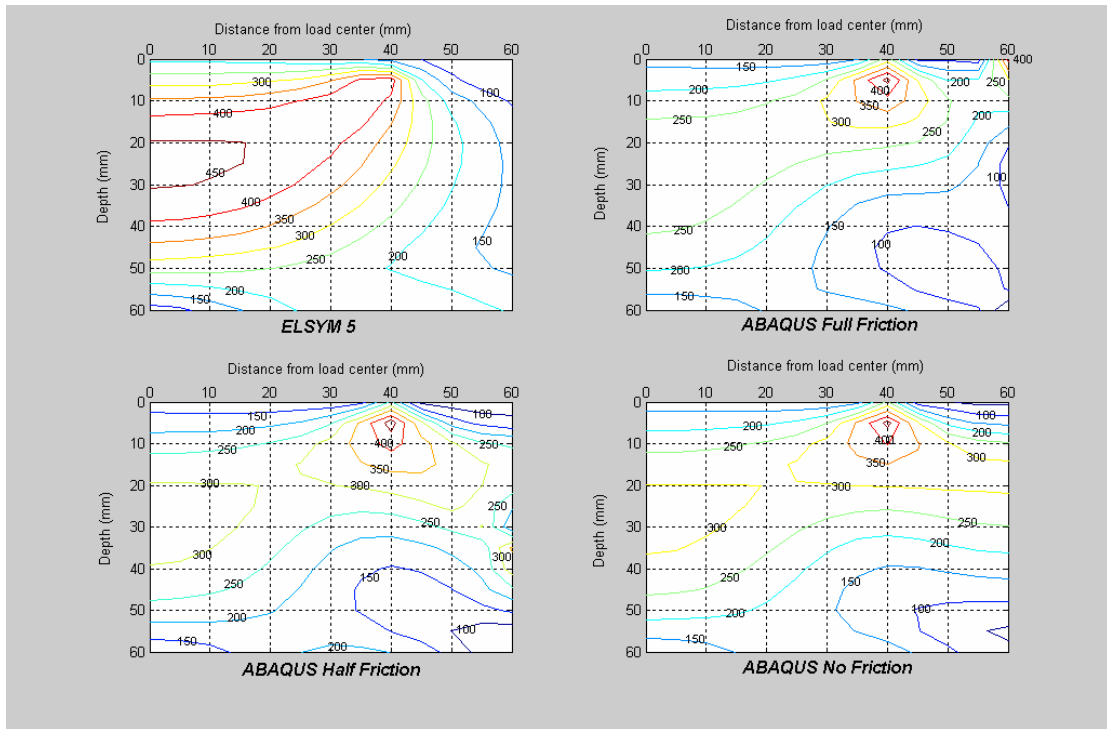


**Figure A - 38: ABAQUS Deviator Stress ( $\sigma_1 - \sigma_3$ ) Contours (in kPa) for Briquette 120mm width; Thickness 60 mm; Stiffness 1500 MPa;  $\nu = 0.45$**

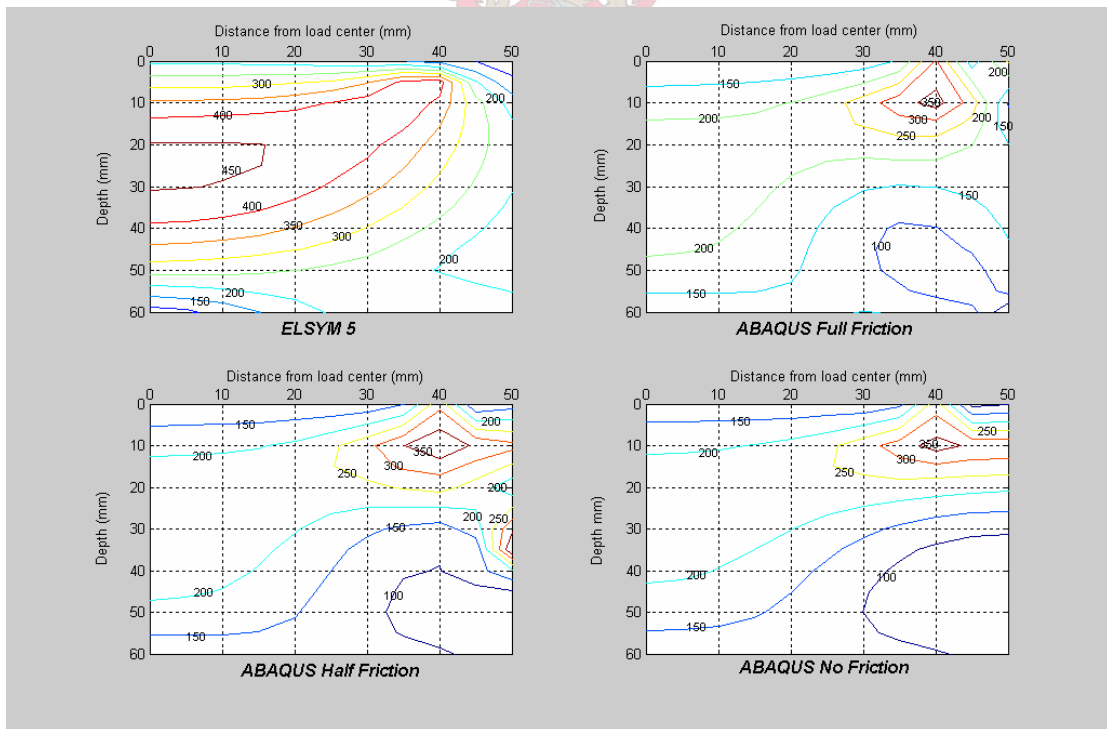


**Figure A - 39: ABAQUS Deviator Stress ( $\sigma_1 - \sigma_3$ ) Contours (in kPa) for Briquette 100mm width; Thickness 60 mm; Stiffness 1500 MPa;  $\nu = 0.45$**

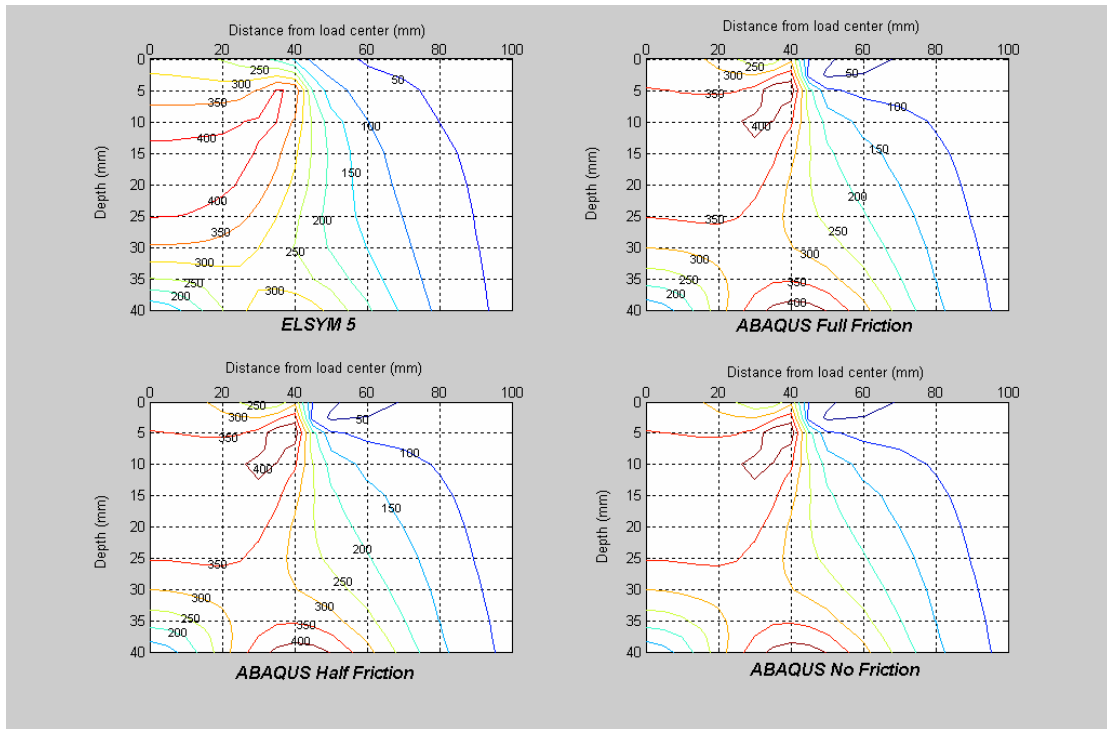
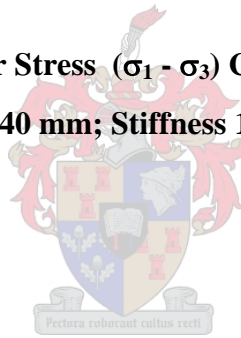


**Figure A - 40: ABAQUS Deviator Stress ( $\sigma_1 - \sigma_3$ ) Contours (in kPa) for Slab 600 mm width; Thickness 40 mm; Stiffness 1500 MPa;  $\nu = 0.45$**

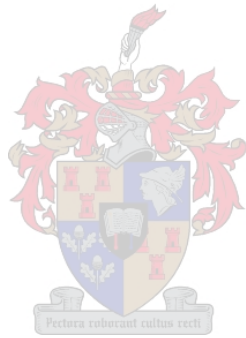


# APPENDIX B

## Input files for Finite Element Analysis

### B.1 ABAQUS Input File for Finite Element Analysis of Briquette 150 mm width

```
*HEADING
MMLS BRIQUETTE 150 MM DIAMETER HEIGHT 60 MM - LINEAR ELASTIC
**UNITS: Length - mm; Load - N; Stress - N/mm2 (MPa)
**NO FRICTION
**PLANE STRAIN
*PREPRINT, ECHO=NO, HISTORY=NO, MODEL=NO
*RESTART, WRITE, FREQ=1
*FILE FORMAT, ZERO INCREMENT
*****
**
**
***   NODE DATA   ***
*NODE, NSET=AMID
101,0.0,0.0
201,0.0,2.5
301,0.0,5.0
401,0.0,7.5
501,0.0,10.0
601,0.0,12.5
701,0.0,15.0
801,0.0,17.5
901,0.0,20.0
1001,0.0,22.5
1101,0.0,25.0
1201,0.0,27.5
1301,0.0,30.0
1401,0.0,32.5
1501,0.0,35.0
1601,0.0,37.5
1701,0.0,40.0
1801,0.0,42.5
1901,0.0,45.0
2001,0.0,47.5
2101,0.0,50.0
2201,0.0,52.5
2301,0.0,55.0
2401,0.0,57.5
2501,0.0,60.0
*NODE, NSET=AOUT
131,75.0,0.0
231,75.0,2.5
331,75.0,5.0
431,75.0,7.5
```

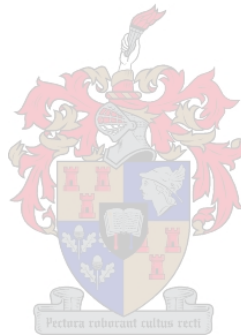


531,75.0,10.0  
 631,75.0,12.5  
 731,75.0,15.0  
 831,75.0,17.5  
 931,75.0,20.0  
 1031,75.0,22.5  
 1131,75.0,25.0  
 1231,75.0,27.5  
 1331,75.0,30.0  
 1431,75.0,32.5  
 1531,75.0,35.0  
 1631,75.0,37.5  
 1731,75.0,40.0  
 1831,75.0,42.5  
 1931,75.0,45.0  
 2031,75.0,47.5  
 2131,75.0,50.0  
 2231,75.0,52.5  
 2331,75.0,55.0  
 2431,75.0,57.5  
 2531,75.0,60.0

\*\*\*\*\*

\*\*\*\*\*

\*NFILL,NSET=SASPH  
 AMID,AOUT,30,1  
 \*NSET,NSET=BOTTOM  
 101,102,103,104,105,106,107,108,109,  
 110,111,112,113,114,115,116,117,118,  
 119,120,121,122,123,124,125,126,127,  
 128,129,130,131



\*\*\*

\*\*\*

\*\*\* ELEMENT DATA\*\*\*

\*\*

\*ELEMENT,TYPE=CPE8,ELSET=WCBIT  
 101,101,103,303,301,102,203,302,201  
 \*ELGEN,ELSET=WCBIT  
 101,15,2,1,12,200,100  
 \*ELSET,ELSET=LSTRIP  
 1201,1202,1203,1204,1205,1206,1207,1208

\*\*\*

\*\*\*

\*\*\*

\*\*\*\*\*MATERIAL DATA\*\*\*\*\*

\*SOLID SECTION,MATERIAL=ASPH,ELSET=WCBIT  
 \*MATERIAL,NAME=ASPH  
 \*ELASTIC,TYPE=ISO  
 1500.0E00,0.45

\*\*\*\*

\*\*\*\*

\*STEP,PERTURBATION

\*STATIC

\*\*\*

```
*****BOUNDARY CONDITIONS*****
*BOUNDARY
BOTTOM,ENCASTRE
AMID,XYMM
AOUT,1,1,0.0
****
****
*****LOADING*****
*DLOAD
LSTRIP,P3,0.690
*****
*****
*NODE PRINT
COORD
U
*****
*EL PRINT, POSITION=AVERAGED AT NODES
S,SP
****
****
*END STEP
```

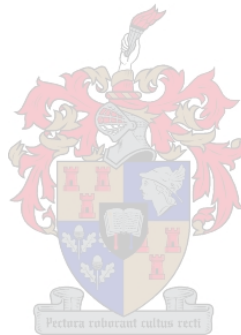
\*\*\*\*\*



## B2. ABAQUS Input File for Finite Element Analysis of Briquette

### 120 mm width

```
*HEADING
MMLS BRIQUETTE 120 MM DIAMETER HEIGHT 60 MM - LINEAR ELASTIC
**UNITS: Length - mm; Load - N; Stress - N/mm2 (MPa)
**NO FRICTION
**PLANE STRAIN
*PREPRINT, ECHO=NO, HISTORY=NO, MODEL=NO
*RESTART, WRITE, FREQ=1
*FILE FORMAT, ZERO INCREMENT
*****
**
**
***   NODE DATA       ***
*NODE, NSET=AMID
101,0.0,0.0
201,0.0,2.5
301,0.0,5.0
401,0.0,7.5
501,0.0,10.0
601,0.0,12.5
701,0.0,15.0
801,0.0,17.5
901,0.0,20.0
1001,0.0,22.5
1101,0.0,25.0
1201,0.0,27.5
1301,0.0,30.0
1401,0.0,32.5
1501,0.0,35.0
1601,0.0,37.5
1701,0.0,40.0
1801,0.0,42.5
1901,0.0,45.0
2001,0.0,47.5
2101,0.0,50.0
2201,0.0,52.5
2301,0.0,55.0
2401,0.0,57.5
2501,0.0,60.0
*NODE, NSET=AOUT
125,60.0,0.0
225,60.0,2.5
325,60.0,5.0
425,60.0,7.5
525,60.0,10.0
625,60.0,12.5
725,60.0,15.0
825,60.0,17.5
925,60.0,20.0
1025,60.0,22.5
1125,60.0,25.0
1225,60.0,27.5
```



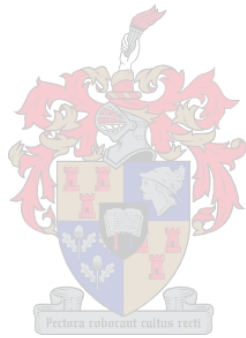
```

1325,60.0,30.0
1425,60.0,32.5
1525,60.0,35.0
1625,60.0,37.5
1725,60.0,40.0
1825,60.0,42.5
1925,60.0,45.0
2025,60.0,47.5
2125,60.0,50.0
2225,60.0,52.5
2325,60.0,55.0
2425,60.0,57.5
2525,60.0,60.0
*NFILL,NSET=SASPH
AMID,AOUT,24,1
*NSET,NSET=BOTTOM
101,102,103,104,105,106,107,108,109,
110,111,112,113,114,115,116,117,118,
119,120,121,122,123,124,125
***
***
***      ELEMENT DATA***
**
*ELEMENT,TYPE=CPE8,ELSET=WCBIT
101,101,103,303,301,102,203,302,201
*ELGEN,ELSET=WCBIT
101,12,2,1,12,200,100
*ELSET,ELSET=LSTRIP
1201,1202,1203,1204,1205,1206,1207,1208
***
***
***
*****MATERIAL DATA*****
*SOLID SECTION,MATERIAL=ASPH,ELSET=WCBIT
*MATERIAL,NAME=ASPH
*ELASTIC,TYPE=ISO
1500.0E00, 0.45
****
****
*STEP,PERTURBATION
*STATIC
***
*****BOUNDARY CONDITIONS*****
*BOUNDARY
BOTTOM,ENCASTRE
AMID,XSMM
AOUT,1,1,0.0
****
****
*****LOADING*****
*DLOAD
LSTRIP,P3,0.690
*****
*****
*NODE PRINT

```

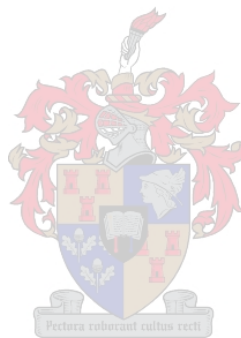


```
COORD
U
*****
*EL PRINT, POSITION=AVERAGED AT NODES
S,SP
****
****
*END STEP
*****
```



### B3. ABAQUS Input File for Finite Element Analysis of Briquette 100 mm width

```
*HEADING
MMLS BRIQUETTE 100 MM DIAMETER HEIGHT 60 MM - LINEAR ELASTIC
**UNITS: Length - mm; Load - N; Stress - N/mm2 (MPa)
**NO FRICTION
**PLANE STRAIN
*PREPRINT, ECHO=NO, HISTORY=NO, MODEL=NO
*RESTART, WRITE, FREQ=1
*FILE FORMAT, ZERO INCREMENT
*****
**
**
***   NODE DATA       ***
*NODE, NSET=AMID
101,0.0,0.0
201,0.0,2.5
301,0.0,5.0
401,0.0,7.5
501,0.0,10.0
601,0.0,12.5
701,0.0,15.0
801,0.0,17.5
901,0.0,20.0
1001,0.0,22.5
1101,0.0,25.0
1201,0.0,27.5
1301,0.0,30.0
1401,0.0,32.5
1501,0.0,35.0
1601,0.0,37.5
1701,0.0,40.0
1801,0.0,42.5
1901,0.0,45.0
2001,0.0,47.5
2101,0.0,50.0
2201,0.0,52.5
2301,0.0,55.0
2401,0.0,57.5
2501,0.0,60.0
*NODE, NSET=AOUT
121,50.0,0.0
221,50.0,2.5
321,50.0,5.0
421,50.0,7.5
521,50.0,10.0
621,50.0,12.5
721,50.0,15.0
821,50.0,17.5
```



```

921,50.0,20.0
1021,50.0,22.5
1121,50.0,25.0
1221,50.0,27.5
1321,50.0,30.0
1421,50.0,32.5
1521,50.0,35.0
1621,50.0,37.5
1721,50.0,40.0
1821,50.0,42.5
1921,50.0,45.0
2021,50.0,47.5
2121,50.0,50.0
2221,50.0,52.5
2321,50.0,55.0
2421,50.0,57.5
2521,50.0,60.0
*NFILL,NSET=SASPH
AMID,AOUT,20,1
*NSET,NSET=BOTTOM
101,102,103,104,105,106,107,108,109,
110,111,112,113,114,115,116,117,118,
119,120,121
***
***   ELEMENT DATA***
**
*ELEMENT,TYPE=CPE8,ELSET=WCBIT
101,101,103,303,301,102,203,302,201
*ELGEN,ELSET=WCBIT
101,10,2,1,12,200,100
*ELSET,ELSET=LSTRIP
1201,1202,1203,1204,1205,1206,1207,1208

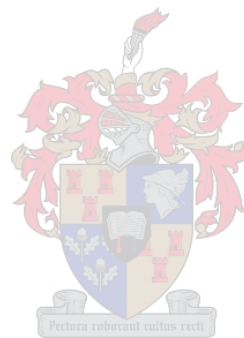
***
***
*****MATERIAL DATA*****
*SOLID SECTION,MATERIAL=ASPH,ELSET=WCBIT
*MATERIAL,NAME=ASPH
*ELASTIC,TYPE=ISO
1500.0E00,0.45
****
****
*STEP,PERTURBATION
*STATIC
***
*****BOUNDARY CONDITIONS*****
*BOUNDARY
BOTTOM,ENCASTRE
AMID,XYMM
AOUT,1,1,0.0
****
****
*****LOADING*****
*DLOAD
LSTRIP,P3,0.690

```



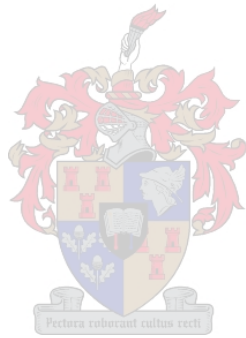
```
*****
*****
*NODE PRINT
COORD
U
*****
*EL PRINT, POSITION=AVERAGED AT NODES
S,SP
****
****
*END STEP
```

```
*****
```



# B4. ABAQUS Input File for Finite Element Analysis of Slab 600 mm width

```
*HEADING
MMLS SLAB WIDTH 600 MM ; HEIGHT 40 MM - LINEAR ELASTIC
UNITS: Length - mm; Load - N; Stress - N/mm2 (MPa)
PLANE STRAIN
**NO FRICTION
***
***
*PREPRINT, ECHO=NO, HISTORY=NO, MODEL=NO
***
*RESTART, WRITE, FREQ=1
***
*FILE FORMAT, ZERO INCREMENT
***
***
***
***      MESH GENERATION      ***
**
**
***      NODE DATA      ***
*NODE,NSET=ACENTR
901,0.0,0.0
1001,0.0,2.5
1101,0.0,5.0
1201,0.0,7.5
1301,0.0,10.0
1401,0.0,12.5
1501,0.0,15.0
1601,0.0,17.5
1701,0.0,20.0
1801,0.0,22.5
1901,0.0,25.0
2001,0.0,27.5
2101,0.0,30.0
2201,0.0,32.5
2301,0.0,35.0
2401,0.0,37.5
2501,0.0,40.0
***
*NODE,NSET=ASIDE
961,300.0,0.0
1061,300.0,2.5
1161,300.0,5.0
1261,300.0,7.5
1361,300.0,10.0
1461,300.0,12.5
1561,300.0,15.0
1661,300.0,17.5
1761,300.0,20.0
1861,300.0,22.5
```

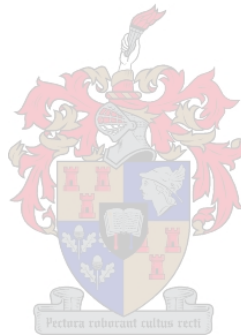


```

1961,300.0,25.0
2061,300.0,27.5
2161,300.0,30.0
2261,300.0,32.5
2361,300.0,35.0
2461,300.0,37.5
2561,300.0,40.0
***,
*NODE,NSET=A1
921,50.0,0.0
1021,50.0,2.5
1121,50.0,5.0
1221,50.0,7.5
1321,50.0,10.0
1421,50.0,12.5
1521,50.0,15.0
1621,50.0,17.5
1721,50.0,20.0
1821,50.0,22.5
1921,50.0,25.0
2021,50.0,27.5
2121,50.0,30.0
2221,50.0,32.5
2321,50.0,35.0
2421,50.0,37.5
2521,50.0,40.0
***
*NODE,NSET=A2
941,150.0,0.0
1041,150.0,2.5
1141,150.0,5.0
1241,150.0,7.5
1341,150.0,10.0
1441,150.0,12.5
1541,150.0,15.0
1641,150.0,17.5
1741,150.0,20.0
1841,150.0,22.5
1941,150.0,25.0
2041,150.0,27.5
2141,150.0,30.0
2241,150.0,32.5
2341,150.0,35.0
2441,150.0,37.5
2541,150.0,40.0
***

***
***
*NGEN, NSET=BOT1
901,921,1
*NGEN, NSET=BOT2
921,941,1
*NGEN, NSET=BOT3
941,961,1

```



```

*NSET, NSET=BOTTOM
BOT1, BOT2, BOT3
***
*NFILL, NSET=SASPH1
ACENTR, A1, 20, 1
*NFILL, NSET=SASPH2
A1, A2, 20, 1
*NFILL, NSET=SASPH3
A2, ASIDE, 20, 1
*NSET, NSET=SASPH
SASPH1, SASPH2, SASPH3
***
***
*** ELEMENT DATA ***
***
*ELEMENT, TYPE=CPE8, ELSET=WCBIT
101, 901, 903, 1103, 1101, 902, 1003, 1102, 1001
*ELGEN, ELSET=WCBIT
101, 30, 2, 1, 8, 200, 100
*ELSET, ELSET=LSTRIP
801, 802, 803, 804, 805, 806, 807, 808
***
***
*** MATERIAL DATA ***
*SOLID SECTION, MATERIAL=ASPH, ELSET=BRIQ
*MATERIAL, NAME=ASPH
*ELASTIC, TYPE=ISO
1500.0E00, 0.45
***
***
*STEP, PERTURBATION
*STATIC
***
*** BOUNDARY CONDITIONS ***
*BOUNDARY
BOTTOM, ENCASTRE
ACENTR, XSYMM
ASIDE, 1, 1, 0.0
***
*** LOADING ***
*DLOAD
LSTRIP, P3, 0.690
***
***
*NODE PRINT
COORD
U
***
*EL PRINT, POSITION=AVERAGED AT NODES
S, SP
***
***
*END STEP
*****

```

